

## University of Southampton Research Repository

Copyright © and Moral Rights for this thesis and, where applicable, any accompanying data are retained by the author and/or other copyright owners. A copy can be downloaded for personal non-commercial research or study, without prior permission or charge. This thesis and the accompanying data cannot be reproduced or quoted extensively from without first obtaining permission in writing from the copyright holder/s. The content of the thesis and accompanying research data (where applicable) must not be changed in any way or sold commercially in any format or medium without the formal permission of the copyright holder/s.

When referring to this thesis and any accompanying data, full bibliographic details must be given, e.g.

Thesis: Author (Year of Submission) "Full thesis title", University of Southampton, name of the University Faculty or School or Department, PhD Thesis, pagination.

Data: Author (Year) Title. URI [dataset]



**University of Southampton**

Faculty of Engineering and Physical Sciences

**Uncertainty and sensitivity of coastal flood risk estimates across the Solent, UK  
from 1920 to 2100**

by

**Jose Alejandro Pinto Rascon**

Thesis for the degree of Doctor of Philosophy

2022





# University of Southampton

## Abstract

Faculty of Engineering and Physical Sciences

Doctor of Philosophy

### **Uncertainty and sensitivity of coastal flood risk estimates across the Solent, UK from 1920 to 2100**

by

Jose Alejandro Pinto Rascon

This thesis develops a methodology to understand the influence of environmental and socio-economic factors on the past, present and future evolution of coastal flood risk on a regional level. The Solent, in the south of England, is selected as a case study region as it encompasses a variety of natural and urban coastal environments along its length, creating the opportunity to transfer the knowledge acquired and the methods developed to other areas in the UK and more widely. The richness of data and previous assessments for this region allow for a better understanding of the coastal processes, leading to more accurate assessments.

The overarching aim of this PhD study is to quantify the influence that each component of the Source-Pathway-Receptor-Consequence conceptual framework has on past, present and future coastal flood risk levels. The analysis uses a 2D inundation model coupled with improved population distributions to determine the risk of coastal flooding using the number of people threatened as the indicator. The uncertainty is assessed using a combination of scenarios and a variance-based sensitivity assessment. Three objectives are defined to assist in the completion of the aim. The first objective is to assess how coastal flood risk has evolved at the Solent between 1920 and 2000. Population growth was the primary driver of coastal flood risk during the 20<sup>th</sup> century, followed by a small contribution of sea-level rise, but defence improvement after 1940 slowed the rise in risk for some areas (e.g. Portsmouth). The second objective is to estimate the present-day risk of coastal flooding and quantify its sources of uncertainty. The average estimate is a risk of 1,480 people/year, equivalent to £145 million/year in 2020. The biggest uncertainties are given by the presence/absence and height of flood defences, but the height of extreme sea levels creates the largest variability for present-day coastal flood risk. The third objective is to determine how coastal flood risk may evolve over the remainder of the 21<sup>st</sup> century, given future sea-level rise, population change, and plausible coastal management strategies. The magnitude of sea-level rise causes the biggest uncertainties, and it is the main driver of coastal flood risk, which reaches an average of 4,581 people/year by 2100. Furthermore, the scenarios of coastal management strategies will not be sufficient to mitigate all of the future effects of climate and population change on coastal flood risk at the Solent. Hence, improved protection or alternative adaptive approaches would be prudent. The approach, methods developed, and learnings of this thesis can be transferred to other regions that follow a similar evolution to that of the Solent and can help steer their coastal management strategies.



# Table of Contents

<b>Table of Contents .....</b>	<b>i</b>
<b>Table of Tables .....</b>	<b>vii</b>
<b>Table of Figures .....</b>	<b>ix</b>
<b>Research Thesis: Declaration of Authorship .....</b>	<b>xvii</b>
<b>Acknowledgements .....</b>	<b>xix</b>
<b>Definitions and Abbreviations.....</b>	<b>xxi</b>
<b>Chapter 1 Introduction.....</b>	<b>1</b>
1.1 Motivation .....	1
1.2 Aim and objectives .....	3
1.3 Thesis structure .....	5
<b>Chapter 2 Literature Review.....</b>	<b>7</b>
2.1 Introduction.....	7
2.2 Coastal flood risk and exposure .....	7
2.3 The Source-Pathway-Receptor-Consequence (SPRC) conceptual framework .....	8
2.3.1 Sources of coastal flood risk.....	9
2.3.1.1 Definition .....	9
2.3.1.2 Temporal evolution of the sources .....	10
2.3.1.3 Previous research analysing the sources of flood risk .....	11
2.3.2 Pathways of coastal flood risk.....	15
2.3.2.1 Definition .....	15
2.3.2.2 Temporal changes on the pathways of flood risk .....	20
2.3.2.3 Previous research analysing the pathways of coastal flood risk.....	22
2.3.3 Receptors.....	25
2.3.3.1 Definition .....	25
2.3.3.2 Temporal Changes.....	25
2.3.3.3 Previous research analysing the receptors of coastal flood risk.....	26
2.3.4 Consequences .....	28
2.3.4.1 Definition .....	28

## Table of Contents

2.3.4.2	Temporal Changes .....	29
2.3.4.3	Previous research analysing the consequences of coastal flood risk...	30
2.4	Hydrodynamic modelling.....	34
2.5	Methods to conduct coastal flood risk assessments.....	37
2.6	Uncertainty in risk assessments.....	39
2.6.1	Previous research analysing uncertainty in flood risk estimates .....	41
2.7	Summary .....	43
<b>Chapter 3</b>	<b>Study Site .....</b>	<b>47</b>
3.1	Introduction .....	47
3.2	Overview of the Solent .....	47
3.3	Coastal flooding at the Solent.....	52
3.4	Previous assessment of coastal flood risk in the area .....	52
<b>Chapter 4</b>	<b>General Methods.....</b>	<b>57</b>
4.1	Introduction .....	57
4.2	Hydrodynamic model set-up .....	59
4.2.1	Boundary conditions (Sources) .....	60
4.2.2	Hydraulic roughness map .....	61
4.2.3	Barriers to flow (Pathways) .....	64
4.2.4	LISFLOOD-FP setup.....	68
4.3	Population distribution methods (Receptors) .....	69
4.4	Summary .....	71
<b>Chapter 5</b>	<b>Historical evolution of coastal flood risk at the Solent .....</b>	<b>73</b>
5.1	Introduction .....	73
5.2	Data and methods.....	75
5.2.1	Historical evolution of the sources of coastal flood risk .....	75
5.2.2	Historical evolution of the pathways of coastal flood risk .....	78
5.2.3	Historical evolution of the receptors of coastal flood risk .....	80
5.2.4	Flood risk analysis .....	88
5.3	Results.....	88

5.3.1	Historical exposure to coastal flooding.....	90
5.3.2	Historical risk of coastal flooding .....	97
5.3.3	Historical drivers of coastal flood risk .....	100
5.4	Discussion .....	105
5.4.1	Historical exposure to coastal flooding.....	105
5.4.2	Historical risk of coastal flooding .....	108
5.4.3	Historical drivers of coastal flood risk .....	111
5.5	Conclusions.....	112
<b>Chapter 6</b>	<b>Present levels and largest sources of uncertainty in coastal flood risk at the Solent .....</b>	<b>115</b>
6.1	Introduction.....	115
6.2	Data and methods .....	116
6.2.1	Uncertainty and sensitivity assessment.....	117
6.2.1.1	Scenario analysis .....	117
6.2.1.2	Probabilistic assessment .....	118
6.2.1.3	Sensitivity assessment.....	118
6.2.2	Sources (Boundary conditions) .....	120
6.2.3	Pathways (Barriers to water flow) .....	123
6.2.4	Receptors (Population distribution).....	124
6.2.5	Preliminary assessment to determine the number of required simulations	126
6.3	Results .....	128
6.3.1	Present-day exposure .....	131
6.3.2	Present-day risk of coastal flooding.....	136
6.3.3	Uncertainty assessment of present-day estimates of exposure and risk of coastal flooding .....	138
6.3.3.1	Scenario assessment of exposure to coastal flooding .....	138
6.3.3.2	Probabilistic assessment of exposure to coastal flooding .....	142
6.3.3.3	Scenario assessment of coastal flood risk.....	149
6.3.3.4	Probabilistic assessment of coastal flood risk.....	151
6.4	Discussion .....	153

## Table of Contents

6.4.1	Present-day exposure .....	153
6.4.2	Present-day risk of coastal flooding .....	154
6.4.3	Uncertainty in present-day exposure and risk of coastal flooding.....	155
6.4.3.1	Sensitivity and uncertainty in exposure estimates.....	155
6.4.3.2	Sensitivity and uncertainty in risk estimates .....	157
6.5	Conclusions .....	158
<b>Chapter 7 Future evolution of coastal flood risk at the Solent over the 21<sup>st</sup> century.</b>		<b>161</b>
7.1	Introduction .....	161
7.2	Data and methods.....	163
7.2.1	Future evolution of the sources.....	163
7.2.2	Future evolution of the pathways .....	165
7.2.3	Future evolution of the receptors .....	170
7.2.4	Future flood risk analysis .....	174
7.3	Results.....	175
7.3.1	Future exposure to coastal flooding.....	175
7.3.2	Future risk of coastal flooding .....	181
7.3.3	Uncertainty in future exposure and risk of coastal flooding.....	186
7.4	Discussion.....	196
7.4.1	Future exposure to coastal flooding.....	196
7.4.2	Future risk of coastal flooding .....	197
7.4.3	Uncertainty in future exposure and risk of coastal flooding.....	197
7.5	Conclusions .....	200
<b>Chapter 8 Synthesis of the past, present and future evolution of coastal flooding at the Solent, England .....</b>		<b>203</b>
8.1	Introduction .....	203
8.2	Synthesis .....	203
8.3	Discussion.....	207
8.4	Implications.....	211
8.5	Limitations.....	212
8.6	Recommendations for future research .....	213

<b>Chapter 9 Conclusions.....</b>	<b>217</b>
<b>Appendix A Accuracy of the hydrodynamic model.....</b>	<b>219</b>
A.1 Coastal flood event March 10, 2008 .....	219
A.2 Hydrodynamic simulation setup .....	222
A.3 Results of the hydrodynamic simulation of the 10 March 2008 flood event .....	223
<b>List of References .....</b>	<b>225</b>





## Table of Tables

Table 2.1 Environment Agency asset condition grading .....	24
Table 4.1 Hydraulic roughness coefficient for different types of land cover .....	64
Table 4.2 Example of the data contained on the Environment Agency Flood Defence dataset. ....	65
Table 4.3 Example of coastal flood defences information included on the 2010 North Solent Shoreline Management Plan .....	67
Table 5.1 Present-day (2020) extreme water levels (m) by the Environment Agency (2018), along with estimates of their historical equivalents. ....	77
Table 5.2 Total number of flood defences at the Solent with and without information of when these were built. ....	79
Table 5.3 Recorded average defence height adjustment in Portsea Island, assumed constant for the whole region.....	80
Table 5.4 Spatial resolution of census data in England from 1921 to 2011 .....	80
Table 5.5 Resolution, publishing data and coverage of Ordnance Survey maps used for urban area digitization and population distribution .....	83
Table 5.6 Input parameters used in the historical flood risk analysis .....	88
Table 5.7 Comparison with Stevens et al. (2015) of Portsmouth historical exposure to extreme water events. ....	108
Table 6.1 Scenarios used for sensitivity and uncertainty analysis.....	118
Table 6.2 Extreme water levels and return periods for Portsmouth tide gauge by the Environment Agency .....	121
Table 6.3 Present economic exposure to coastal flooding .....	134
Table 7.1 IIASA population growth scenarios used in the assessment, including their description .....	171
Table 7.2 SPRC scenarios for future flood risk assessment .....	174
Table 7.3 Main storylines of future SPRC configurations .....	175

## Table of Tables

Table 9.1 Summary of flood locations and failure mechanisms on 10 March 2008. Data from

Wadey (2013) ..... 219

## Table of Figures

Figure 2.1 Sources of coastal flood risk .....	10
Figure 2.2 Evolution of the sources of coastal flood risk .....	11
Figure 2.3 Illustration of the skew surge (McMillan et al., 2011). ....	13
Figure 2.4 Pathways of coastal flood risk.....	16
Figure 2.5 Spatial and temporal scale of processes affecting coastal evolution. Figure inspired by Cowell and Thom (1994).....	22
Figure 2.6 Receptors of coastal flood risk.....	26
Figure 3.1 Location of the Solent, UK .....	48
Figure 3.2 Special Areas of Conservation, Special Protection Areas, Marine Conservation Zones and Ramsar sites within the study region. ....	49
Figure 3.3 Built-up areas in the Solent within the 1 in 10,000-year floodplain.....	51
Figure 3.4 Number and severity of coastal flood events registered at the Solent over the last 100 years by a) month, b) year, c) decade. Data from Ruocco et. al. (2011) and Boza et. al. (2018). Category 1 represents nuisance flooding. Category 2 are minor flooding in open areas. Category 3 are moderate flooding of up to 2.5 feet over localized areas. Category 4 are major floods of over 2.5 feet of water over large areas. Category 5 are severe floods over large areas with livestock drowned and people injured. Category 6 are disastrous events with one or more human lives lost. ....	55
Figure 4.1 Overview of the general methods in relation to the SPRC framework. ....	58
Figure 4.2 Analysis of the 100 largest storm surge curves on record at Portsmouth tide gauge	61
Figure 4.3 Different types of land cover present at the Solent. Data from the Ordnance Survey aggregate class land map.....	63
Figure 4.4 Coastal and fluvial flood defences present in the study region. Data from the Environment Agency (EA) Spatial Flood Defences with Standard Attributes and from the Channel Coastal Observatory (CCO). ....	68
Figure 4.5 Visual representation of LISFLOOD-FP setup.....	69

## Table of Figures

Figure 5.1 Land subsidence and sea-level rise across the Solent .....	76
Figure 5.2 Example of water curve for a 1 in 100-yr extreme water level, and its adjusted maximum height as a consequence of sea-level rise .....	77
Figure 5.3 Difference in the location of tidal lines (red and blue) in Portsea Island as reported by the Ordnance Survey for present-day from those registered in the County Series 3rev.....	78
Figure 5.4 Schematic representation of the population distribution methodology .....	82
Figure 5.5 Representation of population distribution method for an area near Southsea in Portsea Island. a) Location of example area within Portsea Island. b) Representation of original OS historical map (County Series 3 <sup>rd</sup> revision Epoch 4 covering the years 1920 - 1940). This is analysed with the ISO Cluster tool which separated blank spaces and lines (c). The blank spaces are removed (d) and the resulting lines are analysed to remove those that represent streets, parks etc. Lastly, the centroid of each property is obtained (e).....	85
Figure 5.6 Historical evolution of population distribution at the Solent.....	86
Figure 5.7 Initial (1921) and final (2011) population distribution and percentage population change for each timestep from 1921 to 2011 at the Solent. ....	87
Figure 5.8 Historical exposure to extreme water levels of increasing return period based on varying the minimum depth of flood .....	89
Figure 5.9 Historical exposure to extreme water levels of increasing return periods considering a minimum flood depth of 0.3m required to produce damage.....	90
Figure 5.10 Exposure to a 1 in 100-yr extreme water level under all scenarios and a minimum flood depth of 0.3m. Subplot a) present the results when all components are kept variable, showing the relationship between exposure, sea level, standards of protection and population. Subplot b) displays the isolated effect of population variability, illustrating the effect of population growth, c) presents the effect of improving flood defences, highlighting the effect of defence improvement from 1940 to 1960, and lastly d) shows the effect of sea-level rise on exposure.....	92
Figure 5.11 Evolution of flood exposure (area flooded) to a 1 in 100-yr event at the main built-up areas in the Solent, considering all components to be set to the year analysed	

(i.e. the variability caused by changes in components is not analysed) compared to the number of floods reported by Ruocco et al. (2011) .....	94
Figure 5.12 Spatial distribution of population exposure to a 1 in 100-yr extreme water level from 1920 to 2000, considering all components to be set to the year analysed and a minimum flood depth of 0.3m, compared to the number of floods reported at the Solent from 1935-2005 by Ruocco et al. (2011).....	95
Figure 5.13 Evolution of flood exposure (people flooded) to a 1 in 100-yr event in the main built-up areas of the Solent.....	96
Figure 5.14 Evolution of exposure (people flooded) to a 1 in 100-yr extreme water level at Portsea Island (Portsmouth) and Hayling Island.....	97
Figure 5.15 Expected annual damage (people/year) from 1920 to 2000 at the Solent, UK. ....	98
Figure 5.16 Evolution and trends of historical Expected Annual Damage (people) for top cities at the Solent. Note that the y-axis on plots b.1 to b.18 have different units and are only used to present the risk trends.....	99
Figure 5.17 Expected annual damage at the Solent, UK., from 1920 to 2000 based on the combination of input factors and a minimum flood depth of 0.3m. Subplot a) present the results when all components are kept variable, comparing defence standards, mean sea level and population size. Subplot b) displays the isolated effect of population variability, c) presents the effect of improving flood defences, highlighting the effect of defence improvement from 1940 to 1960, and lastly d) shows the effect of sea-level rise on EAD. ....	101
Figure 5.18 Isolated and combined effect of the SPRC components on the historical evolution of expected annual damage. Subplot a) shows the individual effect of each component considering the remainder to be equal to their previous timestep value, showing population growth to be the main driver of EAD increases. Subplot b) presents the evolution of each of the SPRC components as registered, c) shows the combined effect of SPRC factor evolution on EAD. and d) shows the estimated EAD evolution .....	103
Figure 5.19 Individual and combined effect of SPRC components on the historical evolution of coastal flood risk for main built-up areas. When analysing the effect of individual or joint components, the remainder are kept to their previous timestep value. ....	104

## Table of Figures

Figure 5.20 Expected Annual Damage results from (a) Stevens et al., (2015). (b) the EAD estimated in the present assessment, and (c) a comparison of both. ....	110
Figure 6.1 Recorded storm surge lengths for the 100 largest surges on record. A probability distribution is fitted to the data, which is then sampled using the Sobol sequence .....	120
Figure 6.2 a) Extreme water level height distribution across the Solent for a 1 in 300-yr event. b) Spread between the 5 <sup>th</sup> and 95 <sup>th</sup> confidence bounds. c) Shape parameter of each inflow point considering the mean value and confidence bounds. d) Example of the probability distribution fitted to the EA data and the samples generated for the analysis at two locations in the Solent.....	122
Figure 6.3 Difference in defence height when comparing the Environment Agency's dataset against the elevation model-based defence heights. a) Shows the results with a normal distribution fitted to the data. b) Difference data with a stable distribution fitted. ....	124
Figure 6.4 Population distribution method for present-day (objective two) and future (objective three) coastal flood risk assessment. The data is obtained for the census output areas and located within each population-weighted centroid (a). A square grid of 50x50m is generated for each area and the urban squares are determined using the OS building polygons (b). Lastly, the population of the weighted centroid is distributed based on the distance of the grid to the weighted centroid (c). .....	126
Figure 6.5 Variation in the Standard Deviation (STD) and the mean number of people flooded as a consequence of the number of simulations considered for every return period .....	127
Figure 6.6 LISFLOOD-FP simulation times. These are conducted at the University of Southampton IRIDIS High-Performance Computer Facility, using one node and 6 x 2.6 GHz Sandybridge 16-core nodes with 62 GB usable memory. ....	128
Figure 6.7 Present-day exposure (people) based on the minimum depth of flood required for all return periods. ....	130
Figure 6.8 Spread of results (number of people) for all simulations performed for every return period (scenario seven, all components variable). Note that the vertical scale is different for each row of data.....	132

Figure 6.9 Standard deviation of exposure (people) for every return period analysed .....	133
Figure 6.10 Present-day exposure to coastal flooding for some of the main built-up areas at the Solent, considering a minimum flood depth of 0.3m .....	135
Figure 6.11 Present-day Expected Annual Damage in terms of a) people/year and b) assets (GBP millions/year) and based on the minimum depth of flood required to produce damage .....	137
Figure 6.12 Present Expected Annual Damage (people/year) for some of the main built-up areas at the Solent.....	138
Figure 6.13 Standard deviation in population exposure based on a) individual and b) combined effect components being varied, with the corresponding scenario in brackets (note the colour scaling is relative to each row). .....	140
Figure 6.14 Spread of present exposure results for each of the seven scenarios used in the analysis for three representative return periods: 1 on 10; 1 in 100; and 1 in 1,000 years. ....	141
Figure 6.15 Difference in exposure results obtained by using a high-resolution dataset compared to the estimates when using WorldPop data .....	142
Figure 6.16 Distribution of present exposure results for a 1 in 100-year event. These results are obtained by simultaneously varying all three components. However, the results are presented based on the magnitude of two of them. ....	145
Figure 6.17 Distribution of exposure results for three representative return periods. The results are presented as a function of the magnitude of two of the components. The y-axis represents the number of people exposed whilst the x-axis is the height of the extreme water level. The colormaps are based on the range of the input factors, such as the height of defences modified.....	146
Figure 6.18 Exposure results obtained for a 1 in 100-year event following a probabilistic approach where all components are simultaneously varied. The colormap represents the number of people exposed.....	147
Figure 6.19 Variance-based sensitivity indices (Sobol indices). These are presented for every return period analysed and are based on a) local sensitivity, assuming no interaction with other components, and b) global sensitivity, where the interaction and contributions of these interactions are considered. ....	148

## Table of Figures

Figure 6.20 Mean value of people at risk and standard deviation based on the individual and combined variability of the components analysed .....	150
Figure 6.21 Probability distribution of expected annual damage considering a minimum flood depth of 0.3m. This is obtained from 10,000 sample combinations generated with the probabilistic assessment of flood risk.....	151
Figure 6.22 Expected annual damage, risk and exposure estimates, along with confidence bounds for the Solent, UK, considering a minimum flood depth of 0.3m required to produce damage.....	152
Figure 7.1 Sea level rise projections for Portsmouth. Data from the UK Climate Projections (UKCP18).....	164
Figure 7.2 Present-day (2020) and future (2100) extreme water level distribution for a 1 in 100-year return period under different sea-level rise scenarios. ....	165
Figure 7.3 Map of policy units covered in the North Solent Shoreline Management Plan and the Isle of Wight Shoreline Management Plan. Note that colours are only used to differentiate the location of all segments of coast covered by each policy unit. ....	167
Figure 7.4 Present management strategies for the flood defences at the Solent. Information collected from the North Solent Shoreline Management Plan and the Isle of Wight Shoreline Management Plan .....	169
Figure 7.5 IIASA future population projections for England. SSP1 – Sustainable path, SSP2 – middle of the road, and SSP3 – high population growth. ....	172
Figure 7.6 Future population growth for the Solent and difference from the present population distribution for the different IIASA population growth scenarios. ....	173
Figure 7.7 Future exposure to extreme water levels under a business as usual scenario, based on the minimum depth of flood required to produce damage.....	177
Figure 7.8 Map of future exposure to a 1 in 100-year event for the main built-up areas of the Solent under a "business as usual" scenario, considering a minimum flood depth of 0.3m .....	179
Figure 7.9 Future exposure to all return periods for the main built-up areas of the Solent under a business as usual scenario, considering a minimum flood depth of 0.3m....	180



Figure 7.10 Expected annual damage projections for the Solent, considering a minimum depth of flood of 0.3m .....	181
Figure 7.11 Future expected annual damage for four main storylines of SPRC factor configuration .....	182
Figure 7.12 Future expected annual damage for the four main storylines and three additional scenarios relating sea level rise to population growth.....	182
Figure 7.13 Future expected annual damage (EAD – people/year) for main built-up areas at risk at the Solent under four main storylines.....	184
Figure 7.14 Map of future expected annual damage (people/year) at the main built-up areas of the Solent under a business as usual storyline.....	185
Figure 7.15 Future uncertainty in the level of exposure of the Solent to different return periods. ....	186
Figure 7.16 Uncertainty in future exposure to a 1 in 100-year event based on the evolution of the SPRC input factors. Subplot a) shows the estimates when all components vary. For subplots b to d, the components which are not analysed are kept to their business as usual value. ....	188
Figure 7.17 Standard deviation caused by the individual SPRC components on the exposure to different future extreme water levels. Each column presents the uncertainty generated by one component while the remainder are kept to their business as usual value. ....	189
Figure 7.18 Standard deviation on exposure to future extreme water levels caused by the variance of two SPRC components. The remainder variable is kept to its business as usual value .....	191
Figure 7.19 Uncertainty in future projections of expected annual damage caused by variations on the SPRC components.....	192
Figure 7.20 Evolution of expected annual damage based on changes in the SPRC components. The potential individual and combined effect of component evolution on EAD is projected using the different SPRC scenarios at each timestep. ....	194

## Table of Figures

Figure 7.21 Standard deviation of EAD results obtained by maintaining one component constant at its business as usual value (RCP 4.5 for sea-level rise and defence height increments, SSP2 for population growth) while the rest are varied.....	195
Figure 8.1 Evolution of coastal flood risk at the Solent, UK, over the 20 <sup>th</sup> and 21 <sup>st</sup> century as estimated in the present study. ....	207
Figure 9.1 Recorded and modelled water curve for the 10 March 2008 flood event.....	222
Figure 9.2 Modelled flood outline of the March 10, 2008 event, and the locations reported as flooded by Wadey (2013).....	224

## Research Thesis: Declaration of Authorship

Print name: Jose Alejandro Pinto Rascon

Title of thesis: Uncertainty and sensitivity of coastal flood risk estimates across the Solent, UK from 1920 to 2100

I declare that this thesis and the work presented in it are my own and has been generated by me as the result of my own original research.

I confirm that:

1. This work was done wholly or mainly while in candidature for a research degree at this University;
2. Where any part of this thesis has previously been submitted for a degree or any other qualification at this University or any other institution, this has been clearly stated;
3. Where I have consulted the published work of others, this is always clearly attributed;
4. Where I have quoted from the work of others, the source is always given. With the exception of such quotations, this thesis is entirely my own work;
5. I have acknowledged all main sources of help;
6. Where the thesis is based on work done by myself jointly with others, I have made clear exactly what was done by others and what I have contributed myself;
7. None of this work has been published before submission.

Signature: ..... Date:.....



## Acknowledgements

First and foremost, I would like to thank my supervisors, your constant support, advice, guidance, encouragement and understanding helped me achieve something that seemed unattainable at times. You challenged my thoughts and ideas throughout this process, making me more critical of my own work and leading me to develop a stronger thesis.

The last years have been exciting and challenging and I am very lucky to have shared this time with many valuable people. In particular, I want to thank my pals Amy, Ali, Sien, Salma, Esmé, María, Lauren and Kat. Thank you for making this experience enjoyable, for all the good times we shared, the laughs, the long chats, and particularly for being there for me when I needed it the most. This list is by no means complete, and I apologize to anyone not explicitly mentioned.

I want to thank my family for their constant support. I would not have made it this far without your love and constant encouragement. Papá, gracias por tu apoyo. Chepina, gracias por tu cariño y por siempre motivarme a seguir superandome. Tom and Vero, thank you for always having my back and being my family on this side of the world. William and Mattie, best cousins one could ask for, love you guys.

Valentina, my closest companion during these challenging times. Thanks for showing me how much love I can give and how this can be unconditionally reciprocated.

The greatest thanks go to my mum. Muchas gracias por siempre estar conmigo y apoyarme para cumplir todos mis sueños, sin importar que tan locos o difíciles sean. Todo esto es por ti. Te amo ma!

Last but not least I want to thank myself for not giving up, even when it all got too much. For putting in the work and getting myself this far. Who would have thought, eh?

*“Considered a fool ‘cause I dropped out of high school”*

The Notorious B.I.G., *Juicy*, 1994



## Definitions and Abbreviations

1D .....	One dimension
2D .....	Two dimensions
AR5 .....	IPCC Fifth Assessment Report
ARIO .....	Adaptive Regional Input-Output
BODC .....	British Oceanographic Data Centre
BUA .....	Built-up Area
CAM.....	Condition Asset Manual
CCO.....	Channel Coastal Observatory
CFR .....	Coastal Flood Risk
cm.....	centimeters
DEM.....	Digital Elevation Model
DPSIR.....	Driving forces, Pressures, States, Impacts and Responses
DSM.....	Digital Surface Model
DTM.....	Digital Terrain Model
EA .....	Environment Agency
EAD.....	Expected Annual Damage
ED .....	Enumeration District
EWL .....	Extreme Water Level
FRA .....	Flood Risk Assessment
GBP.....	Pound sterling (£)
GDP .....	Gross Domestic Product
GDPppp .....	Gross Domestic Product based on purchasing power parity
GEV.....	Generalised Extreme Value distribution
GIS .....	Geographic Information System
GPD .....	Generalized Pareto Distribution
GTSR.....	Global Tide and Surge Reanalysis

## Definitions and Abbreviations

HBC .....	Havant Borough Council
HTL .....	Hold the Line
IIASA.....	International Institute for Applied Systems Analysis
IPCC.....	Intergovernmental Panel on Climate Change
km .....	Kilometre
LA .....	Local Authority
LECZ .....	Low Elevation Coastal Zone
LIDAR .....	Light Detection and Ranging
IOWSMP.....	Isle of Wight Shoreline Management Plan
m.....	meters
MAFF.....	Ministry of Agriculture, Fisheries and Food
mBar .....	Milibar
MHWS.....	Mean High Water Springs
MLWS.....	Mean Low Water Springs
MSL .....	Mean Sea Level
MR.....	Managed Realignment
NAFRA .....	National Flood Risk Assessment
NAI .....	No Active Intervention
NFCDD.....	National Flood and Coastal Defence Database
NFDC .....	New Forest District Council
NMD.....	No minimum depth
NOAA .....	National Oceanic and Atmospheric Administration
NPFA .....	No Public Funding Available
NSSMP .....	North Solent Shoreline Management Plan
NTGN .....	National Tide Gauge Network
OA .....	Output Area
ONS .....	Office for National Statistics
OS.....	Ordnance Survey



PDZ .....	Policy Development Zones
PPWC.....	Population Weighted Centroid
RCP .....	Representative Concentration Pathway
RD .....	Rural District
RMS .....	Risk Management Solutions
RMSE .....	Root Mean Square Error
RP .....	Return Period
SACs.....	Special Area of Conservation
SLR.....	Sea Level Rise
SMP .....	Shoreline Management Plan
SoP .....	Standard of Protection
SPAs.....	Special Protection Areas
SPRC .....	Source-Pathway-Receptor-Consequence
SRTM .....	Shuttle Radar Topography Mission
SSP.....	Shared Socioeconomic Pathways
STD .....	Standard Deviation
UD .....	Urban District
UHSLC.....	University of Hawaii Sea Level Center
UKCP09.....	UK Climate Projections 2009
UKCP18.....	UK Climate Projections 2018



# Chapter 1 Introduction

## 1.1 Motivation

Many coastal areas around the world are densely populated and have been significantly developed, especially over the last century. Over one-tenth of the world's population currently lives in the low elevation coastal zone (LECZ), defined as the land below 10m above sea level (Lichter et al., 2010). These populations are exposed to coastal flooding from extreme water levels (EWL) today (McGranahan et al., 2007). Coastal flooding presents a severe challenge worldwide. Significant coastal flood events have occurred over the last decades, including Hurricane Katrina in New Orleans in 2005, Cyclone Nargis in Myanmar in 2008, Cyclone Xynthia in France in 2010, and Hurricane Sandy in New York 2012. These events have caused considerable economic losses and are responsible for more than 140,000 deaths (Abramson and Redlener, 2012, Fritz et al., 2009, Lagmay et al., 2015, Vinet et al., 2011). More recently, Hurricane Harvey and Irma impacted Texas and Florida, respectively, in 2017 with combined damages of approximately US\$185 billion (NOAA, 2018). Recent events show some of the most substantial economic consequences when analysing the National Oceanic and Atmospheric Administration (NOAA) data for the costliest U.S tropical cyclones (NOAA, 2018). However, there is a visible decrease in fatalities (Haigh et al., 2020). This can be associated with better preparation, such as earlier flood warnings. However, coastal management through the implementation of hard defences, such as seawalls or dykes, and soft engineering approaches like beach nourishment play a significant role in flood protection. In the future, coastal areas are likely to face more regular and devastating extreme water events as a result of mean sea-level rise and climate change, subsidence and continued development (Hallegatte et al., 2013, IPCC, 2019).

In the UK, coastal flooding is widely recognised as the second leading concern for civil emergency, only outweighed by pandemic influenza, with potential consequences including fatalities, impact on mental health, damage to property, interruption of essential goods and services, and environmental damage (Cabinet Office, 2015). The UK has long experienced the effect of extreme sea levels, with historical data suggesting large populations have been affected by extreme events in the past. For example, in 1607, a large flood around the Bristol Channel caused the death of around 2,000 people and severe damage (Horsburgh and Horritt, 2006). To date, it is the natural hazard event that has caused the greatest loss of life in the UK (Haigh et al., 2020). In England and Wales, approximately £100 billion worth of assets are threatened by coastal flooding (Hall et al., 2006). About 1 in 6 properties and significant infrastructure are at risk of flooding from river and coastal sources, with average annual flood damage estimated to exceed £1 (DEFRA, 2014).

## Chapter 1

Altogether, coastal flooding has caused more than 2,000 casualties in the UK over the last 500 years. The south of England has been particularly prone to experience these events. The prolonged storm of 31 January and 1 February 1953 killed 307 people, and 24,000 fled their homes, with the largest consequences seen at the east coast (Baxter, 2005). More recently, severe flooding affected several cities in this area during the 2013/14 winter storms, with water levels higher than those experienced during the 1953 flood were registered at several sites (Wadey et al., 2015b, Haigh and Nicholls, 2017), causing property and infrastructure damage. Initial damages are estimated at £290 million (Penning-Rowsell, 2015, Thorne, 2014), with collective damages worth over £2.5 billion (Haigh and Nicholls, 2017).

Coastal flood risk is expected to increase as a consequence of climate change and population growth. The latest Intergovernmental Panel on Climate Change (IPCC) assessment (IPCC, 2021) estimates that the global mean sea level is likely to rise by at least 0.33m under a low carbon emissions scenario by 2100. Under a worst-case scenario, the sea level can be expected to rise by up to 0.98m by the year 2100, relative to its 1986-2005 level, with around 70% of the world coastlines experiencing sea-level change (Fox-Kemper et al., 2021). In the south of England, the rise in relative mean sea level (MSL) has increased the likelihood of extreme sea levels over the last decades, with significant widespread coastal flooding in recent years (Haigh et al., 2020). The south of England is expected to experience substantial increments in mean sea level, based on the latest sea-level rise projections by the UKCP18 (Palmer et al., 2018). Under a low emissions scenario, the sea level in this area is projected to rise between 0.29m and 0.7m by 2100. These estimates reach 0.53m and 1.15 m for the same year under the highest-emissions scenario (Palmer et al., 2018).

Based on the above, the UK Government has identified the need to continuously upgrade and invest in new coastal defence infrastructure (Cabinet Office, 2020). Therefore, it is necessary to determine the areas that require protection and the measures needed to maintain or decrease the threat level. This is usually done through a flood risk assessment (FRA), where the extent of the floodplain is estimated and the resulting consequences calculated. However, analysing the flood maps by the Environment Agency, it can be seen that these are obtained using a worst-case scenario, where the presence of flood defences is omitted. Furthermore, it has been argued that the government's estimates of risk overpredict the possible direct consequences of floods by a factor of four, as it utilises financial instead of economic damage to estimate the consequences of flooding. The problem is that the former refers to the cost of replacing assets, which involves "betterment". In contrast, on the latter, the remaining economic life of an asset is considered to estimate its actual value (Penning-Rowsell, 2015). In addition, it has been shown that even

government reports differ on the levels of coastal flood risk for the country, depending on the data and assumptions made for the analyses (Penning-Rowsell, 2015).

One of the most commonly used tools for FRA is the Source-Pathway-Receptor-Consequence (SPRC) framework (Evans, 2004, Narayan et al., 2012) (Figure 1.1), which allows clear identification of all the components of the coastal flood risk system. Several studies have used this conceptual framework at local, regional and global scales (e.g. Nicholls et al., 2008, Hanson et al., 2010, Narayan et al., 2014, Cui et al., 2015). This conceptual model can be particularly beneficial for assessing uncertainties on each of its components and their effect on the overall flood risk estimates. However, to date, research analysing the individual and joint influence of all the SPRC components on past, present and future levels of risk is missing. Furthermore, there is no available research estimating the variabilities on the estimates of risk produced by the uncertainties on the SPRC components.

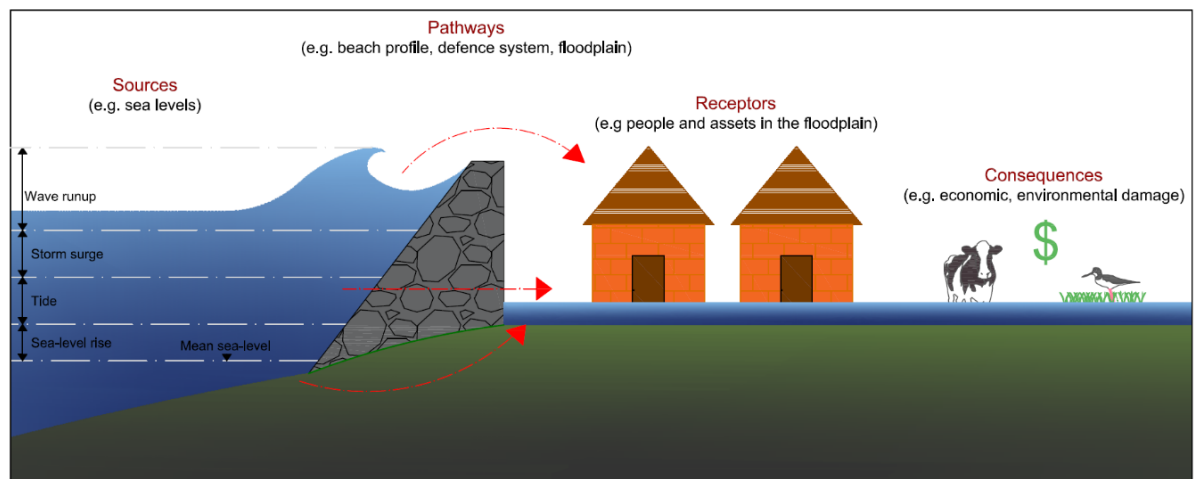


Figure 1.1 Source-Pathway-Receptor-Consequence coastal flood system model.

## 1.2 Aim and objectives

Based on the above, the overarching aim of this PhD study is to quantify the influence that each component of the Source-Pathway-Receptor-Consequence conceptual framework has on past, present and future coastal flood risk levels using the Solent, UK, as a case study. To achieve this aim, the following three objectives are defined as follows:

1. To assess how coastal flood risk has evolved at the Solent, UK over the period between 1920 and 2000.
2. To quantify the largest sources of uncertainty in coastal flood risk at present.

3. To determine how flood risk may evolve over the remainder of the 21<sup>st</sup> century with future sea-level rise and population change, considering future coastal management strategies.

This thesis uses the Solent, in the south of England, as a case study site to explore these objectives. This area is home to a wide variety of coastal environments across its length, from natural designated areas to highly urbanised cities. This creates the opportunity to transfer the knowledge acquired to other areas in the UK and more widely. Furthermore, the richness of data and previous assessments for this region allows for a better understanding of the coastal processes, ultimately leading to more accurate assessments.

Objective one seeks to produce an assessment of the historical levels of coastal flood risk at the Solent since 1920 and until 2000 by individually and jointly analysing all of the SPRC components. This objective seeks to answer the question: *What were the main driving factors of coastal flood risk at the Solent from 1920 to 2000?*. This is done using an inundation model to simulate the effect of combining the SPRC components for the last 100 years and investigating how risk evolves.

The second objective builds on the methods and outputs of objective one and analyses the present-day levels and uncertainties of coastal flood risk for the Solent. This is done by exploring the inherited uncertainties of the input parameters of the inundation and population distribution models and their effect on the variability of coastal flood risk estimates. These uncertainties can be the product of aleatory (e.g. the height of extreme water levels ) and epistemic uncertainties (e.g. the height of coastal defences). The outcomes of objective two will aid in answering the research question: *Which of the SPRC components generates the largest variability and uncertainty for present flood risk analysis?*. By answering this question, resources and efforts can be focused to improve the knowledge and understanding of the risk drivers, ultimately improving coastal flood risk estimates.

The influence of future climate change, socio-economic evolution and coastal management strategies on the future levels of coastal flood risk at the Solent are analysed in objective 3. The overall evolution of the threat levels is assessed by exploring future paths projected for each of the SPRC components. The evolution of the SPRC determines the factors that will have the most significant contribution and the most considerable uncertainties for the future levels of coastal flood risk. The outcomes of objective three will aid in answering the research question: *Which of the uncertain inputs will be the primary driver of coastal flood risk and which generates the most significant uncertainties in the future for the Solent?*

Finally, the results of the three objectives will be integrated to understand the evolution of coastal flood risk at the Solent. Ultimately, the outcomes of this research aim to understand the evolution of feedback mechanisms between natural and socio-economic stressors on the evolution of coastal flood risk. This could help guide future researchers, coastal managers and policymakers by answering the research question: *Is the focus of the current strategies for coastal flood risk management for England and particularly for the Solent given to the relevant SPRC component, and if not, how should these evolve to maintain or decrease coastal flood risk?*. Additionally, this analysis is intended to benefit future assessments of areas that might follow a similar path of evolution to that seen at the Solent.

### 1.3 Thesis structure

This thesis is organised into nine chapters, as follows:

Chapter 2 presents a literature review of the key concepts of coastal flooding, the most relevant studies, their key findings and their utility for the assessment. This chapter starts by introducing the source-pathway-receptor-consequence framework. It follows by expanding on each of these components, their temporal evolution and introducing the relevant knowledge gaps.

Chapter 3 introduces the study area, the Solent on the central south coast of England. It presents the challenges posed by the complexity of the water conditions in the area. An overview of the natural and urban environments found in the area is followed by a brief description of previous studies analysing the SPRC components in the region.

Chapter 4 presents the general data and methods. The present work is based on the development of an inundation and a population distribution model of the Solent. These are used to determine the extent of the floodplain and the number of people living in the area. Both models are built with the possibility to be adequated based on the focus and data availability of each objective.

Chapter 5 presents and analyses the results for the historical evolution of coastal flooding in the study area. The changes in the SPRC components from 1920 to 2000 are presented and used as an input to simulate coastal flood events and their consequences. The individual and combined effect of the SPRC evolution is exposed through the use of scenarios.

The present levels of coastal flood risk and its uncertainties are presented in Chapter 6. This addresses objective two, which seeks to generate accurate estimates of present coastal flood risk and identifies the largest sources of uncertainty.

## Chapter 1

Chapter 7 analyses objective three by exploring the future levels of flood risk in the area and ties them to the projected evolution of climate change, population growth and coastal management strategies.

A synthesis of the evolution of coastal flood risk through the 20<sup>th</sup> century and the projected levels of threat for the 21<sup>st</sup> century are presented in Chapter 8. This is done by summarizing the work and results of each objective, followed by a discussion of the implications of the main findings and their limitations and the recommendations for future work.

Lastly, Chapter 9 provides the key conclusions drawn from each objective and the impacts these have on present and future coastal flood risk management



## Chapter 2 Literature Review

### 2.1 Introduction

Extreme sea levels are one of the greatest challenges coastal managers face as many variables influence the levels of coastal flood risk (CFR). Protecting against every possible extreme water event is nearly impossible, both technically and financially. It is for this reason that methodologies have been developed to analyse a range of possible scenarios that could lead to coastal flooding. FRA has benefitted from the use of conceptual models that help identify the individual characteristics and variability of each of the components that affect the levels of risk. One of the most commonly used is the Source-Pathway-Receptor-Consequence (SPRC) conceptual framework. This chapter starts by defining coastal flood risk. It then presents the SPRC framework, the individual components of the system, as well as their temporal evolution. Section 2.2 gives a general background on coastal flood risk and exposure. Section 2.3 presents the use of the SPRC framework for coastal flood risk assessments. The individual components, Sources (section 2.3.1), Pathways (section 2.3.2), Receptors (section 2.3.3) and Consequences (section 2.3.4), are described in more depth by providing their definition in a coastal context, followed by a detailed explanation of the factors driving their evolution, and a summary of the most relevant studies analysing them. Section 2.5 presents some of the available methodologies for coastal flood risk assessment. The uncertainties found when conducting risk assessments are described in section 2.6, as well as some of the methodologies to quantify them. Lastly, section 2.7 provides a summary of the main knowledge gaps identified in the literature review.

### 2.2 Coastal flood risk and exposure

Risk is defined as a situation that involves exposure to danger and is often described in terms of a combination of probability and consequences. In a coastal framework, this refers to the probability that an event of a certain magnitude occurs which will inundate normally dry land, and the corresponding consequences, which is defined differently depending on the assessment (e.g. the number of affected people, value of assets, damage to the environments or area that can be affected by the flood) (Gouldby et al., 2005). It is clear that if the likelihood of a flood is high (low) and the possible consequences are high (low), the coastal flood risk can be considered as high (low). However, there are other possible combinations, such as low probabilities with high consequences and vice versa. As mentioned, protecting against all combinations can prove challenging. It is then necessary for coastal managers to decide the kind of risk that they are

willing to accept given the probabilities and consequences. The former is given by the magnitude of the extreme water events (Sources) as well as the possible mechanisms through which the water enters the floodplain (Pathways). The latter refers to the presence of people, assets or environments that can be affected by water intrusion (Receptors and Consequences). It is important to differentiate between the concept of risk and exposure to coastal flooding, as flood assessments can be produced with both indicators. This thesis defines exposure as the number of receptors threatened to coastal flooding from extreme coastal water events, considering the presence of flood defences. Exposure is generally reported as the number of people, assets, infrastructure, etc., that are under threat to a specific coastal event. For example, it has been estimated that 23,000 properties are exposed to a 1 in 200-year extreme water level in the Solent region under present conditions (Wadey et al., 2012). Coastal flood risk, on the other hand, is the probability of the receptors experiencing losses. It involves the use of the exposure and the likelihood of occurrence of a group or individual extreme water events. This is generally reported as an Expected Annual Damage (EAD), which considers the probability of a series of extreme water levels to cause flooding, and is obtained by integrating the damage over the probability.

### **2.3 The Source-Pathway-Receptor-Consequence (SPRC) conceptual framework**

Whether a location is flood-risk-prone depends on: a) the likelihood of an extreme water event and b) the presence of vulnerable items (Kron, 2013). A flooding system encompasses those physical and organisational systems that influence or are influenced by flooding (Hall et al., 2003, Evans, 2004). This includes the earth mechanisms that lead to flooding, such as storms; coastal infrastructure; economic, social and environmental assets in the floodplain; stakeholder groups with interest in the impacts of flooding; and the insurers who provide cover for flood risks (Evans, 2004).

Risk assessments often use conceptual frameworks, as these have proved to be useful for identifying the driving forces, pressures, states, impacts and responses (DPSIR). Based on the DPSIR model, several methodologies have been developed and adapted to the specifics of the research topics. In the natural environment, Holdgate (1979) introduced the concept of the SPRC to describe the impact a pollutant (source) would have on a potential receptor based on the conducting pathway. This framework was later adopted in the coastal system by the Foresight Future Flooding project (Evans, 2004). Ever since, it has been utilised by numerous studies (e.g. Kebede and Nicholls, 2011, Narayan et al., 2012, Wadey et al., 2012, Stevens et al., 2015) due to its simplicity to identify the components and feedback mechanisms between the floodplain

system and the external forcing (Narayan et al., 2014). In the coastal environment, sources are water levels capable of producing floods. Pathways are the mechanisms or the routes for the source to reach the receptors. Receptors are the people, infrastructure, natural and built environment affected, which are finally translated into consequences, an indicator of the impact of flooding on the receptors.

Coastal flood risk analyses tend to focus on either the individual components of the SPRC or in the interaction of some but not all of them and their role in the overall risk estimates. Few studies have attempted to incorporate all these factors for flood risk analysis, and those who have often do it on a global scale (e.g. Hoozemans et al., 1993, Nicholls et al., 1999, Nicholls et al., 2008, Hinkel et al., 2014). There is, however, a lack of detail on these derived from the nature of their scale. Regional studies overcome this limitation and incur another one, by focusing on individual or some of the SPRC components. For example, in the Solent region, Quinn et al. (2012) modelled the tide-surge interactions while Ozsoy et al. (2016) analysed the sources with the study of high-frequency sea-level variations and their implications on flood risk. Pathways are reviewed by Wadey et al. (2012) through the analysis of coastal defence systems, whereas Stevens et al. (2015) utilise historical Ordnance Survey (OS) maps to determine the evolution of the receptors. Finally, Ruocco et al. (2011) analysed the consequences by reviewing recorded data of flood occurrence from newspaper sources while comparing these to the occurrence of extreme water levels.

### **2.3.1 Sources of coastal flood risk**

#### **2.3.1.1 Definition**

Sources are the origin of a hazard (Kron, 2013). In the context of this thesis, sources are EWL usually linked to weather events. Extreme sea levels are comprised by the sum of mean sea level, astronomical tide, a non-tidal residual and waves (Figure 2.1). Although these occur at different temporal scales and have distinct variabilities, the most extreme effects are experienced when the occurrence of two or more of the individual sea-level components coincide.

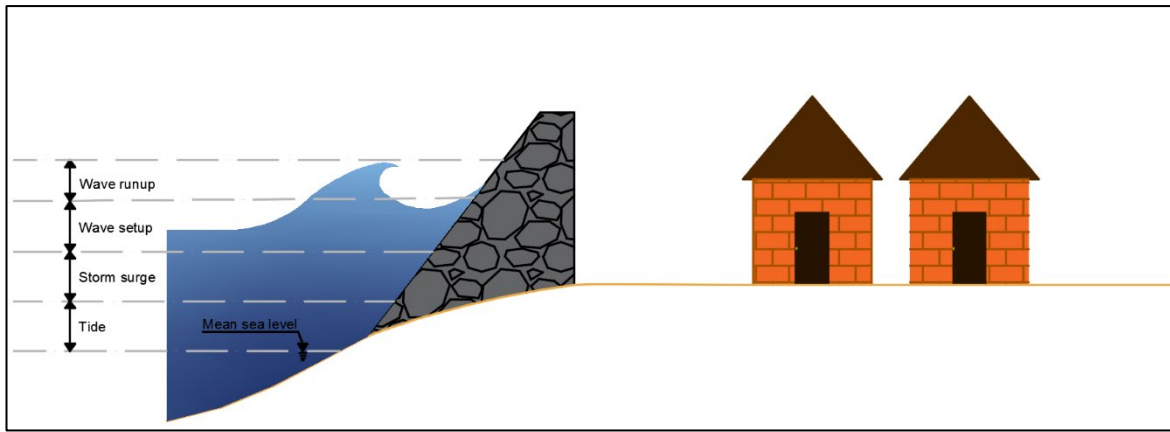


Figure 2.1 Sources of coastal flood risk

### 2.3.1.2 Temporal evolution of the sources

As mentioned, EWL are comprised by the sum of mean sea level, astronomical tide, a non-tidal residual and waves. When assessing MSL, it is essential to understand the difference between eustatic and isostatic factors. The former refers to global factors affecting ocean and basin volume, whereas the latter indicates local factors controlling the Earth's crustal movements. The volume of land ice (glacio-eustasy) is within the primary drivers of changes in the volume of ocean water. This is a function of insolation from the sun on the Earth's surface and varies with the Milankovitch periodicities of Earth's orbit. It works at intervals of tens of thousands to hundreds of thousand years (Emery and Aubrey, 1991) through changes in mean ocean temperature, leading to changes in water density and volume, ultimately affecting sea levels. Changes in the volume of ocean basins can be considered slow –many millions of years- and are a product of the tectonic activity, mainly through the creation of oceanic trenches. In terms of local scale, four isostatic drivers are identified: glacio-isostasy (ice-loading); Hydro-isostasy (water loading); sediment-controlled isostasy (sediment-loading); and Tectonic processes such as local crustal uplift and subsidence, which can be near-instantaneous, i.e. during an earthquake. Isostatic changes in mean sea level are driven by many factors such as atmospheric pressure, winds, ocean currents, levels of land ice and density of seawater, with each of these occurring at different spatial and temporal scales.

The astronomical tide component of sea level is driven by the gravitational attraction and rotation of the Moon-Earth-Sun system (Pugh, 1987). Tide arise as the Sun and Moon generate gravitational forces which attract the Earth and its fluid layer. When the Sun and Moon act together in opposite directions, spring tides (highest) are generated, whereas neap (lowest) tides occur when these act at right angles. The occurrence of spring and neap tides is driven by the lunar month (29.5 days), although the lunar perigee cycle of 8.85 years and the nodal cycle of 18.61-year cause variations in high tide occurrence (Pugh, 1987, Woodworth et al., 2005). Despite

these variabilities, tidal predictions are available for most places around the world. Tides can be classified according to their range (the difference between the lowest and highest tide). These can be microtidal (range <2m); mesotidal (2-4m range); macrotidal (4-6m range); and hypertidal (range >6m). Tides can also be classified based on the mix of periods that are evident. These can be diurnal (24-hour tidal period, one high, one low tide per day); semi-diurnal (12-hour tidal period, two high, two low tides per day); or mixed (a mixture of diurnal and semi-diurnal).

The non-tidal component has the highest variability and acts on the smaller temporal scale. Non-tidal residuals are mainly the product of meteorological contribution and are referred to as storm surges caused by changes in local atmospheric pressure and associated wind stress. In general, a decrease (increase) of 1mbar in atmospheric pressure will increase (decrease) mean sea level by 0.01m. The meteorological forces caused by changes in atmospheric pressure and wind are felt at all depths of the water column; however, these are highly unpredictable, and their influence on sea level is limited to localised areas (Pugh, 1987).

Waves significantly contribute to higher EWL (Figure 2.2). These can be generated by wind, coastal and underwater landslides, and earthquakes. There are various classifications for ocean waves based on their scale and driving factors (e.g. seiches, surface-gravity waves, tsunamis, etc.) (Holthuijsen, 2010). However, the focus is traditionally given to wind-generated waves as there are tools to predict them based on the physical characteristics of the study area, such as fetch length (area of the ocean over which the wind blows) and nearshore depth.

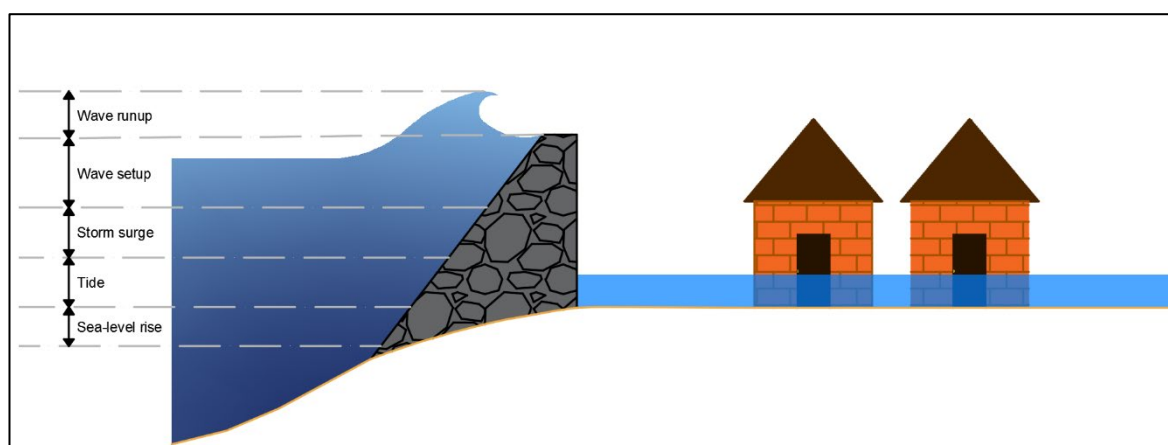


Figure 2.2 Evolution of the sources of coastal flood risk

### 2.3.1.3 Previous research analysing the sources of flood risk

Sources are the most commonly analysed components of the SPRC system. Research tends to rely on the use of local observation of sea levels together with statistical approaches to obtain return levels for periods longer than the observations. Wemelsfelder (1939) was the first person to

introduce extreme value analysis to estimate the probabilities of high coastal waters using ranking sea-level records. Although simple, this approach initiated the use of statistical analysis in coastal systems and further research on the matter. Ever since, several studies have followed a similar approach, with global studies benefitting from statistical analyses of local data to estimate the recurrence probability of EWL.

Long records of tide gauge data are available from various sources. On a global scale, the University of Hawaii Sea Level Centre (UHSLC) holds hourly records of tide gauge data, although some contain significant gaps in the data. In the UK, the British Oceanographic Data Centre (BODC) collects data from 46 quality-controlled gauges, with their longest record dating as back as 1915 at the Newlyn tide gauge. In recent years, there has been an increase in the use of hydrodynamic models of storm surge and waves to simulate water level data in areas where point data is not available. Muis et al. (2016) performed a global reanalysis of storm surges and extreme sea levels. This study developed a hydrodynamic model at a global scale, the Global Tide and Surge Reanalysis (GTSR), the results of which were compared with extreme water levels obtained by fitting a Gumbel distribution to the annual maxima of observed sea levels by the UHSLC. Their results show good agreement with the point data, with an average root mean square error of less than 0.2m for over 95% of the 144 validation sites. The slight differences between modelled and measured data are mainly seen in areas affected by tropical cyclones, most likely caused by the underestimation of extremes derived from the low resolution of meteorological forcing available (Muis et al., 2016). The outputs of these models can then be parameterised with extreme value theory to estimate the height of EWL given a recurrence interval.

Arns et al. (2013) and Wahl et al. (2017) provide a summary of the methods available to estimate the probability of EWL. The different techniques are applied depending on the quality and length of the records. In a global analysis, Wahl et al. (2017) compared the uncertainties in sea level rise projections with the uncertainties in the EWL estimates derived from the selected data processing method. To do so, they compared the results from Muis et al. (2016) with the estimates obtained from fitting statistical distributions to the quasi-global tide gauge dataset GESLA-2. The statistical analysis included: a) Gumbel distribution fitted to a time-series of annual maxima, b) Generalised Extreme Value distribution (GEV) fitted to monthly maxima, and c) Generalized Pareto distribution (GPD) with different percentile threshold exceedances (i.e. the  $r$ -largest values). Wahl et al. (2017) results indicate uncertainties of over 1.5m in sea levels when the range of uncertainties in future sea-level rise projections by the IPCC Fifth Assessment Report (AR5) are combined with the uncertainties in extreme sea level estimates. Although it is argued that these may decrease once lengthier sea level data becomes available. Overall, Wahl et al. (2017) conclude that there is a

need to combine the uncertainties from both extreme value theory and sea-level projections to provide more robust guidance for impact and adaptation assessments.

All of the aforementioned methods consider the combined effects of tide and storm surge components for their analyses, though additional methods that treat them separately are available from the literature. These consider the skew surge, which is the difference between the predicted high tide and the highest tide level observed (Figure 2.3) (Batstone et al., 2013). Some authors suggest that methods considering the skew surge are more robust (Batstone et al., 2013, Williams et al., 2016), although their results have not been tested in enough locations to guarantee their performance (Wahl et al., 2017).

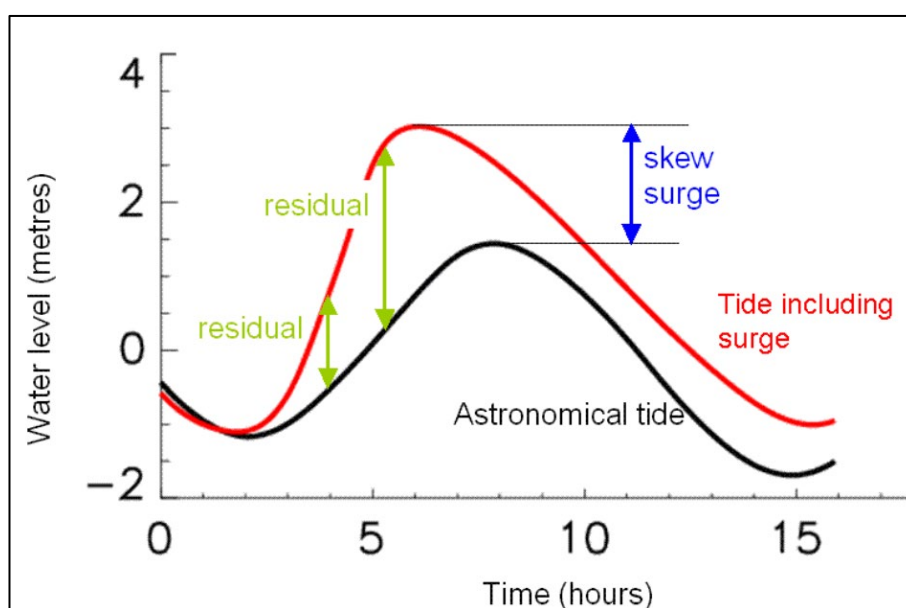


Figure 2.3 Illustration of the skew surge (McMillan et al., 2011).

In the UK, the Environment Agency (EA) provides a set of coastal boundary conditions derived from the analysis of 40 Class A tide gauge records added to 5 supplementary primary sites by the UK National Tide Gauge Network (NTGN). Their study considers the skew surge and uses the skew surge joint probability method as it removes all phase differences between predicted and observed data (McMillan et al., 2011) to provide a series of EWL heights and their associated return period (RP) around the UK coast. In addition to this, the fifteen largest skew surges for each site were identified to obtain standard surge shapes for each location.

Comparing the estimates for past and present high waters generated with the revised joint probability method, it can be seen that there is a notable decrease in the recurrence interval of extreme water heights. For instance, it was found that a surge with a 1 in a 100-yr recurrence interval in 1900 occurred once every 10 to 25 years in 2010. Analysing future estimates, which included the influence of three sea-level rise scenarios given by the UK Climate Impacts

Programme 2009 (UKCP09) assessment, Lowe et al. (2009) find that water levels will be exceeded more frequently by 2100. According to their findings for water heights with a 100-year return period and by the year 2100, a low emissions sea level rise scenario will increase the likelihood to one every ten years. This increase is further exacerbated by a high emissions sea-level rise (SLR) scenario 1800-folding the exceedance frequency from 1 in a 100-years to once every 20 days.

Haigh et al. (2016) followed the previously mentioned global approaches and built on McMillan et al. (2011) by analysing skew surge events around the coast for the period 1915-2014 using the same 40 NTGN gauges. The data was processed to separate astronomical tide from the non-tidal component. This is to identify the time of occurrence, the atmospheric pressure conditions, and the location of the surge. This allowed identifying the spatial footprint of skews according to the associated storm tracks. According to their results, when more than one storm event occurs within close succession, these rarely affect the same stretch of coastline. Furthermore, their findings suggest that the spring/neap tidal cycle prevents successive extreme sea levels from happening within 4-8 days. This has considerable implications for flood management as it is almost safe to assume that areas that have been impacted by high water levels have at least a couple of days to implement flood alleviation measures.

On a similar scale, Haigh et al. (2011) analysed changes in EWL at the English Channel through the twentieth century. To do so, the study collected tide gauge data from 16 sites around the Channel. One of the main limitations the study faced is the lack of long records, as datasets of about 35 years are needed to determine the changes in extreme levels. These 35 years cover two 18.6 lunar nodal cycles, which is required to identify changes in sea level caused by the declination of the moon relative to the plane of the sun (Pugh, 1987, Haigh et al., 2011). After extensive data archaeology, 173 years of new or corrected data were added to the dataset, providing longer records for six sites along the south coast of England. These measurements of sea level were split into mean sea level, astronomical tide predicted through harmonic analysis, and the surge components. The data were analysed using four statistical methods once eustatic and isostatic changes in mean sea level were removed. The statistical methods included the annual maxima, r-largest joint probability and revised joint probability, with the latter recommended for application where possible as it was found to perform best around the study region.



### 2.3.2 Pathways of coastal flood risk

#### 2.3.2.1 Definition

Pathways are the mechanisms that enable floodwater to reach places where it may cause an impact on the receptors (Evans, 2004). In this sense, coastal pathways include coastal processes and failure of sea defences, either natural or anthropogenic (Figure 2.3). Pathways are, in increasing order of severity: 1) overtopping, when wave run-up runs over a defence or stretch of land; 2) overflow caused by still water levels higher than the land level or defence crest; and 3) breaching and erosion of natural or artificial defences. Breaching and erosion are encompassed within the same level of severity as both processes can be classified as a complete defence failure with the potential to allow large volumes of floodwater to reach the receptors, leading to higher flood alleviation costs. For ease of convenience, coastal profiles and infrastructure at the coastline aimed to protect from flooding are hereafter referred to as defences.

Coastal defences have been part of human development around the coast, although some of the early work would not directly fall within what nowadays is called defences. Most of the initial work done in the coastal zone were aimed to modify areas into farmland (English Heritage, 2015, Welch et al., 2017). Early construction of defences in England dates back to before the Norman Conquest in 1066. Land reclamation during the 3<sup>rd</sup> century has been identified at the Severn estuary and parts of Somerset, England (English Heritage, 2015). In the Netherlands, records of this type of procedure are found as early as the 13<sup>th</sup> and 14<sup>th</sup> century with the reclamation of land from the sea and the use of mud-dams (Charlier et al., 2005). Even though defence structures have been present for such a long time, and that pathways are the mechanisms that allow the sources of flood risk to reach the receptors, these remain as one of the least analysed components of the SPRC.

Pathway occurrence is directly linked to the type of driver(s), which can be both natural and anthropogenic. However, identifying the individual or group of actions that triggered a pathway raises complexity to the analysis. In some cases, it is rather clear that, for example, long-period waves cause overtopping of a defence, yet small waves can have a similar effect when combined with raised still water levels. Furthermore, if a defence has experienced weathering of its elements, it is possible for it to fail even with loads far smaller than its design one (Buijs et al., 2007, Simm et al., 2008, Stanczak and Oumeraci, 2012).

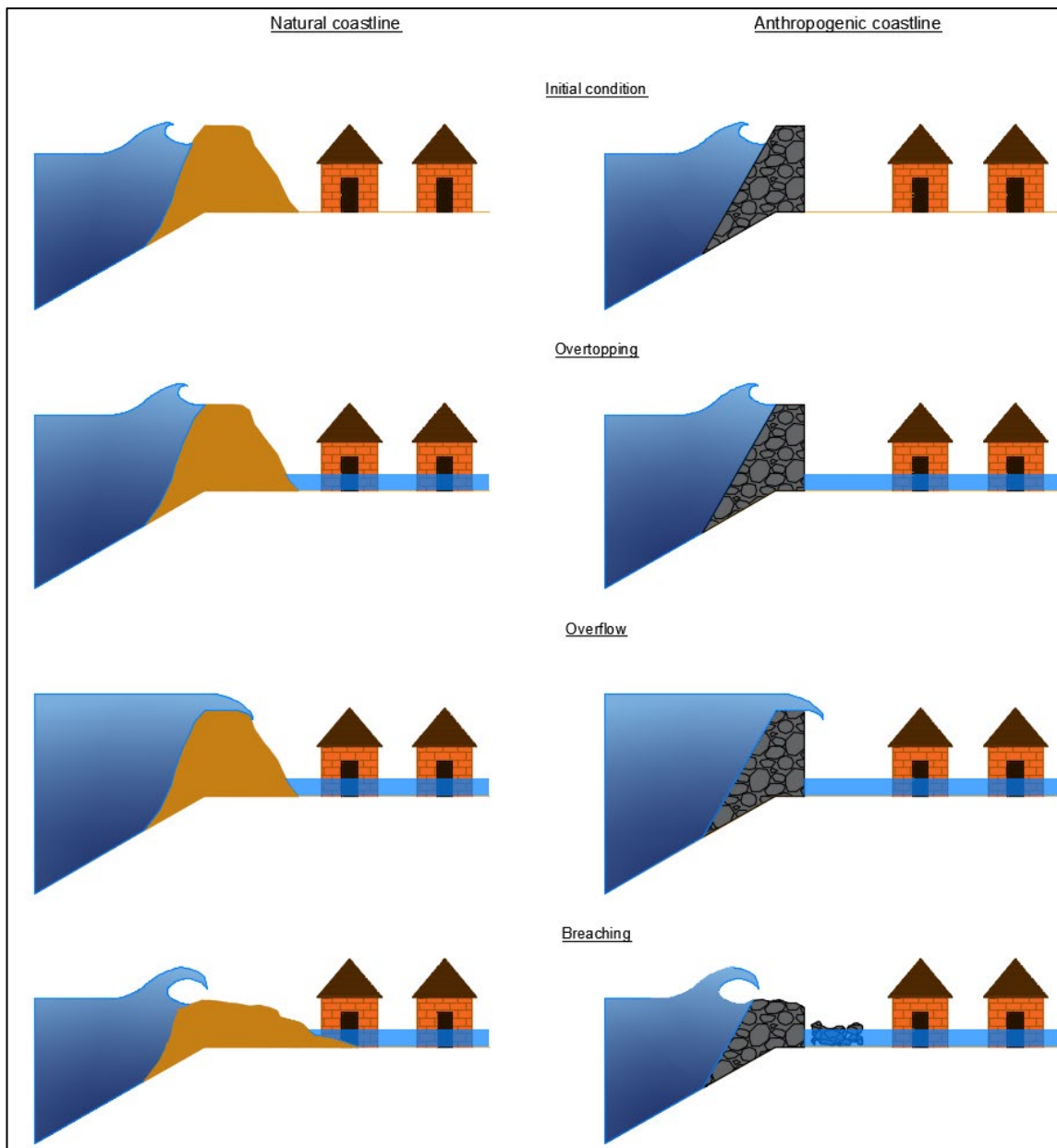


Figure 2.4 Pathways of coastal flood risk

Avoiding the occurrence of every defence failure pathway would require the design of a structure capable of resisting the action of every possible type of forcing. This would result in a design that would not be economically viable nor feasible for construction, let alone realistic. It is for this reason that engineers utilise the concept of limit-states of which there are two, the serviceability limit and ultimate states (Paik, 2018). The former refers to a condition where an element is capable of enduring every action that falls within a design load during its residual life. If for any reason the design load is matched or exceeded, the element will present minor damage, which in cases can be purely aesthetic, but the overall structural integrity would not be compromised. Examples of this would be deflection or cracking of elements. On the other hand, an ultimate state will occur when the actions over the element are so high that it loses its ability to withstand

the action that leads to this state or any following forcing, regardless of their magnitude. This means the element has reached a plastic state where deformations can no longer be recovered. In this sense, it is clear that an ultimate load will be higher in magnitude and/or duration than a serviceability one (Paik, 2018). The selection of these loads is obtained by analysing the forces an element could face throughout its residual life, including the construction period. In the coastal system, this usually relies on the use of probability combined with feasibility analysis. Even though a required standard of protection is arbitrarily set up in occasions, this is still supported by a probability analysis of the likelihood of extreme water levels. For example, the use of the hydrostatic or hydrodynamic pressure caused by the height of a wave or a surge with a recurrence interval of 200 years. The force generated by this event is then multiplied by a safety factor, and this is the load that will be used for the design (Sayers et al., 2002). These factors are obtained from local or national guidelines, and they vary according to the type of load and the defence properties.

The concept of fragility, defined as the probability of a structure to fail under a conditional load (Casciati and Faravelli, 1991), has been applied in the coastal system with the use of fragility curves. However, defining the design loads that could cause failure has and continues to be a challenge for coastal managers. In the case of overflow and some types of breaching, the approach can be rather dull in the sense that it only considers whether the height of extreme water levels is above the defence crest or by analysing the hydrostatic pressure applied to the element. Complexity arises in the case of overtopping and breaching caused by wave pressure. Minikin (1963) describes the early approaches of defence design, which up to the beginning of the last century was done by rule of thumb. Some of these include, for example, the requirement of a vertical breakwater breadth to be slightly less than the full height. It was not until Thomas Stevenson did full-scale experiments at Dunbar, Scotland, that the first records of wave pressure on a vertical wall were obtained (Quinn, 1972).

These experiments relied on the use of a dynamometer to measure pressure against a vertical seawall. Being the early stages of research, there was no systematic analysis, and many assumptions were formulated as to the cross-section of the wall along with other of its properties. Defence failure due to uneducated designs continued to be a constant problem. After the destruction of a breakwater at the east of Genoa, Italy, Professor Luigi Luigi carried out similar experiments to Stevenson (Minikin, 1963). He utilised wave pressure dynamometers but used conical heaps of quarry of different sizes distributed along and across the old breakwater aimed to be moved by wave impact pressure. With this data, he produced one of the first diagrams to represent wave pressure distribution against a vertical wall, which he claimed could be used to calculate any wave height by proportioning the ordinates uniformly. This diagram was greatly

utilised in the design of structures around the world, even though it was utterly empirical (Minikin, 1963). Ever since, research has been conducted trying to develop more robust approaches to defence design, such as the experiments carried out by MM Rouville and Petry in 1935 at Dieppe France with inconclusive results, and the work with a model tank by Major Bagnold and supervised by Professor C.M. White on behalf of the Institution of Civil Engineers (Minikin, 1963).

The development of more sophisticated techniques, such as the work done by Stanczak and Oumeraci (2012), and tools for the analysis of sea levels led to more robust approaches for the design of defences, although most of these calculations still use regression models fitted to hydraulic model tests. Since wave overtopping is unevenly distributed from wave to wave, the design of structures is usually based on average overtopping discharge. Many attribute the first formulae to do so to Owen (1980), who provided a way to predict discharge based on the physical properties of the sea-wall, such as slope and roughness, and empirical coefficients obtained from the analysis of sloping and bermed seawalls (Besley, 1998). These, along with other equations and methods to estimate overtopping, have been produced with the common factor of all being based on empirical analyses of defence performance (see Besley, 1998, Andersen and Burcharth, 2004, Van der Meer, 2017 for an overview).

Finding information on pathway occurrence in a broader perspective (i.e. as a system rather than the analysis of single elements) is not a straightforward process. It is hard to predict where and how each pathway will present and the evolution of the failure mechanism. For example, if a defence starts to present small cracks caused by wave impact, the pressures from any following loads are likely to concentrate on the sidewalls of the cracks (Führböter et al., 1977), potentially leading to greater failure even with smaller magnitude impacts.

The main reason for the lack of studies focusing on the pathways is the limited amount or total lack of data on the defences characteristics (Stanczak and Oumeraci, 2012). In addition to this, a critical aspect is that all elements of the pathways are receptors in their own right and are therefore analysed as such. Due to the complexity of the coastal zone, it is necessary to search for studies built around single objectives, such as physical or biological properties and modes of evolution or geographic occurrence of coastal elements (Finkl, 2004) and incorporate the outcomes of this research into a flood risk context.

Following this principle, most studies look at coastal pathways from a morphodynamic point of view. These analyse the drivers of changes in the coastal system. Pathways in this sense are affected by a range of interacting drivers, which can be catalogued as natural, including the effects of climate change and anthropogenic, derived from direct human intervention. Natural

drivers include acting forces such as the tide, wave and wind, but the formation and maintenance of landforms also depend on suitable sediment supply. The temporal and spatial variation of these components is linked through varying flows of energy, moving the coast towards a state of “dynamic equilibrium” (Burgess et al., 2007, French et al., 2016). These interactions have positive and negative feedbacks working at different spatial and temporal scales. Anthropogenic actions can interfere with coastal behaviour ranging from minor effects, such as temporal erosion of a small coastal area, to catastrophic consequences requiring further intervention, which may lead to a complete loss of the natural system to an artificial one. The effects of human intervention can occur over long periods and extensive areas due to the lag time of the natural system to respond (Burgess et al., 2007). It is for this reason that predictions of coastal evolution through conceptual frameworks are required to understand the possible outcomes of any natural process or anthropogenic alteration and their effects on pathway occurrence.

Coastal areas are also studied for their role as natural habitats. In particular, intertidal areas are the focus of several studies (e.g. Willoughby et al., 2001, Nicholls, 2004, Brander et al., 2006). These have been identified as biologically productive ecosystems with high biodiversity as these benefit from the variation in water levels caused by the tide and the constant exchange between seawater and freshwater. These characteristics have granted them several habitat designations, including the Ramsar site designation, an agreement with over 169 contracting countries seeking the conservation and wise use of wetlands (Bureau, 1971). The European Commission adopted in 1992 the conservation of natural habitats and wild fauna and flora directive, which ensures the conservation of threatened or endemic animal and plant species in Europe (Habitats Directive, 1992). These regulations have been adopted in the UK through the implementation of the Special Protection Areas for Birds (SPAs) and Special Areas of Conservation for over 189 habitat types and 788 species (SACs). Although protected by these designations, intertidal areas are subject to natural and anthropogenic drivers, causing accelerated rates of coastland wetland loss (Spencer et al., 2016). Changes to the natural environment will have an impact on coastal flooding, as these habitats influence water flow by providing hydraulic roughness (Lefebvre et al., 2010).

Within the few studies analysing pathways for their role in flood risk, these tend to focus on the overall performance of a set of defences, rather than on their individual behaviour under specific circumstances (Sayers et al., 2002). The reason for this being that, as mentioned, many coastal works were carried out in the past centuries and early years of the 21<sup>st</sup> century, leaving little if any information on the specifics of the designs. Furthermore, the lack of knowledge on the effect coastal defences have in adjacent areas led to individual parties implementing defences without considering the broader effects. All of this results in a lack of global and regional studies accurately incorporating pathway occurrence, which could be attributed to the level of detail

required for these assessments. In general, most of the research available follows performance or risk-based approaches, whereby alternative forms of intervention are weighted based on the analysis of the costs and benefits (Dawson et al., 2004). Understanding the performance of a set of defences allows assessing the flood system as a whole and improves risk management strategies.

### **2.3.2.2 Temporal changes on the pathways of flood risk**

The likelihood of occurrence of each pathway is strongly linked to the loading the coastal defences experience and the drivers of coastal change, which can be mainly attributed to natural processes acting upon individual features. These are catalogued into three main categories: 1) direct forcing; 2) long-term weathering; and 3) habitat creation, although the latter is a consequence of the formers.

The principal direct driver of change is pressure against a defence, which can be caused by a) static loads derived from the hydrostatic pressure of the weight of the water column and/or b) dynamic loads caused by the fluid in motion and the hydrodynamic pressure applied over short and intermittent periods. Hydrostatic loads in a coastal environment are affected by the continuous fluctuations of water levels experienced all around the globe, and their staticity is relative to periods of time (e.g. the standing tide). The temporal scale of these ranges from large-scale fluctuations on mean sea level to the constant variation of the tide. Although waves produce dynamic loads, the small variations caused by non-breaking waves alter the depth of the water column, effectively altering the hydrostatic pressure acting on the defence. In addition to this, changes in atmospheric pressure have the potential to alter the height of coastal waters. Since the point of action and magnitude of the force applied by the water column are directly related to the depth, the aforementioned variations have the potential to cause defence failure.

Regarding dynamic loads, these will depend on the type of structure and type of wave, of which there are three. 1) Non-breaking waves, which occur when the height of the breaker is smaller than 80 per cent of the water depth in front of the defence. These loads are often caused by reflected waves (clapotis or standing waves) which increase the depth in front of the structure, preventing incoming waves from breaking. 2) Breaking waves that cause short, very high and impulsive pressures. Due to their nature, these are hard to predict, and the methods to do so are not entirely reliable. Some of these methods include the use of the Iribarren number based on seabed slope and wave steepness to determine the type of breaker (Battjes, 1988). The impact load caused by breaking waves is a function of the type of breaker (spilling, plunging and surging), which is controlled by the nearshore properties, such as the slope of the seabed and the state of the breaker when it reaches the defence, as undisturbed breakers generate higher pressures,

ruled by the roughness of the seabed, and the aeration (air content) of the breaker. 3) Broken wave loads generating low pressures through the impact of aerated water. These occur when the height of the breaker approaching the structure is higher than 80 per cent of the water depth in front of the defence (Minikin, 1963, Holthuijsen, 2010).

Long-term weathering processes include variations on the physical properties of seawater, such as temperature and salinity, as these act on natural and anthropogenic structures. Temperature changes have a direct effect on bio-geomorphology (natural defences), water density and water volume. Bio-geoformations are particularly sensitive to temperature fluctuations, with coral bleaching as a clear example of this. As the water temperature rises, density decreases, thus increasing its volume. Salinity, just as the water temperature, has a direct effect on bio-geomorphology. As mentioned, direct and long-term forcing can cause erosion and weathering of defences. However, these processes can lead to habitat creation through sediment and mineral mobilisation. Although wave action can cause erosion by making sediment from the seabed available for cross and longshore currents, this sediment is then mobilised to downdrift areas. Periodic water level variations can have the same erosive effect on coastal areas. This effect is particularly experienced in estuaries, such as Southampton water, where the characteristics of tide propagation cause high-speed currents during ebb tide, flushing sediment from the system (Collins and Ansell, 2000).

The processes affecting pathway evolution work at different spatial and temporal scales. In general, these are regarded as working on four scales: Instantaneous, Event, Engineering, and Geological (Cowell and Thom, 1994) (Figure 2.5). Even though such scales were first adopted for morphodynamic evolution (i.e. natural environments), their scope can also be applied to built environments. It is up to the coastal managers to decide the scale used for their assessment, although a holistic approach looking at all temporal and spatial scales is encouraged (Stive et al., 2008). For instance, the instantaneous effects of a single wave or a tidal cycle can be used to understand the effect of these weathering processes on intertidal bar migration. The event scale can be used to determine the effect extreme loads could have on coastal assets. The weathering processes analysed for both the instantaneous and event scales can be considered stochastic. In a lot of cases, these scales are considered as noise as they do not cover the complete length of time of a coastal project. On the other hand, chronic weathering caused by long term variations on the coastal conditions, such as changes in regional and global sea level and temperature are of interest at an engineering and geological scale. In the case of the engineering classification, the residual life of coastal projects covers from years up to centuries thus making it necessary to anticipate the future coastal stressors. Lastly, the geological scale looks at slow processes that

cover extensive areas and are usually tied to climate change. In many cases, the geological scale is only used as a boundary condition as its scope is far too long into the future.

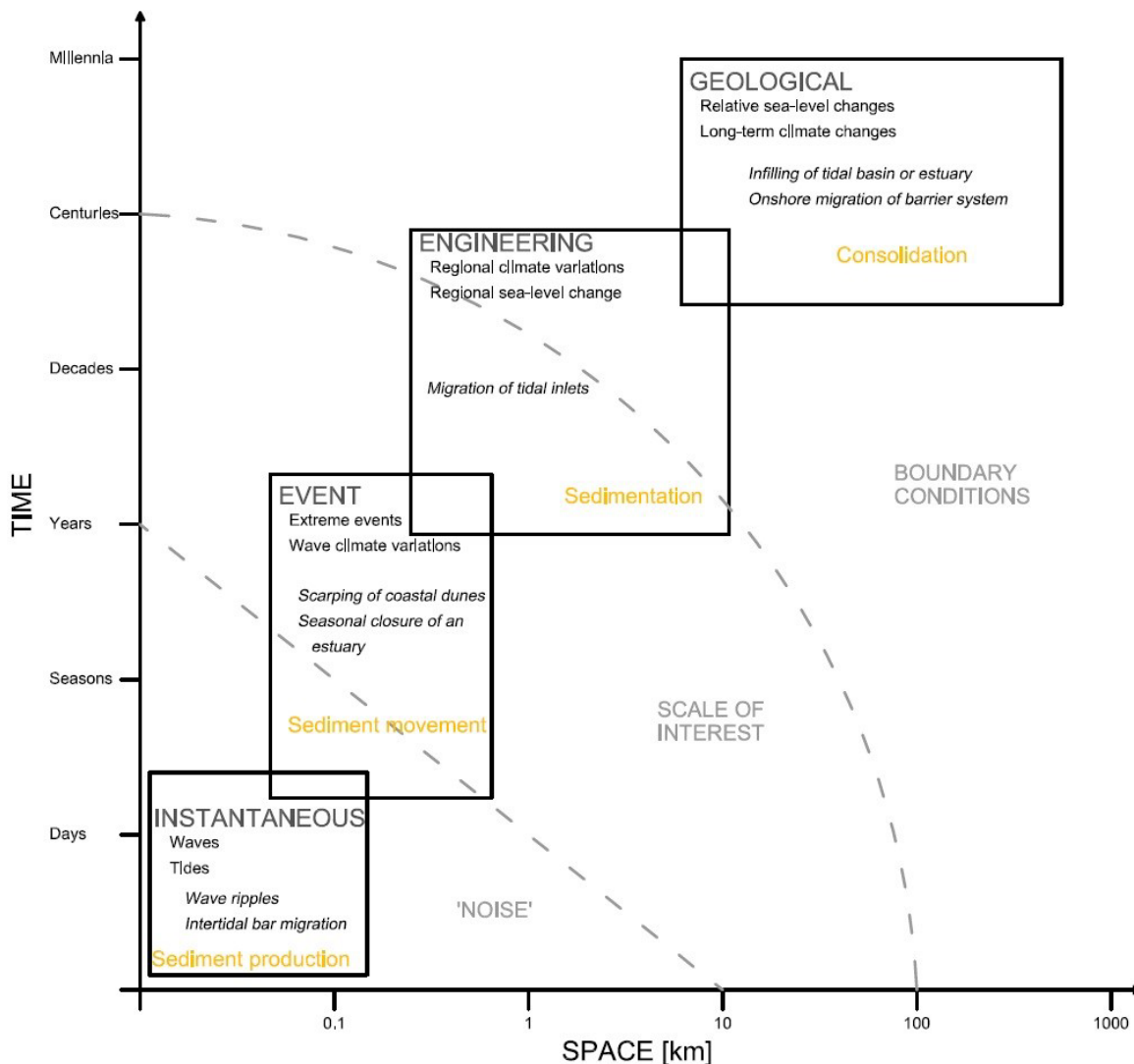


Figure 2.5 Spatial and temporal scale of processes affecting coastal evolution. Figure inspired by Cowell and Thom (1994)

### 2.3.2.3 Previous research analysing the pathways of coastal flood risk

As pathways are one of the essential elements affecting the probability of flood risk, various studies have attempted to determine the conditions under which each pathway could occur. However, there are significant uncertainties in doing so, as the hydraulic conditions in a coastal environment are rapidly changing, and particular sequences and combinations of waves and still water levels (including surge) could cause failure, even if their combined magnitude is below the defence Standard of Protection (SoP) (as mentioned in the previous section). Coastal managers face then the challenge of determining the areas where investment is required to reduce or maintain the levels of risk at tolerable levels. Researchers continue investigating ways to improve our understanding and methodologies to determine defence failure. In this context, failure can be



considered the inability to achieve a defined performance threshold (Gouldby et al., 2005). It is essential to have a distinction between the types of failure, as defences can be allowed to overflow or overtop under specific scenarios but still maintain an adequate level of protection for subsequent loadings, whereas breaching would cause a complete loss of protection. Accurately determining the conditions under which the accepted thresholds are exceeded is still a challenge for flood risk managers. In situ tests of dyke failure (Laustrop et al., 1991), analytical models of wave impact on dune erosion (Larson et al., 2004), and laboratory tests (Stanczak and Oumeraci, 2012) are performed on different configurations of dykes in order to understand the effect of dynamic loads such as breaking waves on breach initiation and pathway evolution. However, many of these results are still case specific and cause uncertainties when applied to constantly varying conditions.

One of the most commonly used approaches to determine the conditions which could cause defence failure is the use of generalised fragility curves. In the UK, these have been used for national risk assessments by Hall et al. (2003) and Gouldby et al. (2008). However, these use a simple representation of the defence condition, as data for the specifics of the defence on a national level is scarce or missing. Simm et al. (2008) argue that these fragility curves should be obtained on a local level to represent the particular conditions of the study areas accurately and continues to explain that the use of deterministic approaches, which consider a variety of load and strength configuration, is far better to obtain fragility curves than the use of a single standard of protection values. In either approach, the fragility curve can be built based on a) empirical and sufficient data on defence failure under loading conditions; b) based on expert judgement; and c) based on structural reliability methods, such as the limit state (Simm et al., 2008). At present, the failure modes most commonly utilised are due to high water levels, without consideration of low water failures modes, such as geotechnical pipping (Simm et al., 2008). One of the biggest uncertainties at present is the effect of sequential loading on assets. Buijs et al. (2009) explored the use of hierarchical process models and stochastic methods where sequence failure trees are determined based on what they define as an initial contributor. In addition to this, they analysed the use of random process models and parametric representations of flood defence deterioration. In general, they found small differences between the parametric and hierarchical models, though the latter gives a better representation of the defences' performance considering time variability (Buijs et al., 2009).

Although the use of fragility curves is widely accepted in coastal flood risk appraisals, these often rely on the collection of data which is often subjective. For example, the EA provides condition grades of its coastal assets in England which are typically visually assessed, thus not considering essential aspects of their structural conditions (Flikweert and Simm, 2008). Simple inspections

assign the condition grades with the help of visual and textual guidance. These inspections have been used since the 1990s by the EA, with the latest guidance given on the Condition Asset Manual (CAM), indicating how the condition grades are assigned based on the type of defence (Flikweert and Simm, 2008). The condition grades, as well as their description, are shown in Table 2.1.

Table 2.1 Environment Agency asset condition grading

Grade	Rating	Description
1	Very Good	Cosmetic defects that will have no effect on performance
2	Good	Minor defects that will not reduce the overall performance of the asset
3	Fair	Defects that could reduce the performance of the asset
4	Poor	Defects that would significantly reduce the performance of the asset. Further investigation needed
5	Very Poor	Severe defects resulting in complete performance failure

One of the critical limitations of these indicators is the lack of information on internal irregularities that can be entirely out of sight, as highlighted by a study in 2008 by the EA and Royal Haskoning. The study analysed the effect of the June and July of 2007 storm and flood events on some of the EA flood defences located in the south of the Humber estuary and the East Midlands. The results indicate that over 1,000km of flood defences were “tested” by the floods, of which half (525km) were overtopped, and only 50m of defences were breached (Pitt, 2008, Royal Haskoning, 2008). With the use of locally collected information and anecdotal evidence as well as existing datasets, the initial defence conditions (i.e. standard of protection) and the forcing mechanisms (i.e. loads caused by the sources) were established to determine the defences failure mechanisms (pathways). One of the most interesting conclusions of the study is the fact that there was not a strong relationship between the EA assigned condition grade and the breaching of defences, as the study found that some of the breaches occurred when water levels were below the crest levels, meaning breaching was caused by geotechnical failures (Royal Haskoning, 2008). Furthermore, when fragility curves for all the failed defences were estimated, it was found that for the defences where breached occurred, the likelihood of breaching was far lower than that of overtopping, whereas, for the overtopped defences, the forcing conditions were more likely to cause breaching than overtopping (Royal Haskoning, 2008, Simm et al., 2008).

### **2.3.3 Receptors**

#### **2.3.3.1 Definition**

Receptors are the people, industries, and built and natural environments in the floodplain (Evans, 2004). In other words, receptors are what can be found in the floodplain or the intrinsic use of this area (Figure 2.4) (Nicholls et al., 2015). In this context, it is necessary to obtain information on the number of people and socioeconomics of the area, the number of assets at the floodplain, as well as their characteristics, types of land use, and detailed mapping of natural areas.

#### **2.3.3.2 Temporal Changes**

A disaster only happens if people are injured or killed, and/or the natural and/or built environment is damaged or destroyed (Kron, 2013). Historically, cities have been established around water bodies as this provided accessibility and facilitated commerce (McGranahan et al., 2007). Even today, major cities around the world are located in estuaries (e.g. London) and around the coastline (e.g. New York and Hong Kong). Areas within the first 100km off the coast show population densities up to 3 times higher than the global average density as development has attracted migration and investment at the floodplain (Smalls and Nicholls, 2003). It is estimated that up to 10 per cent of the world's population live in the LECZ, which encompasses areas with a maximum elevation of 10m above MSL (McGranahan et al., 2007). There is high confidence that the world population will continue to rise during the 21st century, with population projections reaching 8.6 billion by 2030 and 13.3 billion by 2100 (United Nations, 2015). As trends in coastal urbanisation are expected to continue to rise in the future, and given the fact that populations are expected to increase throughout the century, it is vital for coastal managers to understand trends of development at the LECZ. Predicting migration is generally complicated, and trying to do so at the floodplain is even more complex as there is no clear understanding of how populations will react to increasing coastal hazards (Hauer et al., 2016). These threats raise the need for coastal defence implementation. However, it has been shown that coastal defences create positive feedback on coastal development caused by the sense of security these provide (White, 1942, Armstrong et al., 2016, Welch et al., 2017). As populations migrate to these areas, investment in coastal defences to guarantee their safety is required. However, as defences are implemented, the local economy is enhanced, and the population perceives a sense of security, ultimately attracting migration. Migration to the floodplain encourages development in this area, increasing the number and value of assets at risk.

Changes in flood frequency can also affect the natural environments. For instance, intertidal environments are highly sensitive to changes, and constant extreme water events can potentially

move them from their state of equilibrium. Destructive climatic events include erosion, saltwater intrusion, siltation, amongst others (Turner et al., 1996).

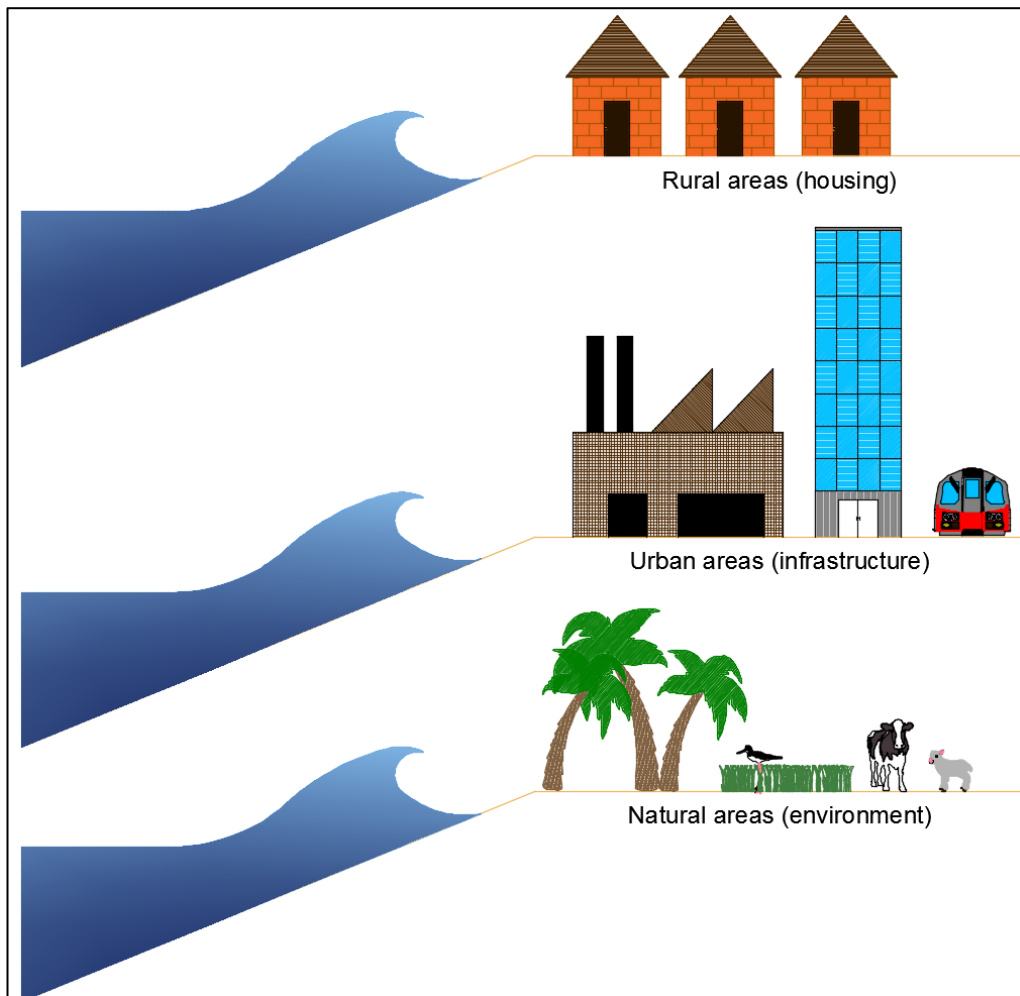


Figure 2.6 Receptors of coastal flood risk

### 2.3.3.3 Previous research analysing the receptors of coastal flood risk

It is important to mention that most of the research analysing the receptors of coastal flooding tend to do so with a focus on the population at the floodplain and its evolution, as understanding human migration remains one of the main challenges not only for coastal managers but researchers in general. It is common to forecast the country's urbanisation rates and assume coastal cities to maintain a constant share of the country's population (Nicholls et al., 2008, Hanson et al., 2010, Kebede et al., 2012). However, coastal areas often show higher rates of urbanisation, thus requiring the implementation of new methodologies based on the country's socio-economic and environmental scenarios and projected urban and non-urban expansion (Neumann et al., 2015). One of the main problems for coastal managers is pinpointing or identifying whether natural processes cause migration or if it happens as a consequence of aspects such as economics, politics, etc. In this sense, previous research has been conducted

trying to predict coastal population evolution, and even though there is a constant improvement in these projections, it is hard to define how populations will react to the effect of natural hazards. Hugo (2011) shows that although there is great uncertainty on future coastal population patterns, climatic stressors are already directly increasing the levels and complexity of population mobility. For example, areas such as New Orleans in the US have experienced migration after coastal flooding (Foresight, 2011), whereas cities like Venice, Italy, maintain stable populations despite the documented flooding (Hauer et al., 2016). Furthermore, predicting migration around the coastline is particularly difficult in deltaic areas where, even though the occurrence of extreme water events has led to billions of dollars in monetary losses and even the loss of human lives, more often than not, residents decide to stay in the affected area, regardless of the existence of future threats.

The Foresight (2011) report analysed global and internal migration trends to estimate rates of the potentially affected population. The report indicates that over 220 million people live in the LECZ. The study finds that populations tend to migrate to threatened coastal areas, particularly in regions of Asia where trends of migration to the coast are far higher than in other regions of the world. It is interesting to see that a lot of this migration is caused by environmental and economic changes in developing coastal zones. The communities' source of income, ability to communicate and overall development highly depends on the resources available in these areas (Foresight, 2011). Given all the variables and detail required to understand migration, research on the effect climate stressors have on population tends to focus on regional and local levels (e.g. Curtis and Schneider, 2011, Penning-Rowsell et al., 2013, Hauer et al., 2016, Hauer, 2017), with the dynamics of coastal receptors analysed for various cities around the world. It is interesting to see that the usual approach relies on an elevation model to define the extent of the floodplain, which is then coupled with population distribution models to obtain the number of people affected by a given water level. The most relevant global studies on this matter which can be considered as stepping stones and whose results and methodology are often cited include the work by Hoozemans et al. (1993), Nicholls et al. (2008) and Hinkel et al. (2014). These studies estimated population growth around the floodplain as a function of the countries urbanisation rates, which are projected by the United Nations (2015). Neumann et al. (2015) identified this as a limitation since observed urbanisation rates are higher on the coast than those at the hinterland and proposed correction factors. These factors vary according to the countries development status and the nature of the coastal area (i.e. urban and non-urban).

Among some of the relevant local studies utilising Nicholls et al. (2008) approach, the work by Kebede and Nicholls (2011) Kebede et al. (2012) on two cities in Africa are most notable. The former analyses Dar es Salaam, the former capital of Tanzania, and the latter studies Mombasa,

the second-largest city in Kenya. Both studies utilised global elevation data from the Shuttle Radar Topography Mission (SRTM) to define their study site's topography. These were then coupled with extreme water levels from the Dynamic Interactive Vulnerability Assessment model (DIVA) and four sea-level rise scenarios from the Fourth Assessment Report by the IPCC to obtain the extent of the floodplain up to the year 2100. Since both studies analysed flood exposure in the future, they required population growth scenarios. For this, both analyses used a city scaled methodology by Hanson et al. (2010), which feeds on the United Nations country projected urbanisation rates. Once the cities populations were estimated, these were distributed to local geographic regions or districts according to their historical share of the city's population obtained from census data. It is important to note that these shares were assumed to remain constant throughout the study periods. Although this was done on the basis that it is unknown if and where people may move, it would be beneficial to identify the areas that are potentially or continuously flooded and remove population from these. Hauer et al. (2016) identified this problem and proposed a simple equation, which in general terms estimates the population at risk at a given time by subtracting the sum of the previously impacted populations multiplied by the land lost due to sea-level rise. By doing so, it is ensured that populations are not double-counted.

As with the studies above, research tends to focus on the human aspect of the receptors and fails to include the natural environment in its assessments. One of the reasons behind this is the complexity of the interaction between social and natural processes. The urbanisation of the coastline and changes to land use have impacted the coastal zone, with human interaction leading to the loss of natural habitats, such as salt marshes, mangroves, coral reefs, and dunes (Turner et al., 1996). Some of these interactions come as a result of the extensive engineering works carried out to protect the coastlines. However, some of these have positive feedbacks on their vulnerability to natural hazards. In the Mississippi Delta, the construction of levees, dams, and canals has led to changes in the freshwater and sediment supply, starving the coastal wetlands. Similar to this, in Bangladesh at the Ganges-Brahmaputra-Meghna river system, sediment flow and deposition rates have been affected by the flood defence system, deteriorating the coastline and changing the frequency and severity of floods (Turner et al., 1996, Welch et al., 2017).

### **2.3.4 Consequences**

#### **2.3.4.1 Definition**

Consequences are the results of coastal flooding. These include the effects of flooding on assets, communities and the environment. There are three main categories of flood consequences. 1) Economic, including damage to assets, such as residential homes and personal and commercial

property and infrastructure; loss of livestock and destruction of crops; public service disruption; evacuation and permanent displacements; looting; injuries and in some cases death. The most common methodology utilises the number of exposed population and sometimes empirical factors to relate the per capita share of the country's gross domestic product (GDPppp) with the expected damage to assets (Nicholls et al., 2008, Hallegatte et al., 2013, Hinkel et al., 2014). 2) Social impacts as floods have the potential to cause loss of community, loss of cultural sites, deterioration of health conditions and cause stress to the population at the floodplain. Many economic consequences can be encompassed as social consequences, such as public service disruption, population displacements, injuries and death. All of these will have an impact on local communities, either by constraining access and communication or by decreasing the economic productivity; and 3) Environmental damage caused by saltwater intrusion, dispersal of weed and nonindigenous species, sediment deposition, loss of natural areas, and release of pollutants, amongst others (Wong et al., 2014).

#### **2.3.4.2 Temporal Changes**

The evolution of consequences is strongly linked to changes in the receptors. For example, migration into the floodplain can induce changes in land use types, increases in the number of properties and the value of assets at the floodplain, etc. However, the type of consequences has changed over time. Economic and social consequences were the common denominator in the past, as there was little to no preparedness or flood protection (Ruocco et al., 2011). With investment in defences and the implementation of early warning systems and evacuation plans, populations can leave the potentially affected area, reducing the social and economic consequences of floods. On the other hand, environmental consequences have increased as natural areas start to become scarce as a consequence of human influence in the climate system. Furthermore, the magnitude of consequences can also be influenced by the characteristics of the flood; for instance, high-speed flows are more likely to cause damage than low energy flows.

Consequences can be decreased by implementing adaptation strategies (Figure 2.5). The Shoreline Management Plan (SMP) policies for adaptation include: 1) Hold the line of defence, meaning the current SoP is maintained. 2) Advance the line, which requires raising the SoP as sources and receptors evolve. 3) Managed realignment, and 4) No active intervention (Environment Agency, 2020b).

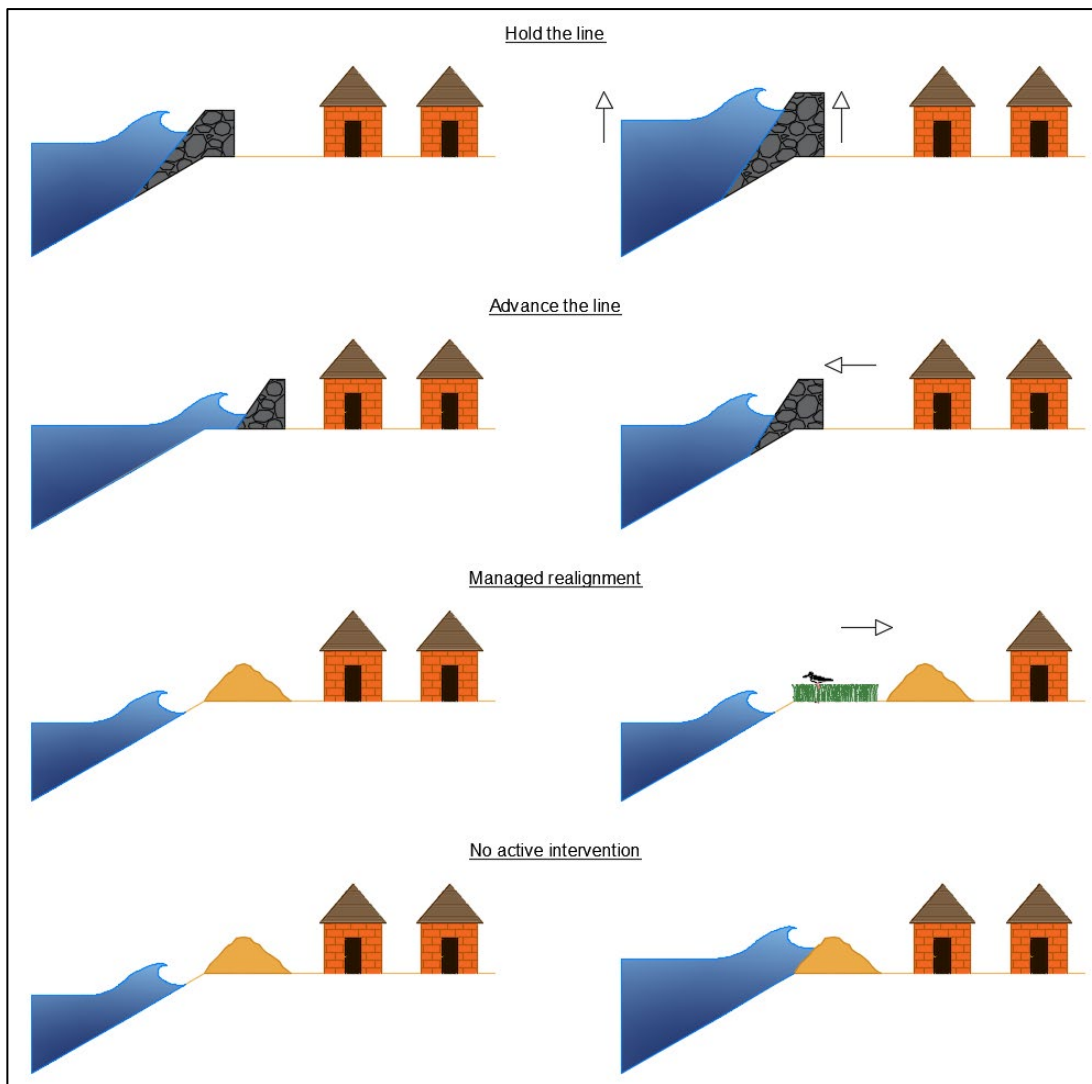


Figure 2.5. Adaptation measures that affect the Consequences of coastal flood risk derived from the principles of the Shoreline Management Plan by the Department for Environment, Food & Rural Affairs (2006)

#### 2.3.4.3 Previous research analysing the consequences of coastal flood risk

The consequences of coastal flooding can be economic, social and environmental. Economic consequences are somehow the easiest to quantify as doing so only requires knowing how much had to be spend to alleviate the effects of a flood. This ability of an area to cope with or resist the effects of a flood is referred to as vulnerability. One of the main problems with defining the degree of vulnerability is that the methodology selected can significantly vary the overall projected cost of a flood. Coastal managers face a significant challenge as investment in coastal defences usually relies on a cost/benefit analysis, where the benefits are obtained as the costs that can be avoided by the implementation of a given defence.



There are a number of ways to calculate the economic consequences according to the scale of the study. In general, there are two main types of consequences, direct and indirect. The former are usually estimated from residential homes, personal property, business and commercial property and insured assets at the floodplain (Hallegatte et al., 2011). It is important to note that public assets, such as energy, water and transport infrastructure as well as government buildings are omitted from direct consequence estimates, although these have been shown to represent up to 40% of direct losses (Environment Agency, 2001, Hallegatte, 2008, Hallegatte et al., 2011). The indirect costs have proved to be harder to estimate, as it is difficult to determine up to which extent of damage and disruption is caused by the inundation. Indirect costs include the interruption in the production of goods and services and the delay in replacing goods.

Direct consequences can be obtained by: a) relating the number of people to the value of their assets, b) giving an economic value to the affected areas according to their land use, and c) estimating the number of properties potentially affected by a flood. Each of these approaches has its advantages and limitations. For instance, the most commonly selected approach, relating people to the value of their assets, is preferred for global and quick analyses, particularly in areas where detailed information is not available. This methodology is often used by insurance companies and was applied by Nicholls et al. (2008) and Hanson et al. (2010) on global studies of coastal exposure. In this case, the population was related to their assets by multiplying the number of people and their share of the GDPppp by a factor of 5. According to the authors, this factor was obtained from previous experience used by Risk Management Solutions (RMS), and by assuming that the per capita value of assets in a city is about 4 or 5 times the per capita GDPppp (Nicholls et al., 2008). Similar to this study, Hallegatte et al. (2013) projected future losses for major coastal cities up to the year 2050. This study translated population to exposed assets with an estimate of produced capital per inhabitant from data by the World Bank, though there is no explicit mention of the multiplying factor.

Hinkel et al. (2014) further built on these results and obtained assets exposure as a function of the number of people at a given flooded depth. In this case, a ratio of 2.8 multiplied the number of people to the subnational per capita GDPppp. It is interesting to compare these studies because all draw on the original work by Nicholls et al. (2008). Hallegatte et al. (2013) use Hanson et al. (2010) estimates, which are derived from Nicholls et al. (2008), and Hinkel et al. (2014) use Hallegatte et al. (2013) results as a baseline. Even though these share the same roots, the factors utilised to relate people to assets vary and interestingly decrease in the more recent studies. It would be somehow logical to assume that more assets are located in the floodplain since populations have become wealthier, acquired more possessions and the fact that there is further investment in the coastal area. However, the fact that early warning systems are available in more

cities has decreased the level of damage produced by extreme water events. These factors combined can be the cause of a decrease in the economic costs of a flood, an effect that has been true since the 1950s (Haigh et al., 2020). It is somewhat difficult to argue which factor is more impartial since all base their assumptions on empirical data. The problem with this is that it is near impossible to compare the consequences of a flood event to another. There are many variables that would be difficult to standardise in order to objectively compare them, such as the duration, intensity and trajectory of the weather event which caused the flood. Furthermore, none of these studies takes account of the different level of development not only between regions but even between coastal cities in the same country. This is somehow overcome by the use of a local per capita share of GDP which varies from country to country but still would not differentiate between cities.

This approach is further limited in the sense that it does not take into account factors such as the characteristics of the properties at the floodplain. For instance, areas with vertical development have high population densities and using the methodology above would result in significant flood cost estimates. However, water is unlikely to reach higher than the first level, and more often than not, this first level is used as a reception and/or for parking spaces, decreasing the consequences of a flood. Furthermore, there is an increasing recognition of the level of flood exposure properties have, which has resulted in more investment in floodproofing old and new infrastructure.

Another way to estimate the direct consequences of a flood involves applying an economic value to areas based on their type of use. This would require a detailed classification of the floodplain and the land uses within it. The most common types of use include residential, commercial and services, industrial, transportation and communications, agricultural, forest land, water, wetland, etc. (Anderson, 1976). One of the problems with this approach is selecting the factors that will determine the economic value of each area. In a study of a Mexican coastal city in the Gulf of Mexico, Pedrozo-Acuña et al. (2015) utilised the level of contribution of each economic activity to the local GDP as a proxy to estimate the value of the flooded areas. This is a practical approach as it prevents the use of any subjective parameters and leads to robust estimates. However, it would lead to some land uses such as residential with low values as these do not significantly contribute to the economic productivity. The same is valid for natural areas where their value is extremely variable across the literature, and published studies are often not directly comparable (Brander et al., 2006). In the case of wetlands and intertidal areas, these are protected by national and international designations. Some of these designations demand compensation of any lost area in order to avoid a net loss, such as the Ramsar convention (Di Leva and Tymowski, 2000). The costs of creating intertidal areas to compensate for any losses can be used as an economic indicator of

their value. Overcoming these limitations would require the use of more biased factors, such as the historical value of an area or the value population assigned to an area based on whether it is used for recreational purposes.

A finer method to estimate direct consequences would be the use of the number and characteristics of the properties at the floodplain. This approach is more likely to be used in regional or local studies where there is accurate and detailed data. This method can be advantageous as it can consider the individual characteristics of the properties, for example, whether this has been flood-proofed or if the property is somehow located above the ground elevation. This would be very beneficial for disaster management purposes, as it would be easy to obtain the number of people affected in finer scales, from property to postcode level.

Indirect economic consequences include service interruption, constraints to communications, job losses, reconstruction duration, amongst others. More often than not, flood risk analyses do not take account of this type of loss, even though direct losses are only a fraction of the overall costs (Hallegatte et al., 2011). To overcome this, Hallegatte (2008) proposed an Adaptive Regional Input-Output (ARIO) model, which can reproduce the impact of a disaster on a local economy taking account of productive capital losses and adaptive behaviour during disasters and their aftermaths. This model was applied to New Orleans, US, with data on the consequences of hurricane Katrina in 2005. Hallegatte (2008) finds indicate the indirect consequences to represent around 40% of the total costs of flooding for an event such as Katrina. Even though that the size of a disaster will increase/decrease the ratio of total losses to direct losses, this ratio is not directly proportional to the size of the disaster. Overall, Hallegatte (2008) concludes that estimating the total consequences of a flood by only analysing direct losses would result in under-predictions, particularly for large-scale disasters, and highlights the need for alternative indicators of the economic losses. Penning-Rowsell (2015) further argues the use of direct losses to estimate flood risk and concludes that the UK Government, through the National Flood Risk Assessment (NAFRA), overpredicts the annual economic risk by a factor of four to five times. Furthermore, it is argued that there is a difference between financial and economic losses, and both are commonly mixed. Financial losses involve a “betterment” of the assets as it is the cost of replacing or restoring a property. The article gives an example of an eight-year-old television, which after a flood is replaced by a new one. In reality, the economic loss should be obtained from the remaining value given the asset’s residual life by including a discount factor to account for damage and deterioration. To convert from financial and economic costs and vice-versa, the estimates should be multiplied by 0.65 and 1.6 respectively.

Environmental consequences of a flood include the loss or adverse effect on natural areas, including but not limited to intertidal habitats and wetlands. This can happen by either waves or large surges causing erosion, by increased levels of saltwater intrusion, or through the input of high volumes of foreign sediment. The consequences can include loss of habitat, damage to the species composition and changes to the biodiversity (Cui et al., 2015). Furthermore, the value of these areas has increased over the last decades as a consequence of the recorded decline in the extent of the global vegetated coastal habitats (Duarte et al., 2005). This can be attributed to the fact that human activities and anthropogenic drivers of climate change have produced large cumulative impacts such as overexploitation and habitat destruction (Wong et al., 2014)

Indirect consequences are the most challenging to quantify as it is difficult to assign a value to the above factors. For instance, some losses can be intangible such as impacts on cultural heritage, which are often overlooked in risk assessments (Hallegatte and Przyluski, 2010, Meyer et al., 2013). Further to this, analysing them requires input from all stakeholders of the area at risk. These can range from local communities, research groups, local services, etc. Identifying all the stakeholder groups and their influence and importance on a CFR assessment can be challenging. Methodologies such as that proposed by Prell et al. (2009) are available from the literature and allow identifying and prioritizing stakeholders.

Altogether, there is a lack of coastal flood research that includes all types of consequences, with the ability to account for tangible and the more subjective factors previously discussed. This could be done on a local scale as detailed information is more likely to be available for small regions. Applying this on a regional to a global scale would result in high uncertainties, which could only be overcome by breaking the analysis into smaller regions and performing exhaustive studies of the latter.

## 2.4 Hydrodynamic modelling

Once all the components of coastal flood risk are identified, the levels of risk for a study area can be evaluated. To this end, several methodologies are available from the literature relying on estimating the depth and extent of the floods. An accurate prediction of the extent of a flood as well as its impacts is one of the most valuable indicators coastal managers have. As computational capabilities have evolved, so has the range of models available for flood risk mapping (Teng et al., 2017). In general, there are three main categories of models to obtain the maximum flood extent: a) the empirical methods, b) hydrodynamic models, and c) the more recently developed conceptual models. Empirical methods rely on measurements of recorded maximum flood extents obtained from geological evidence, remote sensing, historical measurements and descriptions

(O'Connor and Costa, 2004). However, since this method is traditionally used for recording past events, it is difficult to obtain information on all the components that lead to these inundations, such as the magnitude of the EWL. It should, therefore, be used as indicators of possible floodplain extents. Hydrodynamic models aim to represent the mechanisms of water flowing into the study area, and they typically do so by solving the two-dimensional shallow water equations, which are based on the principles of mass and momentum conservation, or simplified versions of these equations. For example, the local inertial simplification to the two dimensional shallow water equations is given by the following equations.

$$\frac{\partial h}{\partial t} + \frac{\partial q_x}{\partial x} + \frac{\partial q_y}{\partial y} = 0 \quad 2.1$$

$$\frac{\partial q_x}{\partial t} + gh \frac{\partial(h+z)}{\partial x} + \frac{gn^2|q|q_x}{h^{7/3}} = 0 \quad 2.2$$

$$\frac{\partial q_y}{\partial t} + gh \frac{\partial(h+z)}{\partial y} + \frac{gn^2|q|q_y}{h^{7/3}} = 0 \quad 2.3$$

Where  $q_x$  and  $q_y$  are the two horizontal components of the flow discharge per unit width,  $g$  is the acceleration of gravity,  $h$  is the cross-sectional averaged water depth,  $z$  is the bed elevation,  $x$  and  $y$  are the two horizontal coordinates,  $t$  is the time (de Almeida et al., 2012). Based on the dimension of their analysis, these models can be 1D, 2D or 3D. Two-dimensional models have become the preferred to model the propagation of floods over complex topography due to their ability to capture complex flow patterns at the appropriate scales and level of accuracy while maintaining acceptable computational costs. These models allow the inclusion of the physical parameters of floodwater propagation, such as the time water is allowed to enter the floodplain with the use of tide, waves or surge curves. In addition, the models are capable of solving the physical problem taking into account factors such as the slope and terrain friction (Néelz and Pender, 2009). The EA has produced a series of reports analysing most of the available flood modelling software (Néelz and Pender, 2009, Néelz and Pender, 2010, Néelz and Pender, 2013). See Table 1 of Teng et al. (2017) for a summary of the most commonly used models. 1D models are the simplest type of hydrodynamic models as these treat flow as one-dimensional. These are typically used to analyse channel or river flow. They do so by averaging the velocity of one cross-section across the channel (e.g. Brunner, 2010) and are preferred for the prediction of water levels on longitudinal profiles (Di Baldassarre, 2012), with some of these models being capable of solving unsteady open channel equations (e.g. HEC-RAS). However, they cannot simulate some characteristics of floods that ultimately determine what areas are flooded, such as the gradual filling of floodplains, blockage and preferential flows driven by the two-dimensional topography, to cite but a few.

Two-dimensional models work by solving the shallow water equations, derived by depth averaging the Reynolds averaged Navier Stokes equations, and represent flow as two-dimensional by assuming the third dimension (vertical) to be shallow. Within the two-dimensional models, there are full two-dimensional depth-averaged codes (e.g. TELEMAC-2D) and simplified two-dimensional models often used for fast risk assessments (e.g. JFLOW and LISLFLOOD-FP) (Bates et al., 2005). Néelz and Pender (2008) provide a review of some of the most commonly utilised 2D modelling software. Finally, 3D models can give further insights into the flow characteristics, as some of these are capable of modelling turbulence, vortices and spiral flow at bends. Given the nature of the present research, many parameter combinations will be utilised to assess the individual influence of the SPRC elements over time, thus requiring rapid assessments of the floodplain extent as the ones obtained with simplified 2D models. LISFLOOD-FP, the model selected for this research, is a 2D inundation model based on a simplified form of the two-dimensional shallow water equations (Eq 2.1-2.3). Water is distributed by the model based on a volume filling process of each cell, mass conservancy and hydraulic connectivity. The accuracy of LISFLOOD-FP was tested against the recorded floodplain extents of Towlyn, Fleetwood, East Anglia and the Thames estuary in the UK by Bates et al. (2010). The results showed good agreement and the capability of the model to reproduce the extent under the storm conditions of observed inundations in 1990, 1977 and 1938, respectively, for the first three sites. In the case of the Thames estuary, there is a lack of information on recent floods as defences have prevented flooding. However, this site was utilised to compare the outputs produced by LISFLOOD-FP to those obtained with a planar approach. Overall, the model proved to be accurate for predictions of floodplain extent.

Finally, the simplified conceptual models make assumptions to simplify the hydraulics and some of the physical processes of inundation. The crudest and perhaps most commonly used method is the planar water surface method, informally referred to as the “bath-tub” method. This method follows a binary approach where areas are either flooded or not, purely based on their elevation relative to the free surface's elevation. This is the most common approach as it requires little information and can often give a fair approximation to what a worst-case scenario would look like (i.e. if all defences failed and water had an unlimited time to spread around the floodplain). There needs to be some consideration in the way the extent of the flood is analysed. It is crucial to understand that there needs to be connectivity between cells in order for water to spread. Therefore, a visual inspection of the outputs is highly recommended. In order to overcome this limitation, models such as the Rapid Flood Spreading Method (Lhomme et al., 2008) later established cell compartments within the study area based on their elevation. The model proceeds to distribute floodwater throughout these cells based on the volume that is available to fill/spill from each cell (Gouldby et al., 2008, Teng et al., 2017).

## 2.5 Methods to conduct coastal flood risk assessments

As previously mentioned, flood risk assessments estimate the area threatened to flood and determine the associated consequences. Gouldby et al. (2005) highlight that the units on which risk is expressed vary according to the scope of the study. Risk can be expressed in monetary terms, fatalities, affected areas or damaged property. Policy and decision making for coastal flood risk management often use methodologies that express the levels of risk in economic terms. These can be given as a function of the number of assets exposed, the costs of flood alleviation.

Some of the most relevant studies analysing coastal flood risk at a global scale include the work of McGranahan et al. (2007), analysing the number of people located at the LECZ. This is done using SRTM elevation data to determine the areas in the vicinity of the coast with an elevation at or below 10m above mean sea level. Data from the Global Rural-Urban Mapping Project (GRUMP) on the population distribution is overlayed onto the LECZ to determine the global number of people exposed to coastal flooding. This assessment finds that 2 per cent of the world's area is located at the LECZ. Furthermore, it estimates over 10% of the world's population to live in this region, with Asian countries being the main contributors as a consequence of their low elevation and high population densities. The characteristics of the study require the use of low-resolution data and therefore are likely to yield larger exposures than those obtained with regional models. For instance, the SRTM data used by McGranahan et al. (2007) has a resolution of roughly 90m at a global scale (USGS, n.d.). The GRUMP data is obtained with the combination of night-time city lights and georeferenced census data with a 1km resolution (NASA, n.d.).

Nicholls et al. (2008) and Hanson et al. (2010) build on the work by McGranahan et al. (2007) and perform a similar assessment analysing flood exposure to a 1 in 100-year event at a global scale. The analysis, however, focuses on port cities and ignores the exposure at non-urban areas. This yields over 40 million people exposed to the 1 in 100-year event. Nicholls et al. (2008) predominantly find Asian cities such as Mumbai, Shanghai, Ho Chi Ming and Osaka-Kobe at the top of the population exposure rankings. Interestingly, the cities of Miami, New York and New Orleans also appear at the top of the charts. However, when the economic consequences of flooding are considered, European and American cities replace some of the Asian cities in the rankings. These include Amsterdam, Rotterdam, Tampa and Virginia Beach. Overall, the study estimates over US\$300 billion exposed to a 1 in 100-year event.

Hinkel et al. (2014) conducted a similar assessment to Nicholls et al. (2008) and Hanson et al. (2010). The analysis provides global estimates of risk to a 1 in 100-yr EWL for the year 2010, although the focus of the assessment is on the future evolution of flood risk. Global SRTM and Global Land One-kilometer Base Elevation (GLOBE) elevation data are coupled with a population

dataset comprised of GRUMP and LandScan data to determine the number of people at risk of flooding. The authors estimate 93 million people are exposed to a 1 in 100-year event. These estimates are twice those found by Nicholls et al. (2008) for the same EWL, although the latter focused on coastal cities. Hinkel et al. (2014) compare the results derived from using the two elevation dataset and both population distribution models. It finds that data obtained with SRTM leads to smaller floodplains than when estimated with the GLOBE dataset. On average, the area found to be exposed with SRTM is 45% smaller than that found with GLOBE. This is expected as the SRTM has a 90m horizontal resolution, capable of capturing the elevation profile on a higher resolution than the one km resolution of GLOBE. The differences found when comparing the results obtained with GRUMP and LandScan have a similar magnitude. Using a GLOBE Digital Elevation Model (DEM), LandScan reduces exposure by 6.5% compared to the GRUMP estimates. With the SRTM DEM, these differences are heightened and using LandScan decreases exposure by 42%. The analysis highlights how some uncertainties are inherent to the nature of a global model and how these can only be overcome with the use of national and regional data.

The methodology by Nicholls et al. (2008) and Hinkel et al. (2014) can be used to obtain coastal flood damages. In general terms, the basis of their method is the determination of the maximum flood extent under the various source and pathway scenarios. Once the flooded area has been determined, a spatial population dataset is overlayed. Due to the scope of their study, the extent of the floodplain was estimated using the planar method coupled with global population datasets. Having overlayed the datasets, a cumulative population exposure function  $e_p$  at given elevations  $x$  was obtained. The exposed population is then translated into number of assets exposed  $e_a$  by multiplying the number of people by their GDPppp and an empirically estimated ratio of assets to GDPppp of 2.8 (Hinkel et al., 2014) (Equation 2.4).

$$e_a = e_p 2.8 \quad 2.4$$

Damage to assets is then estimated with a depth-damage function and by considering the depth to which the assets at elevation  $x$  are submerged by a flood of height  $y$ , and assuming a 1m flood to destroy 50% of the assets (Hinkel et al., 2014). The damage to assets caused by a flood height  $y$  is obtained by integrating the depth-damage and the derivative of the cumulative exposure functions across all the terrain elevations  $x$  (Equation 2.5)

$$d_a(y) = \int_0^y \frac{(y-x)}{(y-x)+1} e'_a(x) dx \quad 2.5$$

Finally, EAD is obtained by computing all the potential damages  $D(y)$  with the probability density function  $f(y)$  of extreme water levels, based on their return periods (Equation 2.6). It is important to mention that damages, in this case, do not consider the probabilities of defence



failure. If an assessment is to be performed with this methodology with the inclusion of probability of defence failure, the density probability function will no longer only be based on the return period (or probability) of extreme water events, as it will have to account for defence failure.

$$EAD = \int_0^{y_{max}} D(y)f(y)dy \quad 2.6$$

## 2.6 Uncertainty in risk assessments

Analysing and modelling natural phenomena are inherently accompanied by uncertainty. As highlighted by Winkler (1996), these can be caused by physical processes (e.g. occurrence of extreme water levels) and social processes (e.g. reaction of people to flooding). However, there are far more sources of uncertainty, ranging from the uncertainty in the random behaviour of natural phenomena, errors in the model processing, uncertainty in the estimation of modelling parameters, uncertainty in human activities, etc. (Kiureghian and Ditlevsen, 2009). These uncertainties can be classified as aleatory and epistemic. The former refers to the intrinsic randomness of a phenomenon. On the other hand, epistemic uncertainties are caused by imperfect or a lack of knowledge or data.

As explained by Ragas et al. (2008), epistemic uncertainty can not be completely measured. The best techniques to quantify it rely on scenarios and models whose outputs can be validated with real-world data. Since this uncertainty lies in the lack of knowledge, its analysis can be used to plan ways to reduce it (Matthies, 2007). Aleatory uncertainty can be quantified, but unlike epistemic, it cannot be reduced. The best approach to handle the randomness of the phenomena analysed is to investigate the most appropriate way to describe the natural randomness of the processes.

These sources of uncertainty are highly present in flood risk assessments. Ranging from uncertainty in the accuracy of the projected extreme sea levels (e.g. Wahl et al., 2017) to uncertainties on the relationship between the time of occurrence of flood events and the presence of the population (e.g. Percival et al., 2019). Given that the outputs of CFR assessments can serve as the basis for legislation or management decisions, it is imperative to explore the range of plausible scenarios and associated uncertainties.

Uncertainty analysis involves determining the uncertainty in the results derived from the inputs and methods used for the analysis (Helton et al., 2006). There are several methodologies to evaluate uncertainty in risk assessments. In general, these can be classified as probabilistic, non-

probabilistic and hybrid (Aven et al., 2013). Poor knowledge of phenomena can lead to the necessity of using specific values rather than probability distributions. For instance, evaluating the model using the lower and upper values of an input. It is difficult to categorise these approaches as they can be considered probabilistic and non-probabilistic. The use of specific quantities for the input factors is equivalent to using scenarios, where the analysis is performed using the maximum and minimum values of an input factor. Probabilistic assessments are best suited to explore aleatory uncertainty. These are used to determine the distribution and probability of the model outputs. This approach is often accompanied by a sensitivity assessment. This indicates how sensitive are the outputs to changes in the inputs (Saltelli et al., 2010) and can serve to determine the contribution of the individual uncertainties to the output of the analysis (Helton et al., 2006). Hybrid approaches are used when there is no certainty on the best way to represent the behaviour of a variable (aleatory uncertainty) due to lack of knowledge (epistemic uncertainty). For example, Palmer et al. (2018) provide values of the projected SLR for the UK; however, it is difficult to establish a probability distribution on the likelihood SLR. In such cases, it is necessary to decide if a probabilistic representation is required or an interval (or scenario) analysis is more appropriate (Aven et al., 2013).

Various methodologies can be used to perform a probabilistic assessment of the uncertainty. Most of these investigate the propagation of the uncertainty of the inputs to the outputs and often rely on sampling techniques to characterise the inputs (Zhang, 2020). Sharma (2017) presents some of the most commonly used approaches for sampling along with their positives and negatives. These include simple random, systematic, stratified, cluster, quota, purposive, self-selection, and snowball sampling, to name but a few. These sampling techniques are commonly used as they can reduce the number of tests performed by producing a number of samples capable of representing the behaviour of a variable.

A commonly used framework for uncertainty analysis is the Monte Carlo (MC) method, whereby the random samples are repeatedly used to compute the results and statistical analysis performed (Caflisch, 2008). In general terms, the samples used in the MC framework can be generated through pseudo-random number generators (PRNG) and low-discrepancy sequences. The former accounts for the probability distribution of the inputs and generate samples accordingly. One of the weaknesses of the PRNG methods is that it can lead to clusters and gaps in the samples (see Burhenne et al., 2011). Low-discrepancy sequences (LDS) overcome this problem by generating equidistributed samples (Dalal et al., 2008). Since the introduction of the LDS removed some of the randomnesses of the assessment, the MC framework becomes a Quasi-Monte Carlo Framework (QMC). Examples of LDS include the Halton sequence, van der Corput sequence, Niederreiter sequence and the Sobol sequence (Dalal et al., 2008).

### 2.6.1 Previous research analysing uncertainty in flood risk estimates

Various coastal flood risk assessments have attempted to explore uncertainty as part of their analysis. The approaches used to investigate the uncertainty generated by their input factors varies. The methodologies fall within the probabilistic and non-probabilistic approaches previously mentioned. For instance, Lewis et al. (2011) explored uncertainty using a scenario (non-probabilistic) assessment. The study analyses the influence of input factors such as the terrain roughness coefficients, SLR projections and methods to interpolate EWL on the coastal flood risk estimates. The authors find mean sea-level rise to be the determining factor of future floodplain extents, with the roughness parameter having a lesser effect. These findings are a result of the focus of the assessment, as it fails to consider the evolution of the pathways and receptors for the study area.

Vousdoukas et al. (2018b) make use of a non-probabilistic approach to measure the contribution of epistemic uncertainties of the input on CFR estimates for Faro, Portugal. The study focuses on the influence of factors within the sources of CFR (i.e. sea-level rise, waves and tidal contributions), uncertainties on the height of flood defences, and the different depth-damage curves available depending on the type of land use. Furthermore, the difference between using a high-resolution elevation model (0.5m resolution) and a coarse SRTM (100m resolution) is explored, although this is only done for a single scenario due to computational costs. The results show large differences in the estimates obtained with a high-resolution and coarse resolution DEM, which the authors attribute to the coarsening of flood defences within the DEM, and suggest treating them separately rather than including them in the elevation model. The DEM resolution is found to almost triple the estimates of EAD. Furthermore, they find that omitting wave contributions to EWL is the largest source of epistemic uncertainty. This is followed by uncertainties in tide and SLR. The errors in the height of flood defences lead to the variance of 30% to 60% on the EAD estimates.

The simplicity of non-probabilistic approaches makes them a useful tool for studies looking at the influence of single components. For instance, Mondal and Tatem (2012) focus on the differences in risk estimates generated by the selection of the population distribution model. The assessment compares the results obtained when the GRUMP and LandScan datasets are employed. The findings indicate that different population distributions can generate high variabilities, particularly for densely populated areas prone to flooding.

More refined assessments include de Moel et al. (2012) incorporating MC frameworks to the analysis of coastal flood risk (probabilistic approach). de Moel et al. (2012) explores the uncertainty and sensitivity of coastal flood estimates for the west region of the Netherlands. The

QMC framework is established by estimating the probability of extreme water levels, a model to simulate beach growth after dike failure, and a model to estimate the associated damages. The authors find the use of a 2D inundation model to be computationally expensive. Instead, the assessment estimates the volume of water that will enter the floodplain under varying conditions and resort to using pre-processed inundation extents and lookup tables. The assessment compared the accuracy of the pre-processing technique against a 2D inundation model, finding the latter to produce larger floodplains likely as a result of connectivity given by local waterways. The study uses a QMC approach to generate input samples for the uncertainty assessment combined with a sensitivity assessment using Sobol Indices. The results highlight that the relationship between depth and damage generates the largest uncertainties. These are followed by the behaviour of coastal defences and the characteristics of the extreme water levels.

Wong and Keller (2017) use the Sobol indices to assess the sensitivity of coastal flood risk in New Orleans. The analysis focuses on the influence of factors contributing to future changes in extreme water levels and different failure mechanisms of coastal defences. Wong and Keller (2017) find CFR estimates to be most sensitive to variations on the characteristic of storm surges and the variance of antarctic ice sheet contributions to sea-level change. Furthermore, overtopping of flood defences is found to be the main failure mechanism for the area, although this is highlighted to be site-specific.

Globally, Rohmer et al. (2021) assess the influence of uncertainties in coastal flood risk estimates. The approach follows an MC framework to estimate the expected annual damage and adaptation costs on a global level. The analysis considers almost all of the SPRC components. In terms of the sources, it includes uncertainties in extreme water level height and future sea-level rise (global and regional). Rohmer et al. (2021) include five different population growth scenarios as well as two population distribution models (Receptors). Lastly, it explores the uncertainties in depth-damage curves as well as factors to translate assets to GDP (Consequences). The study uses a bathtub approach to determine the areas of the coast located below a given elevation to estimate the number of people exposed to coastal flooding. A series of estimates are conducted, and the outputs of the assessment are introduced to a machine learning algorithm. This facilitated the generation of large volumes of results without the computational costs or running a large number of simulations. The analysis finds that at present and for the next 20 years, CFR estimates are highly sensitive to the accuracy of extreme water level heights and the methods to translate damage into costs. In the long range, the authors find population growth to be the largest source of uncertainty for global FRA. However, the analysis finds that if adaptation costs are considered, it is the accuracy on future sea-level rise that causes the most variabilities. One of the key

strengths of this study is the inclusion of dependencies between the variables, namely sea-level rise and population growth.

The probabilistic assessments of uncertainty can also be focused on individual SPRC components. For instance, Le Cozannet et al. (2015) analysed the variance in CFR caused by factors affecting the extreme water levels for a section of the coast in the south of France. These included sea-level rise scenarios and wave parameters. The study indirectly assesses the pathways by exploring uncertainties in the height of coastal defences. The variance-based Sobol indices are used to determine the sensitivity of flood risk to the input parameters. A QMC approach is used to generate input samples for the assessment. The authors find the factors determining the coastal processes of extreme water level propagation to be the main source of uncertainty in CFR estimates for the 21<sup>st</sup> century. These are followed by variability in local sea level and global SLR.

## 2.7 Summary

This literature review has provided a background on the coastal flooding mechanisms, the available methodologies to assess them as well as some of the methods to analyse their uncertainties. As a result of this review, the following knowledge gaps are identified:

In regards to the Sources of coastal flood risk

There is still uncertainty on the possible consequences of climate change to the coastal system, particularly on the possible rate of future sea-level rise. At present, it is still not well understood if and how storminess may change as a consequence of climate change. Variations in the weather patterns can modify the levels of threat, not only by creating exposure in new areas but also by increasing the magnitude of the storm surges. Changes in the ocean conditions (e.g. water temperature and depth) can further alter the propagation of extreme water events.

Statistical analysis of sea-level information to determine the magnitude and return interval of EWL relies on the length of sea-level records or, more recently, in the outputs of hydrodynamic models. These statistical assessments are constrained by the length of sea level measurements and the confidence of the hydrodynamic models. Moreover, there is still debate on the accuracy of analyses that utilise skew surge or residual surge heights for EWL estimates. It has been shown that combining the uncertainties of EWL estimates with those of climate change and associated SLR lead to up to 1.5m uncertainty for the Sources.

## Chapter 2

### In relation to the Pathways

Coastal pathways have constant interaction with the sources, and any changes in the latter will affect the former. There is uncertainty in the evolution of coastal defences as a consequence of climate change. It is possible that areas at equilibrium start experiencing erosion or accretion, as well as defence weathering.

It has been argued that the present data on defence conditions in England has large uncertainties as it relies on visual inspection of the elements by the Environment Agency, which can fail to assess the internal condition of the structures. The lack of specific data has resulted in the use of general fragility curves for each type of defence, depending on their condition. However, it has been shown that these fragility curves are not always representative of the type of pathway that a defence can experience. Furthermore, methods for pathway analysis are based on empirical data, which may not be representative of the conditions that every type of defence will experience throughout its design life. Finally, there are considerable knowledge gaps in sequential loading and pathway evolution. Continuous research is required to better understand the uncertainties derived from visual inspection of coastal elements and the implications this has on estimates of risk.

### In regards to the Receptors of flood risk

Predicting migration to and from the coastal area remains as one of the main challenges coastal managers face. In particular, it is still not well understood how people at the floodplain will respond to natural hazards and the implementation of coastal infrastructure. Present estimates of risk fail to consider the characteristics of properties in the exposed areas for better population distribution, which can lead to overestimating the levels of risk, particularly in areas with vertical development. The national, regional and local assessments of risk can be significantly improved by considering the aforementioned.

### In terms of the Consequences of flood risk

Previous studies tend to estimate the consequences of flood events with the use of empirically obtained factors that relate the number of people exposed to the economic consequences. Most of these studies use the country's GDPppp to determine the number of assets exposed. It is difficult to determine the exact impacts of flood events on a small scale as there is not enough data on the particulars of properties and economics of the exposed areas. However, this fails to represent the spatial wealth distribution of a country. It is then necessary to produce assessments that consider the economics of the threatened areas.

In regards to the methods to assess coastal flooding

The improvement of computational capabilities has lead to the use of more robust methods to simulate inundation of coastal areas. There are still some constraints, and resolution versus computational time are often factors to be considered. New software is available to estimate the extent of floods can be used to compare and update the present estimates derived from simplistic methodologies, such as the planar method and the rapid inundation simulations.

In terms of studies analysing uncertainty in coastal flood risk estimates

Two main approaches can be followed to explore uncertainties in CFR. The first one being a non-probabilistic approach that makes use of scenarios. The second one, on the other hand, relies on probabilistic analyses of the input factors. From the various examples given of the application of both approaches, it can be appreciated that only a few incorporate all of the SPRC components in their analysis. Furthermore, it appears that the computational costs of running inundation models have made the authors resort to basic methods and coarse resolution data to determine the extent of the floodplain. Future research should be conducted incorporating all components of the SPRC framework on either a probabilistic or non-probabilistic framework to investigate their influence on the uncertainties in coastal flood risk. In addition, the improvement in computational capabilities makes it possible for such assessments to incorporate medium to high-resolution inundation models for their assessments. By doing so, more accurate estimates can be performed as uncertainties are reduced.





## **Chapter 3   Study Site**

### **3.1   Introduction**

This chapter provides a description of the Solent, the chosen case study site. First, Section 3.2 provides an overview of the region. Section 3.3 briefly highlights previous coastal flood events in the area. Section 3.4 reviews previous assessments of coastal flood risk in the area.

### **3.2   Overview of the Solent**

The Solent, located in the south of England (Figure 3.1), is the largest estuarine system on the south coast of the UK. It encompasses the 386km of coastline between Hurst Spit at the West, and Selsey Bill, West Sussex at the East (NFDC, 2010). This thesis considers the entirety of the Isle of Wight as part of the study region. The Solent includes Portsmouth, Langstone and Chichester Harbours, Southampton Water, and several tidal rivers, including the Lymington, Beaulieu, Test, Itchen, and Hamble rivers. The Solent formed at the Southern margin of the Hampshire Basin. Before the Holocene, the Solent encompassed river systems, forming one of the major tributaries of the "English Channel River". Progressive inundation caused by the Holocene sea-level rise during the 9000-7000 years before present-day changed the hydrodynamic conditions, shaping the area through erosion and deposition (Velegrakis, 2000).



Figure 3.1 Location of the Solent, UK

The complexity of water circulation in the Solent has been widely recognised. The tidal regime in the Solent is semi-diurnal, with the tidal range increasing from 2.2m at Hurst Spit in the West to 5m at Selsey Bay in the East. The complex geometry and proximity to an amphidromic point create a double high tide and strong asymmetry in the tidal cycle. The duration of the flood tide lasts longer than that of the ebb. This has significant implications for flooding assessment as water coming into the region stays for periods of up to 8 hours. The geometry and tidal characteristics of the Solent create internal resonance (Townend, 2007). At mid-flood tide, the volume of water entering the area remains constant. This is called the "young flood stand" and lasts for about 3 hours (Pugh, 1987), allowing sedimentation of fine material over a more extended period favouring marsh and mudflat creation. These intertidal areas have long been recognised for their ecological value and received natural and international designations. Approximately 80% of the Solent's coastline has a European or International conservation designation as Ramsar sites, Special Areas of Conservation, Special Protection Areas and Marine Conservation Zones (Figure 3.2). This includes Medmerry, one of the most extensive managed realignments (MR) in the UK, covering over 300 hectares. The Medmerry MR is located in the vicinity of Selsey Bill, and it was conducted to provide flood protection and habitat creation (McAlinden, 2015, ABPMer, n.d.).

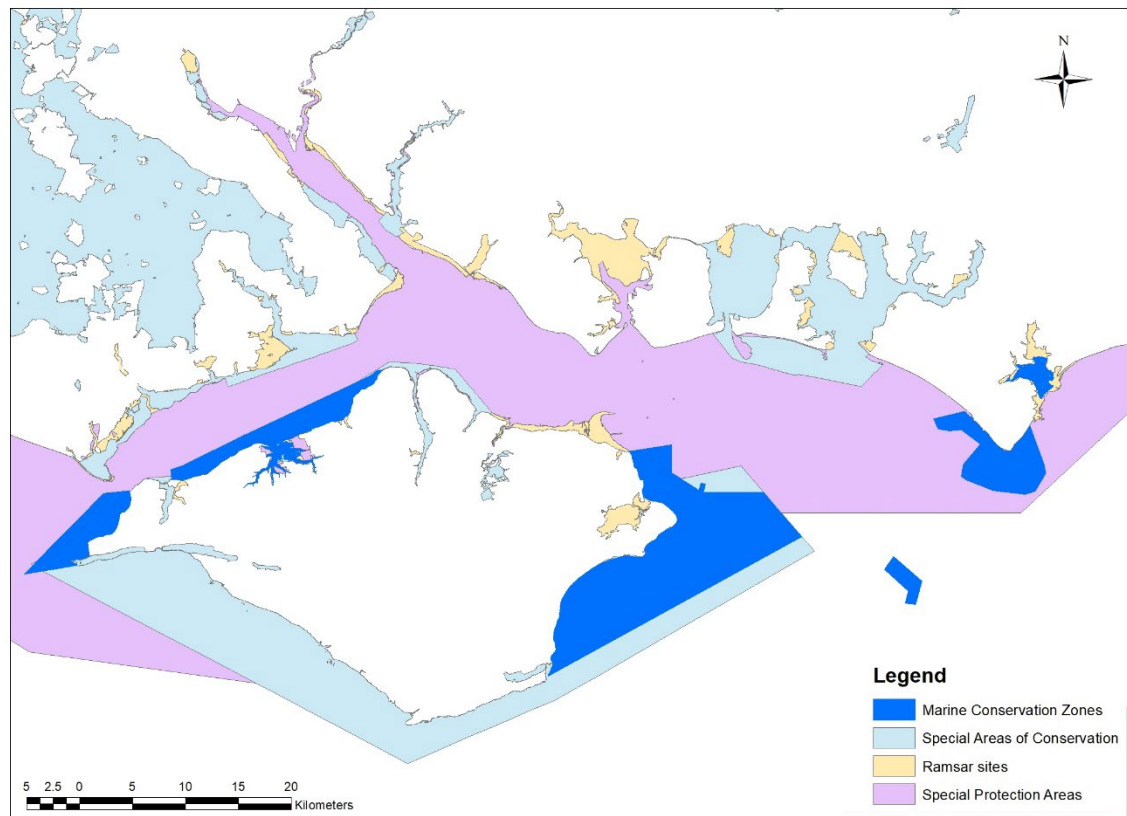


Figure 3.2 Special Areas of Conservation, Special Protection Areas, Marine Conservation Zones and Ramsar sites within the study region.

The wave climate is generally calm in the area as the proximity of the Isle of Wight and orientation of the estuary limits wave fetch. The largest waves found in the Solent are those generated along the East and West. However, the presence of Hurst Spit, a shingle barrier at the western end, constrains wave propagation into the estuary. The Solent area is significantly affected by meteorological induced storm surges of up to 1m caused by low-pressure systems, mostly moving from the Atlantic eastward to the south of England (Haigh et al., 2004a, Haigh et al., 2016).

Throughout modern history, the Solent has experienced large human intervention. Anthropogenic modification of the coastline through land reclamation can be traced back to 1783 (Townend, 2007). Residential, commercial, industrial and agricultural development govern the areas adjacent to the coast. Major cities are in this area, including Portsmouth and Southampton. The former is one of the most densely populated areas in the UK, with a highly urbanised, low-lying coastal area. The latter is home to the primary UK vehicle handling port, the second-largest container terminal and a major destination for cruise lines ships, with over 1.7 million passengers per year (Associated British Ports, 2021). The Office for National Statistics (ONS) identifies 91 Built-up Areas (BUA) within the extent of the study region. The BUA refers to areas with a minimum of 20 hectares and an irreversible urban character, such as major towns or cities (ONS, 2011). Out of

the 91 BUA in the region, 48 are fully or partially located within the 1 in 10,000-year floodplain (Figure 3.3).

The high urbanisation rates of areas within the floodplain at the Solent have created the need for investment in coastal defences. Over 75% of the shoreline is protected from flooding and erosion by natural approaches, such as beach nourishment, and through hard structures like groynes and seawalls. However, many of these are close to reaching the end of their residual or engineering design life (New Forest District Council, 2010). Further problems arise from land ownership, as over 60% of the shoreline is privately owned, and some defences are maintained by third parties (New Forest District Council, 2010). This diversity of stakeholders results in coastal management issues, with the latest North Solent Shoreline Management Plan (NSSMP) identifying over 220 interest groups.

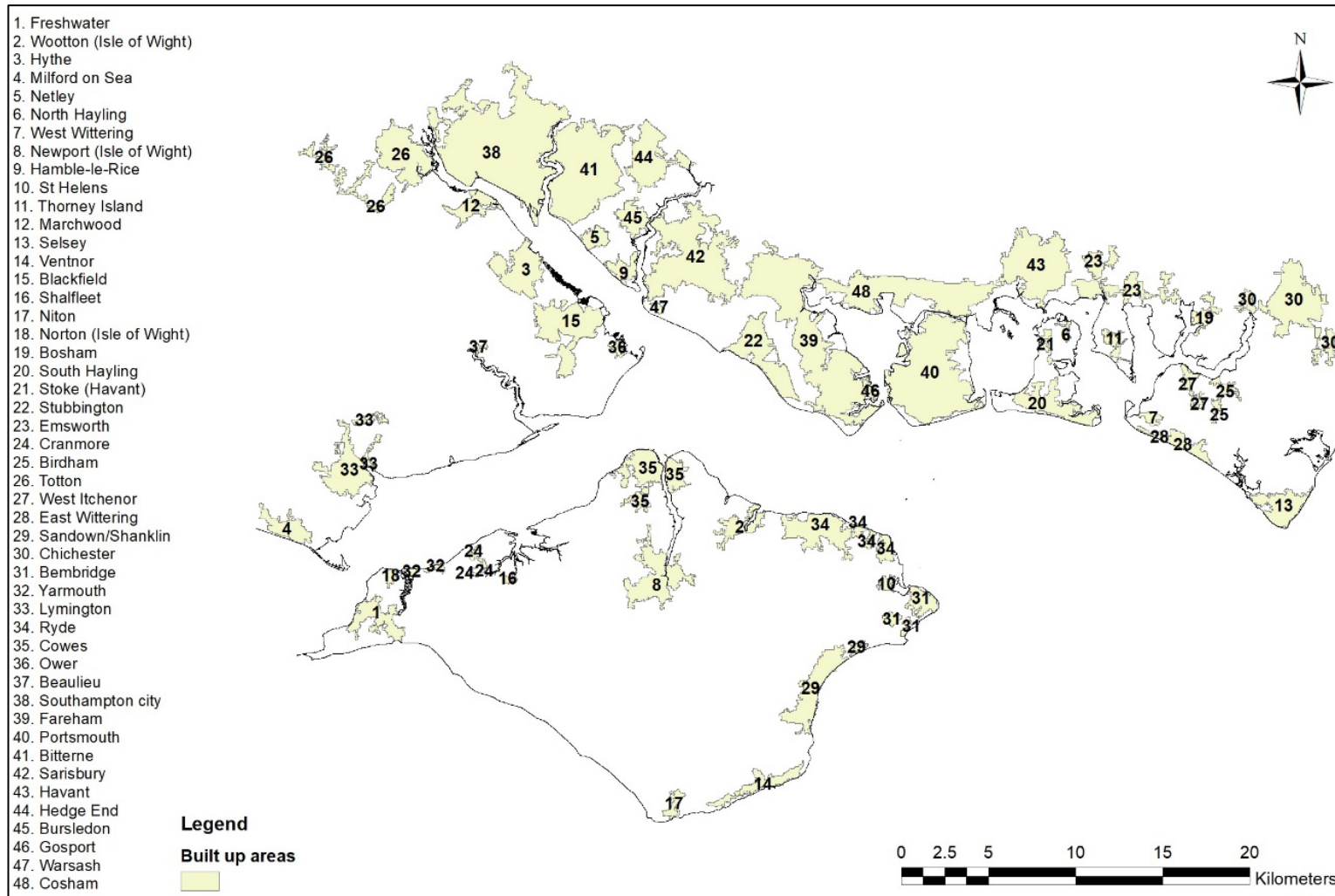


Figure 3.3 Built-up areas in the Solent within the 1 in 10,000-year floodplain.

### **3.3 Coastal flooding at the Solent**

The Solent has experienced the effects of coastal flooding throughout its history. The severity of a series of storms in December 1989 caused the Hurst Spit shingle barrier in the western region to breach (Davison et al., 1993, Stripling et al., 2008, Ruocco et al., 2011). Furthermore, these affected several areas, including Lymington, Pennington, Portsmouth, Fareham, Emsworth, Cowes and Yarmouth. Similarly, high seas resulting from the combination of high tide, large waves and a significant storm surge in March 2008 caused widespread flooding in the area. Most of the affected areas, including Southampton, Fareham, Lymington, Portsmouth, Havant, Chichester, and several areas of the Isle of Wight, experienced nuisance flooding caused by overflow and overtopping of flood defences (Wadey et al., 2013). However, severe flooding occurred at the site where the Medmerry managed realignment is nowadays located and at a holiday park near Selsey. In the last decade, the storm Xavier in December 2013 coincided with large astronomical tides causing flooding in Lymington, Hamble, Havant, Chichester, Cowes and Yarmouth (Wadey et al., 2015b).

Interestingly, the December 6, 2013 event was the second-highest on record at Portsmouth. However, no flooding occurred in this area, highlighting the protection given by flood defences. Further to this, on February 14, 2014, a storm coming from the Atlantic caused a storm surge with an equivalent return period of 1 in 9 years. This storm caused damage to Hurst Spit and flooding in Lymington and some areas in Southampton (Kerins, 2014). However, the possible effect of the EWL on other areas of the Solent was diminished by the presence of coastal defences. In this sense, even though higher and more constant extreme sea levels have occurred in recent decades, the number of damages has been shown to decrease (Ruocco et al., 2011), most likely due to the implementation of coastal defences in urbanised areas. However, a comprehensive analysis of the influence of the SPRC components on the past, present, and future levels of coastal flood risk has not been conducted for the study area.

### **3.4 Previous assessment of coastal flood risk in the area**

Extensive research has been conducted on some of the SPRC components in the Solent. For example, studies analysing the sources include the work by Quinn et al. (2012) on tide surge interactions. In general, the study found a difference of up to 0.3m between recorded and predicted water levels. The latter comprised the height of a storm surge added to the tidal curves obtained with harmonics analysis of the area, which, in general, the study attributes to the underprediction of the tidal range. However, the total water level errors generated when the tide-

surge interaction is considered are expected to be relatively small. These uncertainties are a product of the complexity of tidal predictions in complex estuarine regions like the Solent. The study highlights that tide predictions using harmonics analysis are of adequate quality to analyse the area. More importantly, the assessment finds that tidal elevations can be effectively interpolated from gauge to un-gauge areas. The latter is of particular interest for the present research as the only Class A tide gauge in the area is located in Portsmouth Harbour.

Flood pathways were reviewed by Wadey et al. (2012) and Wadey et al. (2013) through the analysis of coastal defence systems in the area. These are, up to date, some of the most recent and complete assessments of coastal flooding at the Solent. Similar to the present assessment, Wadey et al. (2012) utilised a two-dimensional (2D) flood inundation model to assess the impact of extreme water levels in the area. The analysis is thorough and considers flood defence failure mechanisms such as overflow and overtopping. The latter was analysed separately from the inundation model, with the discharge volume produced by waves translated into a water height added to the still water level used for overflow failure. One of the most significant shortcomings of the analysis is the way flood defences are handled. Initially, flood defences are masked onto the digital elevation model. This prevents the model from analysing the effect of weirs in changing the flow conditions.

Furthermore, under some scenarios, the analysis estimates the theoretical volume of water that could enter the floodplain based on the time that the water level is above the height of the defences. It then proceeds to move the inflow conditions landwards of the defences and inputting this volume as a constant discharge. This is a serious problem as there is no consideration of the drowned weir effect, and the water depth landwards of the defence is assumed not to have an influence on the flow of water over the defence. The drowned weir effect occurs as the level of water landwards of the defence increases and reaches a ratio of 0.9 of the seaside water level. This effect reduces the capacity of water to freely flow into the floodplain until the flow transforms into an open channel flow. In addition, once this condition is reached, the presence of the weir creates high friction losses (Benn et al., 2019). Further to the omission of a drowned weir case, Wadey et al. (2012) assume that the water level inside the defence will never be high enough for flow to reverse directions out of the floodplain. It is not possible to accurately quantify the effect the inclusion of such phenomena on large scale coastal flood modelling as it would require analysing each section of defence at every time step to determine when these occur. However, it is clear that ignoring these scenarios will most likely lead to more extensive floodplains and overestimates of flood risk and exposure.

The effect of changing receptors was analysed by Stevens et al. (2015) and Stevens (2017) through historical mapping of urban extents at the floodplain. The studies mainly focused on the Portsea and Hayling island regions, closely following Wadey et al. (2012). The assessments utilise Ordnance Survey historical maps to determine the extent of the urban footprint and explore the population evolution in the area. The assessments conclude that historical risk for Portsea and Hayling is driven by the combination of increases in population, population density and changes in mean sea level. This is a logical conclusion if the metric used to determine risk is the number of people flooded. The assessments highlight that it was not possible to determine when coastal defences were implemented at Portsea and Hayling Islands.

In terms of consequences, Ruocco et al. (2011) examined the consequences of historical coastal flooding events over the last 70 years (1935-2011). Boza (2018) expanded this analysis and identified coastal flooding events from the 1800s up to the present. The latter assessment utilised a similar technique to Ruocco et al. (2011) to obtain evidence on the consequences of extreme water events and analyse the severity of the flood. Both studies indicate that most recorded events caused nuisance flooding of open areas and streets with no properties flooded. Their results also show that as severity increases, the number of events decreases. Only a few reach a category four or above, equivalent to significant flooding of large areas with more than 0.3m of water (Figure 3.4). Analysing their findings, there is a clear seasonal pattern with more events recorded in the winter months. It can also be appreciated that higher-category events tended to decrease after 1960 and stopped after 1980 (Figure 3.4.c). As suggested by Ruocco et al. (2011) and Boza (2018), this could be attributed to improvements in flood protections and decreasing storm intensity.



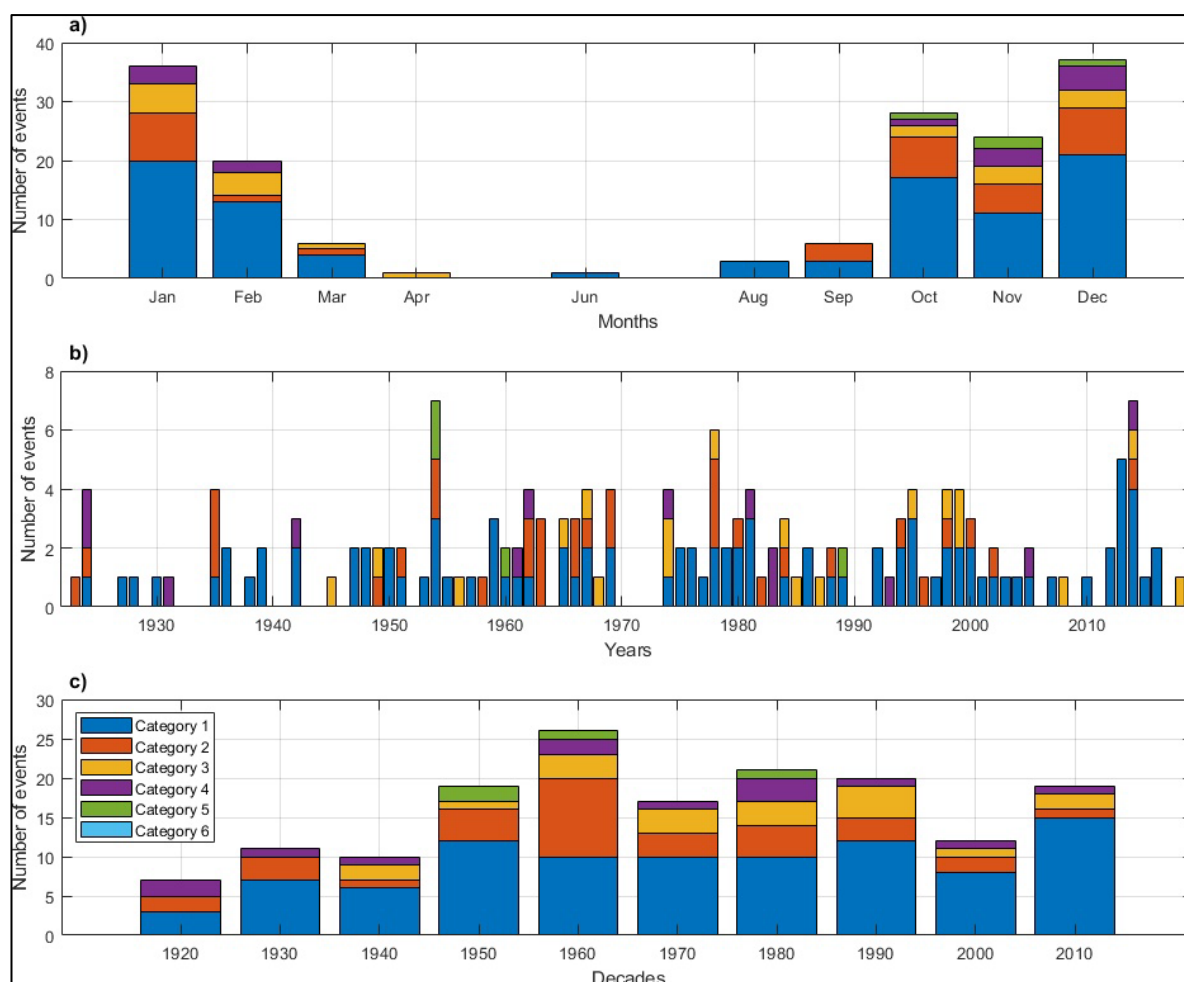


Figure 3.4 Number and severity of coastal flood events registered at the Solent over the last 100 years by a) month, b) year, c) decade. Data from Ruocco et. al. (2011) and Boza et. al. (2018). Category 1 represents nuisance flooding. Category 2 are minor flooding in open areas. Category 3 are moderate flooding of up to 2.5 feet over localized areas. Category 4 are major floods of over 2.5 feet of water over large areas. Category 5 are severe floods over large areas with livestock drowned and people injured. Category 6 are disastrous events with one or more human lives lost.



## Chapter 4 General Methods

### 4.1 Introduction

Coastal flood risk assessments require a systems approach where the individual and mutual interactions of its components are considered. As mentioned, the SPRC framework is a valuable tool to do so. It is known that sea levels have changed, and they are expected to continue changing in the future. Coastal defences have been implemented at the study area, and the increased presence of population and assets is likely to create positive feedback on demand for protection. These variations in extreme sea levels and mean sea level (sources) can be expected to dictate the threat level, whilst the presence and improvement of flood defences (pathways) can decrease the ability of water to enter the floodplain and affect the local population (receptors). However, it is not clear how these components have interacted in the past, leading to the present levels of coastal flood risk. Furthermore, it is imperative to explore their effect on the possible evolution of CFR under future scenarios. Given the above, this thesis presents a methodology where the past, present and future variations of the SPRC components at the Solent are assessed to understand their influence on the threat levels. This methodology uses the best available data for the SPRC components at each timestep. This information is merged in the inundation and population distribution models to estimate the number of people at risk of coastal flooding under different configurations (Figure 4.1).

The metric used throughout this thesis to determine the level of threat is the number of people at risk of coastal flooding. Previous assessments (e.g. Hinkel et al., 2014) tend to report risk in economic terms. Attempting to do this would add another layer of uncertainty to the analysis since, as mentioned in section 2.3.4.3, there is uncertainty on the factors used to translate population to assets. Another metric that could be used to report risk is the number of properties exposed, as done by Wadey et al. (2012). However, it is difficult to predict the areas where future residential developments might occur within the study region. Therefore, the number of people at risk is selected as the most appropriate metric for the analysis. Consequently, it is necessary to determine the population distribution in the study region. The setup for both inundation and population distribution models and their integration to determine the level of coastal flood risk are presented in the following sections.

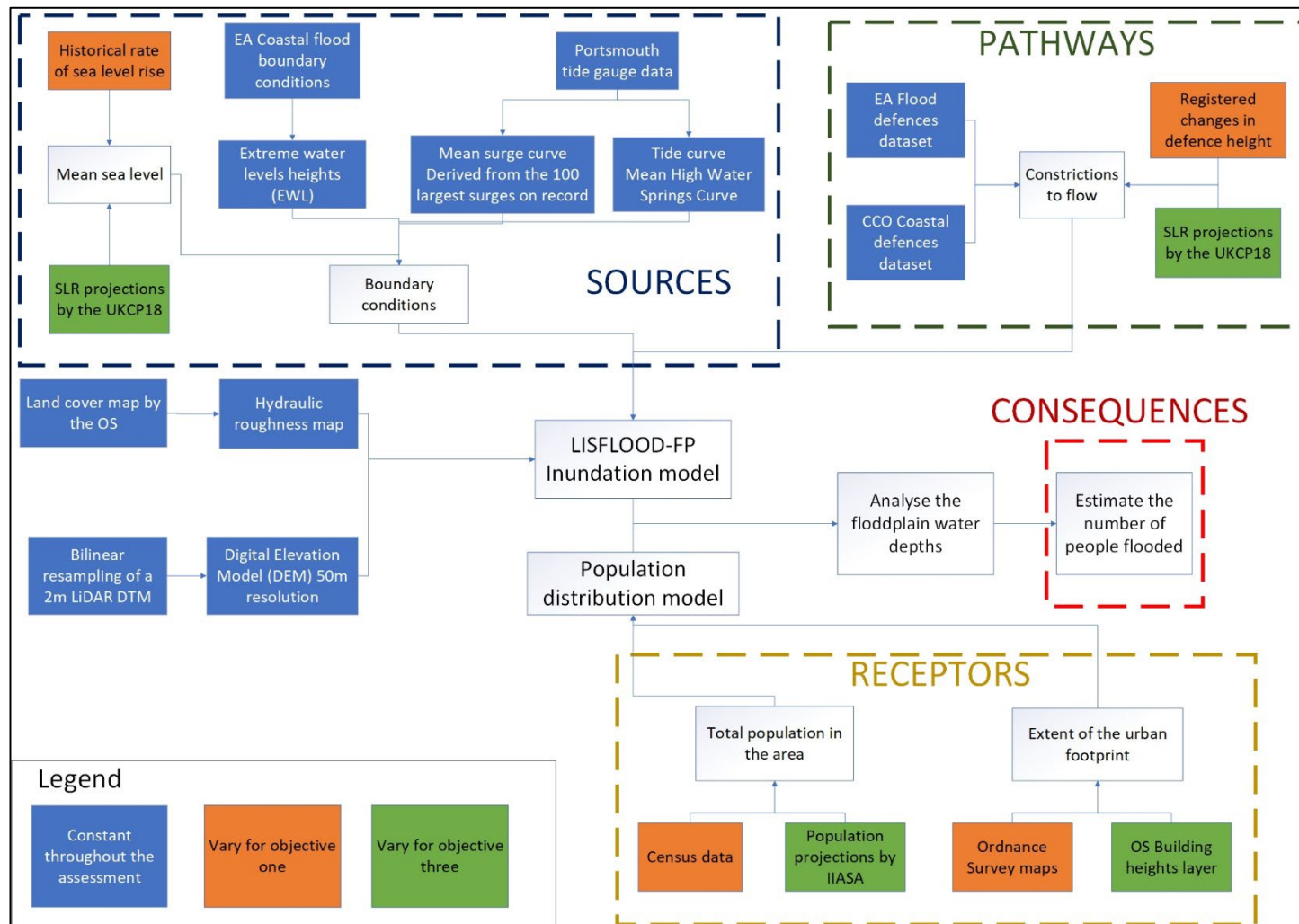


Figure 4.1 Overview of the general methods in relation to the SPRC framework.

## 4.2 Hydrodynamic model set-up

The basis of any flood risk analysis lies in the ability to determine the extent of the floodplain under given extreme water levels. For this purpose, LISFLOOD-FP, a 2D flood inundation model, is selected for the present study due to its simplicity, accuracy and relatively low computational demand. This model has been used in many coastal inundation studies (e.g. Bates et al., 2005, Dawson et al., 2009, Coulthard et al., 2013, Seenath, 2015, Skinner et al., 2015, Christie et al., 2018). Furthermore, some of the most relevant assessments of coastal flooding at the Solent have utilised LISFLOOD-FP (e.g. Wadey et al., 2012, Wadey et al., 2013, Quinn et al., 2014, Stevens et al., 2015), allowing for an almost direct comparison with the estimates of this thesis. LISFLOOD-FP requires some general inputs, such as an elevation model, a set of boundary conditions, indications of the presence of defences or elements that constrain water flow, and a hydraulic roughness map or a general friction value if a constant roughness is selected.

LISFLOOD-FP utilises the topography to determine the routes through which water can spread. The topography of the Solent is input as a DEM obtained from the Environment Agency Light Detection and Ranging (LIDAR) dataset. The EA provides a Digital Surface Model (DSM) and a Digital Terrain Model (DTM) at different resolutions. The DEMs are obtained through an airborne mapping technique. The DTM is generated from the last return LIDAR pulse as it reflects off the ground and surface objects. On the other hand, the DSM is generated by filtering out objects on the surface through automated classification and manual filtering to produce a ground surface model (Environment Agency, n.d.-b). This model is meant to represent, as accurately as possible, the terrain surface without the presence of vegetation, buildings and human-made objects. The EA's specifications indicate that the absolute height error, that is the root mean squared error (RMSE), has to be less than 0.15m when compared with the ground truth survey (Environment Agency, n.d.-a). For the present study, a 2m resolution DTM is obtained and resampled to 50m resolution using a bilinear interpolation technique on a Geographic Information System (GIS). The elevation model extends seaward up to the present-day mean low water springs line by the OS. The 50m horizontal is selected as it offers a good level of detail for the area whilst maintaining a relatively low computational demand. Savage et al. (2016) indicate that there is little gain in performance using elevation models with a resolution higher than 50m and instead utilising these results in high computational demand. Preliminary assessments were conducted analysing the effect of a 10m resolution elevation model against a 50m DEM. The average computational time is 01:03:14 for an inundation model with a 10m DEM, whilst this is reduced to 00:03:39 with a 50m DEM. Furthermore, Savage et al. (2016) find that the variations caused by coarser DEM

resolutions are averaged out over the domain when compared to results from high-resolution models.

### 4.2.1 Boundary conditions (Sources)

In the context of the present assessment and following the SPRC conceptual framework, the SPRC-sources constitute the boundary conditions for the inundation model. The sources are comprised of the EWL, which result from the combination of mean sea level, astronomical tide, a non-tidal residual and waves. Even though waves contribute to the height of EWL, these are not included in this thesis due to the complexity of their analysis. Incorporating waves would require high-resolution information on the bathymetry of the foreshore and data on the individual characteristics of the flood defences, which is not always available for the study region. This information is necessary to determine whether the waves would be capable of reaching the flood defences or floodplain and determine the type of breaker and the consequent effect on EWL. Furthermore, it would be necessary to assess the evolution of the coastal morphology under future sea-level rise scenarios and how these new configurations might affect wave propagation.

Based on the above, EWL are hereon considered as the sum of mean sea level, tidal and non-tidal components. The tide and surge curves are determined by analysing the Portsmouth tide gauge, as this is the only A-Class tide gauge in the area. The data for this site is available from the British Oceanographic Data Centre ([www.bodc.ac.uk](http://www.bodc.ac.uk)). The record extends from 1991 until the present day. The information is provided yearly, with sampling intervals of 60 minutes for data collected before 1993 and every 15 minutes from then onwards. Unfortunately, the information is not complete for every year on record. The BODC applies quality controls, and suspicious data are often flagged as improbable. However, a visual examination of the records was necessary to identify any spurious data that could have bypassed the quality controls. The data is analysed, and a harmonic analysis is performed with T-Tide using the 67 standard tidal constituents (Pawlowicz et al., 2002) to separate the astronomical tide from the non-tidal component (i.e. storm surge). Lastly, the dates on the record when spring tide occurred are identified using tide tables, and a characteristic MHWS tidal curve is obtained.

After separating the tide and non-tidal residual, every storm surge on record is ranked by maximum water level and catalogued using the r-largest method, and declustered using a storm duration of 48 hours to guarantee that only one maximum water level per surge is considered. The 100 largest surge events are extracted, and their data smoothed using a 4-hour moving average as these contain noise, most likely produced by high-frequency variations such as seiches that are not considered for the present assessment. A mean of the smoothed surge curves is

obtained from the identified 100 largest surge events (Figure 4.2). This mean smoothed curve can be added to the MHWS curve and the total height compared and adjusted to match any desired extreme water level.

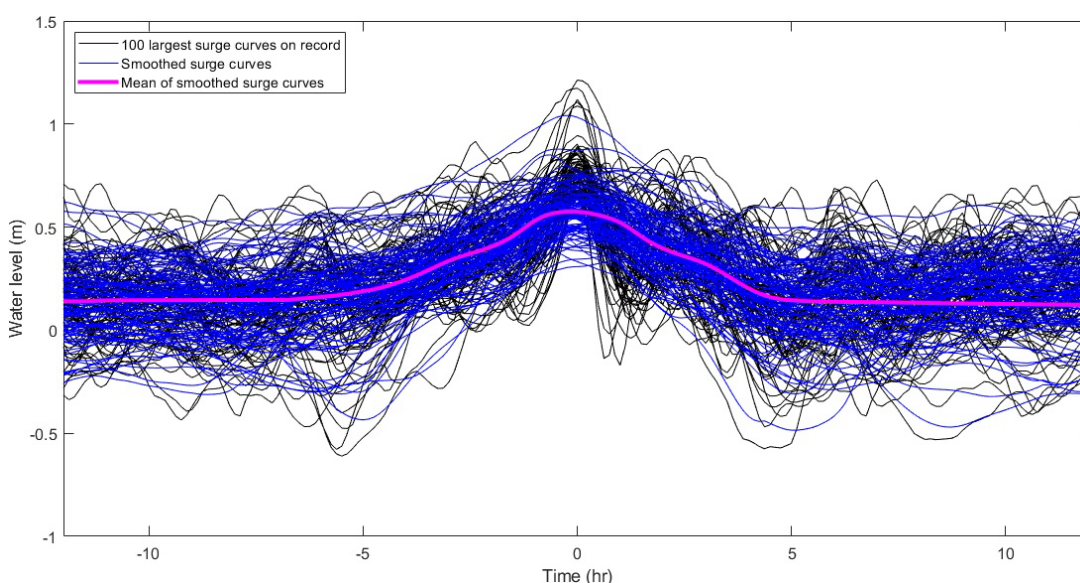


Figure 4.2 Analysis of the 100 largest storm surge curves on record at Portsmouth tide gauge

As done in previous assessments (e.g. Wahl et al., 2011, MacPherson et al., 2019), the mean surge curve is utilised as the basis of the assessment. However, unlike the mentioned assessments where additional variables such as initial, peak and final water levels of the initial surge curves are recorded, the focus is here given to the start and end times as the height of the surge will be modified in later stages. These start and end times are used to determine the length or amplitude of each surge event.

Point sources are used along the coast with a set of dynamic flood boundary conditions. These comprise inflow points located along the Ordnance Survey mean high water springs (MHWS) line at a 50m interval to maintain consistency with the DEM resolution. The inflow points are assigned a time-varying water curve, which results from the combination of a tide and a storm surge curve.

#### 4.2.2 Hydraulic roughness map

Analysing the ability of water to flow within the domain requires the inclusion of a friction factor that accurately represent the constrictions to flow given by the terrain characteristics. Seenath (2015) demonstrated that using spatially distributed friction does not significantly increase the accuracy of the floodplain extents estimated with LISFLOOD-FP. However, it is clear that the terrain conditions greatly vary across the study region. As presented in section 3.2, the topography and characteristics of the Solent's coast range from natural coastlines with estuaries, salt marshes, sandy beaches and rocky shores to rural coastal areas as well as highly urbanised

## Chapter 4

floodplains. For this reason, a hydraulic roughness map of the region is created using the OS aggregate class land cover map at a 1km resolution (Figure 4.3). The equivalent Manning hydraulic roughness coefficients for each type of land cover are obtained from Engman (1986) (Table 4.1).



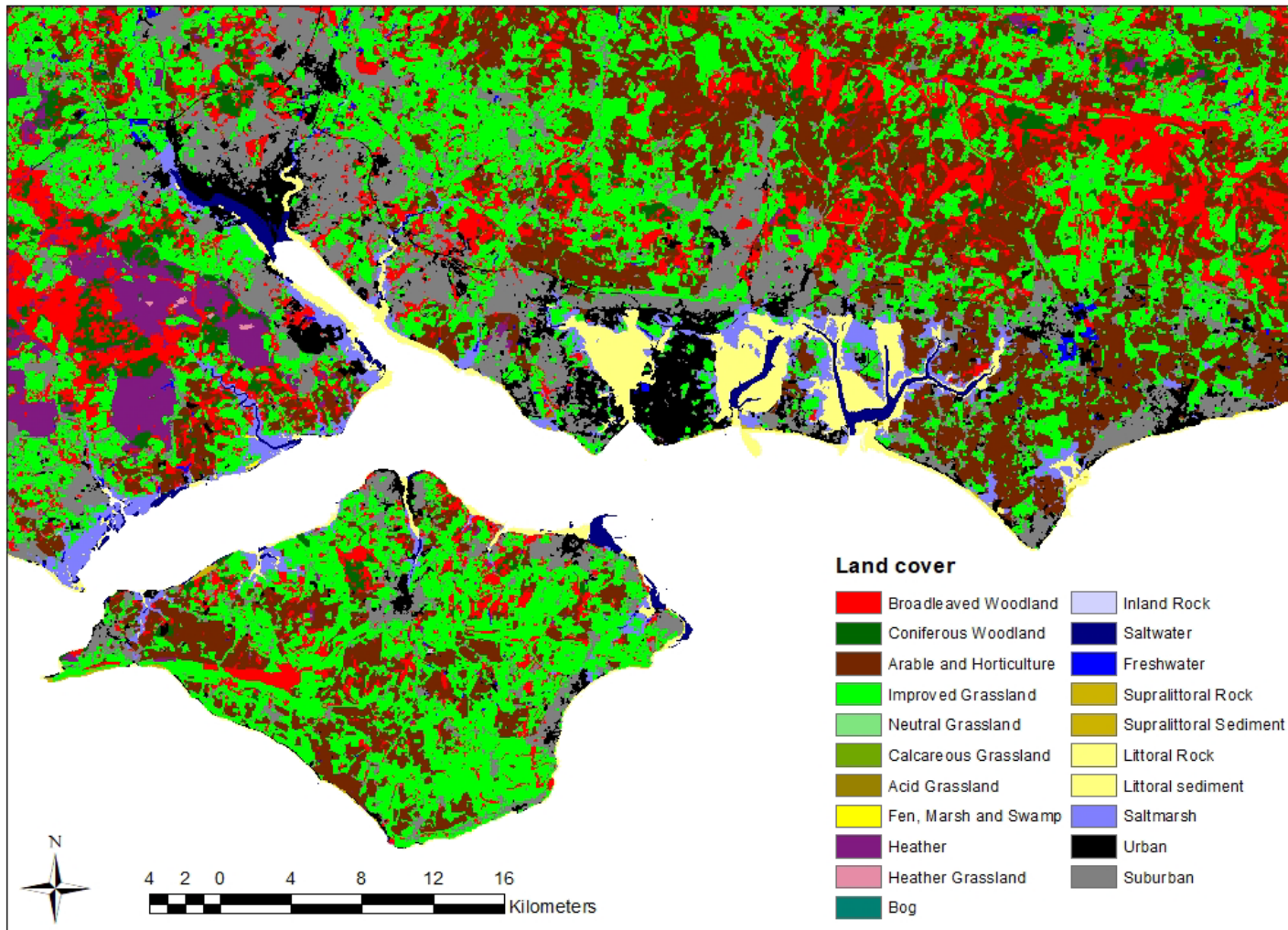


Figure 4.3 Different types of land cover present at the Solent. Data from the Ordnance Survey aggregate class land map

Table 4.1 Hydraulic roughness coefficient for different types of land cover

Ordnance Survey Aggregate class		Equivalent manning number (roughness coefficient) from Engman (1986)
Number	Description	
1	Broadleaf woodland	0.15
2	Coniferous woodland	0.075
3	Arable	0.035
4	Improved grassland	0.035
5	Semi-natural grassland	0.03
6	Mountain, heath, bog	0.6
7	Saltwater	N/A
8	Freshwater	N/A
9	Coastal	0.015
10	Built-up areas and gardens	0.011

#### 4.2.3 Barriers to flow (Pathways)

One of the critical components in flood modelling is the accurate representation of structures that reduce water flow. In this case, these are constituted by flood defences, both inland and at the coast. The presence and characteristics of these are obtained from the EA Spatial flood defences dataset (Environment Agency, 2020a). The EA dataset comprises locally collected data, and the information is provided in a GIS geodatabase in the form of lines representing each defence. Some of the critical information obtained with this data is the type of protection, whether fluvial or coastal, a description of the defence, the standard of protection, defence height, and overall condition (Table 4.2). Previous assessments (e.g. Wadey et al., 2012) have failed to consider fluvial defences in the area. However, the present assessment aims to represent the area's physical conditions accurately, and it is clear that these defences constitute barriers to flood water. Furthermore, preliminary assessments showed that these significantly affect the total extent of the floodplain.

Table 4.2 Example of the data contained on the Environment Agency Flood Defence dataset.

<b>Object ID</b>	<b>Downstream crest level</b>	<b>Upstream crest level</b>	<b>Type of protection</b>	<b>Description</b>	<b>Design SoP*</b>	<b>Condition</b>	<b>Year built</b>
1	48.61	48.72	Fluvial	Wall –(NonFlood) Masonry	2	2	0
2	49.66	50.02	Fluvial	Natural Bank	2	2	0
3	48.1	50.02	Fluvial	Natural Bank	2	2	0
4	8.5	8.08	Fluvial	Natural Bank	2	2	0
5	50.98	51.38	Fluvial	Embankment (NonFlood) Earth	2	3	0
31	2.31	2.31	Fluvial-Tidal	Wall (Abutment) Concrete	0	2	0
32	1.63	1.73	Fluvial-Tidal	Natural Bank	2	3	0
527	3.06	3.06	Tidal	Wall (Abutment) Masonry	2	2	0
556	0	1.71	Tidal	Wall	0	3	0
7709	10.95	10.95	Fluvial	Spillway	100	2	0
7789	0	0	Coastal	Embankment (Flood) Earth-Clay Core	200	2	2007

\*Standard of Protection (SoP)

The EA obtains the defence location and height data from various sources. For instance, local authorities provide insights on their coastal segments, whilst some of the defences' condition is directly assessed by the EA following the asset inspection guidance (Brown et al., 2014). The manual provided to the surveyors informs them of the type of assessment and the procedure required to determine the asset's performance. In general, there are three tiers of assessments, each with different procedures, depending on the nature of the analysis. Tier 1 is the simplest of these and can consist of visual inspections to determine the asset condition and its standard of protection (used to infer its performance) and can be used for judgement on history-based

assessments. Tier 2 requires an engineering inspection and/or a crest survey. This can be used when comparing different options on an assessment through the simple incorporation of the assets on a systems model. Finally, Tier 3 is the most thorough assessment as it requires intrusive investigations by a specialist. The information obtained from a Tier 3 assessment allows for a complete asset and system modelling, which is, for instance, desired in cases when it is needed to confirm the ability of a structure to withstand a specific load (Brown et al., 2014). Unfortunately, there is no information on the type of inspection carried out for each defence. Likely, most of them were analysed under a tier 1, with only a few thoroughly inspected through a tier 3 assessment.

A fundamental limitation of the EA dataset is that it does not contain information on defences that are not owned, operated, managed or inspected by the EA (Environment Agency, 2017). Most notable is the lack of defences in Portsea Island, where most of Portsmouth is located. This is a significant shortcoming as Portsmouth is considered one of the areas with the highest level of coastal flood risk in England. It is then necessary to complement this crucial region's data using the Channel Coastal Observatory (CCO) defences shapefile (CCO, 2014). The CCO Portsea defences are supplied as lines similar to the EA's defence dataset. However, there is no information on the defences conditions, their standard of protection or any other relevant characteristics. The best source of this information is the 2010 North Solent Shoreline Management Plan, which provides maps and tables with basic information of the region's defences. These include the type of defence, its residual life and general condition (Table 4.3).

Table 4.3 Example of coastal flood defences information included on the 2010 North Solent  
Shoreline Management Plan

Management Unit	Unit	Defence type	Residual life (years)	Condition- based on NFCDD* Grades	Source
CPU10	Portsmouth Harbour Entrance	Groynes	1-10	Unknown	HBC**
		Sea Wall	1	4	HBC
		Rock Armour	1	3	HBC
		Revetment	11-20	3	HBC

\* National Flood and Coastal Defence Database

\*\* Havant Borough Council

Unfortunately, there is no mention of the SoP nor the height of the defences, and it is necessary to infer these from the available information. This is done by considering defences with a condition grade of 1 to have an SoP of 1:300; grade 2 with an SoP of 1:250; grade 3 an SoP of 200; Grade 4 with an SoP of 1:150 and grade 5 with an SoP of 1:100. The EA, CCO, and Portsea Island datasets are combined into a single GIS defence layer (Figure 4.4). This layer contains each defence segment's location, the standard of protection, condition, and residual life. The layer is processed, and points are generated every 10m along each defence.

It should be noted that in recent years, the coastal defences in Portsea Island have undergone significant upgrades. In Southsea, over £100 million have been invested in reducing the risk of flooding for Old Portsmouth and Eastney. On the northern end of the island, more than 8km of the coast see improvements in their defences (Coastal Partners, n.d.). Altogether, these projects aim to protect against a 1 in 500-yr extreme water level, including a mean sea-level rise allowance of over 0.80m in accordance with the highest projected rate of future sea-level rise by the year 2100. Given the temporal scope of objectives two and three, the standard of protection of the defences in Portsea is modified to incorporate these upgrades for the assessments of present-day and future levels of risk.

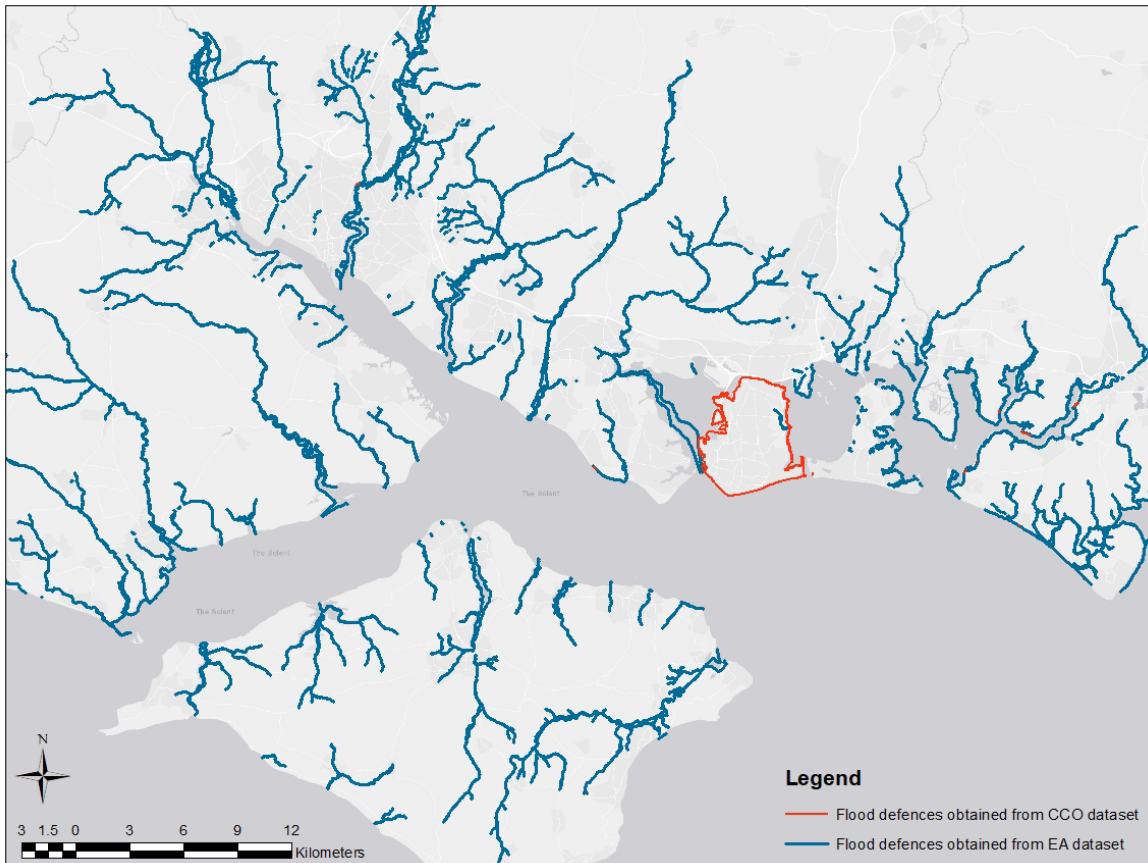


Figure 4.4 Coastal and fluvial flood defences present in the study region. Data from the Environment Agency (EA) Spatial Flood Defences with Standard Attributes and from the Channel Coastal Observatory (CCO).

Out of the three main pathway mechanisms presented in section 2.3.2 (overtopping, overflow and breaching), the only defence failure mechanism analysed in this thesis is overflow. This, as estimating the rate of overtopping, requires information on wave actions, which is not considered in the present study. Furthermore, the occurrence of overtopping and breaching are heavily dictated by the individual characteristics of the flood defences. These include the materials with which these were built (roughness) and their slope, which are not available for all the defences in the area.

#### 4.2.4 LISFLOOD-FP setup

The characteristics and basic equations of LISFLOOD-FP are presented in section 2.4. Out of the floodplain flow solvers available within LISFLOOD-FP, the “acceleration” solver is selected for the present study. This uses a simplified form of the shallow water equations, where the flow between cells is calculated as a function of the water slopes, water acceleration and friction of the terrain. It is the second most complex of the solvers. The so-called “Roe” solver includes all the

terms in the shallow water equations; however, this solver has only been tested on a limited number of scenarios; therefore, it is not yet considered as robust as the acceleration solver.

The initial conditions presented above are inputted to the LIDLOOF-FP model in the form of text files. These are translated by the program to perform the analysis. A visual representation of the model's setup is shown in Figure 4.5. A brief assessment of the accuracy of the hydrodynamic model used in this thesis is presented in Appendix A.



Figure 4.5 Visual representation of LISFLOOD-FP setup

### 4.3 Population distribution methods (Receptors)

Population distribution at the floodplain remains one of the most challenging factors to model for coastal flood risk analysis, particularly since societies have become more aware and better prepared to face and cope with the effects of natural disasters (Neumann et al., 2015, Hauer, 2017). Even though it cannot be directly attributed to it, the implementation of evacuation plans has contributed to the registered decrease in the number of human casualties during flood events. Furthermore, the number of people at the floodplain greatly varies throughout the day, altering the level of impact caused by extreme water levels (Percival et al., 2018).

Coastal managers often rely on models to estimate the number of people located in different areas as spatial information is not widely available. One of the most commonly used datasets for population distribution is that of the WorldPop, which offers almost complete coverage of the world's urban areas. However, the WorldPop dataset often infers the number of people in the area from indirect factors such as land cover data, statistical models from similar areas, etc. (WorldPop, 2021).

More often than not, the only reliable information available comes from a national census, which in the UK are conducted every ten years. However, high-resolution population distribution and its implications on privacy is a sensitive topic in the UK. Therefore, the data is only available at a scale where individual household characteristics cannot be identified to maintain confidentiality. This creates the need to employ models to obtain higher resolution population distributions.

The present assessment builds on Stevens et al. (2015), which was developed for two urban areas at the Solent. The method utilizes historical census data and distributes the population based on different assumptions. The basis of their analysis required manually digitizing the urban footprint of their study sites. This approach is only practical for small scale assessments as it relies on manual processing. Instead, Stevens et al. (2015) methodology is improved for the present study with the automatization of this process. The data availability required the development of two separate methods, one for the digitization of the historical urban footprint and a second one for the present-day and future assessments. The specific details of the urban footprint digitization are presented in sections 5.2.3 and 6.2.4 for the historical analysis and present-day assessments, respectively

Having digitized the urban area, a square grid mesh of 50m by 50m is overlaid to the Solent, and the grids within the urban footprint are identified. The population is then distributed across these grids based on the data available. Unfortunately, no information other than the total number of people in the region is available for most of the data prior to 1980, and different assumptions are made to distribute the population (section 5.2.3). When additional information on the spatial distribution of the census data is available, a more refined method is conducted. Such is the case of information on the 2001 and 2011 censuses, where the concepts of output area and population-weighted centroids (PPWC) are introduced. In this case, the population is distributed as a function of the proximity of each grid to a PPWC. Further details of these processes are presented in the relevant sections of Chapter 5 and Chapter 6.



## 4.4 Summary

Chapter 4 presents the general methods used for the analysis of the past, present and future levels of risk. Particular attention is given to the inundation model setup. This is the base component of the analysis, and accurately determining the extent of the flood is crucial for the estimates of risk. Chapter 4 starts by presenting the different elevation models available for the assessment and justifying the selection of a 50m horizontal resolution as this presents a good balance between detail and computational expense.

This is followed by the process conducted to obtain the boundary conditions. It consists of analysing the 30-year long tide gauge records of Portsmouth and obtaining a characteristic storm surge curve and a typical mean high water springs tidal curve. These are coupled, and the surge curve is stretched so that their total added height matches different extreme water level heights. The ability of water to flow into the floodplain is limited by different factors, such as the slope of the terrain, which is accounted for in the elevation model through the inclusion of the friction given by the types of land use. The friction given by the terrain is obtained with the use of a land cover map. The land cover types are then translated to friction coefficients found in the literature and inputted on the inundation model.

Next, the presence of flood defences, the elements that constrict the flow, is determined using two datasets. The largest source of this information is the Environment Agency's Spatial flood defences dataset. However, a visual inspection revealed that the coastal defences of the city of Portsmouth were missing. Given that Portsmouth is one of the cities with the highest risk of flooding, it is necessary to complement the EA data. This is done with the second dataset, which comes from the Channel Coastal Observatory. The CCO defence data does contain the Portsmouth defences; however, it does not hold any information on the fluvial defences in the area. Furthermore, it only has limited information on the individual characteristics of the coastal defences. The best source for this information is found to be the latest shoreline management plan (2010). However, the information only includes the residual life and a condition grade of the defences. This required inferring the equivalent standard of protection and the equivalent crest height.

For objectives two and three, the work by the Coastal Partners to significantly upgrade the defences in critical areas of Portsea Island is included in the assessment. The defences located within these areas are assigned a standard of protection equivalent to that projected by the Coastal Partners design (i.e. the one they will have once work is completed).

## Chapter 4

Finally, the necessity of employing population distribution models is highlighted as there is no high-resolution information available for the study area. The work by Stevens et al. (2015) is used as guidance to distribute the census data of the area. However, their method requires adjustments, which are briefly introduced as they are dependant on the temporal scope of the analysis. The specifics of the population distribution model are described in the relevant sections of Chapter 5 and Chapter 6.

## Chapter 5    Historical evolution of coastal flood risk at the Solent

### 5.1    Introduction

The south of England, particularly the Solent, has a long history of coastal flooding, with some of the oldest flood events on record in the area dating back to 1804 (Boza 2018). Previous research has looked into the damage caused by extreme coastal water levels in the region. Most notable is the work by Ruocco et al. (2011), Boza (2018), and Haigh et al. (2017), where extensive data archaeology has been conducted on historical tide gauge records, local newspapers, weather reports and photographic evidence to document coastal flood events. Unfortunately, the systematic recording of these events was not common practice in the past.

The events found by the previously mentioned authors are collated into the SurgeWatch database (Haigh et al., 2017). The database provides a catalogue of flood events. Each event has been classified based on the severity, from one representing nuisance flooding to six, which equates to a disastrous event with the loss of human lives. Analysing the registered flood events at the Solent region (Figure 3.4), the data shows the seasonality of coastal flooding at the Solent. The months leading to and during winter show the highest number of events (Figure 3.4.a). The data does not yield any clear trends on the yearly occurrence of flooding in the area. However, it can be appreciated that 1953 to 1954 is one of the most eventful years on record, with eight events. Furthermore, it can be seen that the events of the 26 and 30 November 1954 are two out of the four most severe events on record for the area (Boza, 2018, Haigh et al., 2017). Similarly, the 2013/2014 season is one of the stormiest, with a combined total of thirteen flood events. The particularity of this period has been explored by Wadey et al. (2015b), finding temporal clusters and large footprints of the winter storms. These events are estimated to have caused £1.3 billion worth of damage in England and Wales (Environment Agency, 2016).

The last 100 years of data (Figure 3.4.c) suggest more events occurred towards the second half of the century. However, the events with a more severe magnitude occurred before 1980. There are different factors that could have led to these changes in risk, which can be attributed to the evolution of the SPRC components. For instance, it has been shown that sea levels rose globally at a rate of 1.6 to 1.9 mm/yr over the 20<sup>th</sup> century (Hay et al., 2015). As mentioned in section 2.3.1, isostatic factors can decrease/increase the difference between global and relative sea levels. The south of England has and continues to experience vertical subsidence responding to the pressure

applied by the last glacial maximum. Santamaría-Gómez et al. (2017) estimates this rate of subsidence as  $0.05 \pm 0.23\text{mm/yr}$ . The combined effect of eustatic and isostatic factors led to a relative rate of  $1.89\text{mm/yr}$  sea-level rise in the south coast of England between 1958 and 2018 (Hogarth et al., 2020).

In terms of coastal flood defences, England experienced a move towards a national governance approach following the publication of the first Coastal Protection Act in 1949 and the effects of the 1953 North Sea floods. Following the catastrophic consequence of these floods, a committee on coastal flooding was appointed under Lord Waverley's chairmanship. It aimed to analyse a) the cause and recurrence of such an event; b) determine the necessary improvements to the flood defences system; c) establish any further measures to maintain and decrease the levels of risk; and d) review the lessons learned and analyse the financial and administrative responsibilities of coastal flood risk management (Waverley, 1954). The committee estimated this event to have a recurrence interval of 1 in 200-years, considering the mean sea level of 1953 for the areas of Sheerness and Southend (Waverley, 1954); however, its magnitude varied along the coast (Wadey et al., 2015b). Further to this, population growth has not been linear throughout the study area. As Stevens et al. (2015) presented, the population at Portsea island has fluctuated with an incremental trend up to the year 1931, which is followed by a steady decrease up to the year 1981 when this starts to grow up to present levels.

The complex evolution and interactions of these factors and their role in the evolution of coastal flood risk are, at present, yet to be analysed on a regional level. Based on the above, objective one, the subject of this chapter, is to assess how coastal flood risk has evolved between the years 1920 to 2000. The starting hypothesis of objective one is that population growth and urbanisation have increased the consequences of coastal flooding, whilst improvements to the standard of protection of coastal defences have decreased the likelihood of flooding. In addition, sea-level rise is expected to have had a limited contribution to coastal flood risk. To aid in the completion of objective one, three sub-objectives are defined, as follows:

1. Analyse the exposure to coastal flooding at the Solent between 1920-2000.
2. Estimate the number of people at risk of coastal flooding per year at the Solent during 1920-2000.
3. Determine how the variations on the drivers of risk shaped the level of threat from 1920 to 2000.

Objective one and its three sub-objectives are developed by analysing the level of exposure every 20 years, starting from 1920 up until the year 2000. Assessing the historical evolution of flooding can give an insight into the factors and decisions that have led to present-day risk levels.

Furthermore, understanding the SPRC components' interactions would allow applying the findings to other world areas where development could follow that seen at the Solent.

The structure of this chapter is as follows. First, the data and methodology required to achieve objective one and its sub-objectives are described in section 5.2. The results are then presented in section 5.3. A discussion of the key findings follows in section 5.4, and conclusions are given in section 5.5.

## **5.2 Data and methods**

The following sub-sections present the data, methods and assumptions conducted for the analysis. Firstly, it is necessary to modify the input parameters of the inundation model to represent the changes in mean sea level seen over the 20<sup>th</sup> century and the variations on the presence and standard of protection of coastal flood defences. Secondly, the baseline population distribution method is adjusted based on England's censuses availability and spatial resolution.

### **5.2.1 Historical evolution of the sources of coastal flood risk**

Sources on a coastal flood risk context refer to extreme water levels. These EWLs, included in the inundation model as a set of time-varying conditions, result from the combination of three main factors; mean sea-level, astronomical tides, non-tidal components. Wave action, which contributes to the height of EWL, is not included in this assessment.

The effect of changes in mean sea level is included considering a rate of SLR of 1.89mm/year (Hogarth et al., 2020) (Figure 5.1). The tidal component is included using the mean high water springs curve obtained in section 4.2.1. Haigh et al. (2010), through an extensive analysis of tide gauge records from 1900-2006, found no significant long-term changes on the non-tidal component (storm surge) throughout the century. Furthermore, any changes in the observed extreme sea levels seen during their study period are primarily a consequence of rising sea levels. Therefore, the mean surge curve estimated in section 4.2.1 is used for the non-tidal residual

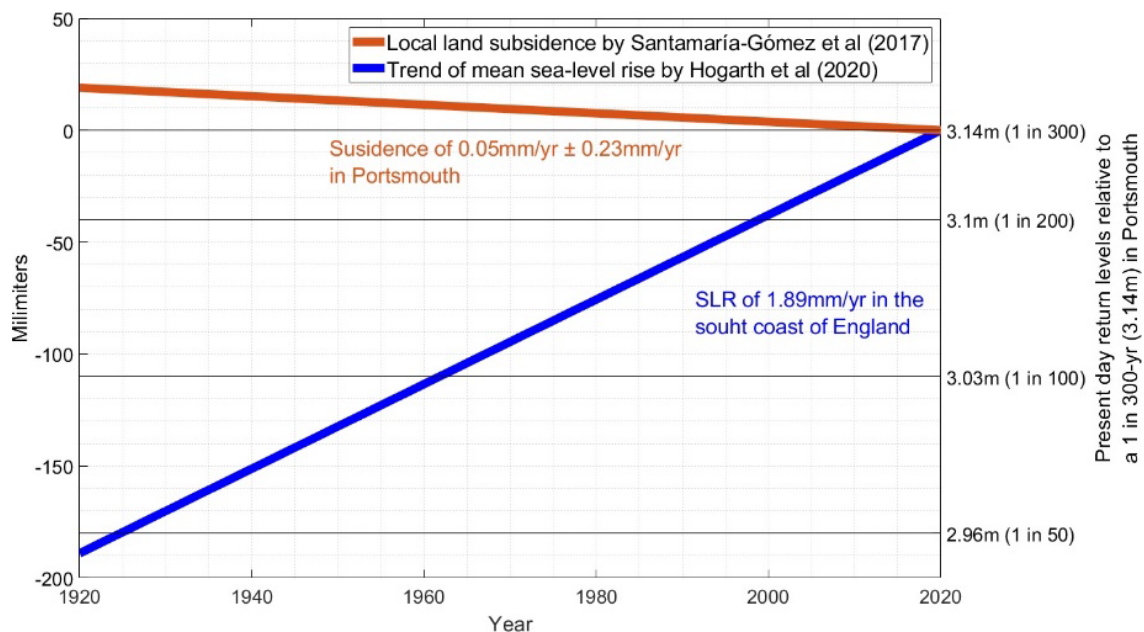


Figure 5.1 Land subsidence and sea-level rise across the Solent

The MHWS and storm surge are joined, and the total height is obtained. This maximum height is compared to the present-day extreme water levels by the Environment Agency (2018) and their equivalents for the years 1920, 1940, 1960, 1980 and 2000 (Table 5.1). As mentioned, the mean surge curve is stretched so that when added to the base MHWS curve, their total height matches that of the EWL under analysis (Figure 5.2).

Table 5.1 Present-day (2020) extreme water levels (m) by the Environment Agency (2018), along with estimates of their historical equivalents.

Return period (years)	Year / Extreme water level height (m)					
	1920	1940	1960	1980	2000	2020
1	2.36	2.40	2.44	2.47	2.51	2.55
10	2.61	2.65	2.69	2.72	2.76	2.80
50	2.77	2.81	2.85	2.88	2.92	2.96
100	2.84	2.88	2.92	2.95	2.99	3.03
200	2.91	2.95	2.99	3.02	3.06	3.10
300	2.95	2.99	3.03	3.06	3.10	3.14
1,000	3.06	3.10	3.14	3.17	3.21	3.25
10,000	3.30	3.34	3.38	3.41	3.45	3.49

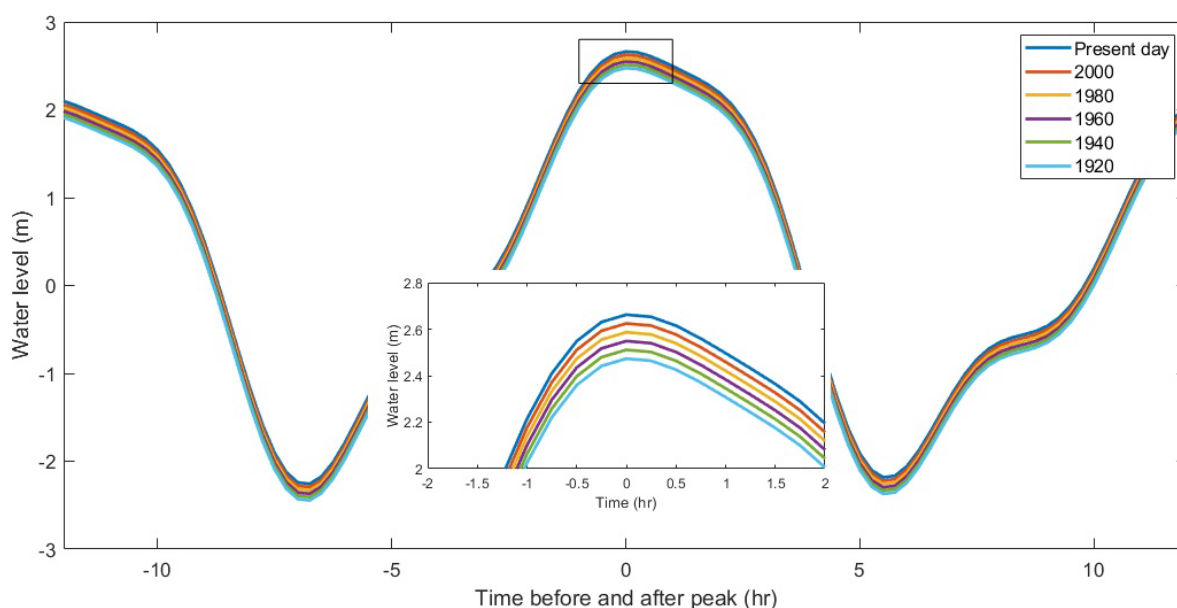


Figure 5.2 Example of water curve for a 1 in 100-yr extreme water level, and its adjusted maximum height as a consequence of sea-level rise

As explained in section 4.2.1, the inflow points containing the boundary conditions are located along the present-day MHWS line. As sea levels are adjusted to represent historical sea levels, this line's location is likely to be modified. However, there are additional factors apart from sea-level

rise that control its position over time. For example, beach nourishment or soft engineering flood defences like dikes can change the beach elevation and impact the average location of the MHWS line. Evidence of this can be seen by comparing the tidal marks shown in the County Series 3<sup>rd</sup> revision (epoch 4) against the present-day MHWS and mean low water springs (MLWS) lines in the city of Portsmouth (Figure 5.3). Unfortunately, there is no clarity of where the MHWS lines locate along all of the Solent's coast on the historical OS maps, and it is not possible to identify their location for the whole area. For uniformity and to avoid uncertainty, it is decided to maintain the inflow points along the present-day MHWS line.

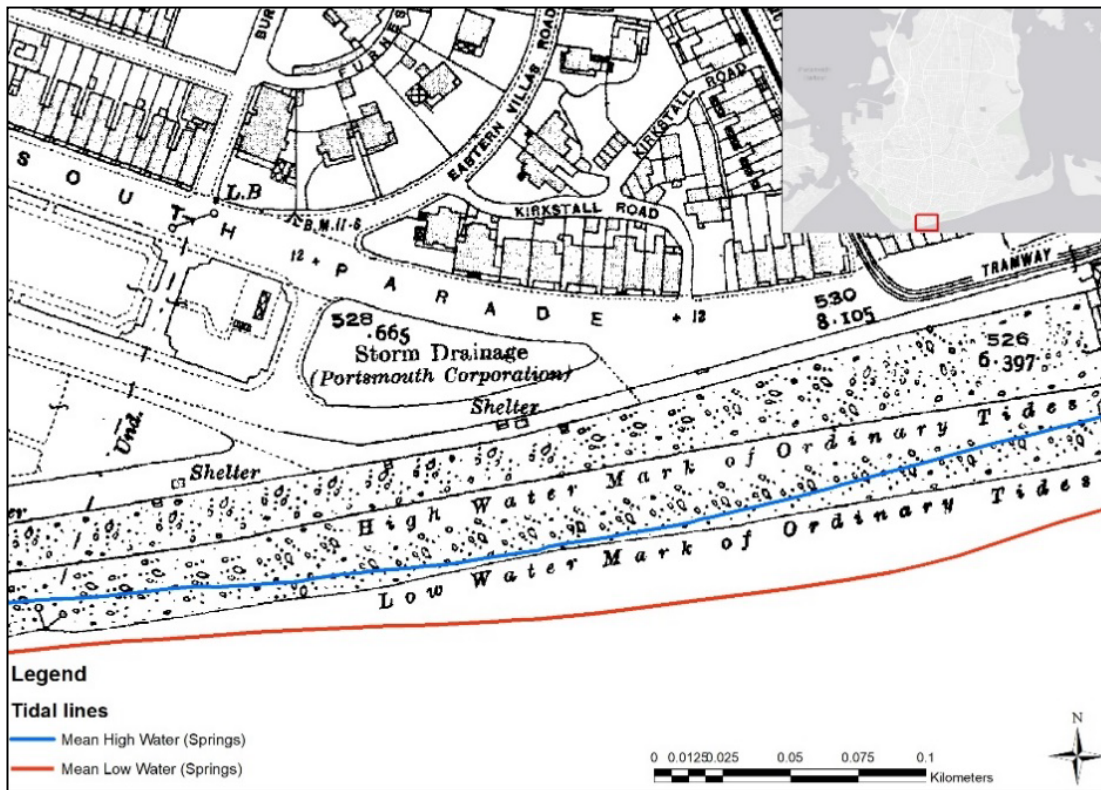


Figure 5.3 Difference in the location of tidal lines (red and blue) in Portsea Island as reported by the Ordnance Survey for present-day from those registered in the County Series 3rev

### 5.2.2 Historical evolution of the pathways of coastal flood risk

The presence of flood defences is one of the critical factors when determining the extent of the floodplain. It is, therefore, necessary to determine when these were first implemented at the different areas of the Solent. Unfortunately, there is little to no data available on when most of these structures were built. This can be the product of various factors. In some cases, the defences are privately owned; hence public information is not available. Some records could be lost in time, and even some defences were not commissioned to act as coastal flood defences but do so now. An example of the latter is the Hilsea line of fortifications at the north of Portsea Island. These were built around the 18<sup>th</sup> century to protect against invasion and now serve as



flood barriers (Slater, 2009). Out of the 5,066 flood defences listed in the EA and CCO data presented in section 4.2.3, only 159 segments, or 3.14%, have information on the year these were built (Table 5.2). Local knowledge suggests that many defences at the Solent were built between 1928 and 1939 to create jobs during The Great Depression. However, there is no information available to support this nor indication of which defences were built in this period. Given the aforementioned, it is decided to assume that the defences found in present-day were built before 1920 and are therefore included in every timestep of the assessment.

Table 5.2 Total number of flood defences at the Solent with and without information of when these were built.

Flood defences within the study area	Defences with information for when these were built	
	Without information	With information
5,066	4,907(96.9%)	159 (3.14%)

Since the evolution of defence presence cannot be analysed, the focus is given to changes and improvements on their standard of protection. Again, information in this matter is generally scarce. However, some information is available for Portsmouth, presented in the “Portsmouth flood defences: Towards 2050 report” (Easterling, 1991) and utilised by Stevens et al. (2015). Given the scarcity of data, it is assumed that all the coastal defences at the Solent uniformly experienced the same rate of improvement as that recorded in Portsmouth (Table 5.3).

Table 5.3 Recorded average defence height adjustment in Portsea Island, assumed constant for the whole region.

Year	The difference in defence height compared to the present value (m)
2000	-0.1
1980	-0.2
1960	-0.3
1940	-0.9
1920	-0.9

### 5.2.3 Historical evolution of the receptors of coastal flood risk

As mentioned in section 4.3, the methodology to distribute the historical population in the study area builds on Stevens et al. (2015). Given the complexity of assessing population evolution, an outline of the process is presented in Figure 5.4, with the particulars of each step shown afterwards.

The method obtains census data on the highest spatial resolution available and distributes it within the urban footprint. Census have been conducted in England every ten years since 1801, except for 1941 during the Second World War (ONS, 2016). However, as the ONS (n.d.-a) pointed out, *“the whole of England and Wales has been divided at different times into various administrative areas with little regard to previously existing divisions”*. The different formats and various spatial resolutions (Table 5.4) required adjustment and preprocessing for the assessment.

Table 5.4 Spatial resolution of census data in England from 1921 to 2011

Census year	Highest resolution available	Data presented as
1921-1951	Administrative County, Municipal Boroughs, Urban and Rural districts	Total residents
1961	Local Authority District (LA), Urban District (UD) and Rural Districts (RD)	Total residents
1981	Enumeration Districts (ED)	Total residents
2001 - 2011	Output Areas (OA)	Population weighted centroids

For the 1921 to 1951 census, the information is obtained as images of the census records. Given that there is no information for 1941, the 1931 and 1951 census data are interpolated to get an approximate figure. Information for 1961 onwards can be obtained through the Office for

National Statistics website (ONS, n.d.-b). Unfortunately, there are no maps available showing the geography used for censuses prior to 1961. This made it necessary to identify the administrative counties, municipal boroughs, and other areas to their most recent equivalents on the 1961 census, of which the ONS has made digital vector boundary files available, allowing to distribute the population spatially.

Once every census has geography attached, the 2001 OAs within each local authority district, urban and rural districts, and enumeration districts are identified. In parallel, the share of the 2001 ED population that each 2001 OA holds is determined. This, as failing to consider that population is not uniformly distributed in the study area could lead to unrealistic results. The percentage of the 2001 population each OA holds is assumed to have remained constant since 1920. The resulting rates are used to distribute the population from the 1921 to 1981 censuses to their respective OA.

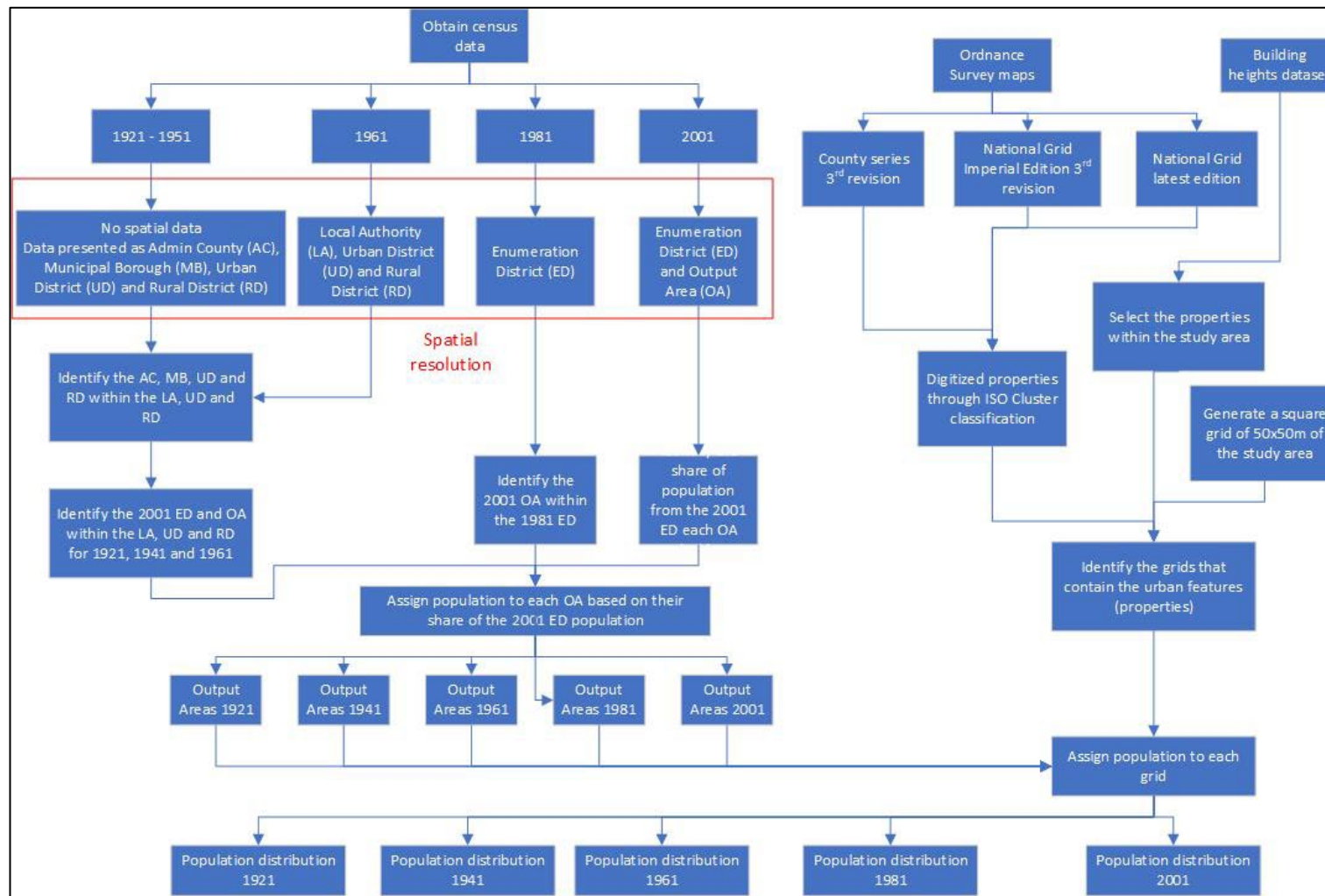


Figure 5.4 Schematic representation of the population distribution methodology

Having the census data ready to be spatially distributed, it is then necessary to determine the extent of the urban footprint. Historical maps for the area by the Ordnance Survey, available through the Digimap service by the University of Edinburgh, are used for this purpose. These are supplied as georeferenced images that can be spatially positioned on a GIS. Even though the resolution, scale and units of each map vary, the main use of these is to indicate the presence of urban elements, and these factors do not affect the outcome (Table 5.5).

Table 5.5 Resolution, publishing data and coverage of Ordnance Survey maps used for urban area digitization and population distribution

Map	Census years covered	Scale	Publishing date range
County Series 3 <sup>rd</sup> revision (Epoch 4)	1920 and 1940	1:10,5600 ("6 inch to the mile")	1922-1969
National Grid 1 <sup>st</sup> Imperial Edition (Epoch i5)	1960	1:10,5600 ("6 inch to the mile")	1948-1977
National Grid latest edition (Epoch m7)	1980	1:10,000	1958-1996
Building heights layer from the OS MasterMap Topography layer	2000	N/A	2018
Source: Historic Digimap Help (Digimap, 2021)			

Stevens et al. (2015) manually digitized these maps; however, their study area is far smaller than the present assessment, only covering Portsea and Hayling Islands. Following their approach would not be practical for a Solent wide analysis, making it necessary to refine the methodology for a more extensive assessment.

Stevens et al. (2015) method is improved by processing the OS maps through ArcMap's ISO Cluster Unsupervised Classification tool. This tool classifies and groups data into attributes with the same characteristics. In this case, the maps by the OS are constituted of blank spaces and black lines showing features such as boundaries, buildings and other annotations. The ISO Cluster tool identifies the lines and isolates them from the empty spaces. These lines, now polygons, are cleaned off of additional features, such as streets, labels, etc., leaving only those that represent properties. Following this, the square grid mesh of the study region generated in section 4.3 is

used, and the grids that contain properties are identified and classified as part of the urban footprint. For the 2001 census, the OS building heights dataset, which is part of the MasterMap Topography layer, is used to determine the grids that fall within the urban footprint. After determining the extent of urban footprint and the mesh grids that fall within this area, the population from each OA is distributed across the urban cells within their domain (Figure 5.5). The resulting evolution in population distribution can be seen in Figure 5.6.

It can be appreciated that there are fluctuations in the number of people living in certain areas between timesteps. This can be attributed to both migration and changes in the resolution of the available census data previously mentioned. To highlight this, the percentage change for each timestep is presented in Figure 5.7. Incorporating the highest resolution, Output Area, for the 2001 census creates the largest changes in population estimates for the smaller areas (Figure 5.7.e). This is critical for areas near the coast and within the floodplain, where simple variations on the number of people can lead to significant changes in the level of risk.

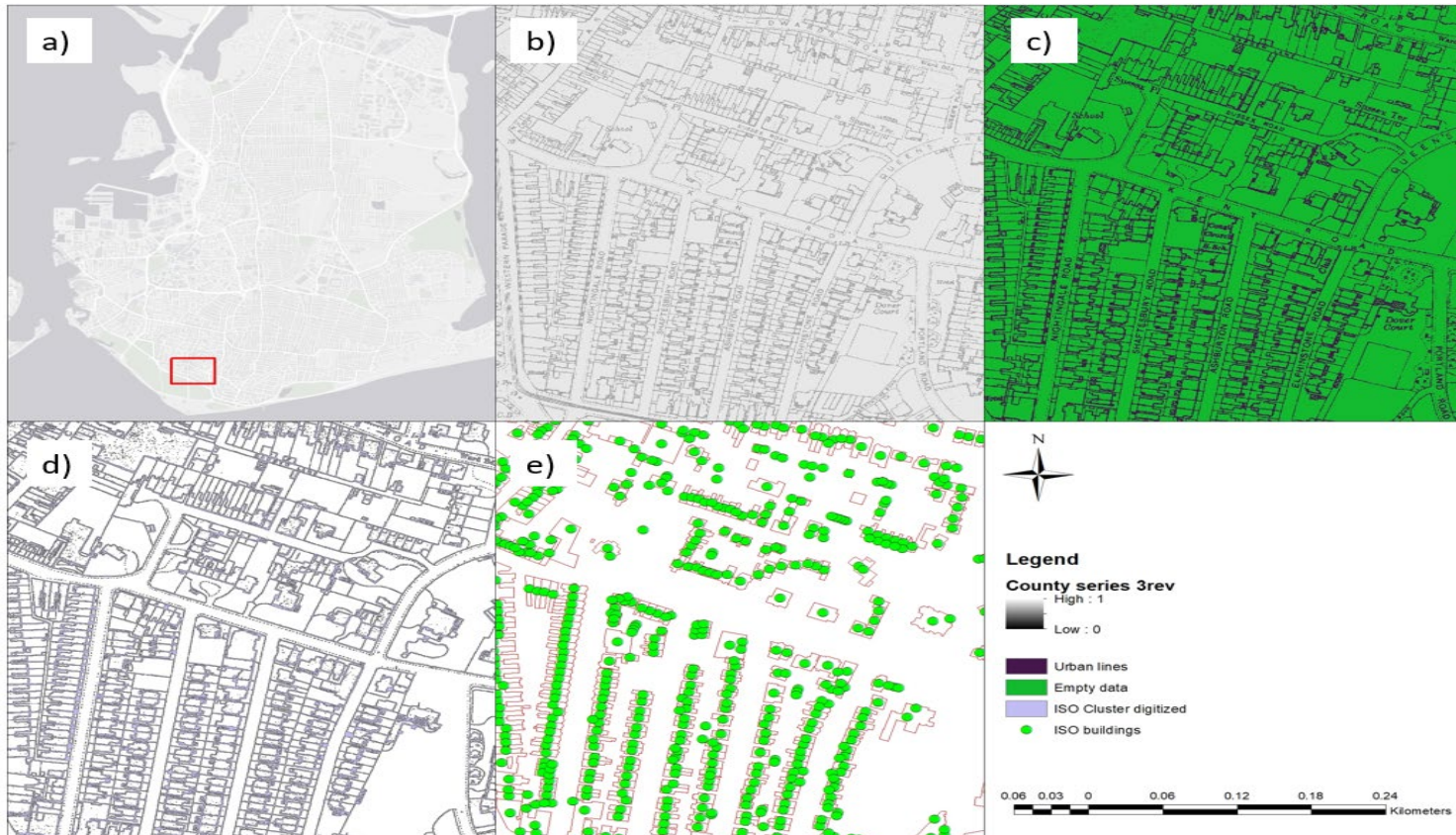


Figure 5.5 Representation of population distribution method for an area near Southsea in Portsea Island. a) Location of example area within Portsea Island. b) Representation of original OS historical map (County Series 3<sup>rd</sup> revision Epoch 4 covering the years 1920 - 1940). This is analysed with the ISO Cluster tool which separated blank spaces and lines (c). The blank spaces are removed (d) and the resulting lines are analysed to remove those that represent streets, parks etc. Lastly, the centroid of each property is obtained (e).



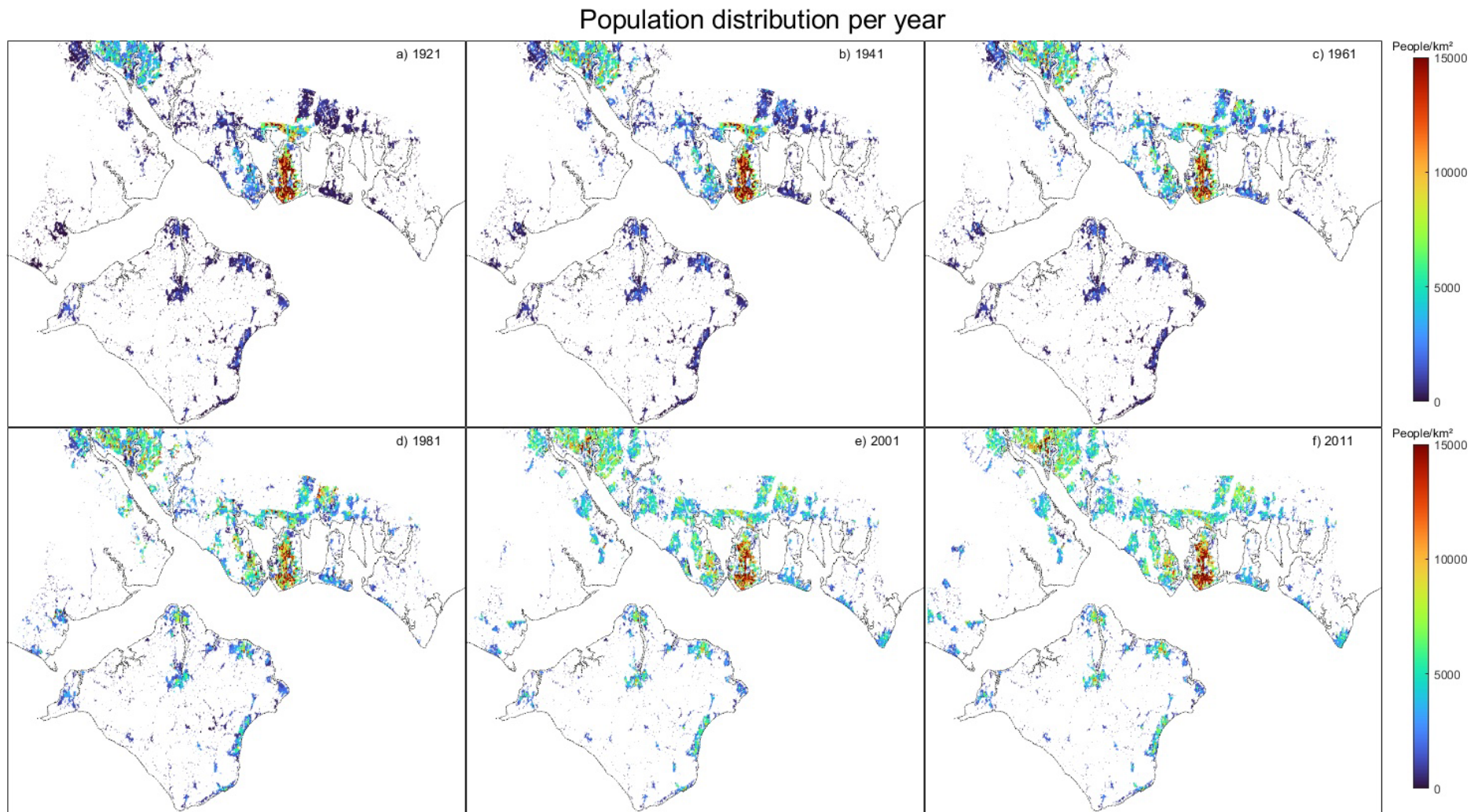


Figure 5.6 Historical evolution of population distribution at the Solent



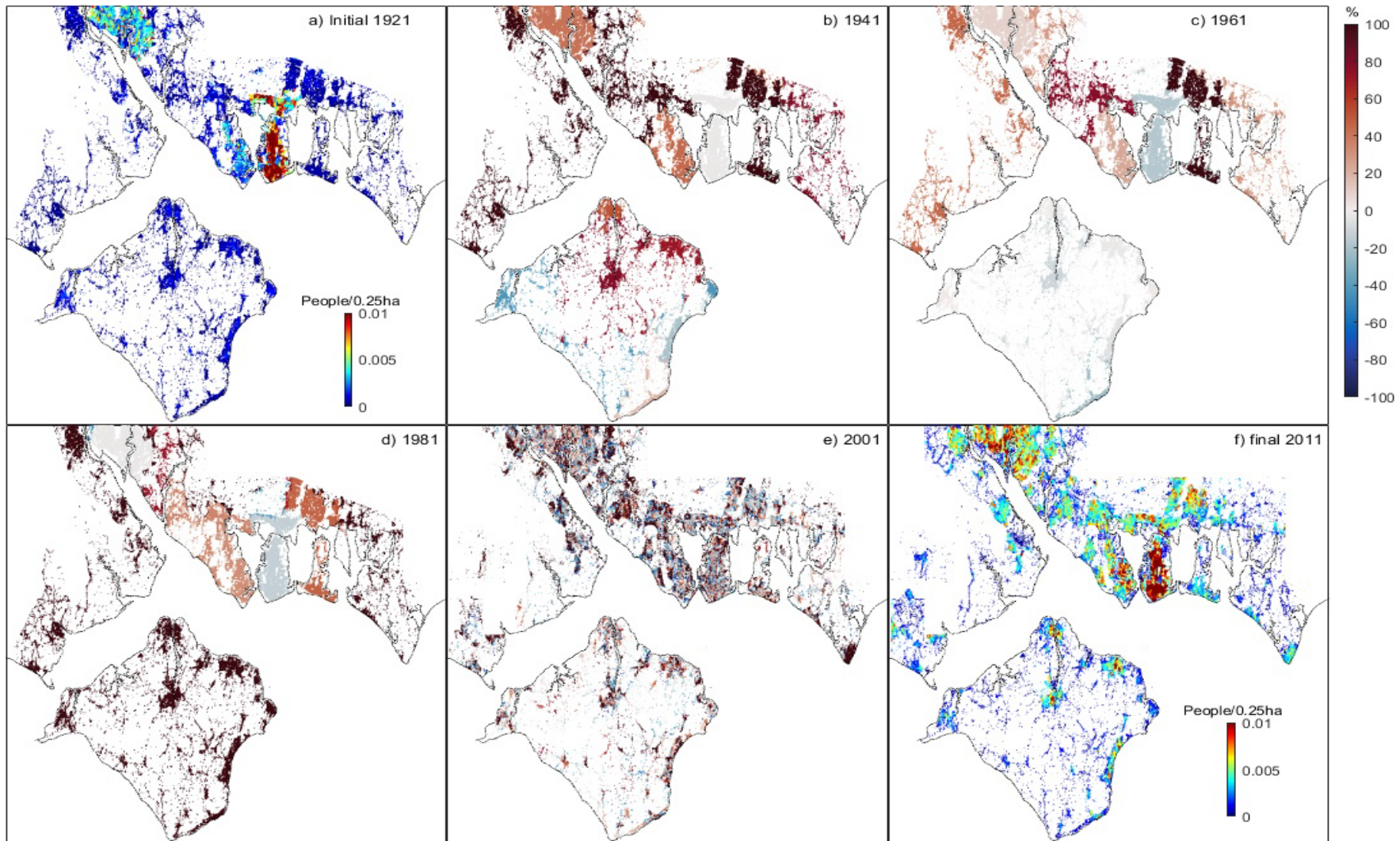


Figure 5.7 Initial (1921) and final (2011) population distribution and percentage population change for each timestep from 1921 to 2011 at the Solent.

### 5.2.4 Flood risk analysis

This first objective aims to understand the evolution of coastal flood risk at the Solent from 1920 to 2000. In addition to this, it seeks to analyse how each of the SPRC components' development has contributed to the experienced levels of risk. Their influence is assessed with the use of scenarios, where each element is evaluated against a mixture of the others (Table 5.6). For example, one scenario used the estimated mean sea level of 1920, the assumed standard of protection for the same year and the population distribution of 1941. Comparing the results of such a scenario against one where all components are kept at their 1920 (and 1921 for the census) value can highlight how much influence population growth had on the levels of risk for 1940 (Equation 5.1). This combination of elements resulted in 125 scenarios for each of the parameters presented in Table 5.6.

$$\Delta EAD_i | \Delta P_i = (EAD | SL_{i-1}, SoP_{i-1}, P_i) - (EAD | SL_{i-1}, SoP_{i-1}, P_{i-1}) \quad 5.1$$

Table 5.6 Input parameters used in the historical flood risk analysis

Year	Lower mean sea level at a rate of -1.89mm/yr	Lower flood defences (in meters)	Population	
			Census	Map used for distribution
1920	-0.19m	-0.9	1921	CS epoch 4
1940	-0.15m	-0.9	1941	CS epoch 4
1960	-0.11m	-0.3	1961	NG epoch i8
1980	-0.07m	-0.2	1981	NG epoch m7
2000	-0.03m	-0.1	2001	OS Buildings database

The results are then integrated to estimate the expected annual damage for every timestep and input configuration. In broad terms, the EAD considers the results obtained for every return period and summarizes the damage expected in any given year. LISFLOOD-FP is systematically run using every input combination presented in section 5.2.4 for the ten return periods presented in Table 5.1. The outputs are combined with the population distribution of each time step to determine the number of people at risk.

## 5.3 Results

The objective of this chapter is to analyse the evolution of coastal flood risk at the Solent from 1920 to 2000. However, it is necessary to determine the influence of the depth and velocity of

floodwater on flood risk and exposure. Depending on the characteristics of the population and properties, different combinations of velocity and depth can cause damage. It is then crucial to consider the depth to which people and assets are exposed. Unfortunately, there is no information available on the specific characteristics of buildings in the area. Therefore, the focus is solely given to the flood depth.

The exposure results are presented for minimum flood depths of 0.1m, 0.3m, 0.5m, 1m and no minimum depth (Figure 5.8). It can be seen that exposure can be overestimated if no minimum depth (NMD) threshold is considered. For instance, for the year 1920 and a return period of 1 in 100-yr, exposure decreases by 53% when 0.1m of depth are required, compared to an NMD scenario. Similarly, the results decrease by 71%, from 4,140 people exposed under NMD to 1,190 for a minimum depth of 0.3m. Similar differences can be seen for all return periods and all the years analysed, highlighting the importance of a flood depth threshold.

Given the above, the following results are reported considering a minimum flood depth of 0.3m. This depth falls within the required depth to produce damage to buildings by infiltrating and causing external damage, even under minimal water velocity (DEFRA, 2003, Kelman, 2002, Dawson et al., 2011).

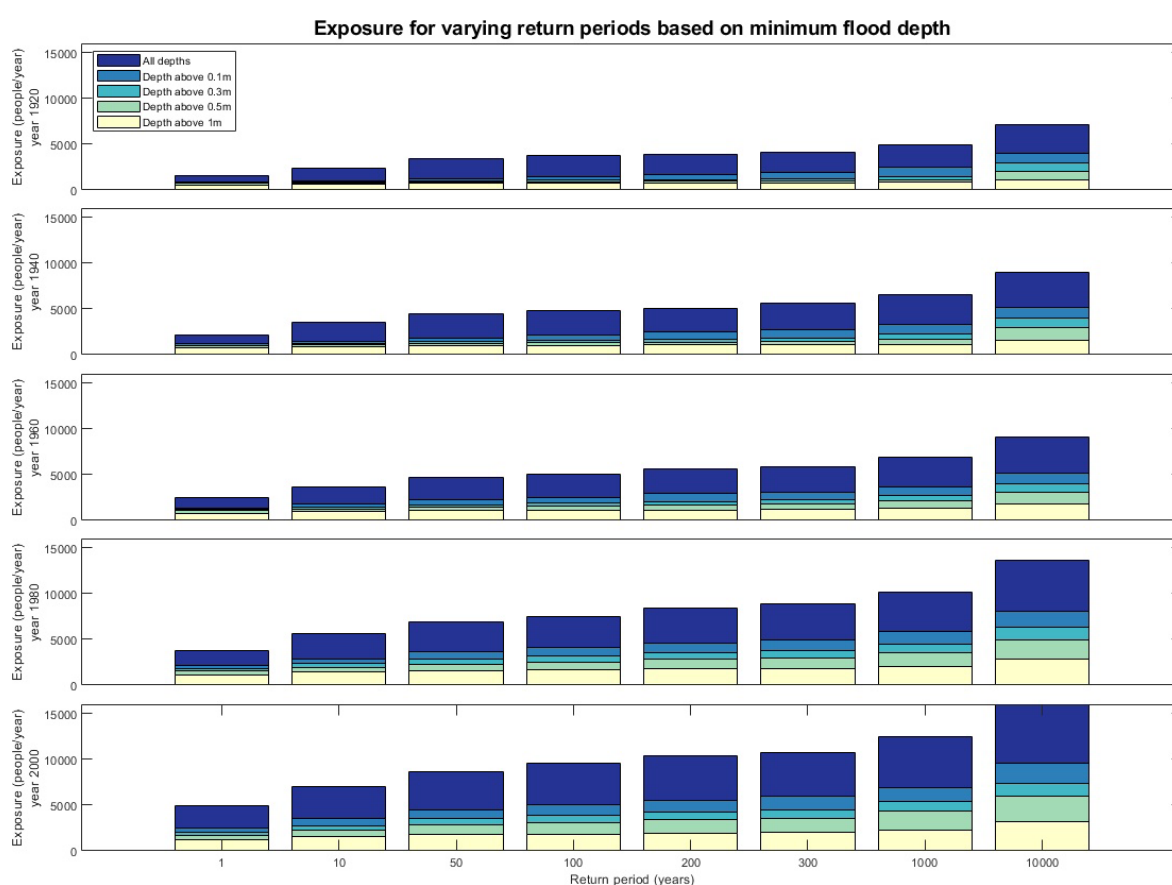


Figure 5.8 Historical exposure to extreme water levels of increasing return period based on varying the minimum depth of flood

### 5.3.1 Historical exposure to coastal flooding

Having determined the adequate flood threshold, the analysis continues to the development of the first sub-objective of this chapter, which is to analyse the past exposure to various extreme water levels of increasing magnitude. The exposure analysis then starts by keeping all the components according to the year analysed (i.e. no mixture of sea levels, populations, nor the standard of protection) and only varying the return periods. The results show that, overall, exposure increases from 1920 to 2000 (Figure 5.9). It doubles in this period for the highest return period and triples for its lowest one. For instance, a 1 in 1-yr event in 1920 would have lead to 800 people being flooded. This exposure increased to over 2,000 people by the year 2000. Relative to the initial exposure of 1920, exposure more than doubled by the end of the 20<sup>th</sup> century. For the highest return period, 1 in 10,000 years, this grew from 3,000 to 7,400 people. Furthermore, the results suggest that exposure rapidly increased from 1920 to 1940, followed by a slowed increment up to 1960. The trend rapidly increased from 1960 to 1980 and appears to slow down again by the year 2000.

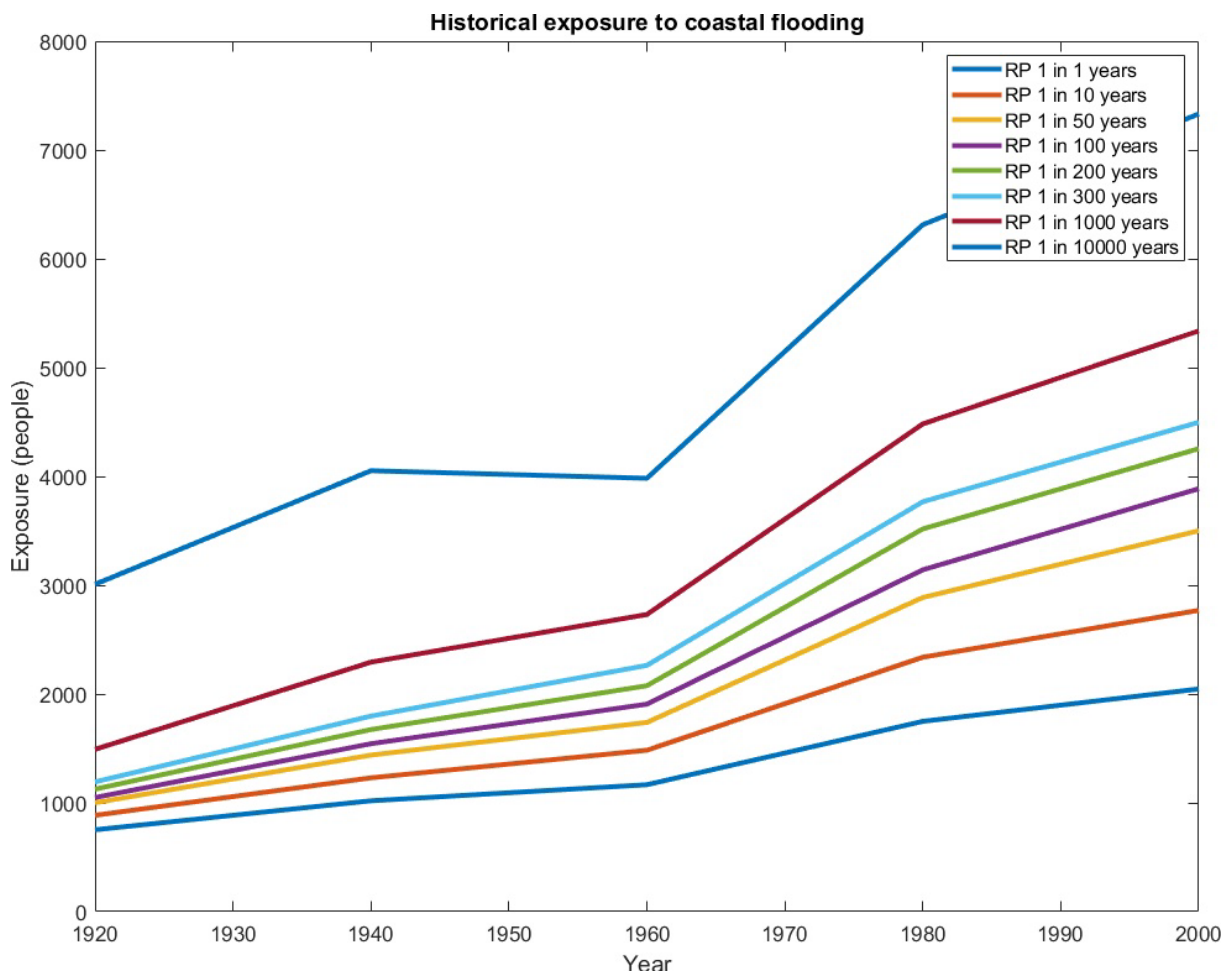


Figure 5.9 Historical exposure to extreme water levels of increasing return periods considering a minimum flood depth of 0.3m required to produce damage

Having assessed the exposure maintaining the components at their value for the year analysed, it is of interest to understand and quantify the individual and compound effect that changes in these had on exposure to coastal flooding. A simple analysis of Figure 5.10, which shows the results of such exercise for a 1 in 100-yr event, highlights that lower defences combined with higher sea levels and populations lead to the highest exposures. The two-dimensional plots b), c), and d) of Figure 5.10 give more detail on the interaction of these components. The aim of these is to understand, for example, what would have happened if mean sea-level and defence standard of protection stayed at their 1940 value. For this, two components are kept according to the year analysed whilst the remainder is varied. Looking at the vertical axis of Figure 5.10.a, it is clear that population growth leads to more significant consequences.

Figure 5.10.b displays the isolated effect of population variability. This variability remains close to 4,000 people for all the years analysed. Interestingly, there is not much increment in exposure comparing the results obtained for 1920 and 1940, with a decrement by 1960. Overall, the population within the study region is roughly estimated to have grown by 60,000 from 1940 to 1960. This estimate is far lower than the one registered from 1921 to 1941 (over 118,000 people), 1961 to 1981 (232,000) and between 1981 and 2001 (98,000).



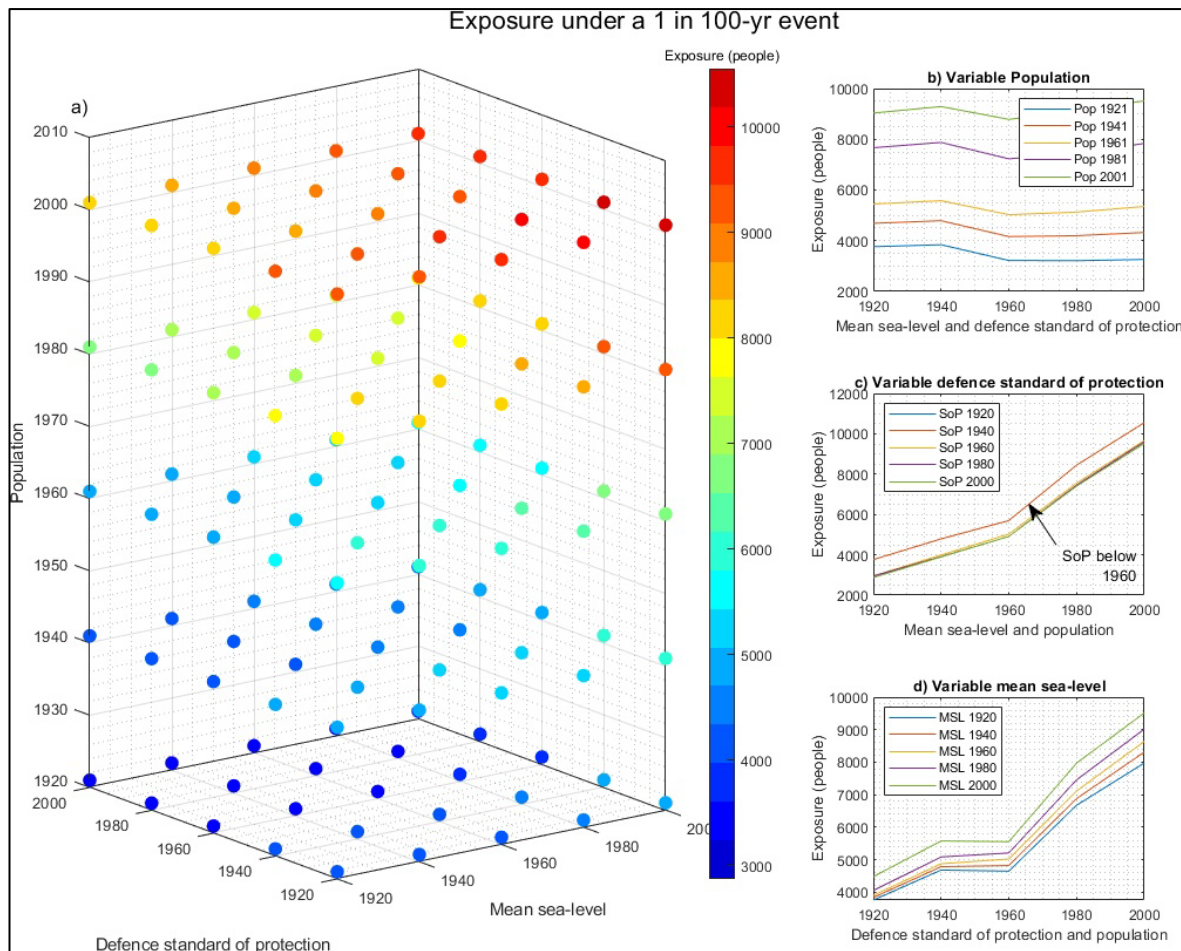


Figure 5.10 Exposure to a 1 in 100-yr extreme water level under all scenarios and a minimum flood depth of 0.3m. Subplot a) present the results when all components are kept variable, showing the relationship between exposure, sea level, standards of protection and population. Subplot b) displays the isolated effect of population variability, illustrating the effect of population growth, c) presents the effect of improving flood defences, highlighting the effect of defence improvement from 1940 to 1960, and lastly d) shows the effect of sea-level rise on exposure.

When the defence standard of protection is analysed in Figure 5.10.c, exposure decreases with defence improvement. Here, it is necessary to highlight the two regions of the graph. The top lines with the most exposure are the results obtained when a SoP below that of the year 1960 is considered. The bottom lines are the result of having higher defences after 1960. It is interesting to see that the central variability is given at the 1940-1960 time-step. However, the results do not present a considerable variance otherwise. The increment in defence height from 1940 to 1960 (0.6m) resulted in roughly 1,000 fewer people flooded for a minimum depth of 0.3m. This number increases to 2,100 when no minimum flood depth is required. As expected from the defence height inputs, after the defence improvement of 1960, there is little change in the protection given by the defences. In fact, the average decrement of 1,000 people from 1940 to 1960

coincides with the overall average exposure variability. Finally, looking at the isolated effect of mean sea-level rise in Figure 5.10.d, the results show increases from 1920 to 1940, followed by a plateau from 1940 to 1960 and abrupt increases in the number of people exposed to coastal flooding from 1960 to 1980.

Determining the levels of exposure for the whole region is a valuable management tool. However, the levels of threat differ across the Solent. Here, the level of exposure for the main 48 built-up urban areas defined by the ordnance survey (Figure 5.11) is analysed. It should be noted that some areas have extensive land coverage, and flood risk might only be prevalent in certain regions. Initially, the area at risk without incorporating the number of people exposed is analysed. The results show a slight spatial trend, with areas at the east experiencing more extensive flooding. This trend is maintained throughout the 20<sup>th</sup> century and agrees with the findings of Ruocco et al. (2011) (Figure 5.11.f).

Incorporating population onto the analysis does indicate the areas with large populations present high levels of exposure. Interestingly, Portsmouth, one of the areas with the largest populations, is also located in the eastern region (Figure 5.12). As mentioned throughout this text, Portsmouth is regarded as one of the towns in England with the highest level of exposure, which is confirmed in the findings (Figure 5.12). Even though Southampton is the second most populated city in the region, its exposure is far smaller than that of Portsmouth, with only an average of 33 people exposed throughout the 20<sup>th</sup> century, compared to Portsea's 230 (Figure 5.13).

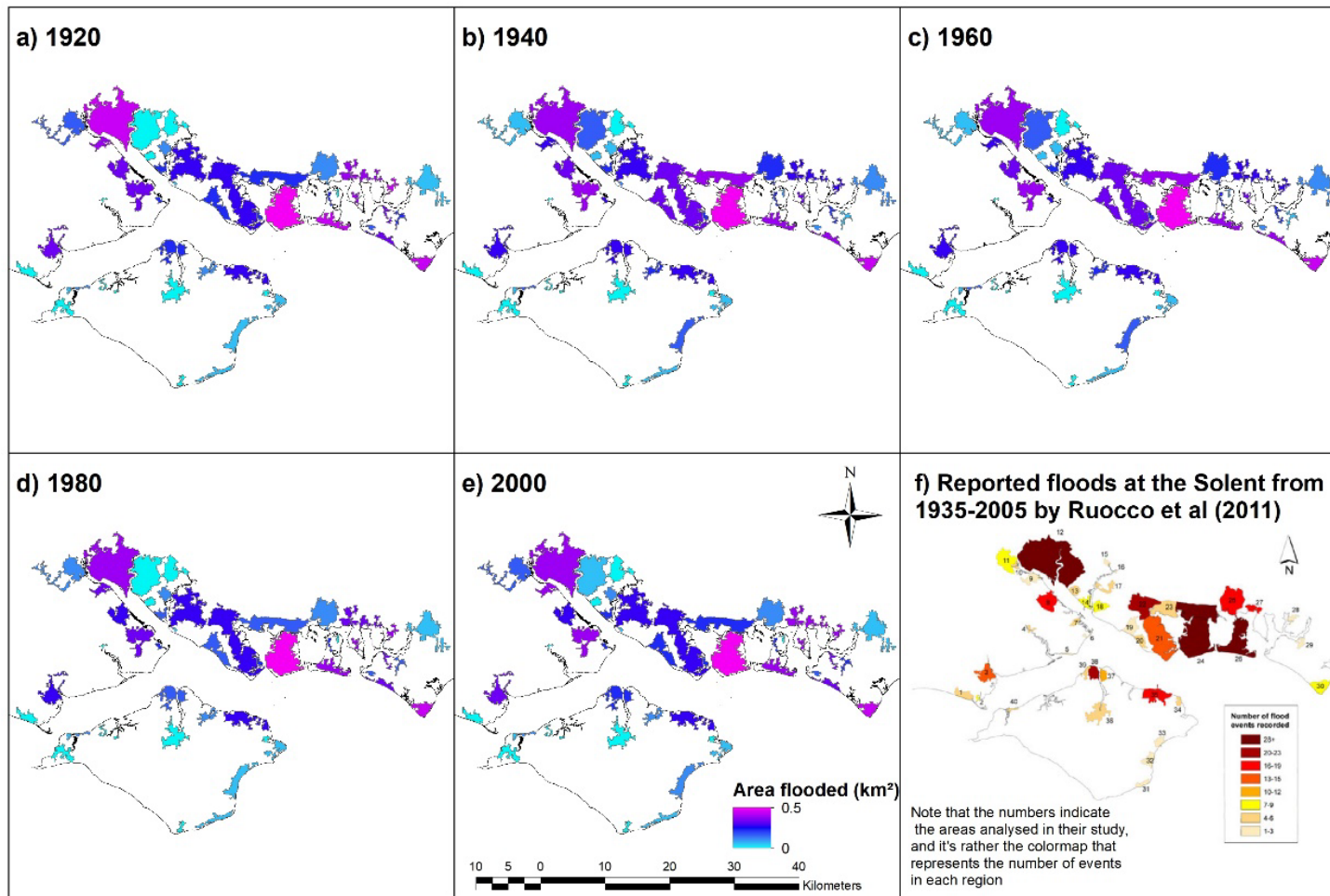


Figure 5.11 Evolution of flood exposure (area flooded) to a 1 in 100-yr event at the main built-up areas in the Solent, considering all components to be set to the year analysed (i.e. the variability caused by changes in components is not analysed) compared to the number of floods reported by Ruocco et al. (2011)



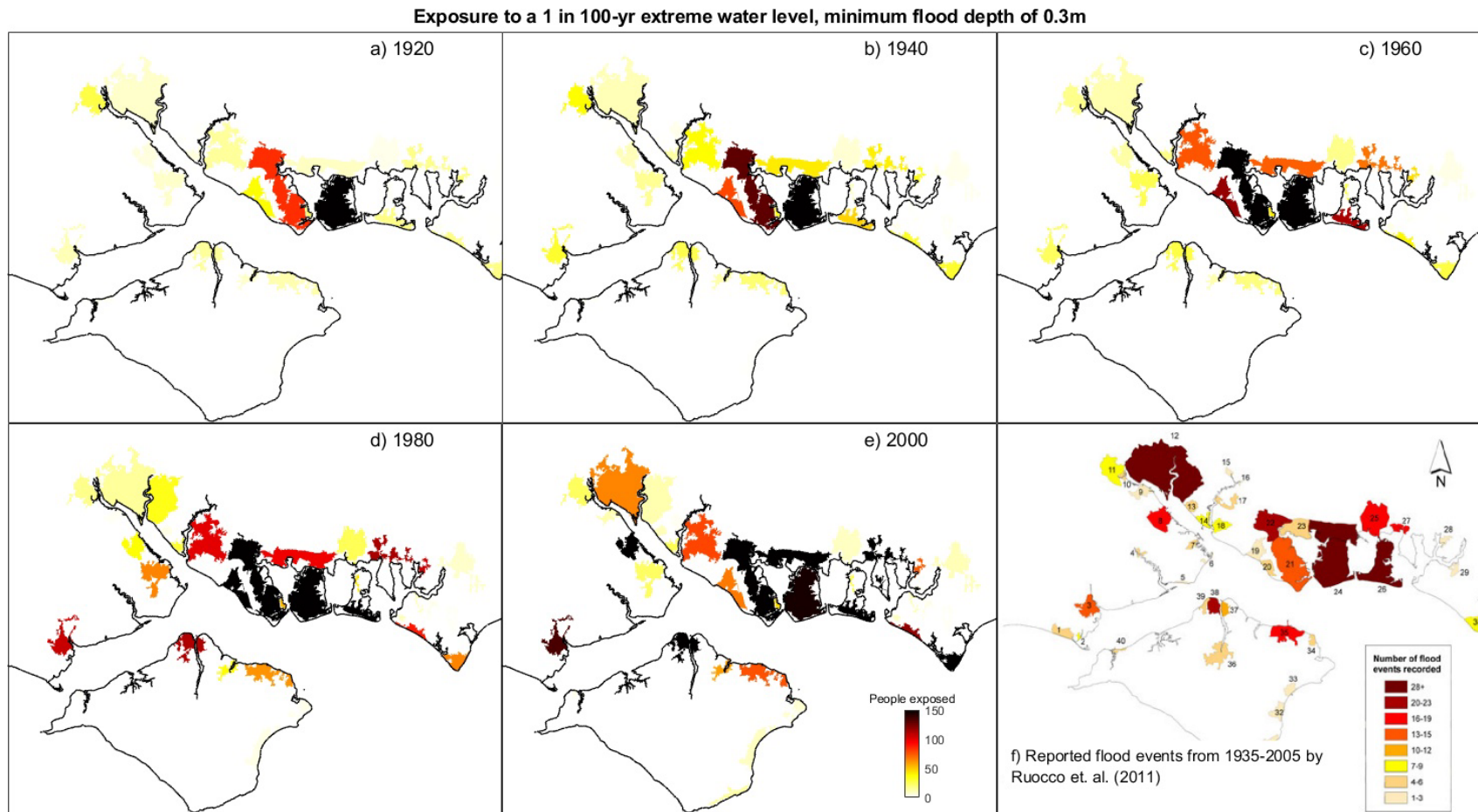


Figure 5.12 Spatial distribution of population exposure to a 1 in 100-yr extreme water level from 1920 to 2000, considering all components to be set to the year analysed and a minimum flood depth of 0.3m, compared to the number of floods reported at the Solent from 1935-2005 by Ruocco et al. (2011)

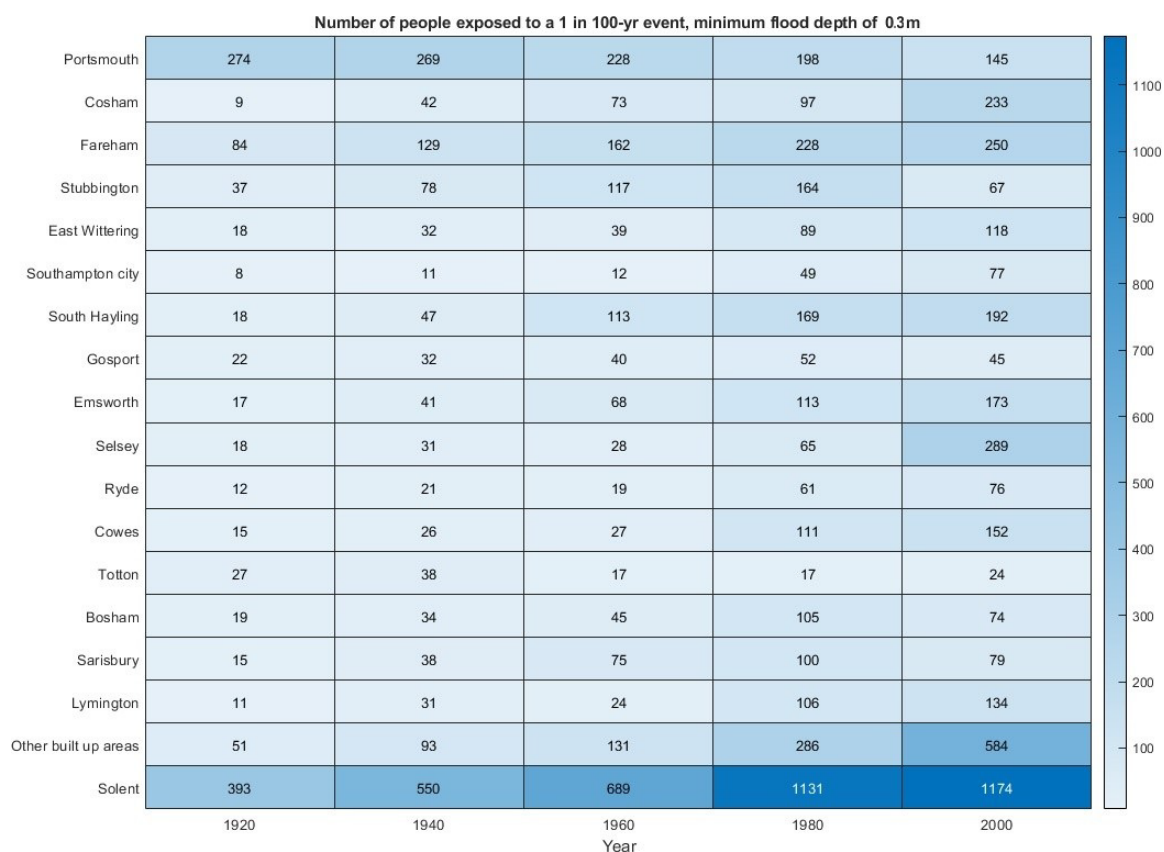


Figure 5.13 Evolution of flood exposure (people flooded) to a 1 in 100-yr event in the main built-up areas of the Solent

As mentioned, the initial hypothesis of objective one is that population was the main driving factor of exposure in the whole area. However, it is necessary to closely look at the evolution of each of the SPRC components in this main built-up area. The results suggest that Portsea Island, where most of Portsmouth lies, has particularly benefitted from defence presence and improvement, as can be appreciated in Figure 5.14. Instead of rising with time, as seen for Hayling Island, the exposure numbers fall after 1960 for a 1 in 100-yr event. Interestingly, Fareham sees a steady increase in exposure.

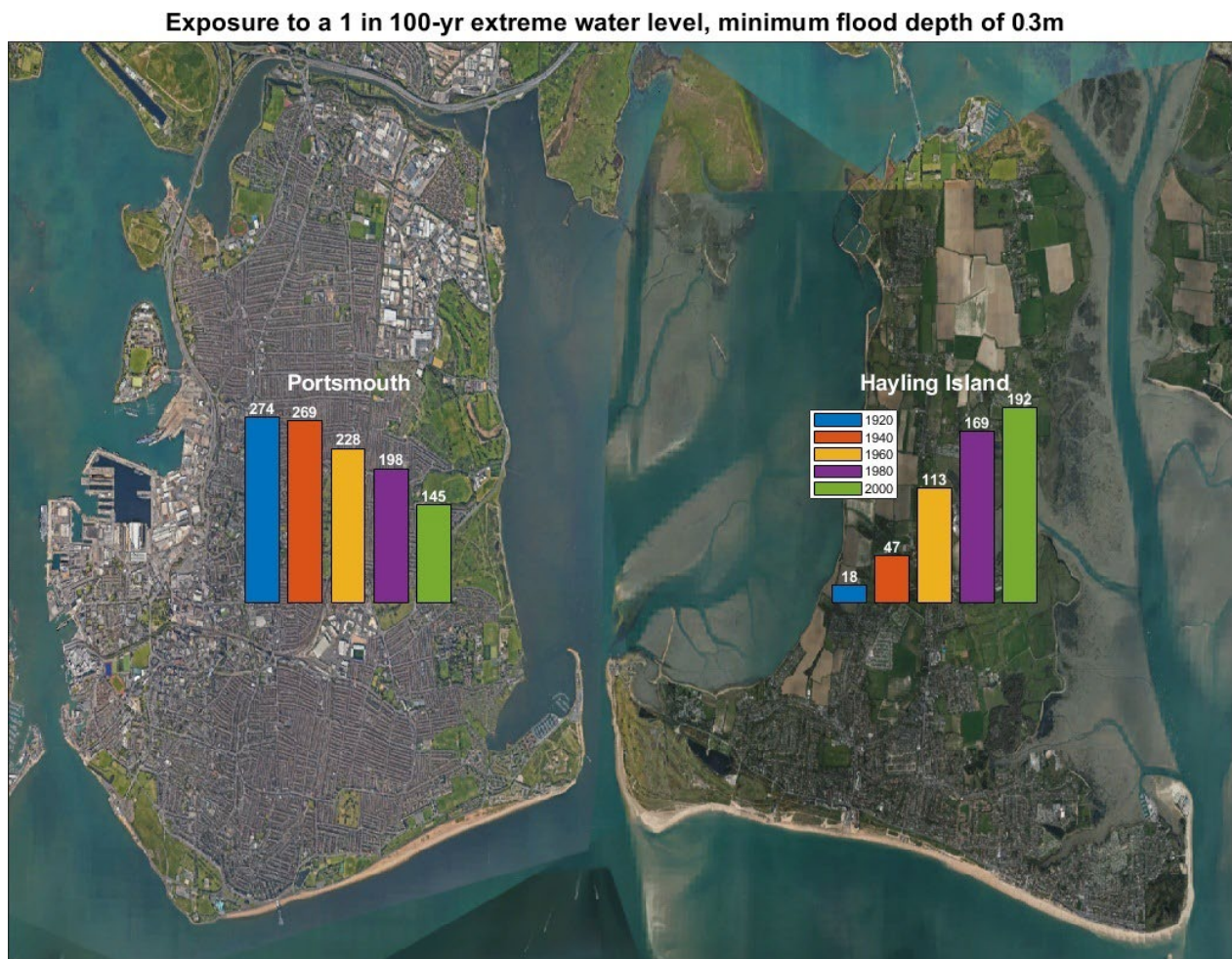


Figure 5.14 Evolution of exposure (people flooded) to a 1 in 100-yr extreme water level at Portsea Island (Portsmouth) and Hayling Island

### 5.3.2 Historical risk of coastal flooding

The second sub-objective of this chapter is to determine the average number of people at risk of flooding per year, which is equivalent to expected annual damage with a metric of people/year. The analysis shows that EAD has grown from 836 people/year in 1920 to 2,500 people/year by the end of the 20<sup>th</sup> century (Figure 5.15). EAD follows a steadily increment from 1920 to 1960, with roughly 260 people/year added in each timestep. This is followed by a rapid increment from 1960 to 1980 of 754 people/year (55.36%). This rate of increment is halved after 1980, with less than 400 people/year added to the EAD from 1980 to 2000.

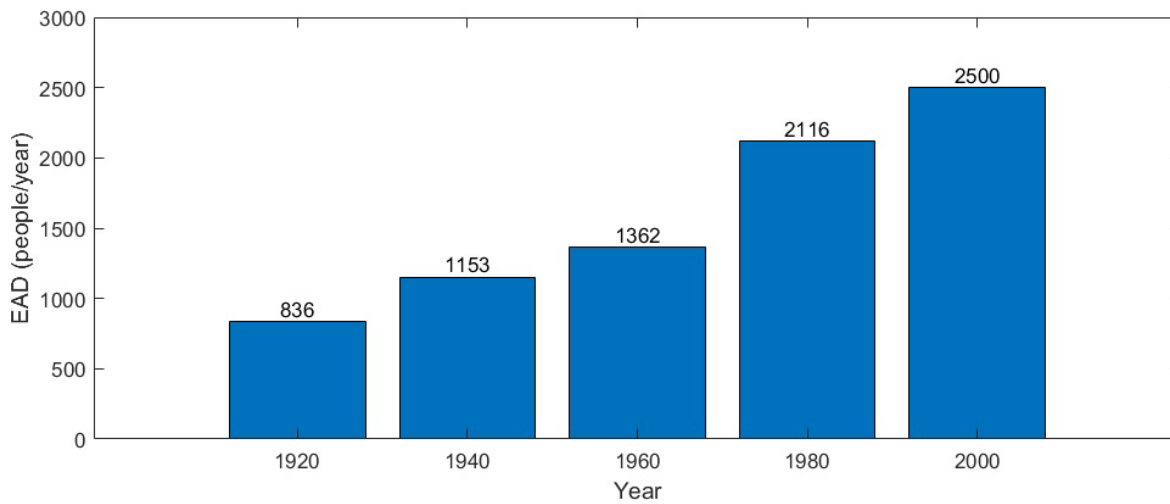


Figure 5.15 Expected annual damage (people/year) from 1920 to 2000 at the Solent, UK.

In terms of risk of coastal flooding, Portsmouth is the area with the highest average risk for the study period. It can be seen that the level of threat it experiences (246 people/year) is equivalent to almost a third of that seen for the Solent (836 people/year) at the beginning of the century. It can be seen that the level of threat for most of the top cities in the area falls below 100 people at risk per year, with a few exceptions going above this threshold from the outset and throughout. Overall, the remainder of built-up areas in the region sees an exponential increase in their risk, almost doubling the number of people threatened at every timestep, except from 1940 to 1960 (Figure 5.16.b.17). Similarly, the risk of coastal flooding for the Solent as a whole region steadily increases from 1920 until 1980, when it almost reaches a plateau (Figure 5.16.b.18). However, some BUA show a decrease in their level of risk from 1980 to 2000. These include Stubbington, Gosport, Totton, Bosham, East Wittering and Sarisbury.

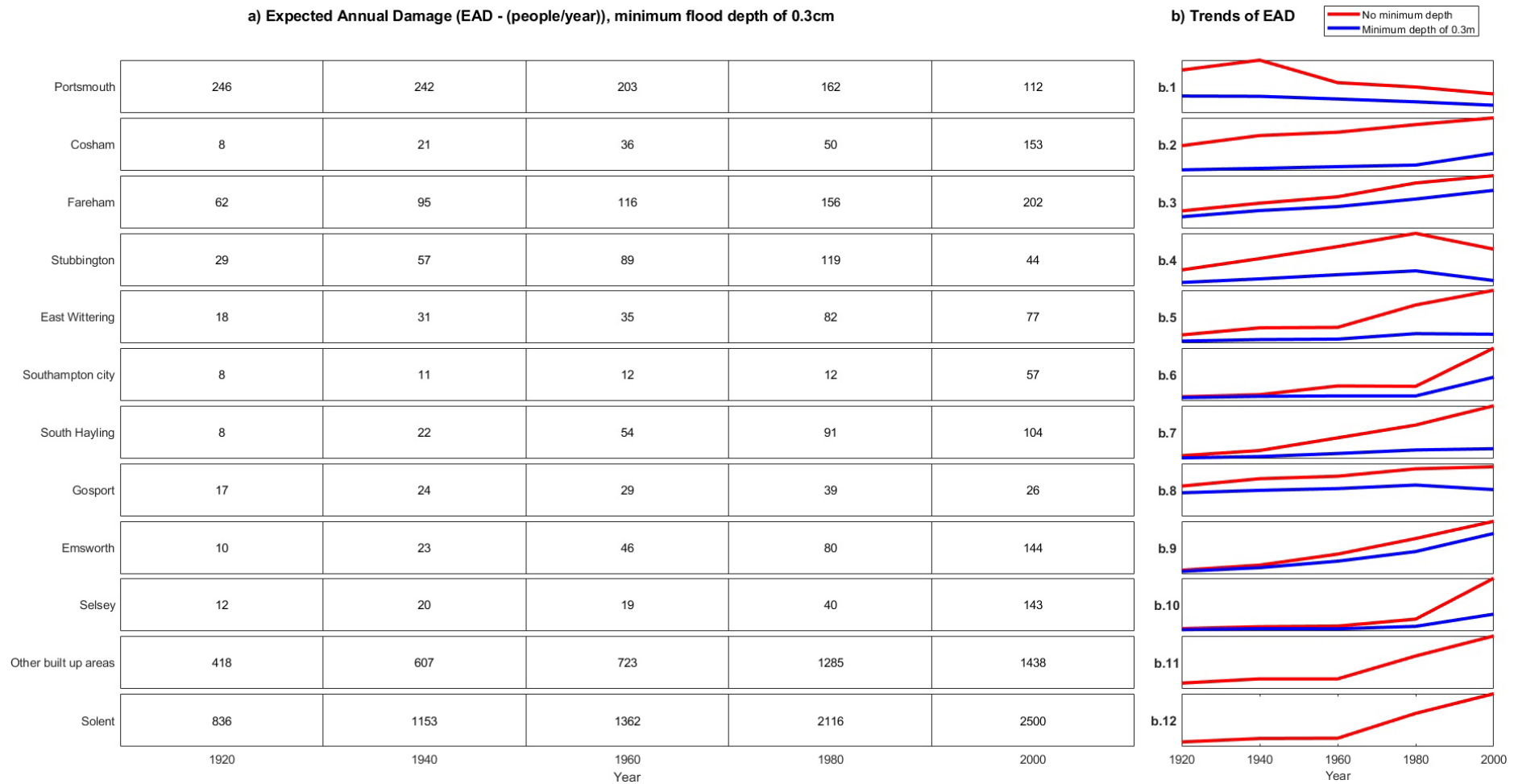


Figure 5.16 Evolution and trends of historical Expected Annual Damage (people) for top cities at the Solent. Note that the y-axis on plots b.1 to b.18 have different units and are only used to present the risk trends.

### 5.3.3 Historical drivers of coastal flood risk

The third sub-objective of this chapter is to determine how the variations on the drivers of risk shaped the level of threat from 1920 to 2000. As done with the exposure analysis, each of the input SPRC factors are varied to analyse their influence on risk. Figure 5.17 presents the results of this exercise. Here, the colourmap represents the average number of people expected to flood per year. The 3D plot shows that lower defences (e.g. equivalent to the year 1920) combined with larger populations and higher sea levels (e.g. the year 2000) lead to the highest EAD.

The variability seen for a 1 in 100-yr event is still highlighted in Figure 5.17.b when mean sea-level and defence standard of protection are kept equal, and only population growth stays variable. The effects of improving the defence standard of protection after 1940 are still highlighted in Figure 5.17.c. Here, two general sections can be appreciated, the top one with the EAD when a SoP prior to that of 1960 is considered, and the bottom one where the height of defences are improved. Sea level has a lower variability than population growth, though it leads to higher increases in exposure from 1920 to 2000.



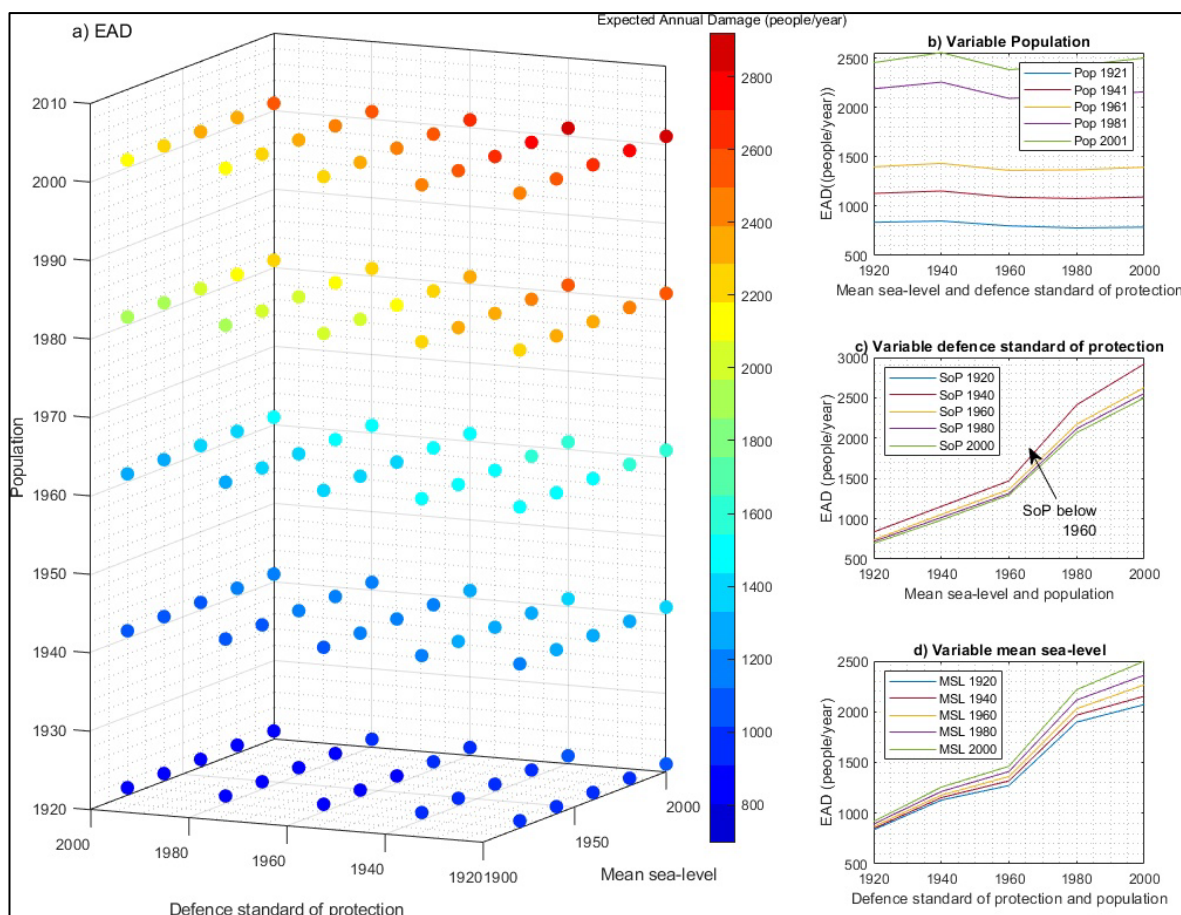


Figure 5.17 Expected annual damage at the Solent, UK., from 1920 to 2000 based on the combination of input factors and a minimum flood depth of 0.3m. Subplot a) present the results when all components are kept variable, comparing defence standards, mean sea level and population size. Subplot b) displays the isolated effect of population variability, c) presents the effect of improving flood defences, highlighting the effect of defence improvement from 1940 to 1960, and lastly d) shows the effect of sea-level rise on EAD.

The influence of each SPRC component by decade is analysed following equation 5.1 (Figure 5.18). For instance, there was no recorded defence improvement from 1920 to 1940 and only a relatively small sea-level rise (Figure 5.18.b), with the EAD increment of 317 people/year directly attributed to population growth (Figure 5.18.a). The increment in EAD from 1940 to 1960 is smaller than that seen for the rest of the timesteps at 200 people. Here, the individual and collective effect of extensive improvement of coastal defences limit the effect of sea-level rise and population growth. However, the effect of population growth can be appreciated from 1960 to 1980, where its isolated effect adds over 700 people/year to the EAD. This increment accounts for over 90% of the EAD increment between 1960 and 1980.

The smaller defence improvements seen from 1960 to 2000 (Figure 5.18.b) still help decrease the level of risk by roughly 30 people in each step. However, its effect is not as prevailing as that of population growth. Similarly, the rate of SLR in the area only started to peak in the late 20<sup>th</sup> century and can be accounted for EAD increases of around 200 people/year in 1980 and 2000, far lower than those generated by population growth.

Similar to the assessment for the region as a whole, the influence of each SPRC component is analysed for the areas with the largest risk. The results show that population growth dictates the level of threat (Figure 5.19). For almost every city, population growth increases the number of people at risk, with the rest of the SPRC components barely affecting. In areas such as East Wittering, Selsey and Totton, the increases in EAD caused by sea-level rise and population growth, combined with the decreasing effect of defence improvement, appear to even out, leading to almost no change in the level of risk (Figure 5.19e, j, m). The decrease in the Portsmouth population found in the census data is again responsible for a decrement in coastal flood risk until 1980. There is still a visible risk reduction driven by population after 1980, even though the census data suggest more people living in this area.



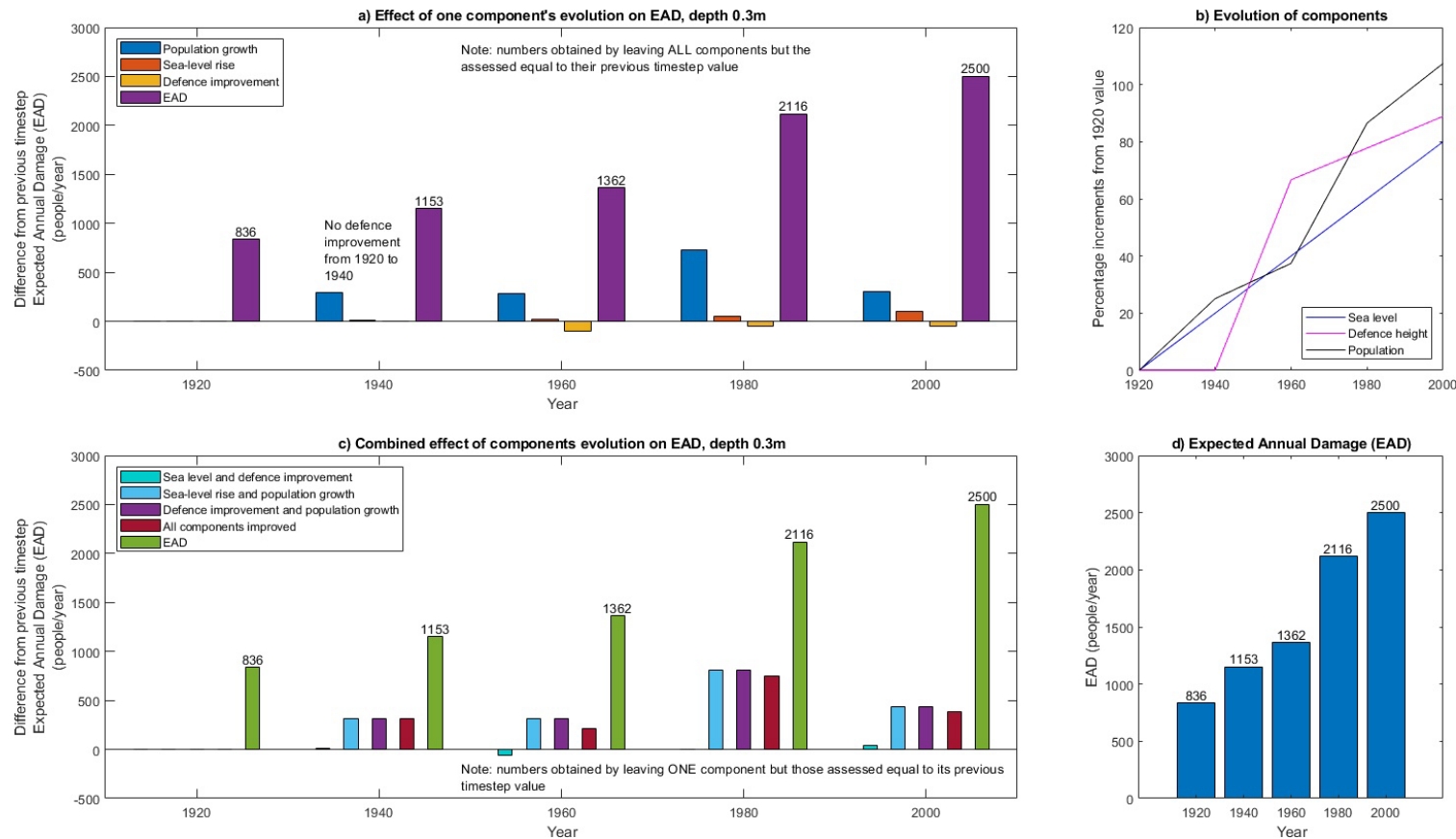


Figure 5.18 Isolated and combined effect of the SPRC components on the historical evolution of expected annual damage. Subplot a) shows the individual effect of each component considering the remainder to be equal to their previous timestep value, showing population growth to be the main driver of EAD increases. Subplot b) presents the evolution of each of the SPRC components as registered, c) shows the combined effect of SPRC factor evolution on EAD. and d) shows the estimated EAD evolution

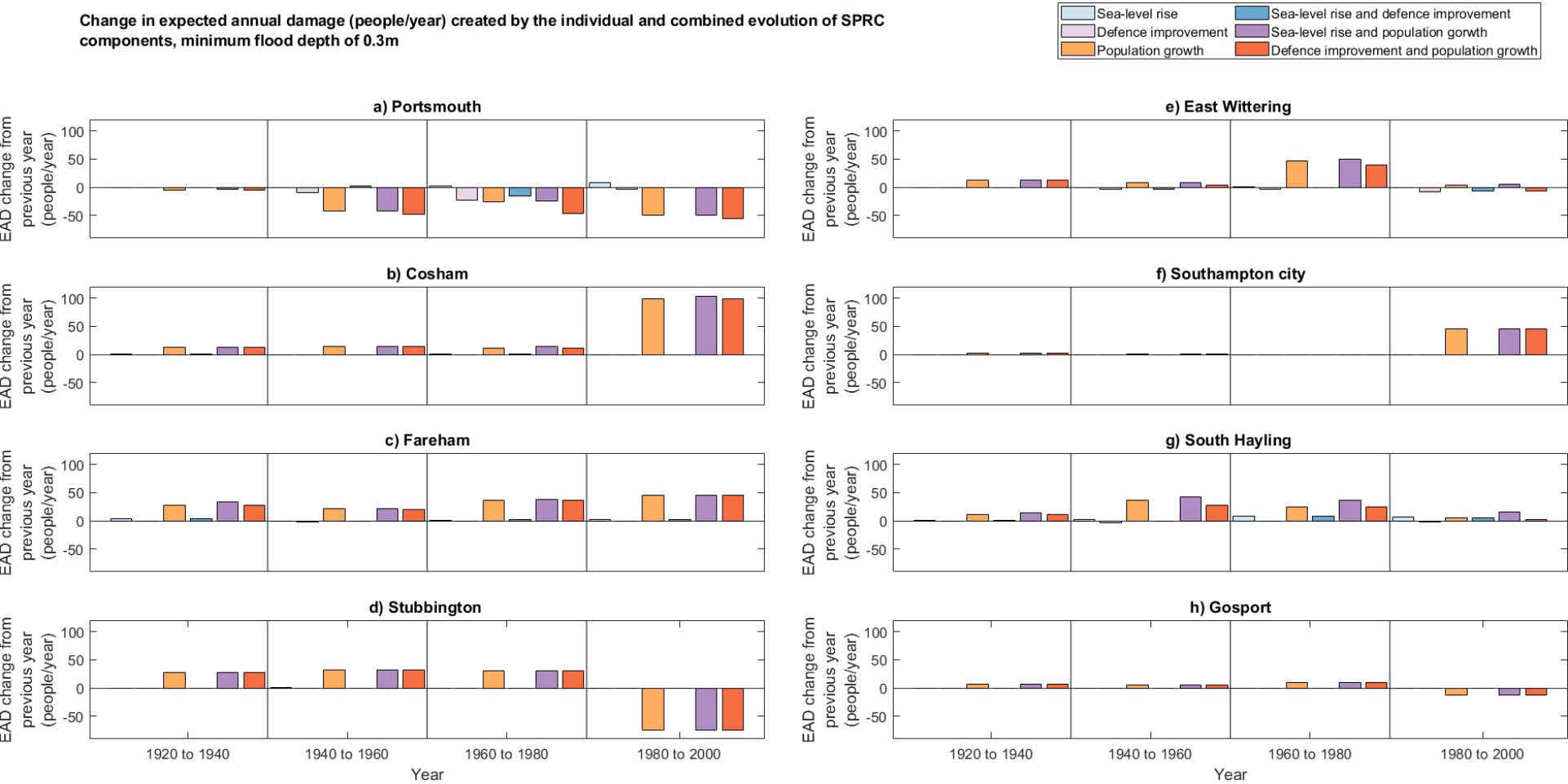


Figure 5.19 Individual and combined effect of SPRC components on the historical evolution of coastal flood risk for main built-up areas. When analysing the effect of individual or joint components, the remainder are kept to their previous timestep value.

## 5.4 Discussion

The present chapter presents the work conducted to complete objective one, which is to assess how coastal flood risk has evolved from 1920 to 2000. The analysis starts by analysing the influence of a flood depth threshold on the estimated levels of risk. This threshold should be determined based on the depth and velocity of water entering the floodplain. However, the assumptions and resolution of the present study create the need for some considerations. Firstly the study uses a DTM for the inundation modelling, meaning all artificial structures such as buildings are removed. This creates an unrealistic scenario where water can accelerate without being affected by these obstructions, leading to high estimates of water velocity. Secondly, the characteristics and materials of each structure will determine its vulnerability. Unfortunately, there is no specific data on the characteristics of the buildings in the area. Even if all properties are assumed to have brickwork on their walls, there are additional factors to consider, such as their height and width. Therefore, a minimum depth of 0.3m is selected as it falls within the required to produce damage to buildings, even at low water velocities.

### 5.4.1 Historical exposure to coastal flooding

The study then moves to complete the first sub-objective of this chapter, which is to analyse the exposure to extreme water levels of increasing magnitude from 1920 to 2000. The results show that exposure rapidly increased from 1920 to 1940, followed by a slowed decrease up to 1960. Most likely, this is tied to two factors. The first one is the substantial defence height improvement assumed in the analysis by the year 1960. As stated by Ruocco et al. (2011), the North Sea floods in 1953 could have led governments and people to prioritize flood defence protection. This, in turn, decreased the ability of water to enter the area and the subsequent consequences of flood events. The effect caused by defence improvement is roughly seen on a similar scale for almost every return period, with the highest reductions in exposure seen for the highest return periods.

The second factor influencing the slow increase in exposure seen from 1940 to 1960 is the registered migration and population decrease in Portsmouth since 1931. It is interesting to see how a single area can steer the overall exposure for the whole area and highlights the city's importance on coastal flood risk assessments.

Analysing the results for a 1 in 100-year event under different input factors gives a better idea of how the evolution of SPRC components shaped the level of exposure to EWLs. Since the increment in mean sea level is regarded at a constant rate of 1.89mm/yr (Hogarth et al., 2020), any increases in the number of people exposed could be expected to be uniform (considering the

pathways and receptors are kept constant). However, there are additional factors to extreme water levels that should be considered. It could be possible that many defences' standard of protection lies at or just over the 1 in 100-yr EWL of 1960, and any increases in the EWL height could lead to flooding in new areas.

Furthermore, it is also possible that higher sea levels and larger volumes of water entering the area led to deeper floodplains, ultimately increasing their extent. Analysing the size of the floodplain, it can be seen that increments in mean-sea level for a 1 in 100-yr event lead to an average increment of 1.73% in the flooded area. Sea-level rise between 1960 and 1980 creates a more extensive floodplain, with an average increment of 1.95%. Altogether, it is interesting to see that population growth is the primary driver of exposure, and it leads to the highest variability under a 1 in 100-yr event.

The study then moves to analyse the spatial distribution of exposure in the region. This indicates that areas at the east of the Solent presented the largest levels of exposure to a 1 in 100-year event. This can be tied to the extreme water level distribution presented by the EA for the region, where EWL height increases from west to east. Furthermore, the eastern regions are indeed more threatened by coastal flooding when wave action is considered. Unlike the western part, this area does not benefit from natural features such as Hurst Spit and the shelter provided by the Isle of Wight. There are, however, areas at the west where the effect of high sea levels is compounded by fluvial influences, such as the case for Lymington. Here, extreme sea levels combined with high river flows have led to considerable flood damage in 1909, 1989 and 1999 (Ruocco et al., 2011, Haigh et al., 2015, Hendry et al., 2019).

The initial hypothesis has been that population is the main driving factor of exposure in the whole area. Although Portsea's large population would confirm such an assumption, its level of threat can also be attributed to its location and low elevation. The decrease in exposure for Portsmouth seen after 1960 is in line with the increasingly higher occurrence of extreme sea levels but lower flood events found by Ruocco et al. (2011) and Boza (2018). This can be evidence of defence improvement benefitting the city, showing the effect pathways can have on the overall risk.

Assuming population distribution to be the factor dictating the exposure would suggest that Southampton, the second most populated city in the area, would have high levels of flood exposure. However, there are different factors that prevent this from happening. Most importantly, Southampton's more elevated topography and location further up Southampton Water. The latter directly affects the magnitude of the extreme water level, with a 1 in 100-yr event being almost 0.2m lower in Southampton compared to Portsmouth. Furthermore, industrial

development, particularly the land reclamation where most of the port of Southampton lies, results in fewer people located within areas where floodwater can reach.

These insights for some of the most important cities in the area provide information that can steer flood management approaches. The approach followed in Portsmouth and here assumed uniform for the whole area could be corresponding with the “hold the line” (HTL) strategy by the Environment Agency (2020b). In general terms, HTL refers to building defences to maintain or improving existing ones to keep the SoP at certain levels, as done between 1940 and 1960. As mentioned, the long-lasting effect of this approach is apparent for Portsmouth when assessing exposure to a 1 in 100-yr event.

Stevens et al. (2015) is the most relevant source of information for a historical assessment of the Solent. Unfortunately, their assessment only covers two cities of the Solent, with only the results from 1960, 1980 and 2000 overlapping with the present assessment. Comparing their results for six return periods, it can be seen that their estimates of exposure are higher for almost every return period, even without a minimum flood depth (Table 5.7). These differences are enhanced when a minimum flood depth of 0.3m is considered. Even though the present study uses a similar approach to Stevens et al. (2015), some distinctions can cause the disparities. Firstly, Stevens et al. (2015) inundation model uses a mean tidal curve of December 1989. The study does not justify the reasoning behind selecting the data for this month and year. It could be assumed that this is done as two major flood events occurred on the 14 and 17 of December 1989, and the authors wanted to represent a worst-case scenario. However, more severe events occurred during the 2013/2014 winter months, and the quality of the data for this period is superior to that of 1989. The only real reason behind the use of such curve is that Stevens et al. (2015) uses Wadey et al. (2012) inundation model to estimate the extent of the floodplain. Wadey et al. (2012) use the water curve of 17 December 1989 to simulate the flood event of this date. Furthermore, as described in section 3.3, Wadey et al. (2012) treatment of flood defences and how these are inputted on the inundation model is likely to overestimate inundations.

Thirdly, and as highlighted by Stevens et al. (2015), their analysis is limited by the assumption of uniform population distribution across the residential areas. In contrast, the present approach uses the highest geographical resolution available for each census combined with the latest Output Areas of the 2001 census to accurately represent the population distribution through time. This is critical for densely populated areas like Portsmouth, where minor fluctuations in the population distribution could lead to significant variations of risk estimates.

Table 5.7 Comparison with Stevens et al. (2015) of Portsmouth historical exposure to extreme water events.

Year	Return period (years)					
	1	10	50	100	200	1,000
Stevens et al. (2015)						
1960	0	907	2,381	3,893	4,573	5,669
1980	0	681	2,011	2,753	3,124	3,898
2000	0	2,139	4,837	5,660	6,219	7,206
Present study, no minimum depth						
1960	342	500	644	704	781	1,156
1980	296	425	559	601	642	1,022
2000	224	304	402	422	472	791
Present study, minimum depth of 0.3m						
1960	189	214	228	228	233	266
1980	146	172	198	198	202	248
2000	98	122	130	145	145	186

#### 5.4.2 Historical risk of coastal flooding

The second sub-objective of the present chapter is to estimate the average number of people at risk per year from 1920 to 2000. The results indicate that the average number of people at risk per year triples from 1920 (836 people/year) to 2000 (2,500 people/year). This represents an average growth of 80 people/year. The results suggest a steady increase in EAD from 1920 to 1960. There is, however, a rapid increment of almost 55% from 1960 to 1980, which is then followed by a minor increment from 1980 to 2000.

Given the fact that the evolution of the SPRC components was not linear in the area, EAD is analysed for the main cities at the Solent. As mentioned, Portsmouth is the area with the highest average risk for the study period. However, migration from the area and coastal defence improvement made its overall risk decrease, with other cities overtaking its top position. Interestingly, various cities show a decrease in their level of risk from 1980 to 2000. These include Stubbington, Gosport, Totton, Bosham, East Wittering and Sarisbury when a minimum flood depth of 0.3m is considered. However, these decremental trends are less evident when a minimum flood depth is disregarded (Figure 5.16). There are areas and even periods of time when these differences increase or decrease. For instance, Portsmouth started the century with a large distinction on the EAD depending on the minimum flood depth, which was reduced after 1960. The factors behind this are flood defence improvement and migration from the area. In contrast, other cities in the area started the century with almost no difference in the number of people

threatened regardless of the minimum depth of flood. However, the difference in the trend of their risk estimates when a minimum depth of flood is required becomes evident moving towards the second half of the 20th century (Figure 5.16 b.3, b.5, b.7, b.8, b.10, b.11). Other top cities maintain the distance between the risk estimated when a minimum depth of 0.3m is required and their no minimum depth results (Figure 5.16 b.2, b.4, b.6, b.9, b.12). Finally, a small number of the main built-up areas experience the same level of threat regardless of the minimum depth required. These include Totton (Figure 5.16 b.13), Bosham (b.14), Sarisbury (b.15) and Lymington (b.16).

As with the exposure assessment, the best source of comparison for historical risk estimates in the area is Stevens et al. (2015). Considering expected annual damage is obtained using exposure and the information presented in Table 5.7, Stevens et al. (2015) estimates are expected to be larger than the present study's findings. Unfortunately, the study does not explicitly give their EAD numbers (called annual average exposure for their study), which are only shown in a graph (Figure 5.20.a). This required using their exposure estimates to obtain the equivalent EAD (Figure 5.20.b). The results confirm that the estimates of risk in this study fall below those of Stevens et al. (2015) regardless of the minimum flood depth required to produce damage. Interestingly, the results of both studies concur with the decreasing trend seen from 1960 to 1980, with relatively low differences between them. However, Stevens et al. (2015) find a sharp risk increment in EAD from 1980 to 2000, with their results almost trebling (Figure 5.20.c). This could be a product of their assumption of uniform population distribution. Even though the overall number of people living in Portsea increased from 1980 to 2000, the new population is not evenly distributed across the area, as shown in Figure 5.6

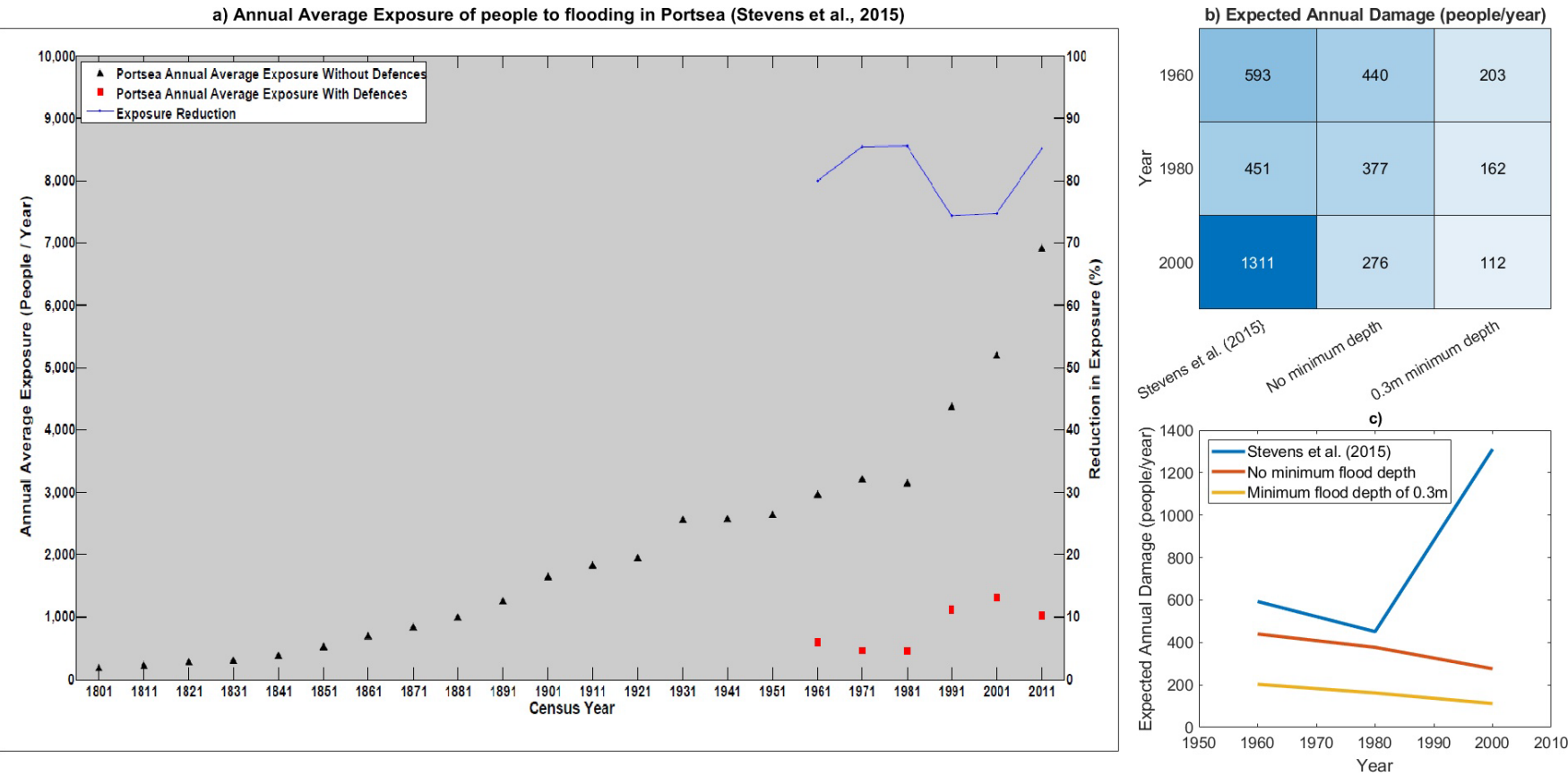


Figure 5.20 Expected Annual Damage results from (a) Stevens et al., (2015). (b) the EAD estimated in the present assessment, and (c) a comparison of both.



### 5.4.3 Historical drivers of coastal flood risk

The influence of each SPRC component on the level of risk from 1920 to 2000 is analysed on the third sub-objective. These indicate that population growth was the main driver of risk. However, its evolution was not linear, and neither was its effect on risk. Most notable is the case of Portsmouth, which strongly contributes to the EAD of the area. Here, the population decreased from 1940 to 1960. However, the overall effect of population evolution on coastal risk is close to that seen from 1920 to 1940. This is interesting as it could suggest people migrated to and developed areas within the coastal floodplain. Even though the population at the Solent continued to rise from 1960 to 2000, its effect on EAD reached its peak by 1980 and rapidly decreased by 2000. This could be caused by population growth occurring in areas outside of the floodplain.

Furthermore, the improvement in census data resolution for the year 2001 modified the estimated risk. As noted, 2001 was the first time the Office for National Statistics introduced Output Areas to a census. These areas are, up to date, one of the lowest geographical levels at which population estimates are available. By improving the resolution of the data, a more accurate representation of the population distribution may have led to fewer people being located at the floodplain. This becomes a critical aspect for highly densely populated areas such as Portsmouth, where small changes can significantly impact the estimated level of coastal flood risk. Similarly, Stubbington and particularly Lee-on-the-Solent are areas that see the largest difference in population distribution from 1981 to 2001 (Figure 5.7.e). The opposite seems to occur for Selsey, where the percentage difference in population was almost negligible between timesteps until 2001, when this drastically increases.

It should also be considered that expected annual damage is the integration of all risks and probabilities to generate an average number of people who could experience flooding every year. Being affected by their likelihood, the events with a higher probability (i.e. low return period) and the largest associated damages have the most influence on EAD. Following the defence improvements before 1960, likely driven by the first coastal protection act, the effect of low return period events was reduced, leading to a fall in the overall number of people flooded. Furthermore, following the North Sea flood event of 1953, people could have migrated from areas prone to coastal flooding.

## 5.5 Conclusions

Objective one seeks to analyse the evolution of coastal flood risk at the Solent from 1920 to 2000. This, to understand how each SPRC component influenced coastal flood risk. This can provide general indications of what could happen in regions that might experience a similar evolution to that seen at the Solent from 1920 to 2000. Three sub-objectives were defined to aid in the completion of objective one. The first sub-objective was to analyse the past exposure to various extreme water levels of increasing magnitude. The baseline assumption is that population growth had increased the consequences, whilst defence implementation actively decreased the probabilities of coastal flooding. The analysis of the Solent agrees with the baseline hypothesis, and overall it is clear that larger populations lead to increases in the level of threat. The assessment finds that exposure to extreme water levels increased from 1920 to 2000, although the increments were not linear. It can be appreciated that lower return periods saw their resulting exposure steadily increase between 1920 and 1960. In contrast, the higher return period saw fast increases from 1920 to 1940, plateaued from 1940 to 1960, followed by sharp increments by 1980. Similar trends are found for the average number of people at risk per year.

The second sub-objective was to estimate the number of people at risk per year from 1920 to 2000. The results indicate that coastal flood risk tripled from 1920 to 2000, with an average increment of 21 people at risk per year. Analysing the trends of EAD, it can be seen that there was a steady rate of increment from 1920 to 1960, which abruptly increased from 1960 to 1980. This can be tied to a rapid increment in the population at the Solent seen for this period. The results are compared to previous estimates by Stevens et al. (2015), showing agreement for the data prior to 1980. Interestingly, Stevens et al. (2015) estimates of risk have an unexplained sharp increment from 1980 to 2000, which can be a product of the assumptions made by their assessment, most likely the uniform distribution of population at the study area. This highlights one of the key improvements of the present approach to population distribution presented in section 5.2.3, where the highest quality data available is used to procure a more accurate representation of people at the study area.

Lastly, the third sub-objective was to determine how the variations on the drivers of risk shaped the level of threat from 1920 to 2000. The results indicate the population growth was the primary driver of coastal flood risk for the Solent during the 20<sup>th</sup> century. The magnitude of change caused by the overall increments in population is larger than that of sea-level rise and defence improvement combined. This is interesting as there is a widespread belief that sea level being the cause of coastal flood risk in the past. This assessment has shown that the rate of sea-level change from 1920 to 2000 did increase the threat level, but its effect was limited. Furthermore, the data

shows that defence improvement prior to 1960 had a long-lasting effect on the regional level of risk. Analysing the effect of SPRC components on a city level also shed light on the importance of finer scale analysis. The city of Portsmouth is regarded as the highest contributing area to the regional levels of risk. The analysis shows that migration from the area combined with defence improvement actively decrease the level of threat. Although the city started the 20<sup>th</sup> century as the area with the highest coastal flood risk, other areas overtook this after 1960. The remainder built-up areas of the region had the opposite effect, with migration into their areas and subsequent increments in coastal flood risk. It can be seen that population growth varied across the Solent. It is not possible to determine the factors that drove migration into specific areas. Although certain factors such as local economics could influence this trend, the possibility of migration to these areas being caused by a sense of safety provided by improved defences should not be discarded.

The assessment highlights the need to create an accurate representation of the historical distribution of the population and the effects this has on risk estimates. This is clearly shown for Stubbington, an area where housing development occurred near the coast. Here, using the highest geographical resolution available for census data resulted in fewer people living within the floodplain. Similarly, a better distribution of the Portsmouth and Fareham populations led to a decrease in the average number of people at risk per year by 2000.

Both sea-level rise and defence improvement show minor effects on the level of risk for individual cities compared to that of population growth. The isolated effect of mean-sea level rise from 1940 to 1960 barely produced any increments in the EAD, which could indicate that people were aware of the areas prone to flooding and avoided developing them during this period. Analysing the individual effect of SLR after 1960, this increases exposure for cities such as Fareham, Stubbington and Cosham, which indicates development in areas within the floodplain, again possibly linked to a sense of security provided by coastal defences. However, sea-level rise began to appear as a driving factor in 2000. Although a small finding, it should be considered for future assessments as the rate of registered sea-level rise for the 20<sup>th</sup> century of 1.8mm/yr is lower than the lowest projected future sea-level rise scenario for the UK (2.9mm/yr UKCP18).

Some assumptions are made for this assessment which directly affect the estimates of risk. The most critical being that all of the defences found in the present-day were built before 1920. This is unlikely as, more often than not, defence implementation is driven by a necessity to protect people, assets or the environment. As mentioned, the first coastal protection act came in place in 1949. It is not clear if this triggered coastal protection in the area as recording when these were built was not common practice even for built-up areas such as Portsmouth or Southampton, let

alone for rural sections around the New Forest. Unfortunately, it is not possible to quantify the effect of this assumption on risk estimates as the only option to compare against would be a “worst-case” scenario where no defences exist, which is far less realistic.

Furthermore, there is no data available indicating the improvements in the standard of protection of coastal defences throughout the 20<sup>th</sup> century. It is assumed that all the defences in the region followed the trend seen in Portsea. In reality, some areas required improvement before others and even the level to which these were improved varied. It is clear from the spatial analysis that areas in the eastern regions were more threatened by flooding, requiring higher levels of protection than those in the west.

This study built on previous methodologies to distribute population within the study area. Unfortunately, the resolution in which censuses were reported before 1980 generates significant uncertainties on the accuracy of these distributions. Given what has been highlighted by the findings, and considering the metric used to determine the damage caused by coastal flooding is the number of people, accurately determining the population distribution at the floodplain is one of the most critical factors for a flood risk assessment. Some authors (e.g. Neumann et al., 2015) provide correction factors to estimate the population in urban and non-urban coastal areas. However, it is impossible to determine if the numbers that would yield for the Solent using such factors would considerably impact the present results as there is no data available for comparison.

## Chapter 6 Present levels and largest sources of uncertainty in coastal flood risk at the Solent

### 6.1 Introduction

Coastal flooding is a constant global hazard. In England, the risk posed by extreme sea levels is considered the second largest concern for civil emergency, only outweighed by pandemic influenza, with potential consequences including fatalities, impact on mental health, damage to property, interruption of essential goods and services, and environmental damage (Cabinet Office, 2015). Recently, significant coastal flood events have occurred in England, with the most notable events occurring during the winter of 2013/2014 (Wadey et al., 2015b, Haigh et al., 2020). These events have caused catastrophic economic consequences with collective damages worth over £2.5 billion (Haigh and Nicholls, 2017). However, there is a visible decrease in fatalities when the consequences of these floods are compared to historical events (Haigh et al., 2020). This can be attributed to different reasons, such as the improvement of coastal defences and the adoption of early warning systems. However, the likelihood of coastal flooding is expected to increase as a consequence of climate change (IPCC, 2021). Furthermore, socio-economic factors such as population growth and migration and the demands this creates for protection can impact the consequences of coastal flooding (Hauer, 2017, McMichael et al., 2020).

Conducting a coastal flood risk assessment is a complex task that requires a good understanding of the characteristics of natural phenomena and anthropogenic behaviour. The SPRC framework is a valuable tool to identify all of the components driving coastal flooding (Evans, 2004, Narayan et al., 2014). However, up to date, no research has been conducted analysing the interactions between all of its components and the uncertainties these generate. Most of the previous assessments exploring uncertainty in coastal flood risk focus on one of two options. The first group of studies focuses on highly specific factors, such as the influence of elevation model resolution (e.g. Savage et al., 2016) or friction factors (e.g. Seenath, 2015) on the inundation extent. On the other hand, the second family of assessments aims to tackle the variability generated by the epistemic uncertainty in the main components of the SPRC. However, the latter group tend to do so for one or more but not all of the components (e.g. Lewis et al., 2011, Muis et al., 2015). A more in-depth analysis of some of the most relevant studies available has been presented in Chapter 2.

Furthermore, coastal flood risk assessments rely on the use of models to estimate the level of hazard. These models are built to represent, as closely as possible, the natural phenomena occurring in the study area. However, to achieve the required computational performance, most of the models available adopt simplifications. Often, the model results obtained, which are then used for the coastal flood risk assessments, are strongly dictated by these assumptions adopted by the models, which is one of the sources of uncertainty affecting the accuracy of the predictions. However, this particular source of uncertainty is often, if not always omitted, either knowingly or unintentionally, in coastal flood risk estimates.

Based on the above, the overreaching aim of objective two, the subject of this chapter, is to analyse the present-day levels of coastal flood risk at the Solent and its main sources of uncertainty. For this purpose, three sub-objectives are established, as follows:

1. Analyse the present-day exposure to coastal flooding at the Solent
2. Estimate the present-day number of people at risk of coastal flooding at the Solent.
3. Quantify the influence of the characteristics of the SPRC components on the estimates of exposure and risk of coastal flooding

The analysis starts from the assumption that extreme water levels will produce the largest sources of uncertainty, but it is the variability of defence height what controls the outputs of the inundation model and therefore dictates the level of risk. Along with this, it is expected for population resolution to be an important factor, and using a coarse-resolution population model will markedly overestimate the level of risk compared to a fine-resolution population model.

The structure of this chapter is as follows. First, the data and methodology required to achieve objective two and its sub-objectives are described in section 6.2. The results are then presented in section 6.3. A discussion of the key findings follows in section 6.4, and conclusions are given in section 6.5.

## 6.2 Data and methods

This section presents the specific data and methods applied for objective two, building on the general methodology presented in Chapter 4. It starts by introducing the basics of uncertainty analysis and the sample generation for a sensitivity assessment. This is followed by a discussion of the parameters of the hydrodynamic model, such as the boundary conditions and elements that act as barriers to water flowing at the study area. Following this, the improvements introduced in this thesis to Stevens et al. (2015) methodology for population distribution, which consist of including new and more accurate data, are presented. The resulting population distribution and

the risk estimates obtained with this distribution are compared to those using WorldPop, a global population distribution model. A preliminary analysis is conducted to determine the number of simulations required for the assessment. As previously mentioned, the focus is given throughout this chapter to the analysis of the uncertainty associated with each input variable.

### **6.2.1 Uncertainty and sensitivity assessment**

Uncertainty can be addressed in many ways depending on the scope of the assessment and the nature of the uncertainty. Epistemic uncertainty derived from a lack of knowledge tends to be assessed with conceptual models. However, it is not easy to assess and quantify it unless very extreme scenarios are considered. For example, quantifying uncertainty due to the presence of coastal defences can only be explored by comparing the results of models with/without defences. On the other hand, aleatory, or random, uncertainty can be systematically explored based on the knowledge of the phenomena. In general, the simplest approach to analysing uncertainty relies on the use of scenarios where plausible conditions are combined. The use of a scenario-based approach is often driven by the need to simplify the analysis, product of methodological or data limitations. Another approach to estimate uncertainty is the use of statistical assessments of the critical flood risk parameters considering their probability of occurrence. This approach usually yields a large range of results and introduces the likelihood of each one based on the probability of different model configurations. Here, the focus is on the aleatory uncertainty and explored with two general methods. The first one makes use of a scenario approach, whilst the second follows a probabilistic assessment of the SPRC components.

#### **6.2.1.1 Scenario analysis**

In a very simplistic way, the use of scenarios relies on having a set of statuses for each component. For instance, three scenarios for extreme water levels. One where the lowest height for each return period is used, one where the mean value is utilised and one with the maximum. Here, instead of the scenarios dictating the value of a component (i.e. lowest, mean or highest), they indicate whether the components are constant or variable. These are used to investigate the influence of each SPRC component's uncertainty on the overall uncertainty of coastal flood risk estimates.

The scenarios start by maintaining all but one component constant. Then, one by one, the additional components are changed. By following this approach, the variations in the spread of results caused by the individual SPRC elements can be quantified. The mean value obtained in the preliminary assessment of each component is used as their constant value.

Table 6.1 Scenarios used for sensitivity and uncertainty analysis

Scenario	Surge length	Extreme water level	Defence height	Length of defences modified
1	Constant (mean value)	Constant (mean value)	Variable	Constant (50%)
2	Constant (mean value)	Variable	Constant (mean value)	Constant (50%)
3	Constant (mean value)	Variable	Variable	Constant (50%)
4	Variable	Constant (mean value)	Constant (mean value)	Constant (50%)
5	Variable	Constant (mean value)	Variable	Constant (50%)
6	Variable	Variable	Constant (mean value)	Constant (50%)
7	Variable	Variable	Variable	Constant (50%)

#### 6.2.1.2 Probabilistic assessment

The probabilistic assessment is done using a Quasi-Monte Carlo framework (Sobol, 1998, Caflisch, 2008). Firstly, the individual parameters are analysed and their possible configurations determined. This is done by producing a probability distribution for each component. Following this, the parameters are (quasi-)randomly sampled to produce a space of inputs. One of the problems with a probabilistic approach that relies on sampling techniques is the large number of combinations and simulations required to reach convergence on indicators such as the standard deviation of the results, creating high computational costs. This problem is tackled using a Sobol' sequence, an efficient sampling technique demonstrated to result in faster-converging results and decrease computational expenses (Burhenne et al., 2011, Renardy et al., 2021).

#### 6.2.1.3 Sensitivity assessment

Along with the uncertainty assessment, it is possible to determine the components that generate the highest variabilities and those to which coastal flood risk estimates are most sensitive. Here,



and based on the QMC framework used for the uncertainty analysis, a variance-based sensitivity analysis of the Sobol' indices for the first order ( $S_i$ ), second-order ( $S_{ij}$ ), and global ( $S_{Ti}$ ) sensitivities is followed. The first order, or local sensitivity, refers to the individual effect of each component over the averaged variation of the rest of the components. The second-order indices analyse the fractional contribution of the interactions between individual variables. On the other hand, the global, or total effect, estimates the contribution of each variable considering all the possible interactions between components.

Alongside the uncertainty analysis of each SPRC component presented in the following sections, the methods and equations described by Saltelli et al. (2010) are used to determine the local and global sensitivities of coastal flood risk to each SPRC components. Firstly, two sampling matrices,  $A$  and  $B$  of size  $N \times j$ , and  $a_{ij}$  and  $b_{ij}$  elements are generated. The  $a_{ij}$  and  $b_{ij}$  elements are obtained by sampling each component's probability distribution using the Sobol' sequence. The  $N$  dimension of the  $A$  and  $B$  matrices represents the number of sample points, whilst the  $j$  dimension is equivalent to the number of input factors. Secondly, the matrix  $A_B^{(i)}$  is generated by keeping all the columns but the  $i$ -th of matrix  $A$ , and replacing the  $i$ -th  $A$  column with the  $B$   $i$ -th column. The same procedure is followed for each input factor, replacing the  $i$ -th column of  $A$  with the  $i$ -th of  $B$ . The matrices  $B_A^{(i)}$  are built in the same way. Saltelli et al. (2010) proposes simple estimators to compute  $S_i$  and  $S_{Ti}$ . Here,  $f(X)$  is the result obtained from conducting the analysis with the  $X$  inputs, and  $V(Y)$  is the variance of all the results obtained in the analysis.

$$S_i = \frac{\frac{1}{N} \sum_{j=1}^N f(B)_j (f(A_B^{(i)})_j - f(A)_j)}{V(Y)} \quad 6.1$$

$$S_{Ti} = \frac{\frac{1}{2N} \sum_{j=1}^N (f(A)_j - f(A_B^{(i)})_j)^2}{V(Y)} \quad 6.2$$

Dr Sergei Kucherenko and O. Zaccheus through the Imperial College London have made available a Sobol global sensitivity analysis software capable of computing the first and higher-order indices as well as the total effect of each input variable (available at <https://www.imperial.ac.uk/process-systems-engineering/research/free-software/sobolgsa-software/>). This model is employed in the present thesis as it offers simplicity and accuracy. The model feeds off the quasi-random samples and evaluates them against the model outputs to obtain the sensitivity indices.

### 6.2.2 Sources (Boundary conditions)

To create the boundary conditions, as mentioned in section 4.2.1, the 100 largest storm surge events on record are identified, and their characteristics are obtained. Previous assessments (e.g. Wahl, Mudersbach and Jensen, 2011; MacPherson *et al.*, 2019) analysing the boundary conditions of flood risk assessments tend to characterise water curves (e.g. hydrographs, surge curves, tide curves) with parameters such as initial, peak and final water levels, and time to peak. Here, the focus is on the start and end times as the surge height is modified at later stages. The start and end are the times when water starts to rise before it reaches maximum height and the time it takes until the surge event ends. The elapsed time between start and end is recorded as the length of each surge.

A probability distribution of the recorded lengths is generated (Figure 6.1), and 1,000 quasi-random samples are obtained. These samples are used to modify the length of the mean surge curve presented in section 4.2 to capture the behaviour of all the storm surges recorded in the study area. It should be noted that all the start and end times of the generated surges are symmetrically modified to reach the desired length. Each of these surge curves is added to the MHWS curve, and their total height is recorded.

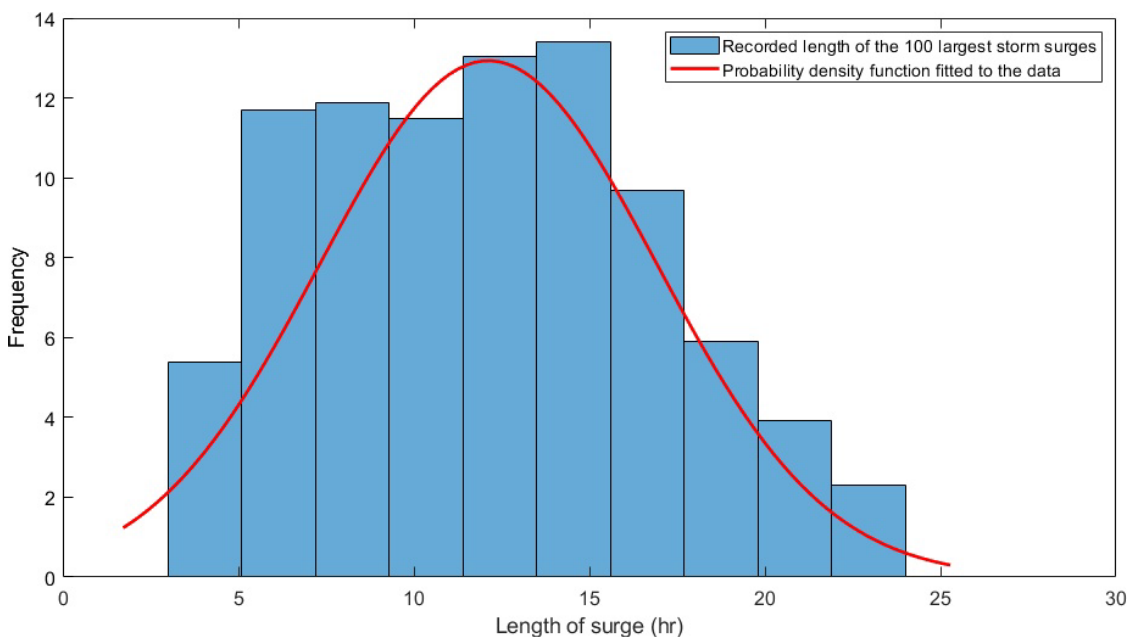


Figure 6.1 Recorded storm surge lengths for the 100 largest surges on record. A probability distribution is fitted to the data, which is then sampled using the Sobol sequence

The water curves do not have a particular return period or maximum height assigned to them and are modified depending on the extreme water value to analyse. The extreme water level heights are obtained from the latest EA data (Environment Agency, 2018). The EA estimates these EWL for 46 of the National Tide Gauge Network (NTGN) and seven non-NTGN gauges provided by Forth

Ports, the National Oceanography Centre, the British Oceanographic Data Centre and the UK Hydrographic Office (Environment Agency, 2018). The tide gauge data is used to estimate the joint probability of possible peak tide and skew surge combinations (Environment Agency, 2018). This probability, referred to as a return period, is the geometric mean of the probabilities of all the skew surge and peak tide combinations that add up to the total extreme water level. The EWL are calculated at the 53 tide gauge locations and interpolated along the coastline with the UK operational tide-surge numerical model at a 12km resolution. The 12km resolution was later increased by the EA to 2km based on inverse distance weighting coupled with the high-resolution north-east Irish Sea model, as well as local modelling of estuaries, tidal rivers and harbours (Environment Agency, 2018).

The EA provides the data for each tide gauge location as well as for points along the coast for a total of 16 return periods (Table 6.2). One of the benefits of this is that, since data is available for locations between tide gauges, it better represents the reality of EWL distribution in complex areas such as the Solent and mainly Southampton water (Figure 6.2.a). There is a clear decrement in the EWL height from east to west, which can be a consequence of western travelling surges doing so against the tidal waves of the English Channel (Haigh et al., 2004b). In addition to the mean EWL height, the EA includes the values for the 97.5% and 2.5% confidence intervals derived from the joint probability analysis for each EWL (Figure 6.2.b).

Table 6.2 Extreme water levels and return periods for Portsmouth tide gauge by the Environment Agency

Return period (years)	Extreme water level height (m)	Return period (years)	Extreme water level height (m)
1	2.56	100	3.04
2	2.54	150	3.08
5	2.73	200	3.11
10	2.81	250	3.13
20	2.88	300	3.15
25	2.9	500	3.2
50	2.97	1,000	3.26
75	3.01	10,000	3.49

Analysing the EWL and the confidence bounds, it is clear that a skewed shape parameter resulted from the EA model (Figure 6.2.c). The EA presents the shape parameters in a graph as part of the Coastal flood boundary conditions (Environment Agency, 2018). However, these are presented as boxplots without a clear indication of the value utilised for the assessment. Given the uncertainty generated by the possible range of EWL height within each return period, it is necessary to analyse their influence on the overall level of risk. Therefore, the probability distribution of each EWL is obtained by solving for the generalised extreme value cumulative density function (Figure 6.2.d). Then quasi-random samples are generated for each EA point along the Solent.

The EWL heights are then interpolated to each inflow point located every 50m along the coast as presented in section 4.2.1. Finally, each surge curve is stretched so it matches the water height for each point and return period once added to the MHWS tide.

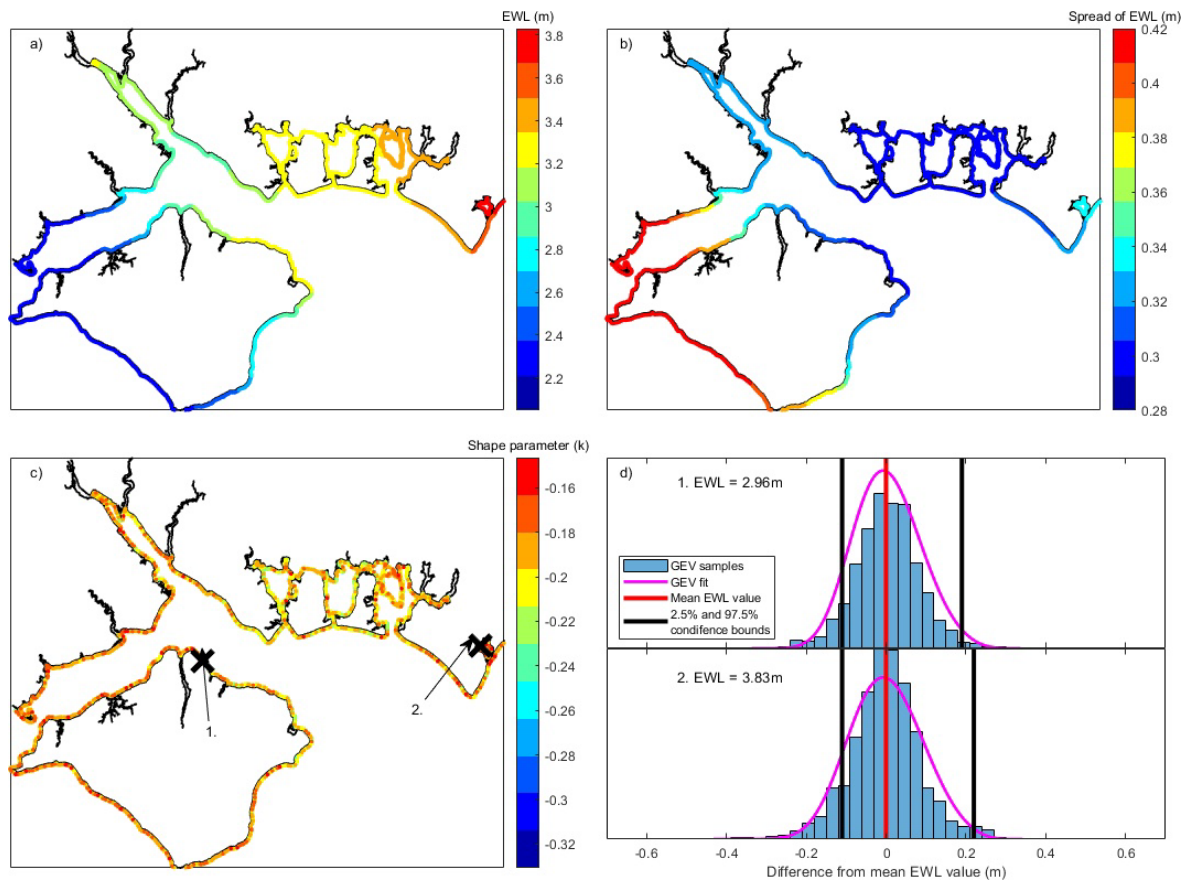


Figure 6.2 a) Extreme water level height distribution across the Solent for a 1 in 300-yr event. b) Spread between the 5<sup>th</sup> and 95<sup>th</sup> confidence bounds. c) Shape parameter of each inflow point considering the mean value and confidence bounds. d) Example of the probability distribution fitted to the EA data and the samples generated for the analysis at two locations in the Solent.

### 6.2.3 Pathways (Barriers to water flow)

The flood defence data by the EA and the Channel Coastal Observatory presented in section 4.2.3 are used as an input for the barriers to flow in the LISFLOOD-FP model. The data comprises the location of flood defences and includes some of the main characteristics for each structure, such as maximum height, the standard of protection and overall condition. As mentioned in section 4.2.3, there are several sources of epistemic uncertainties tied to the data. Inaccurate assessments of the defence's conditions and heights are the primary source of concern in the present study, which could only be overcome entirely with in-situ assessments of every defence in the area. Unfortunately, this falls outside of the scope of the present assessment as it would require a tremendous amount of time and resources.

Based on the above and considering objective two includes the exploration of uncertainty, it is decided to create an additional dataset of defence height obtained from elevation datasets. This is done using the points generated along each coastal defence structure in section 4.2.3 to extract the elevation values from the EA LIDAR DSM and DTM at a 2m horizontal resolution.

The height difference between the DSM and DTM can be considered the height of the defence derived from a high-resolution elevation dataset. This elevation-derived defence height dataset is used to compare the elevation reported by the EA against the elevations obtained from an indirect assessment. The reasoning behind this being a) it serves to assess the accuracy of the elevation-based data by comparing the height differences, and b) transferability to areas where data is scarce, and the only source of information available is satellite data.

The difference between the heights reported by the EA and those obtained from the elevation models are gathered, and a probability distribution is obtained (Figure 6.3). It can be appreciated that in most cases (66%), the heights obtained from the elevation models are lower than those in the EA data. The majority (36%) of the overall differences are within 0 to 0.1m. The peak seen at 0 to 0.1m would make it so that a Gaussian distribution is assigned to the data if this is automated in software such as Matlab (Figure 6.3.a). However, a stable distribution seems to better fit for the probability distribution (Figure 6.3.b). The stable probability distribution is sampled, and this data is used to modify the height of the defences. Once the height by which the defences are modified, the structures which will be modified are selected. Those modified are randomly selected only considering those that offer protection against coastal flooding, and the total length of defences modified is set at 50% of the total defences.

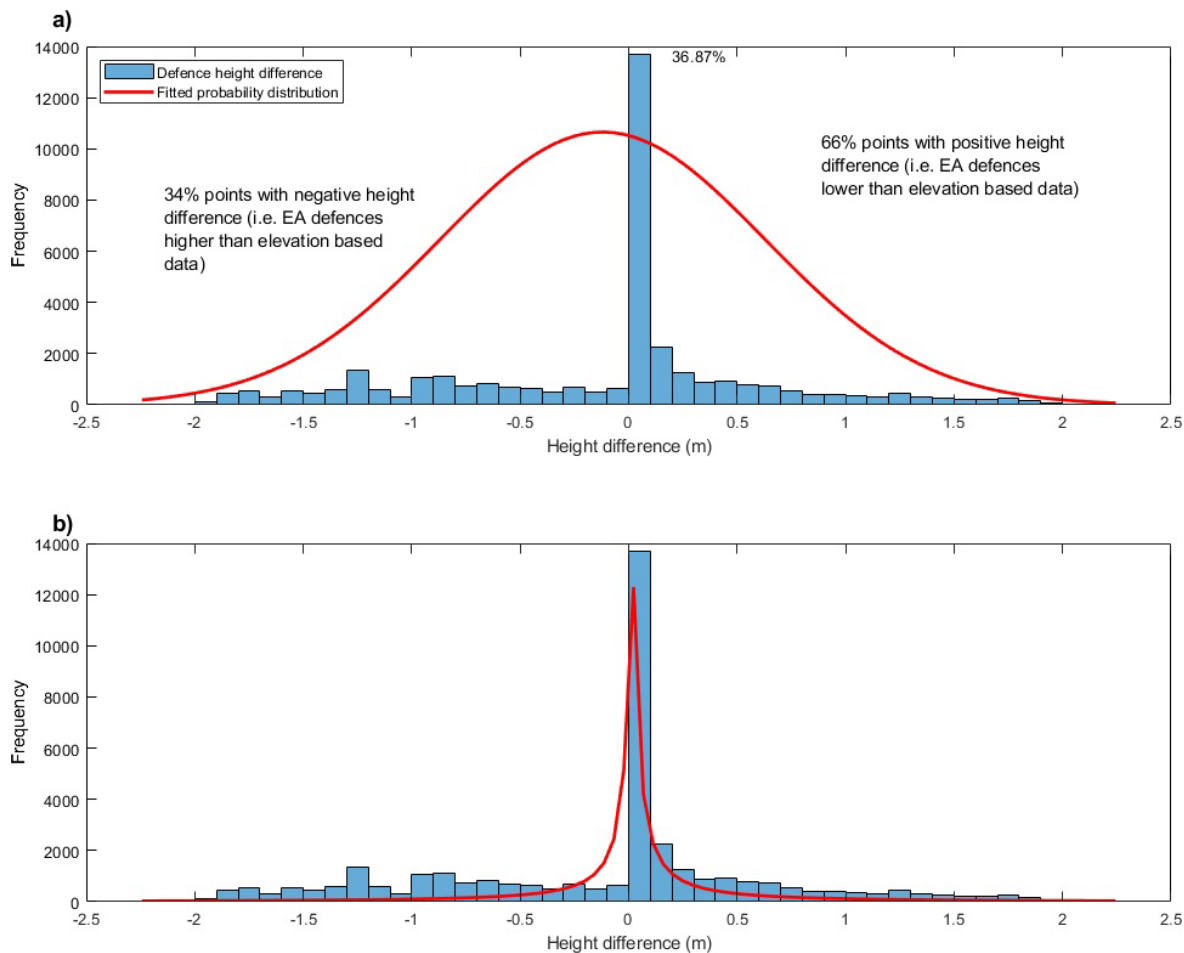


Figure 6.3 Difference in defence height when comparing the Environment Agency's dataset against the elevation model-based defence heights. a) Shows the results with a normal distribution fitted to the data. b) Difference data with a stable distribution fitted.

#### 6.2.4 Receptors (Population distribution)

As mentioned in section 4.3, the methods used to distribute the population in the study area have to be adjusted depending on each objective's data availability and temporal scope. Here, the improvements on the population distribution method by Stevens et al. (2015) using the latest available data are presented.

As mentioned in section 5.2.3, since 2001, the Office for National Statistics has made available census data on an Output Area resolution. These OA have associated population-weighted centroids, representing the spatial distribution of people within each OA (Figure 6.4.a). The PPWC are generated using a median centroid algorithm for the 2011 census (ONS, 2011). Following the methodology presented in section 4.3, the urban extent is digitized so that the population is distributed in areas with development. At present, the Ordnance Survey has made available a building height dataset as part of the Master Map Topography Layer. This dataset contains

polygons that represent individual properties in the area (Figure 6.4.b). Each polygon includes information such as the total height of the building and relative height from the ground to the roof (Ordnance Survey, 2016). The layer contains any roofed building, residential homes, covered tanks, horticultural glasshouses with an area over 50m<sup>2</sup>, and mobile or park homes that are permanent and have a postal address (Ordnance Survey, 2016, Ordnance Survey, 2017). However, the OS does not differentiate between residential, commercial or industrial properties. This creates a problem as the population should only be distributed within the residential extent. Unfortunately, this is hard to overcome unless additional knowledge of specific areas is available.

Since it is not possible to overcome this limitation with the data publicly available, all of the properties in the dataset are assumed as residential. Having done so, a new square grid of 50m by 50m is created over the study area and the urban grids that contain the building polygons identified. It should be noted that the shape of each output area causes some of the square grids to overlap between OA. When this occurs, the percentage area of the square that lies within each OA is calculated, and the polygon is assigned to the OA with the highest share.

The urban grids within each OA are identified, and the population is assigned to them based on the proximity of each square to the PPWC (Equation 6.3) (Figure 6.4.c). Stevens et al. (2015) investigate the influence of selecting an influence radius of 50m, 100m, 200m, 300m, 400m and 500m for each PPWC, concluding that there is no significant variation on the results.

$$P_x = \left( \frac{\frac{\sum_{i=1}^n d_i - d_x}{\sum_{i=1}^n d_i + d_x}}{\sum \frac{\sum_{i=1}^n d_i - d_x}{\sum_{i=1}^n d_i + d_x}} \right) P_{PPWC} \quad 6.3$$

Where  $P_x$  is the population of each urban grid,  $d_x$  is the distance from the PPWC to the urban grid,  $\sum_{i=1}^n d_i$  is the total distance of all urban grids to the PPWC, and  $P_{PPWC}$  is the total population of the PPWC.

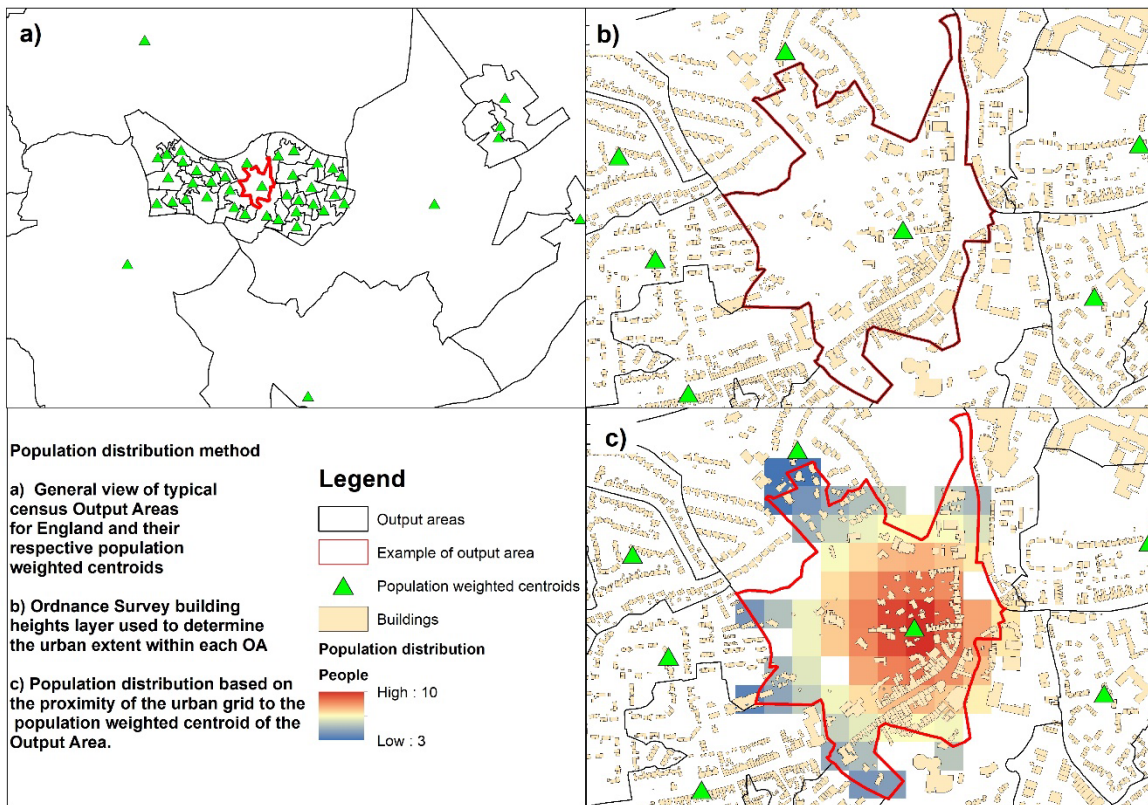


Figure 6.4 Population distribution method for present-day (objective two) and future (objective three) coastal flood risk assessment. The data is obtained for the census output areas and located within each population-weighted centroid (a). A square grid of 50x50m is generated for each area and the urban squares are determined using the OS building polygons (b). Lastly, the population of the weighted centroid is distributed based on the distance of the grid to the weighted centroid (c)

As with coastal defences, there is no data available that can be used to estimate the accuracy and level of error in the population distribution. Given this, it is assumed that the population distribution generated in the present assessment is the best data available and with the highest resolution. The results obtained with this dataset are compared to those obtained using coarse-resolution data, the WorldPop population distribution, available at a 100m horizontal resolution. This data is derived from indirect data such as satellite and cell phone data (Tatem, 2017). Comparing the results of both models can offer some insights on the accuracy of the latter and inform future assessments of areas where little to no information on population distribution is available

### 6.2.5 Preliminary assessment to determine the number of required simulations

A preliminary assessment of the inundation model's behaviour is performed to determine the number of simulations required to obtain stable results. This is done for scenario 7 (S7), where all



components are variable. First, the mean ( $\mu_{1000}$ ) and standard deviation ( $\sigma_{1000}$ ) of the number of people flooded are obtained, considering a thousand simulations. Secondly, the results for each return period are randomly reordered. Following this, a mean ( $\mu_x$ ) and standard deviation (STD) ( $\sigma_x$ ) are obtained considering an increasing number of simulations ( $x$ ), from 2 simulations to 999. Then the difference between  $\mu_{1000}$  and  $\sigma_{1000}$  and each of the  $\mu_x$  and  $\sigma_x$  is calculated (Figure 6.5). It can be seen that for around 400 simulations, this difference stabilized at around zero. Hence, 400 simulations per scenario and return period are regarded as the minimum leading to stable and representative results. Considering the initial thousand used in the stability analysis and the 400 required for the six remainder scenario, the number of simulations performed is 3,400 per return period. With the 16 return periods considered, this equals 54,100 simulations required for the analysis. It is clear that identifying and narrowing down the number of simulations required to obtain stability in the analysis is essential to reduce computational costs. This is one of the benefits of the quasi-random samples, such as those obtained with Sobol sequences, used for the sampling, as it leads to better uniformity than random sampling techniques even under small sample sizes (Renardy et al., 2021).

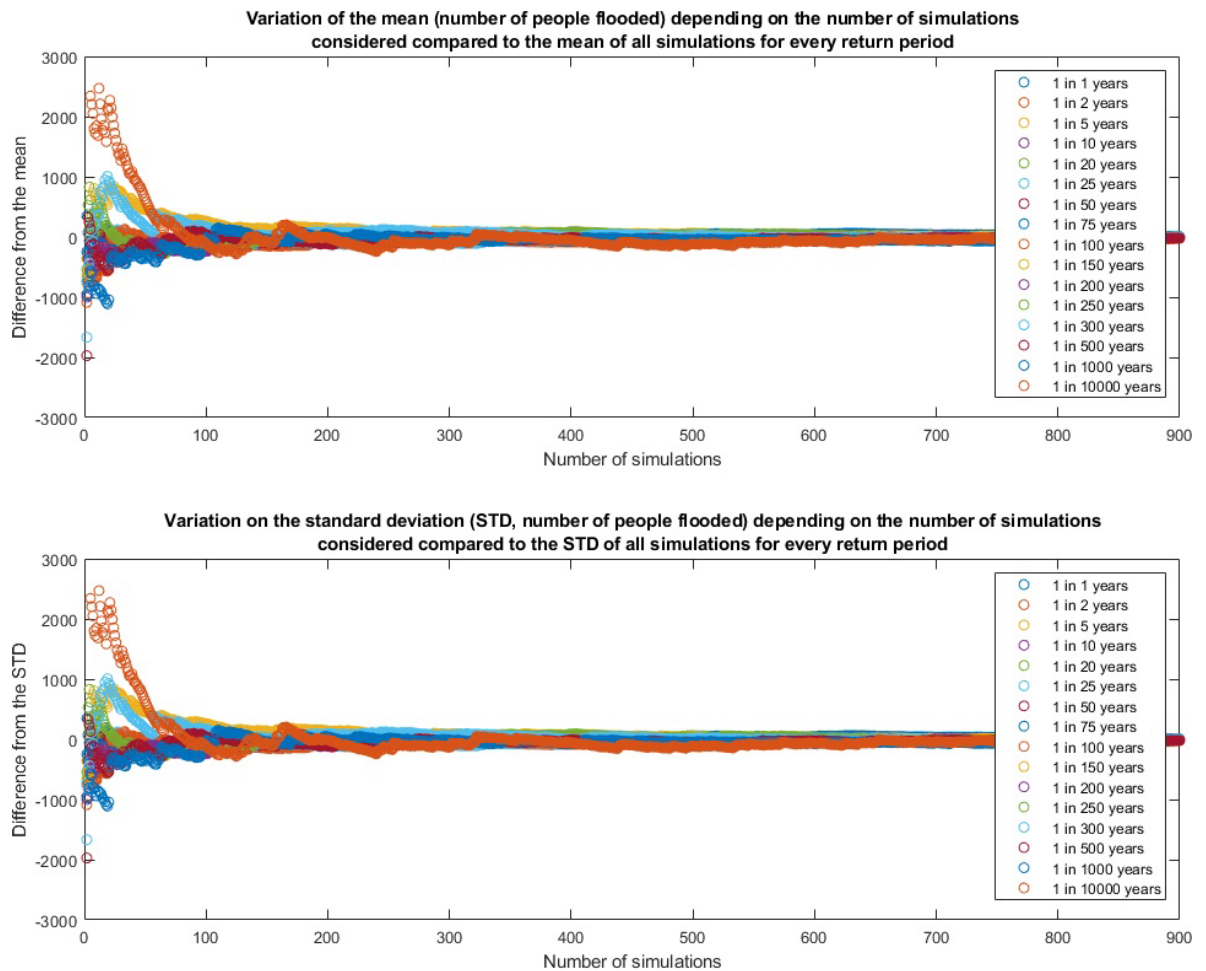


Figure 6.5 Variation in the Standard Deviation (STD) and the mean number of people flooded as a consequence of the number of simulations considered for every return period

This is of considerable interest as the average computation time for the LISFLOOD-FP simulations is three minutes and thirty-nine seconds (Figure 6.6). The overall computational times for the analysis, including estimating the number of people flooded, is seventeen minutes and thirty-four seconds. These computational times are obtained with the University of Southampton IRIDIS High-Performance Computer Facility, using one node and 6 x 2.6 GHz Sandybridge 16-core nodes with 62 GB usable memory. These times do not consider the time spent in the IRIDS computer cluster queue waiting for the simulation to start.

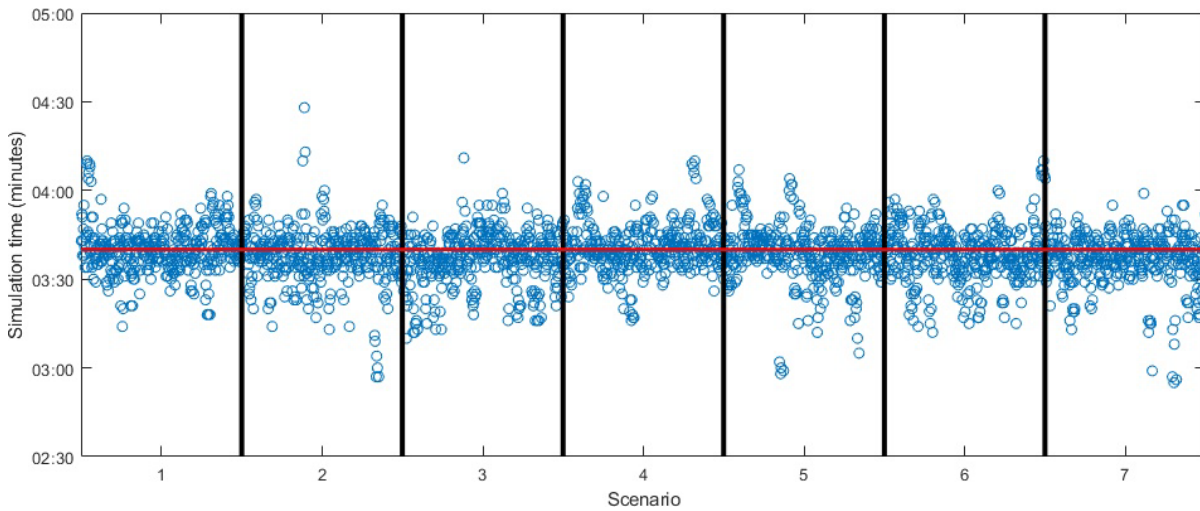


Figure 6.6 LISFLOOD-FP simulation times. These are conducted at the University of Southampton IRIDIS High-Performance Computer Facility, using one node and 6 x 2.6 GHz Sandybridge 16-core nodes with 62 GB usable memory.

### 6.3 Results

The overall objective of this chapter is to analyse the risk of coastal flooding at present, its uncertainty and driving factors for the Solent region. The complexity and number of simulations required for the analysis prevent assessing the variability of the estimates for each area within the Solent. Nonetheless, a brief analysis of the threat level for some of the built-up areas presented in Figure 3.3 is included. However, the majority of results and discussion of this chapter are given for the Solent as a whole.

As highlighted in Chapter 5, whether people and assets are affected by a flood is determined by the velocity of water entering the area and the depth of the flood. As done with the historical assessment of Chapter 5, five minimum depth thresholds are defined: 0.1m, 0.3m, 0.5m, 1m and no minimum depth. The focus is given to depth as using a DTM for the analysis likely leads to overestimating the flow velocities. Figure 6.7 shows values of exposure as a function of the return period and for different depth criteria. It can be appreciated that the exposure results are greatly

affected by the minimum depth adopted. Even by selecting a minimum depth of 0.1m, the exposure results decrease by 45% on average for all return periods, compared to the zero-depth criterion. As highlighted in section 5.3, a minimum depth of 0.3m is selected for the assessment as this complies with the minimum required to produce damage, even under minimal water velocity (DEFRA, 2003, Kelman, 2002, Dawson et al., 2011). Introducing this threshold reduces exposure estimates by an average of 58% compared to a no minimum depth scenario for all return periods.

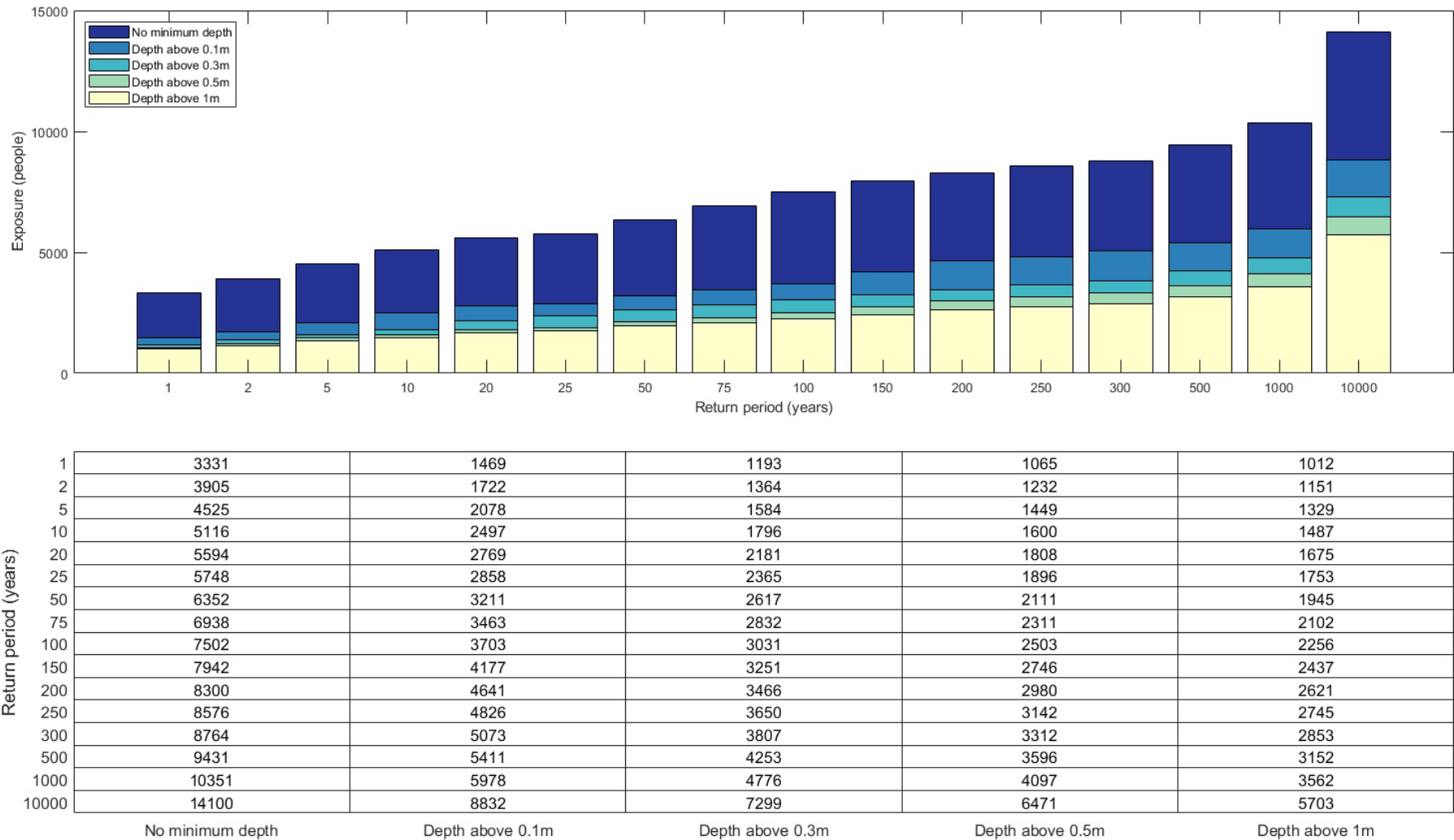


Figure 6.7 Present-day exposure (people) based on the minimum depth of flood required for all return periods.

### 6.3.1 Present-day exposure

After establishing the flood depth threshold of 0.3m, the analysis continues to the development of the first sub-objective, which is to analyse the present-day exposure to coastal flooding at the Solent. This is done by looking at the results of scenario seven, where all components are variable. The results show a positive-skewed Gaussian distribution. The mean number of people flooded increases with the return periods, from 1,197 people for a 1:1-year to 7,306 for a 1:10,000-year event (Figure 6.8). Most exposure assessments focus on events with a medium and high likelihood (e.g. return periods at or below 1 in 200-years) and often dismiss the residual risk posed by extreme events with a higher return period than the defences standard of protection. Considering a 1 in 300-year event, the mean exposure is 3,807 people, with a minimum of 2,588 and a maximum of 7,716. These 7,700 is above the mean value of 7,300 obtained for the highest return period in the assessment, 1 in 10,000-year.

As mentioned in previous sections, the most recent defence protections schemes are designed to achieve a 1 in 500-year standard of protection. If all defences in the area followed this trend, an average of 4,250 people would be protected against coastal flooding through overflow mechanisms. In reality, most modern coastal flood defence schemes aim to protect against a 1 in 200-year, which means an average of 3,464 people are benefitted from flood prevention structures at the Solent.

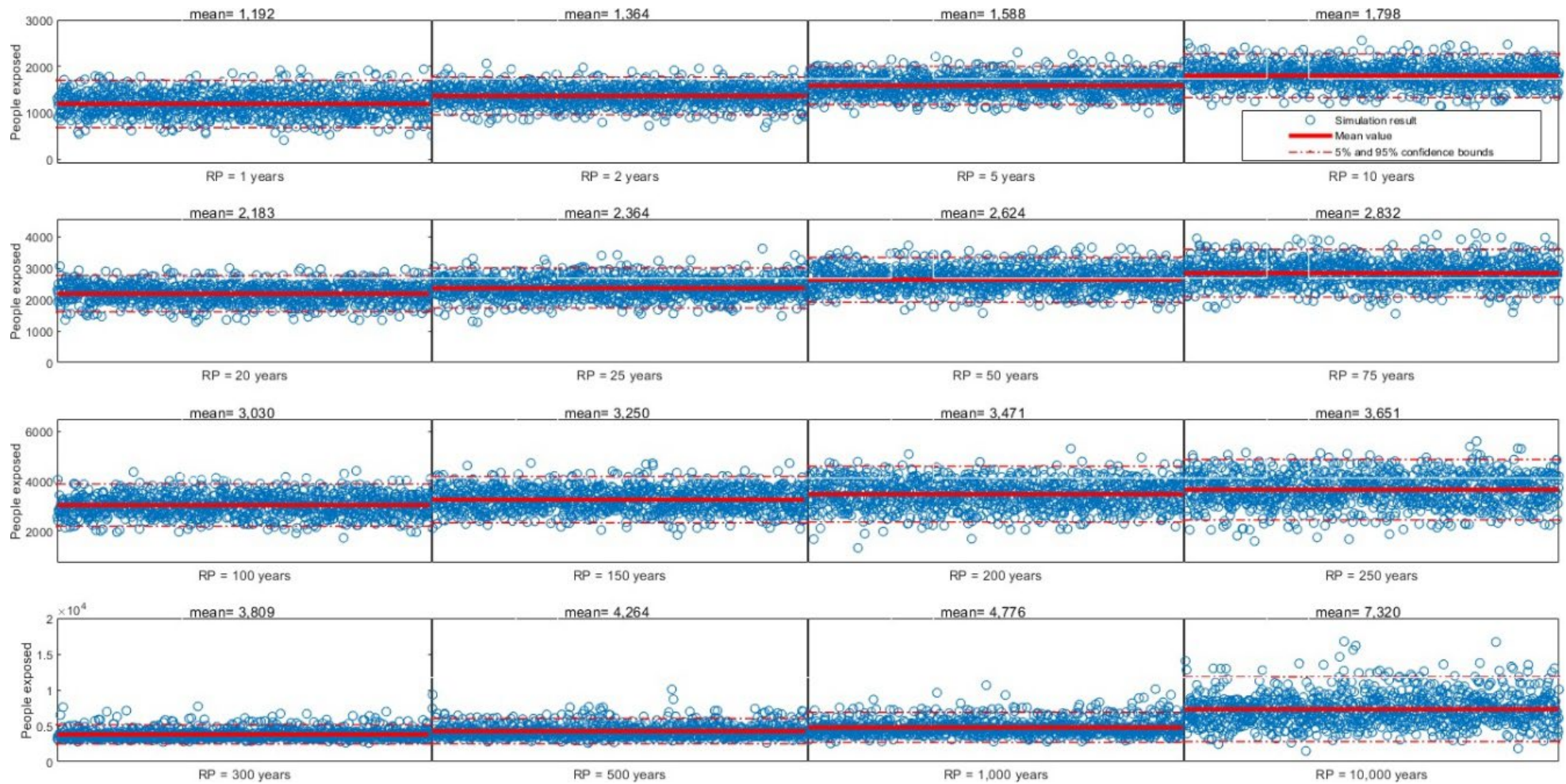
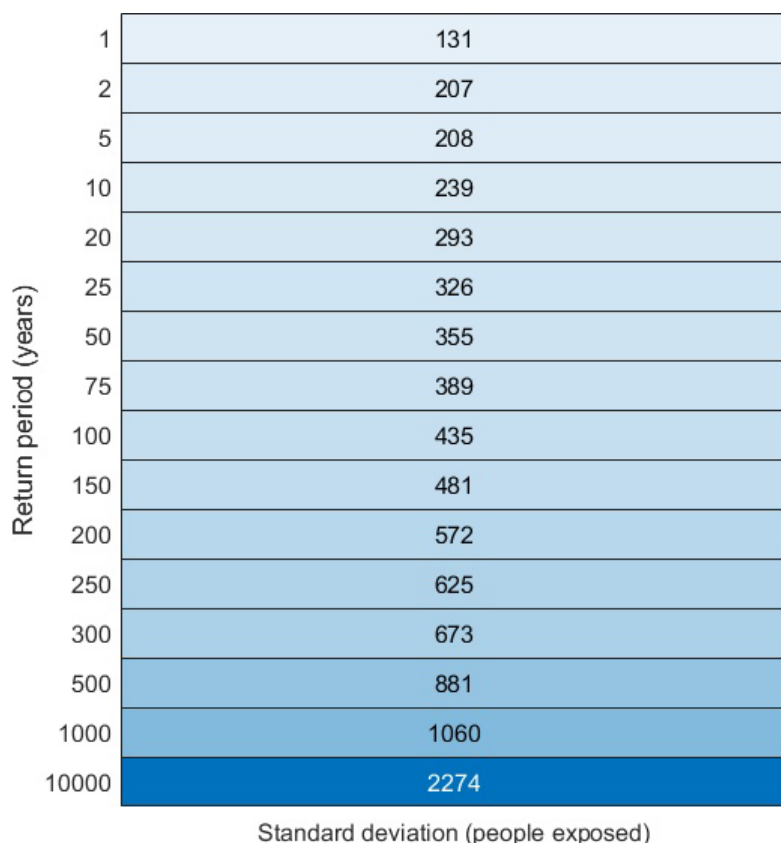


Figure 6.8 Spread of results (number of people) for all simulations performed for every return period (scenario seven, all components variable). Note that the vertical scale is different for each row of data.

Analysing the spread of the results can indicate the variability of the estimates. A good measure of the spread is the variation and the standard deviation, which indicate how close the results are from the mean. For all return periods, the average standard deviation is 571 people, ranging from 130 to 2,274 people for a 1:1 and 1:10,000-yr event, respectively (Figure 6.9). As expected, the spread increases with the magnitude of the return period.



1	131
2	207
5	208
10	239
20	293
25	326
50	355
75	389
100	435
150	481
200	572
250	625
300	673
500	881
1000	1060
10000	2274

Figure 6.9 Standard deviation of exposure (people) for every return period analysed

Along with the number of people threatened, the assessment estimates the economic consequences of risk. This as doing so with present-day economic indicators of risk does not add uncertainty to the assessment. Hinkel et al. (2014) factor of 2.8 is used to translate population to assets exposed. The economic consequences directly follow the trends seen in population exposure. Considering the average household income of £35,9000 for the UK in 2019 (ONS, 2020), over £104 million is exposed to a 1 in 1-year event. This number increases by a factor of 3.8 to £401 million for a 1 in 10,000-year event. Damages worth £289 million and £326 million can be expected for a 1 in 100-year and 1 in 200-year extreme water level, respectively (Table 6.3).



Table 6.3 Present economic exposure to coastal flooding

Return period (years)	Exposure (GBP million)	Return period (years)	Exposure (GBP million)
1	104	100	289
2	128	150	309
5	154	200	326
10	169	250	346
20	206	300	365
25	223	500	401

As with the population results, the spread of results and variability increases with the magnitude of the return periods. The standard deviation ranges from £13 million to £65 million, with an average standard deviation of £32 million for all return periods

In addition to estimating the exposure for the Solent as a whole, the results for some of the main urban areas introduced in Figure 3.3 are presented. These results are estimated using the baseline value of all components (i.e. without considering the uncertainty). This, as the present work is focused on the Solent as a whole. Furthermore, the computational power required to downscale the analysis from a regional to a city level would result in extensively long processing times.

Portsmouth presents the largest exposure for every return period. On average, the city contributes to over 27% of the Solent's exposure to extreme water levels with a return period below 1 in 10,000-years. There is a sharp increment for the 1 in 10,000 year event, with the city holding over 53% of the total exposure for the Solent. In general, the eastern cities and those in the vicinity of Portsmouth show the largest exposure, such as Fareham, Emsworth, Thorney Island and Cosham. (Figure 6.10). Their combined exposure is equivalent to that given by the city of Portsmouth.



Exposure for built up areas at the Solent for present extreme water levels												
Lymington	74	80	80	80	80	133	138	138	152	156	178	225
Ower	1	1	3	3	3	3	3	3	4	5	6	12
Blackfield	5	6	10	11	11	12	12	12	13	14	14	15
Hythe	24	51	155	155	155	166	181	190	192	192	192	239
Marchwood	9	18	26	26	26	34	35	35	35	37	37	222
Totton	0	0	0	0	0	0	0	0	0	0	0	2
Southampton city	14	14	15	18	23	23	23	23	24	25	48	51
Netley	0	0	9	9	9	9	9	9	9	9	9	15
Hamble-le-Rice	0	0	15	15	15	22	22	22	22	22	25	29
Bursledon	0	4	4	4	4	4	4	4	4	4	4	4
Sarisbury	6	8	9	9	13	16	16	16	26	26	31	53
Stubbington	27	41	47	52	59	76	84	84	84	84	85	122
Gosport	23	23	33	33	33	33	82	82	87	95	101	140
Fareham	157	167	175	217	286	307	360	360	360	378	523	775
Cosham	80	84	93	93	120	166	245	249	249	275	317	497
Portsmouth	242	365	548	556	568	665	709	732	785	1045	1106	1935
Havant	3	3	3	3	3	3	3	3	3	7	7	17
Stoke (Havant)	0	0	0	0	0	0	0	3	3	9	16	47
South Hayling	11	11	179	179	179	186	186	186	186	186	239	502
Emsworth	55	72	72	72	72	78	78	84	84	89	96	129
Thorney Island	25	36	95	95	95	118	118	195	209	235	283	338
West Itchenor	0	0	0	0	0	0	0	0	1	3	3	3
East Wittering	0	0	0	0	0	0	0	0	36	45	45	82
Selsey	29	29	31	32	33	42	88	91	93	104	137	212
Cowes	97	127	208	210	213	231	238	238	238	238	250	275
Wootton (Isle of Wight)	11	26	26	26	26	29	29	29	31	32	32	32
Ryde	0	0	9	9	9	9	13	14	14	22	25	58
Bembridge	0	0	8	8	8	8	8	8	8	8	8	11
Ventnor	7	7	7	7	7	7	7	7	7	7	7	7
Freshwater	3	3	3	3	5	8	8	8	8	8	8	18
Norton (Isle of Wight)	1	1	1	1	1	1	2	2	2	2	2	2
Yarmouth	0	4	4	4	4	4	9	9	9	13	13	43
	1	5	10	25	50	100	200	250	300	500	1000	10000
Return period (years)												

Figure 6.10 Present-day exposure to coastal flooding for some of the main built-up areas at the Solent, considering a minimum flood depth of 0.3m

### **6.3.2 Present-day risk of coastal flooding**

The second sub-objective of this chapter is to estimate the present-day risk of coastal flooding at the Solent. This is done by analysing the exposure to all events and return periods to determine the expected annual damage. As seen with the exposure, the level of reported risk is highly dependent on the minimum depth of flood considered to cause damage (Figure 6.11). The introduction of a small depth threshold such as 0.1m halves the risk estimated for a no minimum depth case. Throughout the present study, it has been established a flood depth of 0.3m as the minimum required to consider people and assets at risk. By doing so, the estimates of risk are reduced to an average of 1,488 people at risk every year, almost a third of the 4,157 under a no-minimum flood depth scenario (Figure 6.11.a). Following Hinkel et al. (2014), the number of people at risk are multiplied by a factor of 2.8 and by the average household income of £35,9000 for the UK. These estimates are equivalent to £145 million of expected annual damage for the Solent, assuming a minimum depth of 0.3m (Figure 6.11.b).

Along with the estimates of coastal flood risk for the Solent, the expected annual damage for the cities presented in section 3.2 is estimated. Portsmouth is the city with the highest number of people expected to experience flooding every year (Figure 6.12). This is expected as it has been identified as being the urban area with the largest exposure to coastal flooding. The city's EAD represents almost a quarter of the mean total EAD for the Solent. For some areas, the exercise of estimating the EAD yields zero people at risk. This is a product of integrating the exposure across the probability of each extreme water level. Five out of the 48 built-up areas in the analysis (Portsmouth, Fareham, Cowes, Cosham and Lymington) accumulate more than fifty per cent of the areas EAD.

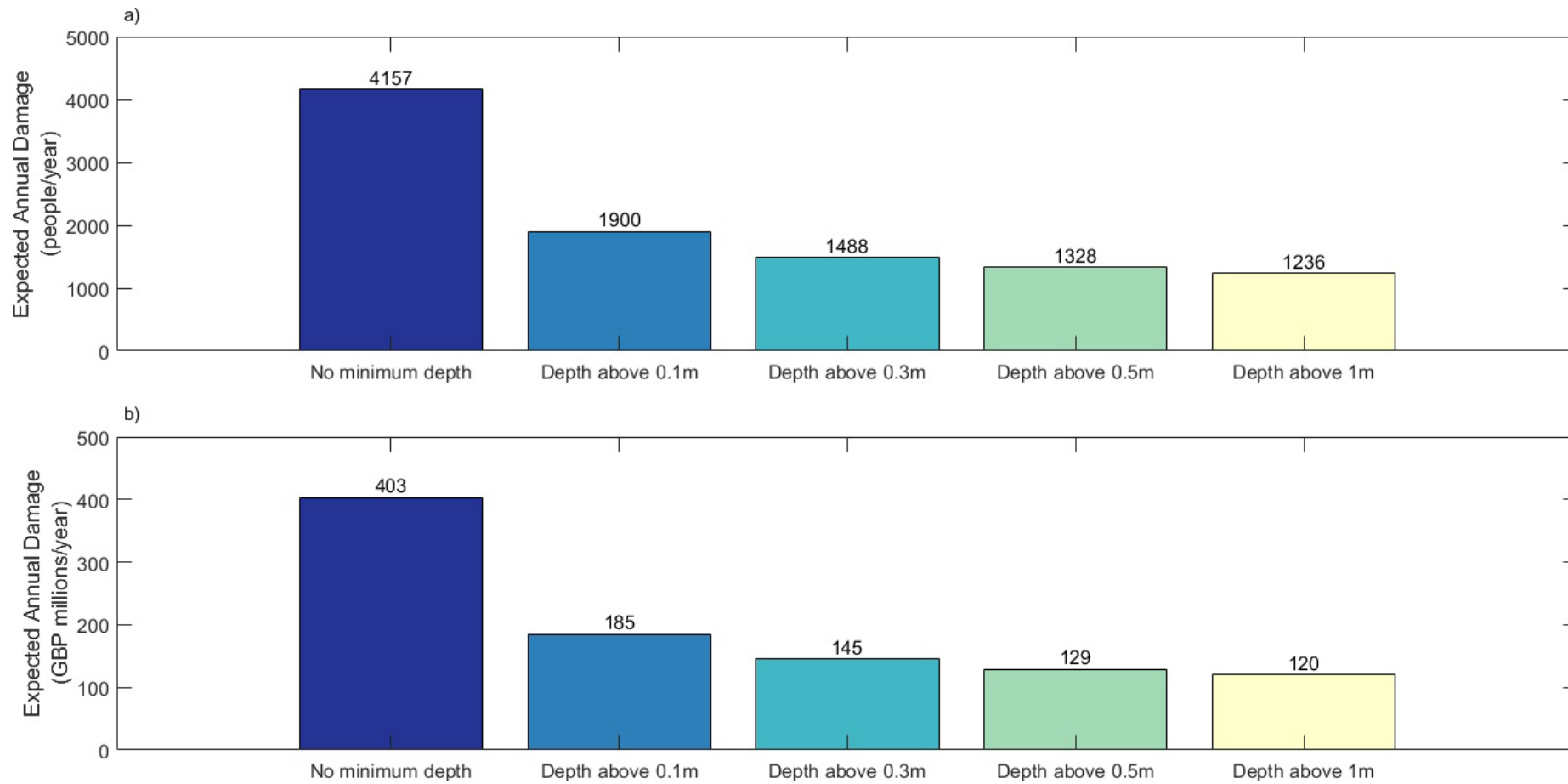


Figure 6.11 Present-day Expected Annual Damage in terms of a) people/year and b) assets (GBP millions/year) and based on the minimum depth of flood required to produce damage

Expected Annual Damage by city	
Lymington	78
Ower	0
Blackfield	5
Hythe	51
Marchwood	15
Totton	0
Southampton city	14
Netley	1
Hamble-le-Rice	1
Bursledon	2
Sarisbury	7
Stubbington	36
Gosport	23
Fareham	170
Cosham	85
Portsmouth	340
Havant	2
Stoke (Havant)	0
South Hayling	29
Emsworth	64
Thorney Island	38
West Itchenor	0
East Wittering	0
Selsey	29
Cowes	124
Wootton (Isle of Wight)	19
Ryde	1
Bembridge	0
Ventnor	6
Freshwater	2
Norton (Isle of Wight)	0
Yarmouth	1

EAD (people/year)

Figure 6.12 Present Expected Annual Damage (people/year) for some of the main built-up areas at the Solent

### 6.3.3 Uncertainty assessment of present-day estimates of exposure and risk of coastal flooding

An uncertainty and sensitivity assessment is conducted to complete the third and last sub-objective of this chapter, which consist of analysing the influence of the characteristics of the SPRC components on the estimates of exposure and risk of coastal flooding. The two main approaches to analysing sensitivity and uncertainty in flood risk assessments consist of a) using scenarios and b) conducting a probabilistic assessment. The following sub-sections present the results of these analyses for the exposure and risk estimates.

#### 6.3.3.1 Scenario assessment of exposure to coastal flooding

As presented in Table 6.1, seven scenarios are used to assess the individual and combined influence of the SPRC components on the exposure. The analysis is conducted by gradually incorporating each component's variability while the remainder are kept constant to their mean value.

Taking scenario one, where the only variable component is the height of the defences, this has the highest variability for flood events with a high likelihood (and low return period) (Figure 6.13.a). The variability given by defence height decreases with the magnitude of the extreme water levels. Isolating the effect of extreme water levels in scenario two reveals that this is a dominant factor for higher return periods. Surge length on its own does not appear to cause much variability for any return period compared to the other two components. The dominance of these factors can be seen by looking at the combined variability of components on the overall uncertainty in the results (Figure 6.13.b). Scenario three, where extreme water levels and the height of the defences are modified, leads to the highest variability in the exposure results for all return periods.

Analysing the results of each scenario for three representative return periods gives a better indication of the effect of each components uncertainty on the overall variability (Figure 6.14). It is interesting to see that varying the surge length leads to decreased mean exposure for all return periods, compared to the mean of scenario seven, where all the components are variable. Scenario two, where the height of extreme water levels is the only variable component, generates the largest uncertainties for all return periods. However, it leads to a lower mean exposure than that of scenario 7. When the joint variability of components is introduced, it can be seen that scenario three (extreme water level and defence height variable) creates the largest uncertainties. This is followed by scenario six (variable length of surge and extreme water levels) and then by scenario five (variable surge length and defence height).

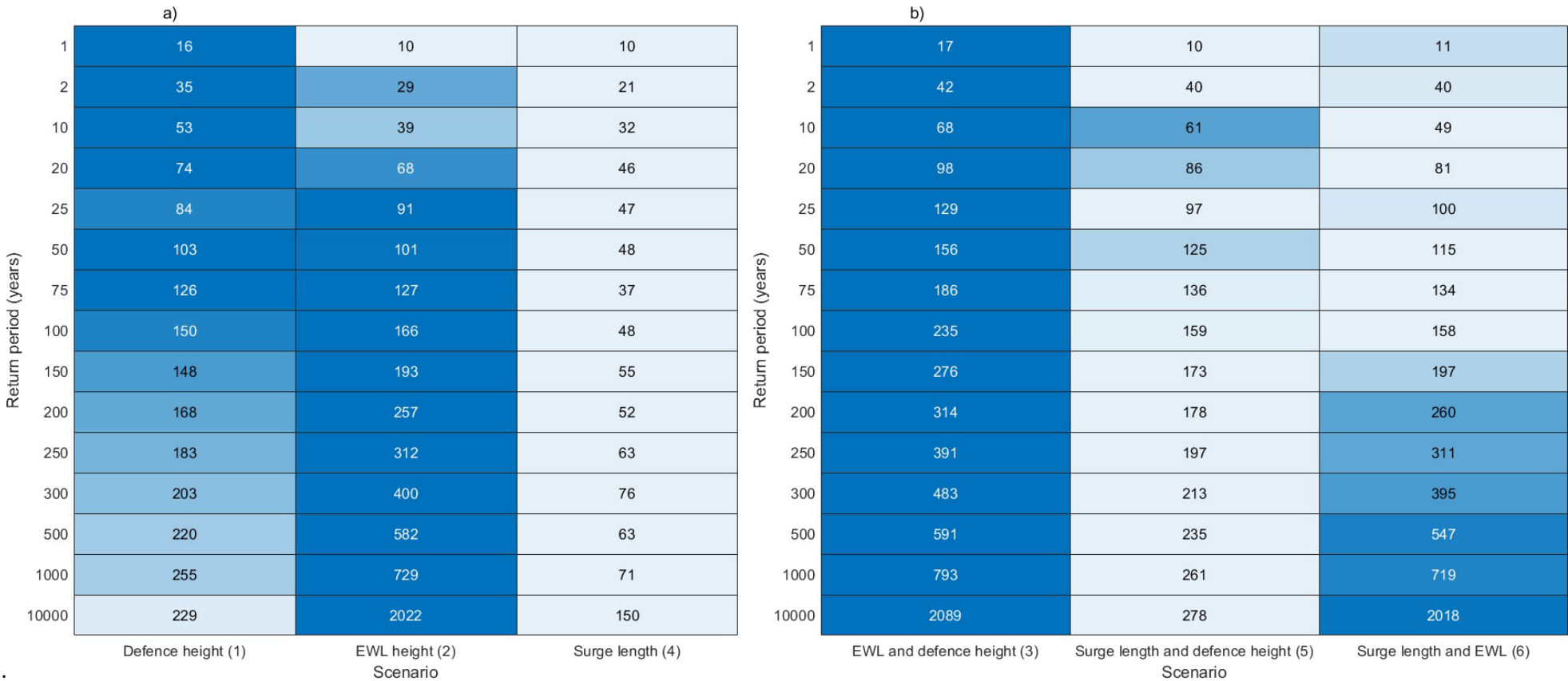


Figure 6.13 Standard deviation in population exposure based on a) individual and b) combined effect components being varied, with the corresponding scenario in brackets (note the colour scaling is relative to each row).

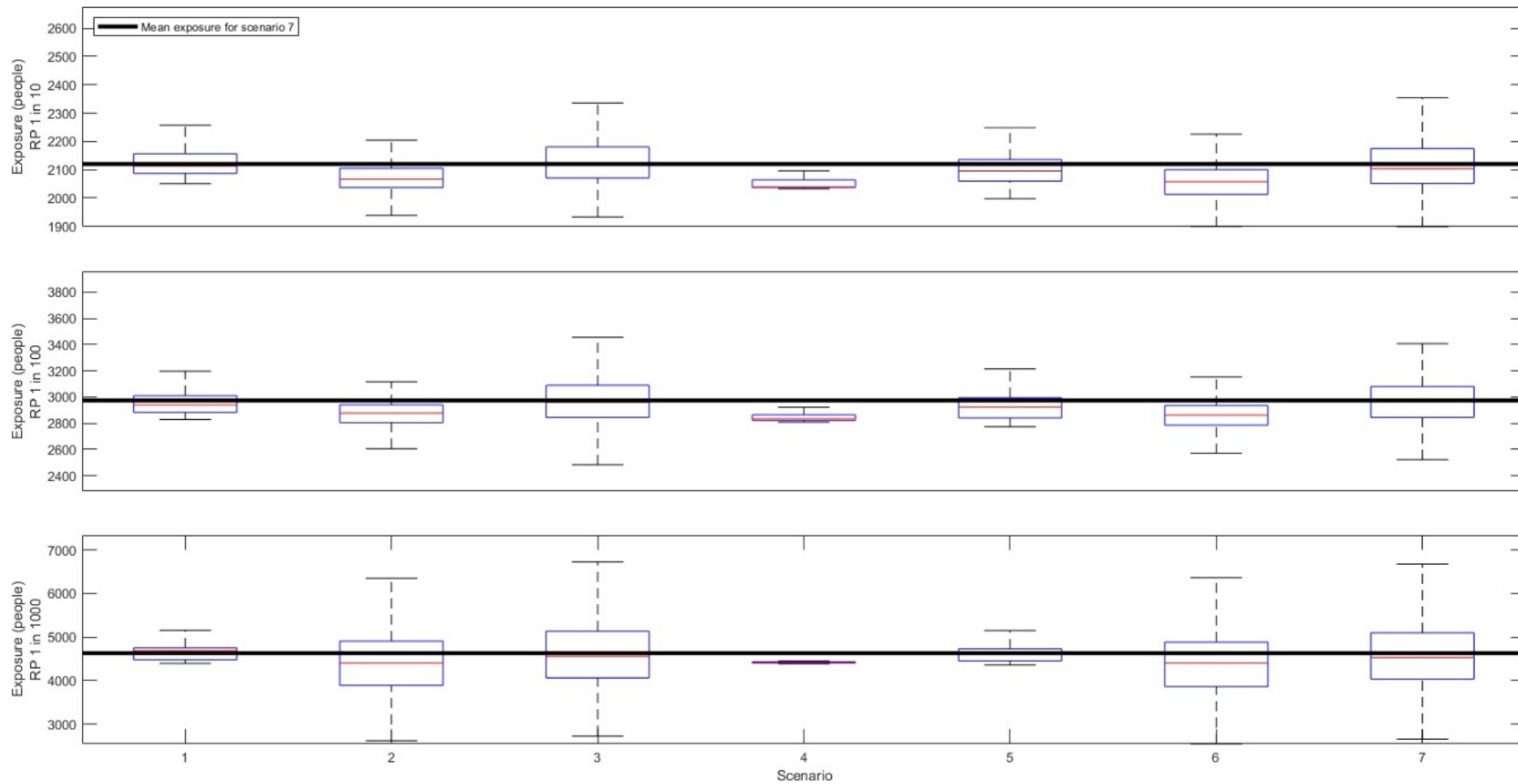


Figure 6.14 Spread of present exposure results for each of the seven scenarios used in the analysis for three representative return periods: 1 on 10; 1 in 100; and 1 in 1,000 years.

The results above are obtained using the high-resolution population distribution generated in this study with the most accurate census information for 2011. The influence of receptors on exposure estimates is assessed by quantifying the difference in the number of people estimated at risk when a coarse resolution dataset such as that of WorldPop is employed. The outputs of LISFLOOD-FP are overlayed to the WorldPop data for the area, and the results are presented in Figure 6.15. Using the coarse population data has a considerable influence for low return periods, more than tripling the exposure for the 1 in 1-year event. These differences decrease as the return period increases, although the results are always larger than those obtained using a high-resolution model.

	Exposure results		Difference		
	High-resolution data	WorldPop (corase) data	People	Percentage	Ratio Coarse/High
1	1072	3646	2574.00	240.11	3.40
2	1314	4114	2800.00	213.09	3.13
5	1474	4536	3062.00	207.73	3.08
10	1741	4871	3130.00	179.78	2.80
20	2121	5583	3462.00	163.22	2.63
25	2298	5705	3407.00	148.26	2.48
50	2544	6276	3732.00	146.70	2.47
75	2782	6767	3985.00	143.24	2.43
100	2975	7051	4076.00	137.01	2.37
150	3187	7543	4356.00	136.68	2.37
200	3361	7905	4544.00	135.20	2.35
250	3570	8277	4707.00	131.85	2.32
300	3763	8616	4853.00	128.97	2.29
500	4136	9020	4884.00	118.09	2.18
1000	4628	9368	4740.00	102.42	2.02
10000	7141	1.109e+04	3948.00	55.29	1.55

Figure 6.15 Difference in exposure results obtained by using a high-resolution dataset compared to the estimates when using WorldPop data

### 6.3.3.2 Probabilistic assessment of exposure to coastal flooding

Having analysed a scenario where all the components are kept variable, the probabilistic approach is used to determine the SPRC components that cause the most variability in the results. Here, the focus is on the behaviour of the results for scenario 7, where all components are variable. Figure 6.16 presents the interaction between components for the 1 in 100-year event. Each row and column present the variation of one component. Looking at subplots a.1 and c.3 of Figure 6.16, the interaction between defence height and surge length does not produce any trends, nor do the results form any clusters. The opposite occurs when the height of extreme



water levels is combined with the height of flood defences being modified (subplots a.2 and b.3). The largest exposure comes from the scenarios with the highest EWL and the lowest defences. Analysing the interaction between surge length and extreme water levels (subplots b.1 and c.2), it is the latter that drives exposure.

A similar approach is followed for three representative return periods, 1 in 1, 1 in 100 and 1 in 1000 (Figure 6.17). Looking at the diagonal trend in all the plots, exposure is heavily driven by the height of the extreme water level for all return periods. This is confirmed by looking at plots a.2, b.2 and c.2, where increasing the height of the water level increases the number of people exposed. In the case of the length of storm surge, there is a slight trend of longer surges leading to more exposure that can be particularly appreciated for the 1 in 1-year event (Figure 6.17.a.1), where the largest storm surges lead to the highest exposure. However, the effect of the surge is overrun by the magnitude of the extreme water level as the return period increases.

Other than metrics such as the standard deviation of the results, the above are purely visual assessments that do not always reveal the whole picture. This certainly cannot be done when the variability of all components is introduced. In such a case, the results seem to cluster around the mean values of each component (Figure 6.18) without showing any clear trends.

Therefore, it is necessary to use the Sobol' indices to mathematically quantify the sensitivity of the results to the variability of each component. Figure 6.19 presents the sensitivity of the results to the length of the surge, height of extreme water level and defence height for every return period. Looking at the individual effect of each component (Figure 6.19.a), the dominant sensitivity factor is the height of extreme water levels. This agrees with the findings of Figure 6.13, with the system presenting the highest sensitivity to the height of the extreme water levels. Interestingly, the sensitivity to the height of flood defences appears to have a Gaussian distribution along the return periods, with the highest sensitivity seen for EWL with return periods in the vicinity of the 1 in 100-year event. Coastal flooding at the Solent is minimally sensitive to the variability in the length of the surge compared to the other variables analysed.

It is clear that the components under scrutiny have interactions, making it necessary to determine the importance of each variable when their combined contribution is considered. This is done with the second-order indices which look at the interaction between two components at the time Figure 6.19.b. It can be seen that the exposure results are most sensitive to the combined uncertainty in extreme water levels and defence heights. On the other hand, surge length creates the least variability, regardless of the combination with other components.

Lastly, analysing the effect of each component considering the joint variability of SPRC, the variance-based sensitivity analysis of the total-effect indices highlights, once again, the dominance of the height of the extreme water levels on the variability of the exposure (Figure 6.19.c). The uncertainty in defence height comes in second place, but its influence on the overall uncertainty is still visible. On the other hand, the length of the surges has a limited effect on the exposure uncertainty when its interaction with variable defence height and extreme water level heights are considered.

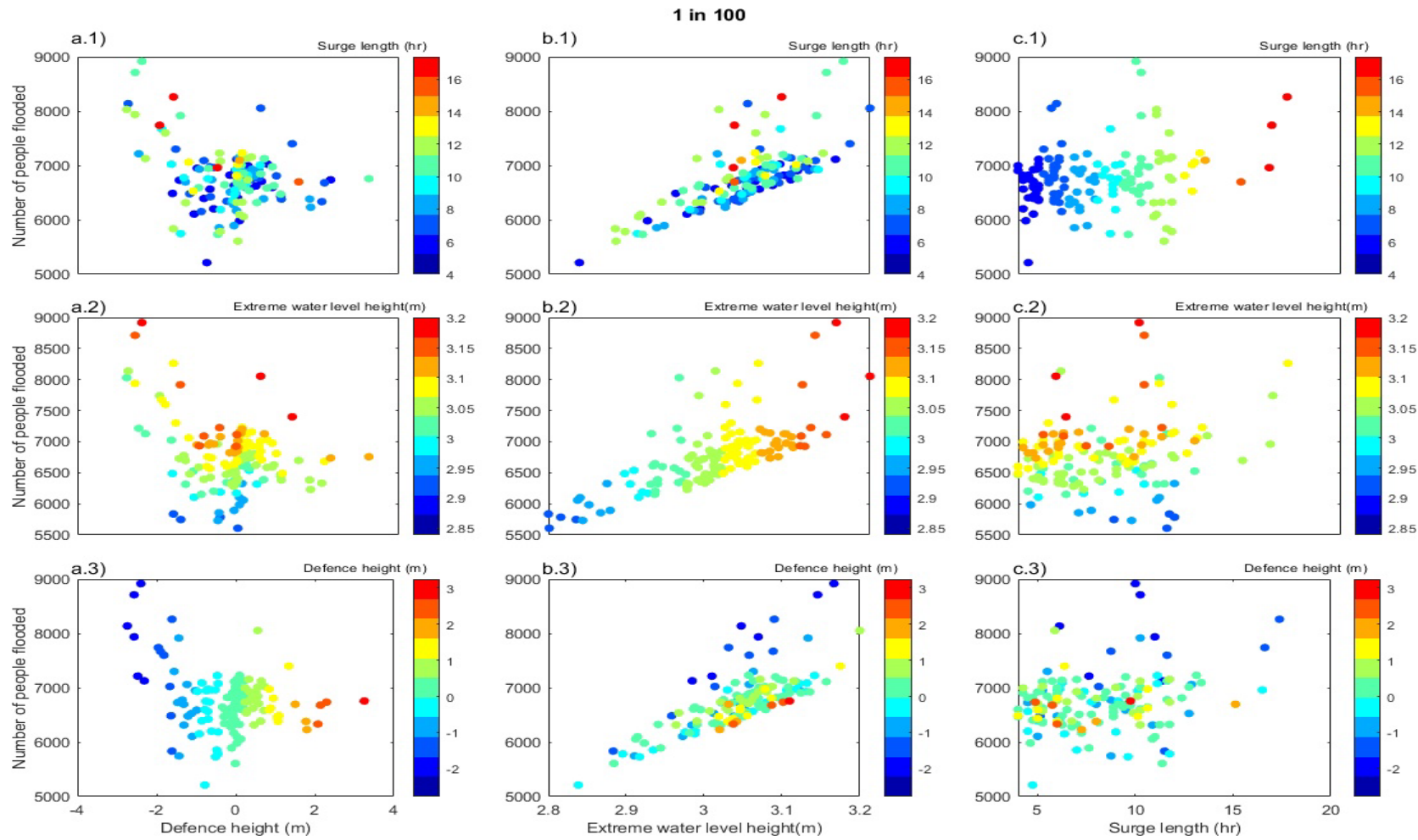


Figure 6.16 Distribution of present exposure results for a 1 in 100-year event. These results are obtained by simultaneously varying all three components. However, the results are presented based on the magnitude of two of them.

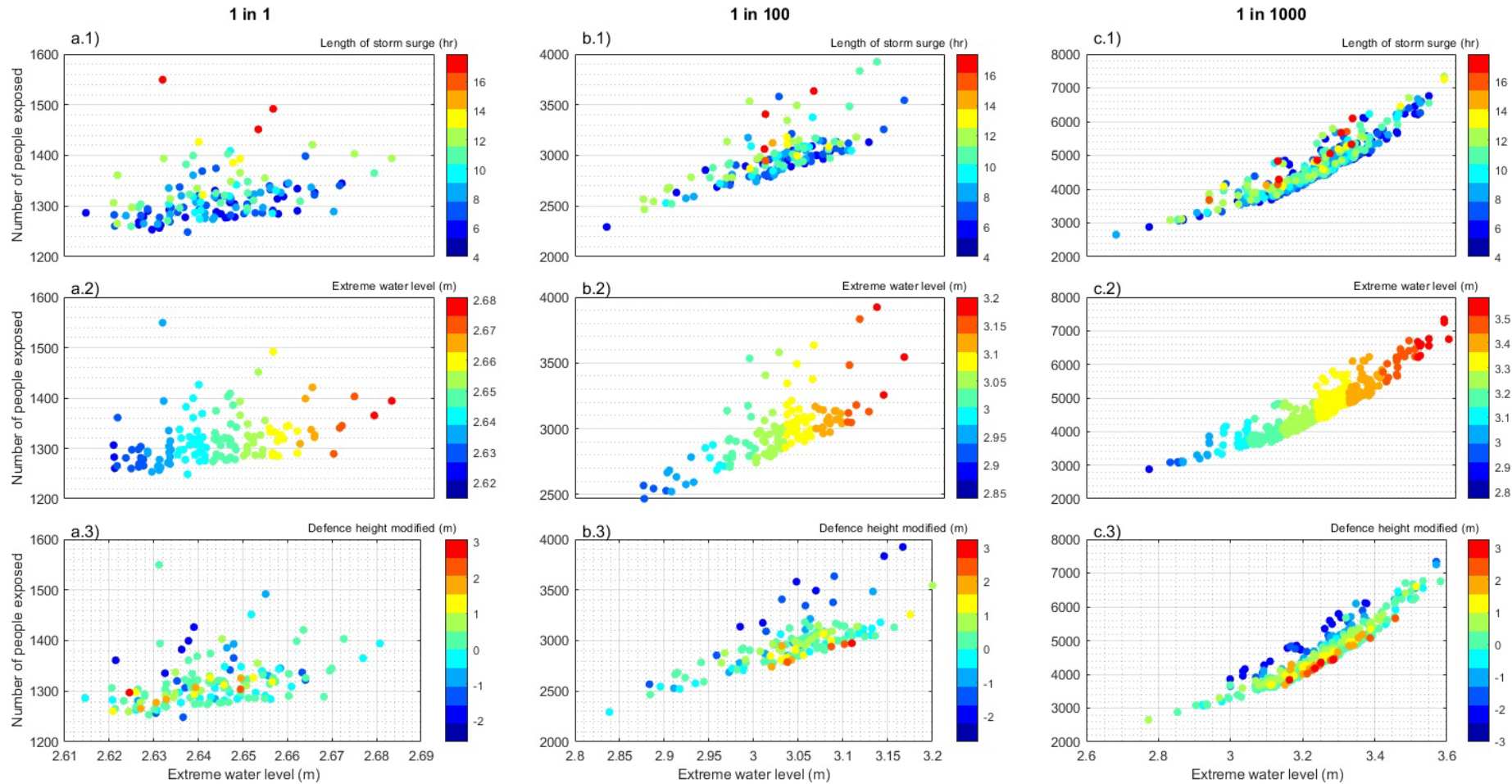


Figure 6.17 Distribution of exposure results for three representative return periods. The results are presented as a function of the magnitude of two of the components.

The y-axis represents the number of people exposed whilst the x-axis is the height of the extreme water level. The colormaps are based on the range of the input factors, such as the height of defences modified.

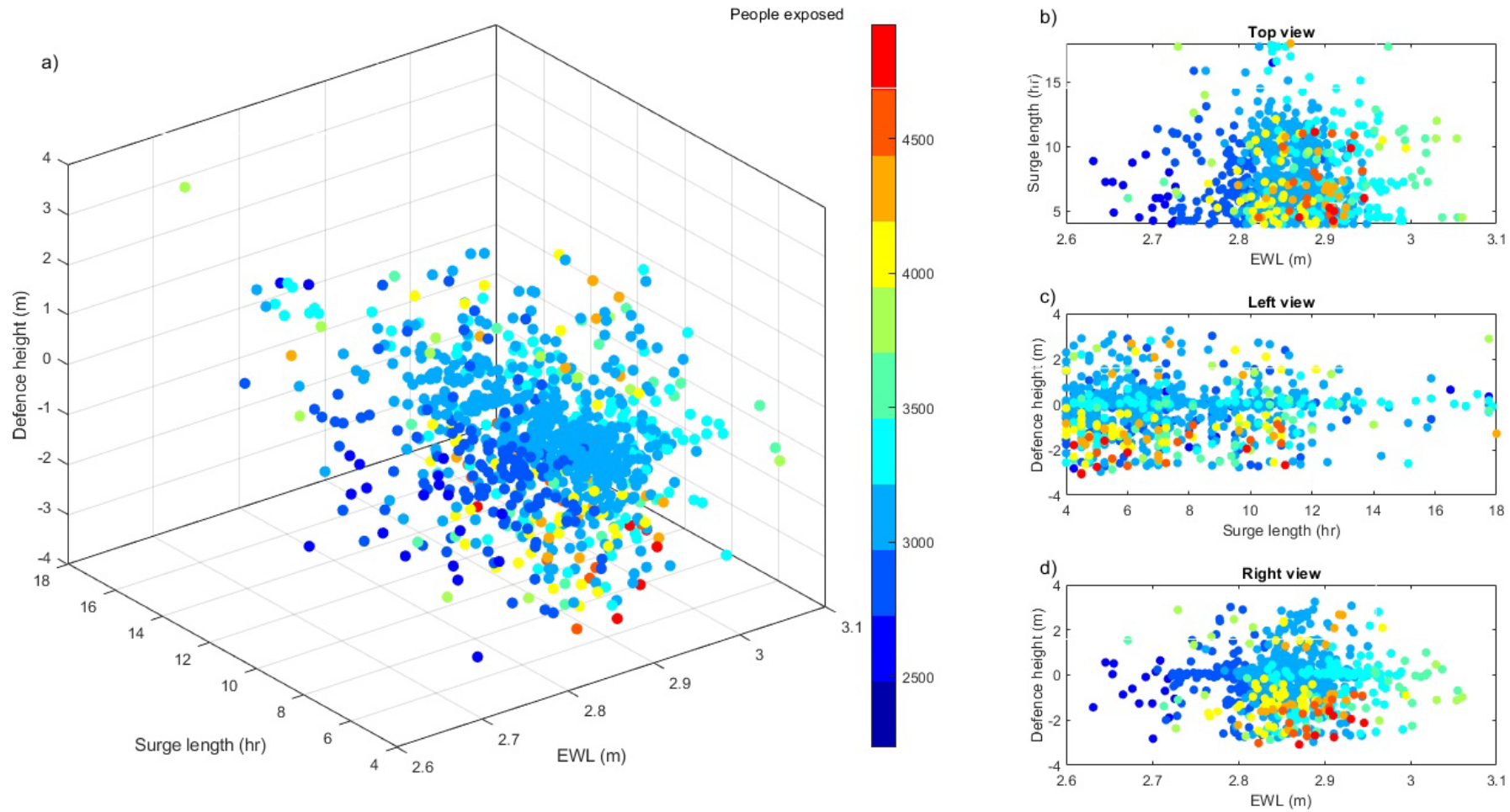


Figure 6.18 Exposure results obtained for a 1 in 100-year event following a probabilistic approach where all components are simultaneously varied. The colormap represents the number of people exposed.

Minimum flood depth of 0.3 m

Return period (years)	a) Local sensitivity (first-order indices)			b) Sensitivity to interactions (second-order indices)			c) Global sensitivity (total effect)		
	Surge length	Extreme water levels	Defence height	SL+EWL	SL+DEF	EWL+DEF	Surge length	Extreme water levels	Defence height
1	0	0.683	0.314	0.001	0.003	0.007	0	0.685	0.317
5	0.001	0.734	0.25	0.001	0.001	0.006	0.002	0.749	0.264
10	0	0.689	0.294	0.001	0.001	0.002	0.002	0.706	0.31
20	0.001	0.687	0.305	0.001	0.001	0.002	0.002	0.694	0.312
25	0.001	0.685	0.311	0.001	0.001	0.005	0.002	0.688	0.313
50	0.001	0.707	0.292	0.001	0.001	0.009	0.001	0.707	0.292
75	0.001	0.633	0.365	0.001	0.001	0.004	0.001	0.634	0.366
100	0.001	0.56	0.438	0.001	0.001	0.006	0.001	0.561	0.439
150	0.001	0.596	0.402	0.001	0.001	0.003	0.001	0.597	0.403
200	0.001	0.632	0.366	0.001	0.001	0.007	0.001	0.633	0.367
250	0.001	0.69	0.308	0.001	0.001	0.003	0.001	0.691	0.309
300	0.001	0.748	0.25	0.001	0.001	0.005	0.001	0.749	0.25
500	0.001	0.784	0.214	0.001	0.001	0.007	0.001	0.785	0.214
1000	0.002	0.771	0.227	0.001	0.001	0.009	0.002	0.771	0.227
10000	0.001	0.843	0.156	0.001	0.001	0.009	0.001	0.843	0.156

Figure 6.19 Variance-based sensitivity indices (Sobol indices). These are presented for every return period analysed and are based on a) local sensitivity, assuming no interaction with other components, and b) global sensitivity, where the interaction and contributions of these interactions are considered.

### 6.3.3.3 Scenario assessment of coastal flood risk

The variability of the expected annual damage estimates given by each component is analysed using the scenarios presented in Table 6.1. First, the effect of the individual components is assessed. The variability in defence height (pathways) generates the largest spread of results (scenario one) with a standard deviation of 64 people/year. This is followed by the effect of extreme water level height (sources) with a standard deviation of 18 people/year. Finally, as seen with the exposure results, the effect of surge length in the variability of the EAD is almost negligible, with a standard deviation of 5 people/year.

Following this, scenarios three, five and six, which explore the combined effect of varying the input factors, are assessed. Interestingly, scenario three, where extreme water levels and defence heights are variable, generate the largest uncertainties when exposure is analysed (i.e. the results were not integrated along all return periods). For the flood risk assessment, scenario six narrowly overtakes scenario three as the one generating the largest uncertainty. This shows how combining components can increase their individual effect on the overall uncertainty, as both extreme water level height and length of surge did not produce a large variability on their own (scenarios two and four).

Something unexpected occurs with scenario five, where surge length and defence height are variable. When exposure is analysed (Figure 6.13), this scenario does not produce large uncertainties. Here, its variability is now closer to that of scenarios three and six (Figure 6.20). Finally, scenario seven, where all components are variable, shows the total uncertainty in the estimates. The results presented in Figure 6.20 can serve as a tool to produce approximations based on the data available. For instance, if an assessment assumes complete knowledge and certainty of the length of a surge (scenario three), the uncertainty in the estimates would be  $\pm 151$  people/year 95% confidence.



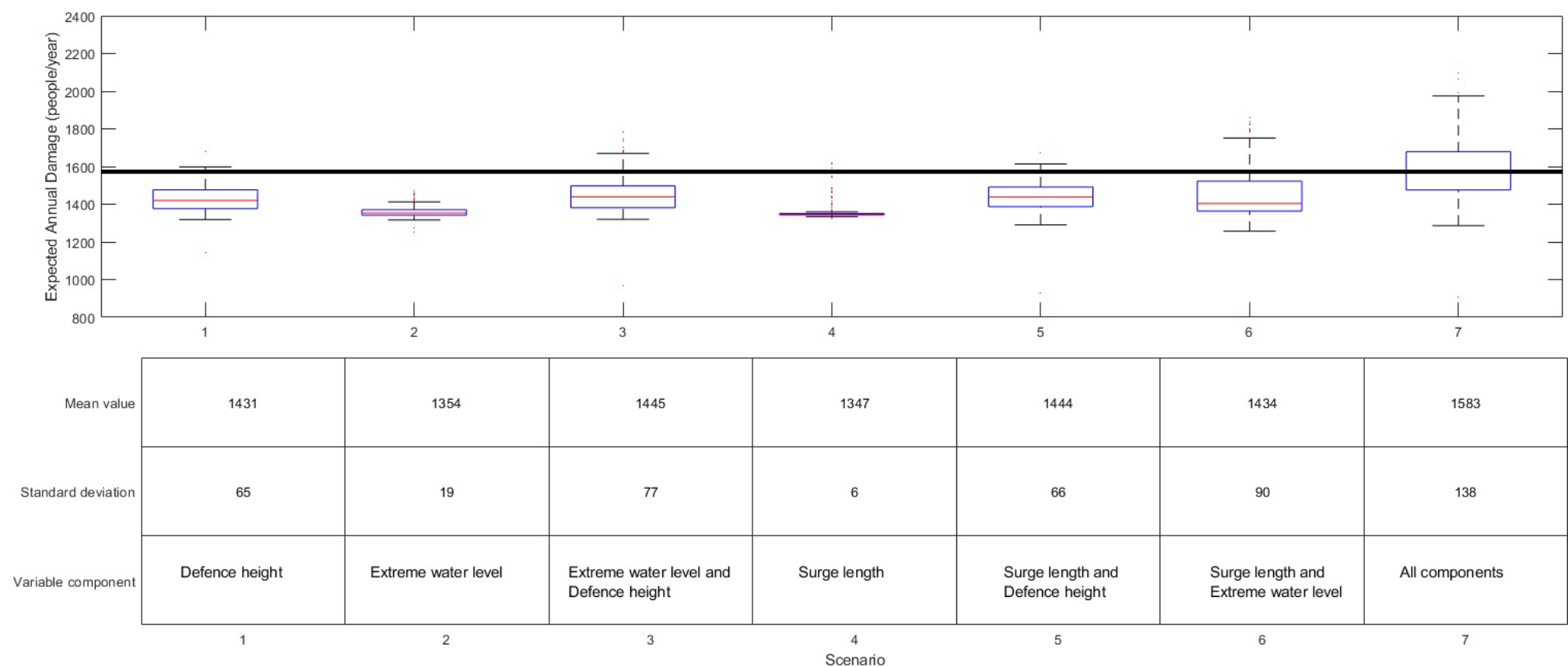


Figure 6.20 Mean value of people at risk and standard deviation based on the individual and combined variability of the components analysed



### 6.3.3.4 Probabilistic assessment of coastal flood risk

Following the probabilistic assessment, the expected annual damage is calculated for all of the input samples generated. This approach is equivalent to the analysis of scenario seven of the previous section. EAD is estimated at 1,488 people/year ( $\pm 460$  people/year at 95% confidence) at risk of flooding with a minimum depth of 0.3m (Figure 6.21). This, in economic terms, is equivalent to £145 million/year ( $\pm$  £44 million/year at 95% confidence). Low return periods seem to have the largest flood risk uncertainties, with up to a 42% variability for a 1 in 1-year event (Figure 6.22). The percentage variability decreases as the return period increases, reaching a 0% variability after a 1 in 75-year vent. An additional benefit of a probabilistic approach is that the likelihood of the expected annual damage can be estimated. For this, 10,000 samples for each return period are selected, and the EAD is calculated for each combination of input factors (Figure 6.21).

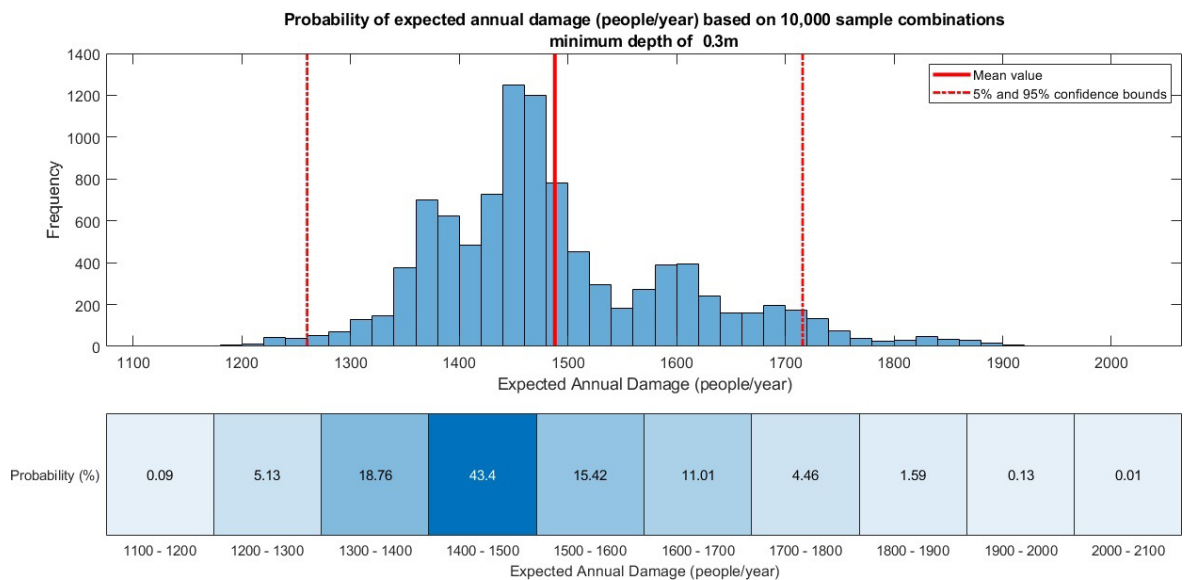


Figure 6.21 Probability distribution of expected annual damage considering a minimum flood depth of 0.3m. This is obtained from 10,000 sample combinations generated with the probabilistic assessment of flood risk.

Chapter 6

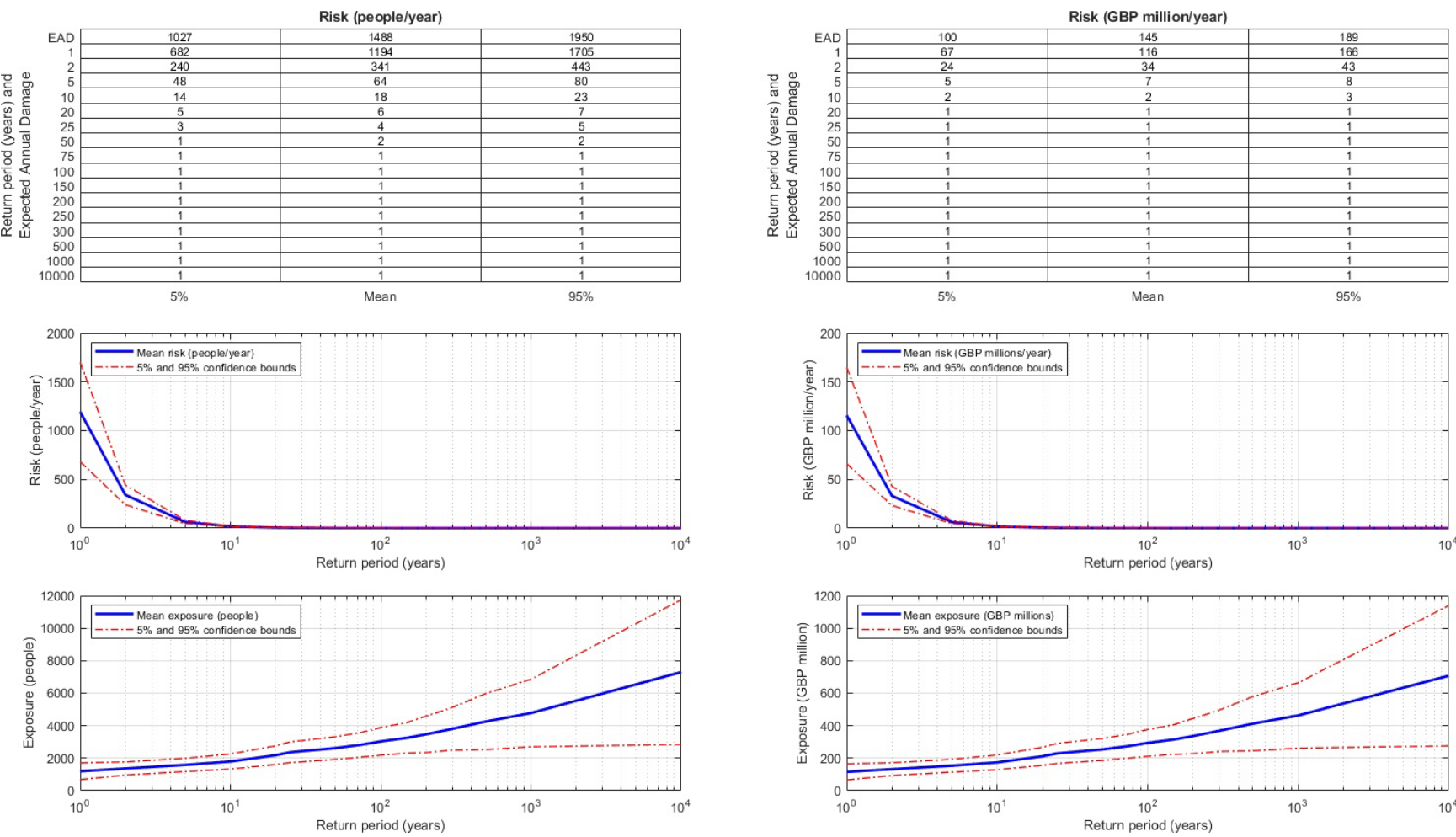


Figure 6.22 Expected annual damage, risk and exposure estimates, along with confidence bounds for the Solent, UK, considering a minimum flood depth of 0.3m required to produce damage

## 6.4 Discussion

The present chapter analyses objective two, which is to determine the present-day level of coastal flood risk at the Solent, as well as to quantify its uncertainty and the factors influencing it. For this purpose, three sub-objectives are defined, and their results are discussed in the following sub-sections.

### 6.4.1 Present-day exposure

The first sub-objective is to estimate the level of exposure to coastal flooding to various extreme water levels. The spread of exposure results resembles the probability distribution of the EWL, and is an indicator of the SPRC-Sources being a crucial driving factor in the overall uncertainty. It can be seen that as the return period increases, so does the spread in results. The wider distance between the mean estimated value for the EWL and their confidence bounds is a result of the statistical assessments necessary to predict EWL. The further the return period is from the length of the tide gauge records, the greater the uncertainty and the wider the spread. This is seen when looking at the distance between the 5% and 95% confidence bounds in the results (Figure 6.8).

One of the most recent works analysing coastal flooding at the Solent is Wadey et al. (2012). Their results are presented as the number of properties exposed to flooding under different conditions. The authors present their results for no minimum depth and a minimum flood depth of 1m. Considering the former, their analysis finds 4,816 properties exposed to flooding from a 1 in 200-year event. Taking England's average household size of 2.3 people per property (ONS, 2013), the 4,816 properties, equivalent to 11,077 people exposed. In this thesis, the analysis yields 8,300 people exposed for the same return period with no flood depth threshold. This difference between Wadey et al. (2012) and the present results is equivalent to a 33% increase. Analysing the 1m flood depth threshold, Wadey et al. (2012) calculate 219 properties, equivalent to 504 people, exposed to a 1 in 200-year event. The present analysis finds 2,621 people exposed to the same conditions, which is more than five times their estimates. In the same study, the authors estimate roughly 10,000 properties exposed to a 1 in 1,000-year extreme water level and a minimum flood depth of 1m. This equals to 23,000 people, which is more than six times higher than the mean exposure of 3,562 people found in the present study for the same conditions. It is unclear the reason why such differences occur. Analysing the baseline assumptions of Wadey et al. (2012), it can be seen that their methodology to incorporate flood defences and the volumes of water entering the floodplain would likely yield more extensive floodplains, as discussed in section 3.4. Furthermore, Wadey et al. (2012) does not consider the presence of river flood

defences. Even though these provide protection, they can also alter the flow of water and confine it, leading to deeper floods with a smaller extent. Interestingly, it would appear that Wadey et al. (2012) exposure estimates rapidly increase for return periods above 1 in 100-year, whereas the present results present a more stable and steady increase along the return periods (Figure 6.7).

Interestingly, Portsmouth has the largest exposure to every return period, although the exposure remains relatively low considering a minimum depth of 0.3m to cause damage (Figure 6.10). This is not surprising as works have been conducted in the city to increase the standard of protection and reduce the level of threat. The area of Fareham, located to the west of Portsmouth, closely follows the results of the latter. In both cases, their low elevation makes them particularly prone to flooding, and both areas have human settlements near the coast and within the floodplain. Furthermore, their location in the less sheltered region of the eastern Solent favours higher extreme water levels, which ultimately exceed the height of the defences. Nevertheless, the area of Selsey should also be highlighted with large exposure numbers as the EWL are the highest within the region. This is not the case as the area, just like Portsmouth, has extensive coastal defences. In addition to this, the areas near Selsey which were prone to tidal flooding have been abandoned and the Medmerry managed realignment placed.

As mentioned, the urban areas at the east present the largest exposures to coastal flooding. Nonetheless, Lymington at the west also has a significant level of exposure, most likely caused by its low elevation. Even though the area is protected against flooding, even low events can generate large impacts (relative to the low population living in the area). This urban area is no stranger to flooding, although the most damaging events have occurred when compound flooding from high river flows are combined with extreme coastal water levels (Ruocco et al., 2011, Hendry et al., 2019).

### **6.4.2 Present-day risk of coastal flooding**

The second sub-objective of this chapter is to estimate the present-day risk of coastal flooding. Expected annual damage is estimated at 1,488 people/year at risk of flooding. This is equivalent to £145 million/year worth of assets at risk. This is the first publicly available estimate of present expected annual damage for the region, meaning there is no data available for comparison. Even the national estimates of risk tend to report the expected annual damage considering the effect of coastal and river flooding, and there is no mention of the assumptions used for their estimates. The present-day expected annual damage caused by coastal, river and pluvial flooding in England is estimated at £1.3bn (Sayers et al., 2020). The estimates in this thesis seem appropriate given the extent of the area covered by the Solent. Looking at the evolution of EAD from the year 2000

to 2020, there is a significant reduction in the average number of people at risk per year. This period sees a decrease of 40% in the number of people at risk of flooding, caused by the increments in the standard of protection of the coastal defences at Portsmouth, highlighting its role as a major contributor to the level of risk for the whole area.

### **6.4.3 Uncertainty in present-day exposure and risk of coastal flooding**

The third and last sub-objective of this chapter is to analyse the influence of the variability of each SPRC component on the estimates of exposure and risk of coastal flooding. The findings are discussed for the exposure (6.4.3.1) and coastal flood risk (6.4.3.2)

#### **6.4.3.1 Sensitivity and uncertainty in exposure estimates**

The height of coastal flood defences is found to produce high variabilities in the exposure to EWL with a low return period. Among the reasons for this is the magnitude by which defence height is modified presented in section 6.2.3. The samples generated can modify the height of the defences by up to two meters up and down. However, most of the 400 simulations will fall below these maximums. It is likely that this will only impact those defences whose height is close to the extreme water level under scrutiny (e.g. low return periods). This variability given by defence height decreases with the magnitude of the extreme water levels as higher magnitude events are likely to have surpassed the coastal flood defences. Further to the magnitude of the samples by which the defence heights are altered, the random selection of structures to modify could have led to non-critical defences being selected. That is defences whose height is well above or far below that of extreme water levels so that any adjustments will not significantly affect the flow rate regardless of the magnitude by which the defence is modified.

The height of extreme water levels appears to become a dominant factor for higher return periods (e.g. above a 1 in 50-year). Looking back at the extreme water level distribution and the confidence bounds for each return period, the higher extreme water levels have confidence bounds further from the mean. When these distributions are sampled, it is likely that the height will be equivalent to that of an EWL with a higher return period.

These findings are consistent with the principles of water entering the floodplain and can be explained by looking at the Manning formulae to calculate the flow rate over each defence used by LISFLOOD-FP. Manning's formulae for rectangular weirs is controlled by the breadth of the defence, which remains constant in the analysis, the weir coefficient and the head of water. The resulting flow rate has volume units divided by time.

$$Q = CL(2gH)^{1.5}$$

Where  $Q$  ( $\text{m}^3/\text{s}$ ) is the flow rate,  $C$  is the weir discharge coefficient,  $L$  (m) is the weir breadth,  $g$  is the gravity constant of  $9.81(\text{m}/\text{s}^2)$ , and  $H$  (m) is the water head over the weir. For low return periods, the elevation head is likely to be of a small magnitude. However, modifying it under scenario one directly impacts the water head and ultimately the discharge into the floodplain.

In the case of extreme water levels, their variability can lead to extreme water levels well below or above the defence's crest. Considering a return period of 1 in 1,000-year, the distance between its mean value and the 2.5 and 97.5 confidence intervals are 0.15m and 0.31m, respectively. Lowering the 1 in 1,000-year event by 0.15m would be the equivalent of having a 1 in 100-year event. Increasing its height by 0.31m falls above the mean height of the 1 in 10,000-year event (3.5m), which is the highest magnitude extreme water level reported by the EA. In both cases, the flow rate will be significantly affected, thus making it a dominant variability factor.

The dominance of extreme water levels and defence height on uncertainty can be still be appreciated when analysing the combined effect of the inputs. For scenario five, where a variable length of the surge is combined with variable defence height, the effect of the former increases for some return periods. However, this can be a product of the combination of very extreme cases where samples leading to the longest surges are combined with defences being substantially lowered. In the case of scenario six, the effect of variable surge length seems to attenuate that of variable extreme water levels for lower return periods. In fact, it prevents the latter from being dominant for return periods below a 1 in 100-year.

The effect of a coarse resolution population model on the exposure estimates is analysed as part of the third sub-objective. The results indicate that exposure estimated using WorldPop is substantially increased when compared to that obtained with the high-resolution population distribution, particularly for low return periods. This means that in low return periods, the floodplain is smaller and any changes in the number of people at the flooded areas create high variability in the results. However, as the area of land flooded increases, the accuracy of the population distribution becomes less relevant. This is an exciting finding, particularly for studies employing a planar (or bath-tub) inundation model. As explained through this research, these studies tend to overestimate the land flooded area as they do not consider the presence of flood defences or the physics of water entering the floodplain. This means for such studies that the accuracy of the population distribution model potentially becomes less of a relevant factor as the accuracy on the extent of the floodplain is limited.

The outcomes of the sensitivity assessment can be utilised to inform future evaluations of coastal flood risk at the Solent and wider areas with similar characteristics. For instance, the local sensitivity of Figure 6.19 indicates that improving the accuracy of extreme water level estimates

would have the highest impact on the overall uncertainty. Several methods are available from the literature (see section 2.3.1.3) to estimate the height and likelihood of EWL. However, it is difficult to determine the accuracy of this component, therefore the focus should be given to improving the quality of the data of coastal flood defences. On the other hand, the total effect indices show that the uncertainty in the length of the storm surge has little to no impact on the exposure uncertainty.

#### **6.4.3.2 Sensitivity and uncertainty in risk estimates**

In terms of uncertainty on coastal flood risk, the variability in extreme water level height generates the largest spread of results. This is followed by the effect of variability in defence height, and lastly by that of surge length, with the effect of the latter on the variability of the EAD almost negligible. Interestingly, de Moel et al. (2012) find flood risk estimates in the Netherlands to be most sensitive to the duration of the storm surge. However, the duration of their surge is far longer than that seen at the Solent, estimating a mean length of 35 hours with a standard deviation of 10 hours. The results obtained for uncertainty in EAD are consistent with the effect seen on the exposure assessment. Furthermore, it is clear that the combination of varying defence height and extreme water levels directly impact the volume of water entering the floodplain. On the other hand, the length of the surge indirectly impacts the extent of the floodplain by only modifying the duration in which the water level is higher than the height of the defences.

Unlike the exposure assessment, scenario five, where surge length and defence height are variable, increases the variance of the risk results. This could be caused by combining long surges with low defence heights, deriving larger EAD. The opposite would occur with short surges and high defences. This is what creates the wide spread of results seen in Figure 6.20 for scenario five. Surprisingly, the distribution of the results (Figure 6.21) closely follows that seen for the exposure, likely driven by the probability distribution of the extreme water levels (Figure 6.2). Previous assessments of coastal flood risk on a regional scale yield similar findings, concluding that the accuracy of extreme water levels produces large variations on risk estimates (Vousdoukas et al., 2018a). Wong and Keller (2017), using a Sobol' sensitivity assessment, find the characteristics of the flood sources to be the key drivers of risk on a regional assessment for New Orleans.

Wing et al. (2019) produced one of the few studies exploring the effect of the accuracy of defence height on risk estimates. The study focuses on the impact of masking these structures onto the elevation model. This approach is constantly used in flood risk assessments (e.g. Lewis et al., 2011, Wadey et al., 2012) as it simplifies the setup of the inundation model. However, the present thesis incorporates these structures on the LISFLOOD-FP model giving their exact characteristics,

rather than including them on the DEM. This approach is taken as modifying the elevation of the square grids of 50mx50m could have severe implications for critical areas such as Portsmouth. Unfortunately, no studies analyse the uncertainty generated by the variability in defence height following a similar approach to this thesis.

In addition to the uncertainty on defence heights, there are deep epistemic uncertainties in the presence of flood defences in the area. Similar problems have been highlighted on several occasions for regional and global assessments (e.g. Apel et al., 2004, Hinkel et al., 2021, Rohmer et al., 2021). For the present study, these are overcome by complementing the incomplete data with additional sources.

Unfortunately, it is not possible to conduct the variance-based sensitivity assessment to determine the component that causes the largest uncertainty. This, as calculating the Sobol' indices relies on the mathematical approximations presented in section 6.2.1.3. These approximations make use of the input matrices generated through random sampling. The problem with this is that when EAD is estimated, the results obtained with each input matrix are integrated with those of other return periods, and the effect of individual components is masked.

## 6.5 Conclusions

Chapter 6 presents the work undertaken to complete objective two, which seeks to analyse the present levels of coastal flood risk at the Solent and to analyse the largest sources of uncertainty. Three sub-objectives are defined to aid the completion of this objective. Regarding the first sub-objective, which is to analyse exposure to extreme water levels, this is estimated for sixteen return periods. It can be seen that the shape of uncertainty for each return period resembles the uncertainty in the height of the extreme water levels. However, the sensitivity assessment reveals that it is indeed the variation in the sources that generate the largest standard deviation for most return periods, although this is overtaken by the effect of defence height for low return periods. The exposure estimates of a 1 in 200-year event are compared to Wadey et al. (2012). This comparison indicates that the present assessment leads to smaller estimates when no minimum flood depth is required to cause damage. Interestingly, the opposite occurs when a minimum depth of 0.3m is incorporated. It is unclear the reasons that lead to such variations, but it is speculated that they are a product of the inaccurate population distribution method followed by Wadey et al. (2012) and their failure to consider the presence of river and pluvial flood defences.

The second sub-objective is to estimate the present-day risk of coastal flooding at the Solent. An average of 1,488 people are estimated at risk of flooding every year, considering a minimum depth of flood of 0.3m required to produce damage. The number of people at risk is equivalent to



£145 million/year. These estimates are presented along with their confidence bounds. In the case of people at risk, the expected annual damage of 1,488 has an uncertainty of  $\pm 460$  people/year at 95% confidence. For the economic risk, the 95% confidence bounds are  $\pm$  £44 million/year.

Overall, these are the first publicly available estimates of present-day exposure to a range of extreme water levels and expected annual damage for the Solent. This means there are no other estimates of coastal flood risk available for the area, and even national assessments tend to report river and coastal flooding within the same figures.

The third sub-objective, which is to analyse the influence and uncertainty generated by different SPRC components on the level of threat, is developed with two approaches. The first one uses a scenario approach where the behaviour of individual and combined components is introduced, and the uncertainty of the output is assessed. The second one follows a probabilistic technique and looks at the sensitivity of the results based on the input variables.

Initially, the assessment explores the range of results obtained from varying the characteristics of the sources of flood risk. As done throughout the present work, the sources are considered as the extreme water levels caused by the combination of astronomical tide and a storm surge component. For the present objective, the focus is on two factors that dictate the magnitude of the source. The first one is the length of the storm surge event, and the second one is the total height of the extreme water levels and the uncertainty these have. Using the scenario-based and probabilistic approaches, the length of the surge produces an average standard deviation of 53 people from the mean exposure of all return periods. Analysing the sensitivity of the system with the Sobol' indices, the results do not appear to be highly sensitive to either the individual effect of surge length or its effect when combined with the variability of other components (global sensitivity).

Analysing the effect of the uncertainty in the extreme water level estimates, these produce an average standard deviation of 322 people from the mean exposure of all return periods. However, it is clear that it becomes a dominant factor of uncertainty for high return periods and those above the average standard of protection of coastal defences (1 in 100-years). Looking at the Sobol' indices, this component has the most influence on the exposure estimates both individually and when combined with other factors.

The influence of variations on the coastal flood defences at the Solent is then analysed. The information on defence presence is obtained from the Environment Agency's dataset. Upon investigation, major gaps in the data were identified. The EA's data is complemented with information from the Channel Coastal Observatory and establish what is considered as a complete dataset of defence presence. Unfortunately, it is not possible to assess the accuracy and

subsequent uncertainty of the number and location of defences included in this data. This, as assessing it would require visiting the whole length of the Solent's coastline to record the location and characteristics of these structures. Instead, the focus is given to the information on the defences characteristics, particularly the standard of protection and the total defence height, and the accuracy of this information is assessed. As there are no additional datasets that could be used to compare this information, a new flood defence height dataset is created derived from an analysis of high-resolution elevation models. The heights of the defences from the government data are compared to those in the elevation-based dataset, and the differences obtained are used as a reference for the uncertainties in flood defence heights. Considering this, the uncertainty in the height of the defences causes a standard deviation of 133 people from the mean exposure of all return periods. Interestingly, the height of defences seems to be the main driver of uncertainty for low return periods. However, when analysing the sensitivity of the results, exposure is moderately sensitive to the height of defences, both when individually and jointly assessed. This is expected as several assumptions are made from the outset of the analysis. Firstly, that extreme water events occur, with the only variable being their magnitude. Secondly, that people will be present at the time of these events and that the properties do not have flood mitigation devices such as flood gates. Given this, the only variable that can potentially stop water from entering and spreading through the area are the flood defences. Since the uncertainty behind the presence of defences cannot be assessed, the only variable that influences the severity of the flood is their height, hence the high sensitivity of the model to this factor.

Lastly, the results obtained with a high-resolution population distribution model are compared with those using a coarse-resolution global model. This is done with the use of a population distribution model developed using the latest and most accurate information from the 2011 UK census and a second one using the information from the WordlPop dataset. On average, the number of people exposed to flooding is severely increased when the coarse dataset is used. This is particularly evident for low return periods, with the magnitude by which the results are overestimated decreasing as the return period increases. This happens since lower return periods generate smaller floodplains, and any changes in the population distribution significantly affect the results. As the area flooded increases, the accuracy of the population distribution becomes a less significant factor, although the results using WorldPop data are still twice as double compared to the estimates with a high-resolution model. The findings presented for this sub-objective can be beneficial and used as correction factors for more superficial studies or extensive geographical-scale analysis, which employ simplified methods to determine the extent of the floodplain. Altogether, this is the first study where the individual and joint uncertainty on the risk estimates generated by different components has been quantified for the Solent.

## Chapter 7    Future evolution of coastal flood risk at the Solent over the 21<sup>st</sup> century

### 7.1    Introduction

Coastal flooding presents a considerable threat for the south of England. The risk it poses at present is likely to be enhanced throughout the 21<sup>st</sup> century as a consequence of the interactions between climate change and socio-economic development. The former is expected to increase the severity of extreme water levels through increments in the global mean sea level. The IPCC, in its latest report, has projected up to 0.82m of global sea-level rise by the year 2100 (IPCC, 2021). In the UK, the Met Office projects it to be 1.12m (Palmer et al., 2018). In addition to actively increasing the height of EWL, their occurrence is likely to increase, further increasing the possibility of flooding.

In terms of socio-economic drivers, the most direct impact will come from population change. This is expected to continue to rise in the future, with coastal areas presenting higher rates of growth and urbanisation (Neumann et al., 2015). In the UK, and under the most extreme scenarios, the population is projected to reach as much as 83 million people by 2060 and 98 million people by the year 2100 (Lutz et al., 2014). Some authors argue that the extent of the urban footprint within the low elevation coastal zone is expected to rise as this area is less land-locked than the hinterland. Although this could be true for rural areas, the extent to where development can occur in coastal areas is limited by the extent of the floodplain. In fact, the latest North Solent Shoreline Management Plan indicates that residential development is restricted to already developed areas. Any housing projects will only take place outside of the potential floodplain (NSSMP, 2010 Appendix F). Regardless of where development occurs, the value of properties and assets within the floodplain is likely to increase, increasing the potential consequences of coastal flood events.

The latest NSSMP, published in 2010 (NFDC, 2010), highlights that the majority of coastal flood defences within the study area have a residual life of around 10-30 years, with only a few reaching a residual life of 50 years. As these defences reach the end of their service life, it is necessary to determine the actions required to maintain or reduce future risk. The Environment Agency, along with local governments, have a duty to develop and maintain a flood risk strategy in England. However, not all flood risk management approaches are viable, making it necessary to identify the management strategies that can produce the best outcomes.

Several assessments have been produced aiming to determine the future levels of flood risk and its driving factors. Globally, Hinkel et al. (2014) estimate a range of over 20 to 400 million people per year at risk of flooding by the end of the 21<sup>st</sup> century under a constant protection scenario. These numbers equate to flood damages of up to 100,000 billion US\$/yr. By enhancing protection, these damage costs can be reduced to a maximum of 90 billion US\$/yr (or three orders of magnitude). For England, Hall et al. (2005) estimated that without an integrated approach to flood risk management, the levels of risk could potentially be twenty-fold from their 2002 value. That is, going from £1 billion of Expected Annual Damage to £20.5 billion EAD by 2080. However, the same study finds that with an effective portfolio of adaptation, EAD only increases to £1.5 billion for the same year.

At present, there are no published assessments of coastal flood risk at the Solent. Various articles have been published looking at the characteristics of significant flood events (e.g. Wadey et al., 2015a, Wadey et al., 2013) and the overall flooding mechanisms in the area (e.g. Wadey et al., 2012). Nevertheless, neither of these has looked at more than one specific event or return period. Furthermore, there has been no inclusion of scenarios that incorporate future climate scenarios, socio-economic development, nor the adoption of flood risk management strategies.

Determining the threat level at different stages during the 21<sup>st</sup> century can inform policy development and dictate the actions that need to be taken for long-term planning in the area. Identifying the components which would play a key role in managing the levels of risk is a useful tool to try and avoid disaster in the area. As highlighted by Muis et al. (2015), the uncertainties generated by socio-economic development at the floodplain tend to be neglected, and the number of future assessments of flood risk that combine climate and socio-economic scenarios is scarce. Examining the behaviour and evolution of coastal flood risk at the Solent would shed light on the possible range of future risk for the area.

Given the above, objective three, the subject of this chapter, is set to determine how flood risk will develop over the remainder of the 21<sup>st</sup> century, considering the evolution of the SPRC components. To achieve this objective, the following sub-objectives are established.

1. Estimate the future exposure to coastal flooding at the Solent.
2. Estimate the future levels of coastal flood risk for the Solent.
3. Quantify the uncertainty in exposure and risk estimates produced by climate change, socio-economic drivers and coastal management strategies.

The initial hypothesis of this objective is that population growth will be the primary driver of exposure and flood risk as increments in the number of people in the area will raise the

consequences of flooding. Furthermore, the uncertainty in future extreme sea levels is expected to be the primary source of uncertainty in the overall level of risk.

The structure of this chapter is as follows. First, the data and methodology required to achieve objective two and its sub-objectives are described in section 7.2. The results are then presented in section 7.3. A discussion of the key findings follows in section 7.4, and conclusions are given in section 7.5.

## **7.2 Data and methods**

In order to assess the future levels of coastal flood risk at the Solent, the present study uses scenarios for climate, socio-economic and coastal management scenarios. The specifics of these are presented in the next subsections.

### **7.2.1 Future evolution of the sources**

As the IPCC indicates in its latest report, climate change will increase extreme sea levels throughout the 21<sup>st</sup> century. These increments will be primarily caused by mean sea-level rise. It could be expected that the recurrence interval of some of these EWL would increase; nonetheless, there is low confidence in the regional projected variations of storminess (Church et al., 2013). Given this, and having established in Chapter 6 the relatively low impact that variations of the average length of the surge have on flood risk uncertainty, the focus is given to the future variations on the total heights of the extreme water levels caused by increments in the mean sea-level.

For this purpose, data from the latest UK Climate Change projections (UKCP18) through its marine report are employed. The UKCP18 provides three SLR scenarios that build on three Representative Concentration Pathways (RCP) first introduced in the IPCC's Fifth Assessment Report. These are the RCP2.6, which represents a "stringent mitigation scenario" where the number of emissions and atmospheric concentration of greenhouse gases start declining by 2020 and reach zero by 2100; the RCP4.5 which is a mid-range case, with emissions declining after 2045 and halve by 2100; and the RCP8.5 which is the worst-case scenario and portrays a very high emissions future (IPCC, 2014). In all scenarios, the mean sea level is expected to rise around the UK.

Under an RCP2.6, SLR is projected at 0.29-0.7m in London, 0.27-0.69m in Cardiff, 0.11-0.52m in Belfast and 0.08-0.49m in Edinburgh by the year 2100. Similarly, under an RCP8.5, SLR is projected at 0.53-1.15m, 0.51-1.13m, 0.33-0.94m, 0.3-0.9m for London, Cardiff, Belfast and Edinburgh, respectively (Palmer et al., 2018).

At the Solent, these ranges are lower and narrower than those found for the rest of the country. In Portsmouth and for the RCP2.6, SLR could range between 0.22 to 0.57m by the year 2100. For a mid-range scenario, this increment is projected at 0.3m to 0.7m. Under the most extreme scenario, RCP 8.5, the sea level is expected to rise by 0.46m to 1m by 2100 (Figure 7.1).

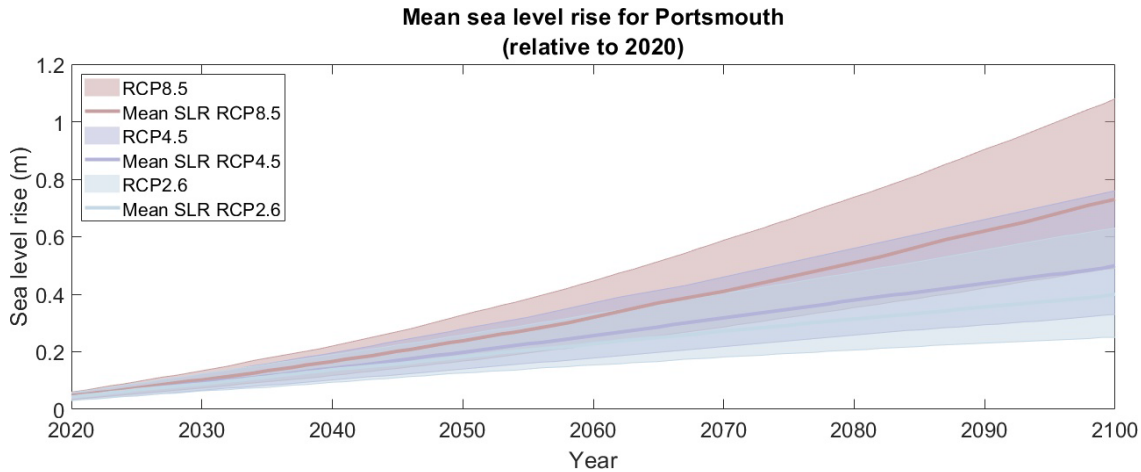


Figure 7.1 Sea level rise projections for Portsmouth. Data from the UK Climate Projections (UKCP18)

The UKCP18 provides the estimated extreme water level height for various return periods. However, unlike the present coastal design levels by the EA, where data is supplied for points along the coast, the UKCP18 estimates are only available at tide gauge locations. Given this, it is decided that the rate by which the present extreme water levels are increased as a consequence of sea-level rise will be maintained equal across the study area. This means that the EWL height differential between areas east and west of the Solent is maintained. For instance, the lowest EWL for a 1 in 100-yr event are experienced at Hurst Spit in the east, with a height of 1.94m, while these reach a height of 3.35m at Selsey Bill in the west. This is equal to a spread of 1.41m across the Solent. Under the lowest SLR scenario, the 1 in 100-yr EWL reaches 2.31m and 3.72m for Hurst Spit and Selsey Bill, respectively, by the year 2100. For the highest RCP scenario, these reach 2.61m at Hurst Spit and 4.02m at Selsey (Figure 7.2).

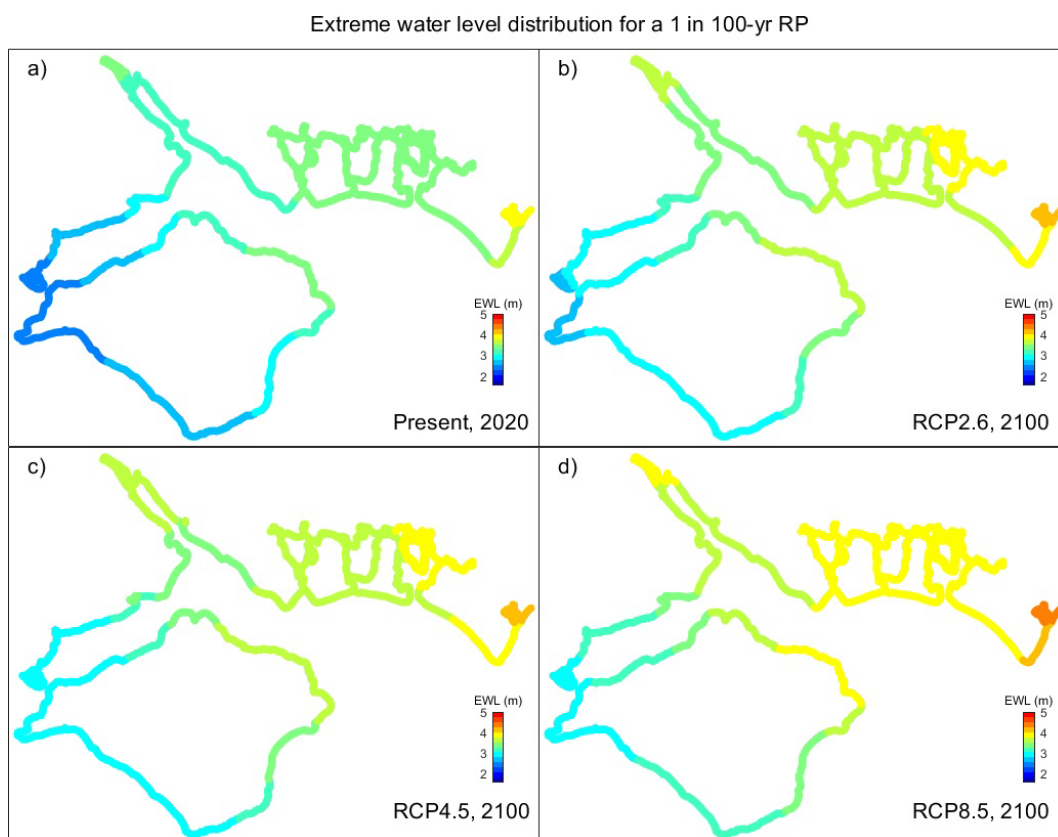


Figure 7.2 Present-day (2020) and future (2100) extreme water level distribution for a 1 in 100-year return period under different sea-level rise scenarios.

### 7.2.2 Future evolution of the pathways

Since 1995, the Ministry of Agriculture, Fisheries and Food (MAFF), now DEFRA, introduced guidance for the creation of the Shoreline Management Plans. Back then, the UK coast was divided into cells based on sediment boundaries. Local authorities analysed the risks posed by flooding and erosion and developed their SMP's based on MAFF's guidance, resulting in the first generation of SMPs being published in 2000. Some shortcomings were identified, and the second generation of plans was released in 2010.

This latest generation of SMPs overcomes the shortcomings of the first edition and, following DEFRA guidelines, has two baseline response scenarios for coastal management. The first one is no active intervention, which assumes that defences are no longer maintained and will therefore fail over time. The second one, called "with present management", assumes that all defences are maintained to provide a similar level of protection to that seen at present (DEFRA, 2006).

Within the second baseline scenario, there are four main policy approaches for coastal management provided by DEFRA. The first one is to "hold the line". This refers to maintaining or upgrading the level of protection provided by the existing defences. The second one is "advance

the line”, which, as the name suggests, implies advancing the line of defences seawards by building new defences asea of the existing ones. The third approach, called “managed realignment”, requires a retreat from or abandonment of areas subject to tidal flooding to create inter-tidal habitats. This approach is usually applied in areas that, along with being subject to tidal flooding, are designated as special areas of conservation or special protection areas, both of which are highly present at the Solent (Figure 3.2). Finally, the decision to not invest in maintaining or upgrading the existing defences is called “no active intervention” (NAI) (Environment Agency, 2020b). Although the NAI policy is similar to the overall NAI management approach, the former is implemented after other management policies have already been completed. In contrast, the NAI management approach means there will not be any intervention from the outset and throughout the scope of the SMP.

These approaches are projected onto three epochs, which cover short, medium and long term scenarios. These are built by analysing the consequences of adopting specific policies through the 21<sup>st</sup> century and the possible socio-economic evolution of their coverage area. The plans then set the best approach to defend or manage flood and erosion risks, considering the broader environmental and social benefits.

The study area is covered by two SMPs (SMP 13 and 14), the North Solent Shoreline Management Plan and the Isle of Wight Shoreline Management Plan (IOWSMP). The leading authority in charge of preparing the NSSMP is the New Forest District Council (NFDC). The NFDC has divided the 386km of the coast from Selsey Bill to Hurst Spit into 62 policy units of varying length, based on the area's coastal processes (Figure 7.3). These 62 policy units are then grouped into nine management areas. In the case of the IOWSMP, this was developed by the Isle of Wight Council Coastal Management Unit. The Isle of Wight is divided into seven large segments of coast called Policy Development Zones (PDZ). Each PDZ is divided into smaller sections where specific management policies are proposed based on the needs of each site.



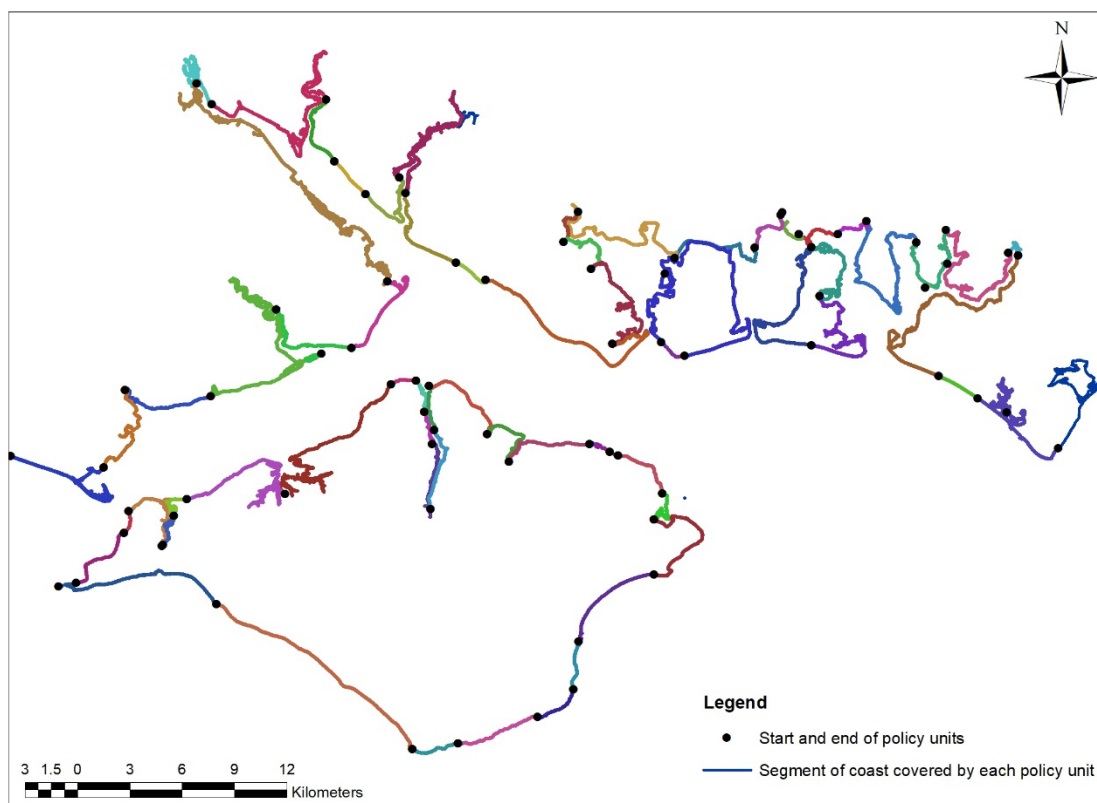


Figure 7.3 Map of policy units covered in the North Solent Shoreline Management Plan and the Isle of Wight Shoreline Management Plan. Note that colours are only used to differentiate the location of all segments of coast covered by each policy unit.

Various assumptions are made for the present assessment. As done in objective 2, all the defences present in the Solent and included in the EA and CCO flood defence datasets are included in the assessment, regardless of whether these provide protection from coastal or river flooding. In the case of river defences, it is assumed that these are kept at their 2010 standard of protection reported by the EA. In other terms, no active intervention is assumed for these as they fall outside of the scope of the SMPs. Furthermore, the defences located in the north area of Portsea Island and Southsea are upgraded to their latest standard of protection. This represents the current works being carried out by the Coastal Partners to upgrade the defences up to a standard of protection equivalent to a 1 in 500-years return period plus an allowance for sea-level rise by the year 2110 (Coastal Partners, n.d.).

In terms of each management policy, these are included in the assessment in different forms. Under present management, the height of the defences with a HTL policy is increased by the rate of SLR of each of the RCP scenarios (Figure 7.1). As shown in Figure 7.4, for areas around Chichester Harbour, the preferred policy is HTL though there is no public funding available (NPFA). In this case, it is assumed that funding will be obtained, this could be through public or private

investment, and their SoP will be increased at the same rate as the remainder defences with a HTL policy.

Under epoch 1 of the 2010 NSSMP, the defences around Medmerry, Sussex are assigned a “managed realignment policy”. The works to create the managed realignment were completed in 2013. Therefore defences at the shorefront are removed from the future assessment, and only those located behind the created intertidal habitat are kept. Finally, for those defences where the preferred policy is NAI, their last standard of protection is kept throughout the study. In addition, it should be noted that all defences are assumed to be present throughout the study period. This, as their presence will continue to provide protection even after the end of their design life. Furthermore, it is not always feasible to decommission or remove some of these structures, as these often have secondary uses, such as promenades.

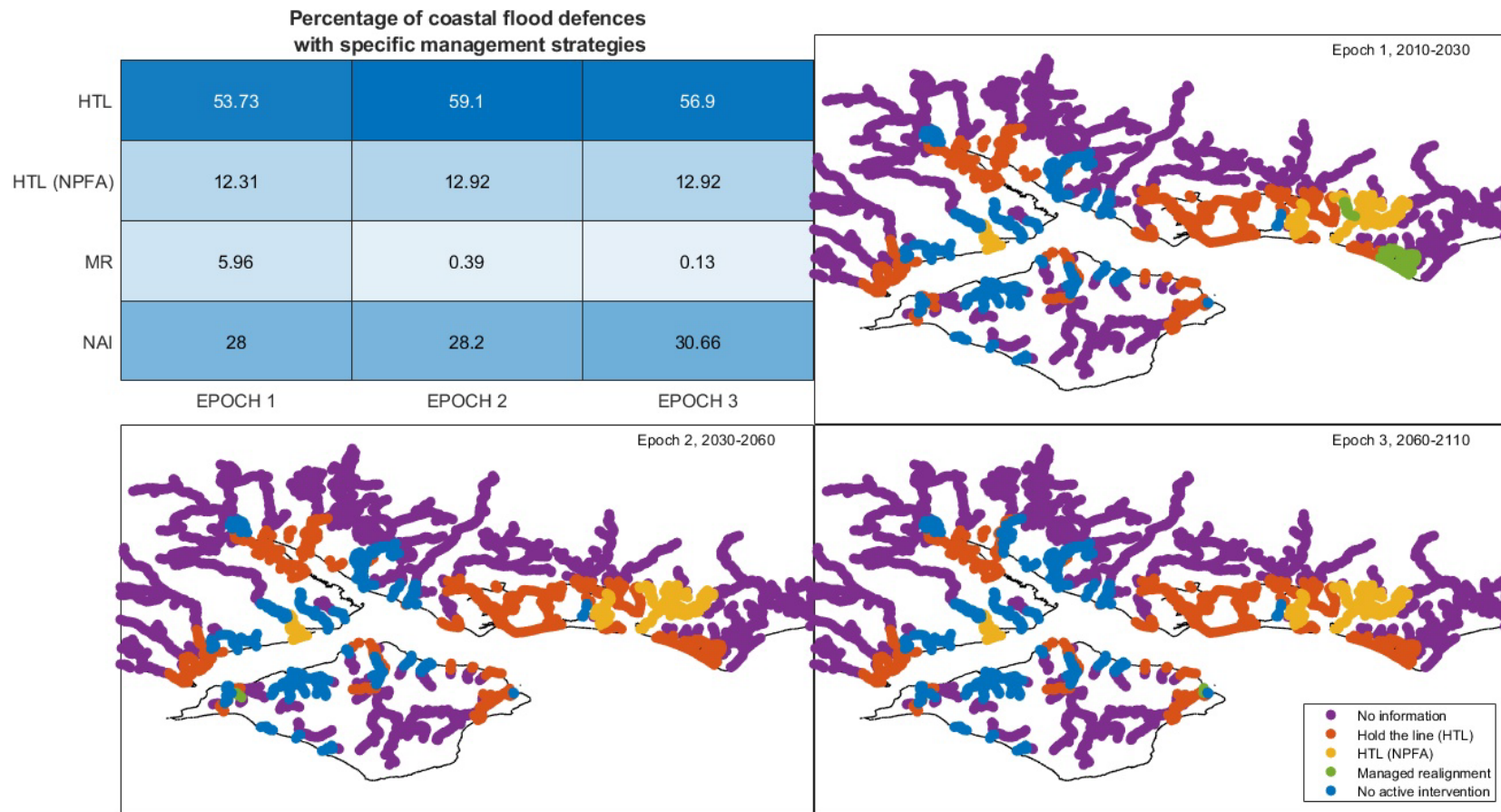


Figure 7.4 Present management strategies for the flood defences at the Solent. Information collected from the North Solent Shoreline Management Plan and the Isle of Wight Shoreline Management Plan

### **7.2.3 Future evolution of the receptors**

Globally, coastal areas have historically attracted migration as these areas offer cultural and economic activities and provide access points for trade. These trends of migration are expected to grow despite the various natural threats these areas face. Any future assessment of coastal flood risk should then include scenarios of socioeconomic development that represent the anticipated trends of migration and wealth development for the coastal region. Previous studies have analysed coastal population growth (Merkens et al., 2016) and its implications for flood risk (Neumann et al., 2015), as well as the possible adaptation scenarios that coastal communities could carry out to decrease their levels of risk (Hinkel et al., 2010).

In England, the ONS offers population projections on a country, local authority, and high administrative areas level. However, these are only projected up to the year 2043 and fall short of the scope of the study. Instead, the present assessment uses the population growth scenarios for the UK by the International Institute for Applied Systems Analysis (IIASA). These projections, called Shared Socioeconomic Pathways (SSP), are closely linked to the RCPs as some of the factors used to determine future population growth are also indicators of the level of future climate change. These include technological and economic development, cultural and institutional changes, and social and population dynamics and aim to depict how the world might evolve over the century (van Vuuren et al., 2011).

For the present assessment, three of the five SSP narratives available by the IIASA are used (IIASA, 2018). These are SSP1, SSP2 and SSP3, representing a sustainable path, the “middle of the road”, and regional rivalry, or rocky road. In general terms, the three scenarios cover the broader spread of socio-economic growth under the future narratives (Table 7.1).

Table 7.1 IIASA population growth scenarios used in the assessment, including their description

IIASA Scenario	Description from Riahi et al. (2017)
SSP1 – Sustainability	The world tends to a more sustainable path. Increasing commitment to achieve development goals, inequality is reduced. Educational and health investments. Low energy and resource consumption
SSP2 – Middle of the road	Economic, social, and technological trends do not shift markedly from historical patterns. Development and income growth proceed unevenly. Environmental systems degrade, although there are improvements and energy and resource use declines.
SSP3 – Regional rivalry	Countries focused on achieving energy and food security goals. Investment in education and technological development decline. Inequalities persist or even worsen. Strong environmental degradation in some regions.

As mentioned, the IIASA population projections are available on a UK level. Therefore, it is necessary to downscale them to obtain the future number of people living in the study area. Neumann et al. (2015) find that coastal areas have higher rates of urbanization and migration than those seen at the hinterland. However, a fundamental limitation of Neumann et al. (2015) is that the study fails to consider migration from the coastal areas caused by sea-level rise. Moreover, the same study finds that coastal populations in Europe are expected to decrease in the future. Given this and the uncertainty behind population movement, it is assumed that England and particularly the study area keep their present share of the UK's population throughout the 21<sup>st</sup> century. Furthermore, it is assumed that no migration from the study area will occur.

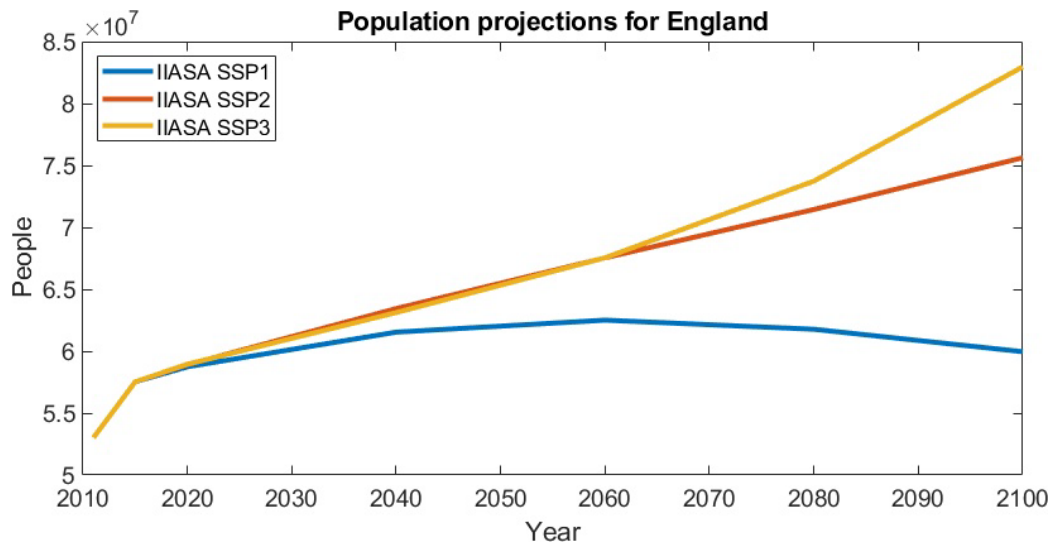


Figure 7.5 IIASA future population projections for England. SSP1 – Sustainable path, SSP2 – middle of the road, and SSP3 – high population growth.

Given the assumptions above, the population within the study area is expected to grow by more than 70,000 people in 2060, reaching a minimum of 1,250,000 and a maximum of 1,360,000 people by the same year (Figure 7.5). Under an SSP1 – sustainability scenario, the population is expected to decline by the year 2100, decreasing by over 50,000 from its 2060 estimate. In contrast, the SSP3 scenario – regional rivalry – creates an increment in the population of over 300,000 people, compared to the 2060 estimates in the same scenario (Figure 7.5). It is important to remember that these numbers are projections for the study area and do not represent the totality of people expected to live in Hampshire, West Sussex, and the Isle of Wight.

Once the total number of people in the area is defined, a similar methodology to that presented in section 6.2.4 is utilised. People are assigned to each population-weighted centroid within the study region. The population is then distributed on the urban grid identified in section 6.2.4, as the present extent of the urban footprint is assumed to be maintained in the future. This, as it is not possible to determine where new development might occur. Furthermore, any development in the floodplain is highly discouraged by the Environment Agency through the National Flood and Coastal Erosion Risk Management Strategy for England (Environment Agency, 2020b).

Figure 7.6 shows the difference from the baseline population for each of the SSP projections for the years 2060 and 2100. In all cases, most population growth is seen around the main urban areas, Portsmouth and Southampton. These are closely followed by areas in Fareham and Havant. However, within each urban square grid of 50m by 50m, the increments in the population are of up to 8 people.

Difference in population distribution under future scenarios compared to the 2020 distribution

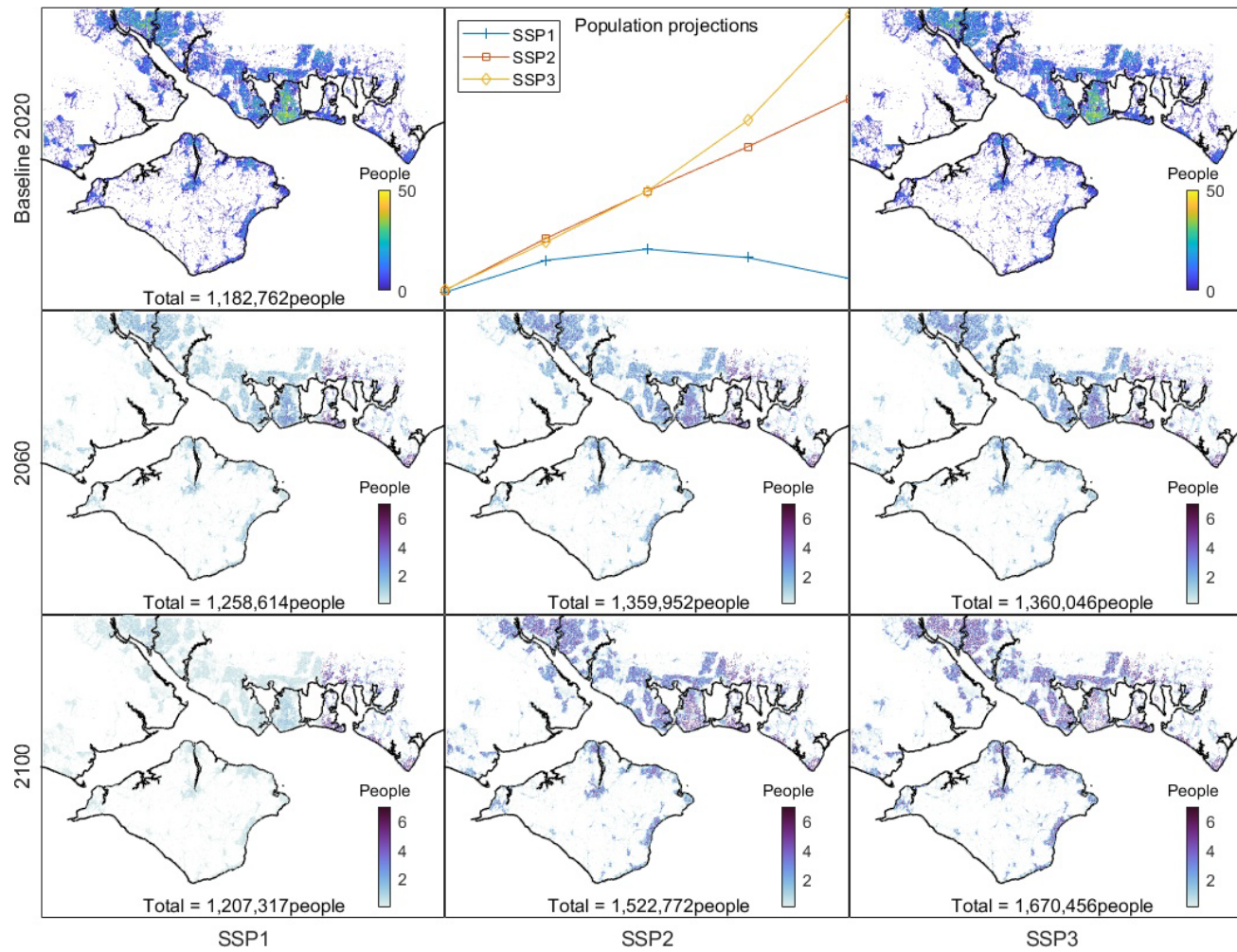


Figure 7.6 Future population growth for the Solent and difference from the present population distribution for the different IIASA population growth scenarios.

### 7.2.4 Future flood risk analysis

Having established the future evolution of each of the SPRC components under study, the future levels of coastal flood risk at the Solent are estimated utilising the hydrodynamic model presented in Chapter 4. The input parameters of this model are modified to match the specific characteristics of the sources and pathways of each of the scenarios in Table 7.2. Once the total extent of the inundation is determined for each scenario combination, the output of the LISFLOOD-FP model is overlayed onto each of the population distributions to obtain the number of people exposed. The process is repeated for 12 return periods, which results in 2,028 simulations. Combined with the population growth scenarios, this yields a total of 26,364 results of future exposure.

Table 7.2 SPRC scenarios for future flood risk assessment

<i>Sources (sea-level rise)</i>				
RCP Scenario		Years analysed		
No SLR		2020		
2.6	2040	2060	2080	2100
4.5	2040	2060	2080	2100
8.5	2040	2060	2080	2100
<i>Pathways (defence improvement)</i>				
RCP Scenario		Years analysed		
No improvement		2020		
2.6	2040	2060	2080	2100
4.5	2040	2060	2080	2100
8.5	2040	2060	2080	2100
<i>Receptors (population growth)</i>				
Scenario		Years analysed		
No growth		2020		
SSP1	2040	2060	2080	2100
SSP2	2040	2060	2080	2100
SSP3	2040	2060	2080	2100

Along with the mix of all scenarios, the focus is given to seven main storylines, presented in Table 7.3. These are selected as they portray some of the most likely conditions that can be expected in the future. The last three scenarios, SCEN 1, SCEN 2, and SCEN 3, are set as climate change, and particularly the RCPs can be closely tied to the socio-economic evolution (SSPs) (van Vuuren and Carter, 2013).



Table 7.3 Main storylines of future SPRC configurations

Storyline	Sea-level rise	Defence height	Population growth
Business as usual	RCP 4.5	RCP 4.5	SSP 2
Best case – Present management	RCP 2.6	RCP 8.5	SSP 1
Worst case – Present management	RCP 8.5	RCP 2.6	SSP 3
Worst case – No active intervention	RCP 8.5	No intervention	SSP 3
SCEN 1	RCP 2.6	RCP 8.5	SSP 1
SCEN 2	RCP 4.5	RCP 8.5	SSP 3
SCEN 3	RCP 8.5	RCP 8.5	SSP 3

## 7.3 Results

This section presents the main findings obtained by performing a series of simulations of coastal flooding using LISFLOOD-FP. The outputs of this analysis are then coupled with the projected population distributions of the area and the number of people at risk estimated. The following sections highlight some of the main findings for both the Solent and some of the main built-up areas in the region.

### 7.3.1 Future exposure to coastal flooding

The first sub-objective of this chapter is to analyse the future exposure to coastal flooding at the Solent. In order to provide the future levels of threat, it is necessary to explore the effect of selecting a minimum depth of flood required to produce damage and its influence over time. This is initially done by using a “business as usual” storyline (see Table 7.3 for a description). It can be seen that for the lowest return period, exposure increases from 4,240 people in 2040 to over 8,180 by 2100 when no flood depth threshold is employed. This rate of increment, equivalent to exposure almost doubling by the end of the century, is maintained for all return periods.

It has been established in previous chapters that a minimum depth of flood of 0.3m is an appropriate threshold, as it is the lowest depth in which water can damage properties, even under low water velocity (DEFRA, 2003, Kelman, 2002, Dawson et al., 2011). Introducing this minimum depth of flood has a considerable effect on the estimates of future exposure. For example, in a 1 in 1-year event, the number of people expected to be flooded by 2100 is less than the exposure obtained for 2040 without a minimum flood depth threshold (Figure 7.7). However,

the influence of the minimum threshold appears to decrease over time. For a 1 in 100-year event, introducing the minimum threshold of 0.3m decreases exposure by 57.27% in 2040. This changes to 49.12% by the year 2100. On average, the flood depth threshold creates a reduction of 57.02% in 2040, 54.54% in 2060, 52.37% in 2080, and 50.59% by 2100.

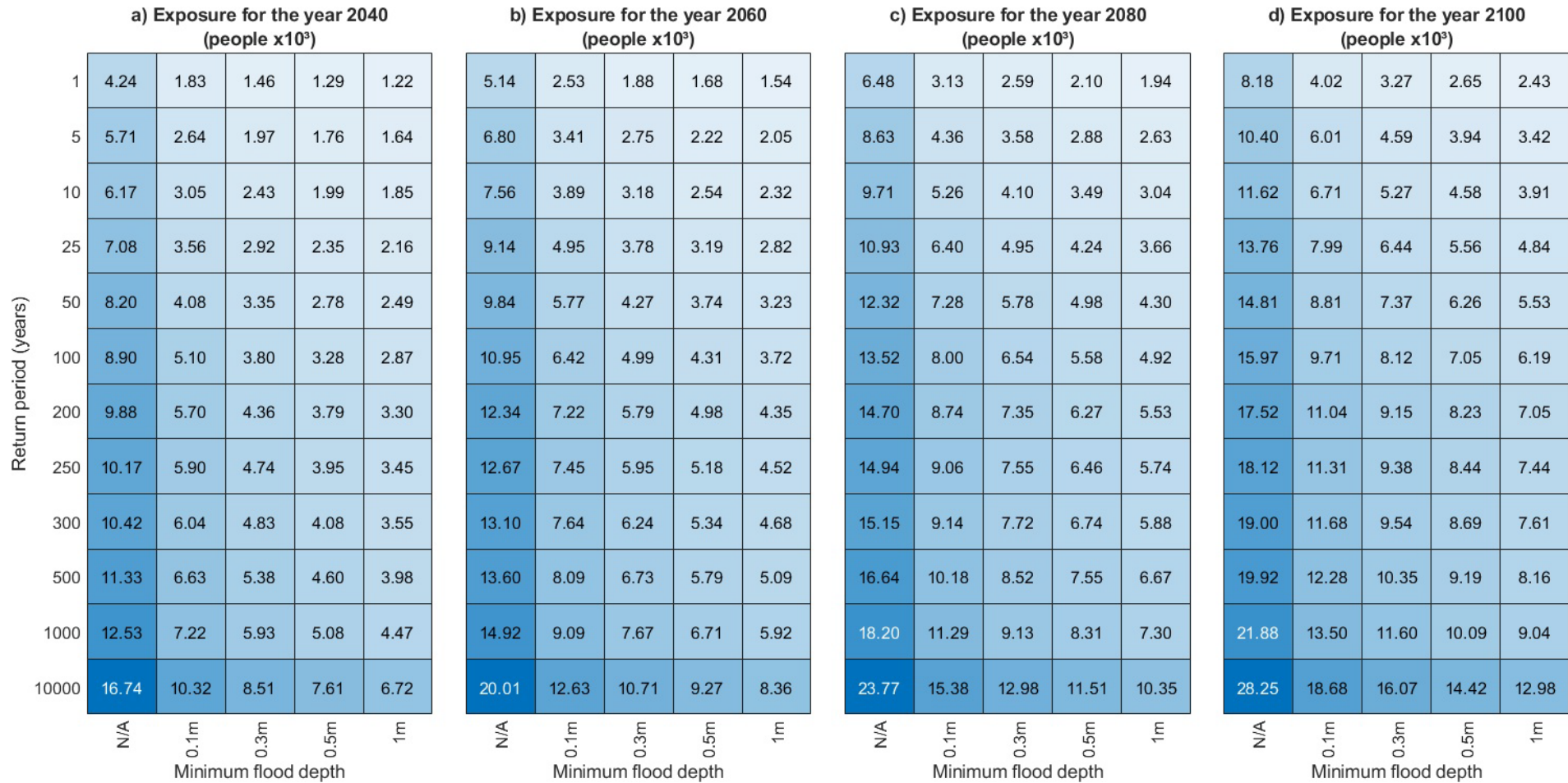


Figure 7.7 Future exposure to extreme water levels under a business as usual scenario, based on the minimum depth of flood required to produce damage

Exposure is estimated for the built-up areas presented in Figure 3.3. The results for a 1 in 100-year event are presented in Figure 7.14. It can be seen that Portsmouth and Fareham are the areas with the largest level of threat for this return period along all timesteps. Portsmouth initiates with over 700 people exposed and finishes the century with more than 1,900 people threatened to flooding by a 1 in 100-year event. Fareham sees its exposure almost treble from 380 in 2040 to more than 990 by the year 2100. The areas around Portsmouth and Chichester Harbour also experience the largest exposure. Cosham, located at the north of Portsmouth, has a similar level of threat to that of the latter, with 268 people exposed in 2040 and almost 600 by 2100. Hayling Island more than triples its exposure from 200 people in 2040 to more than 640 by the year 2100.

Even though all of the Solent is estimated to increase its exposure through time, some areas see a lower rate than those in the vicinity of Portsmouth. Lymington's exposure to a 1 in 100-year event is nearly doubled in the 60 years between 2040 to 2100, going from 148 to 272 people. The city of Southampton is projected to have 25 people exposed to the 1 in 100-year event in 2040. This number only increases by 18 people, finishing the century with 43 people exposed to the same extreme water level.

Overall, the rate of increment in exposure from the year 2040 to 2100 under the business as usual scenario here presented has an average of 2.45. However, the reality of these increments is far different along the coastline (Figure 7.9). Areas such as Havant increase their exposure by a magnitude of 5.25, rising from 4 people in 2040 to 17 by the year 2100. However, these 17 people represent less than 2% of the increment of 1,198 people seen in Portsmouth for the same period. In this sense, the areas located in the eastern-central region of the Solent experience the highest level of risk and the highest increments in the number of people exposed throughout the 21<sup>st</sup> century for all return periods (Figure 7.9).

Exposure to a 1 in 100-yr event for the main built up areas of the Solent under a business as usual scenario - present management

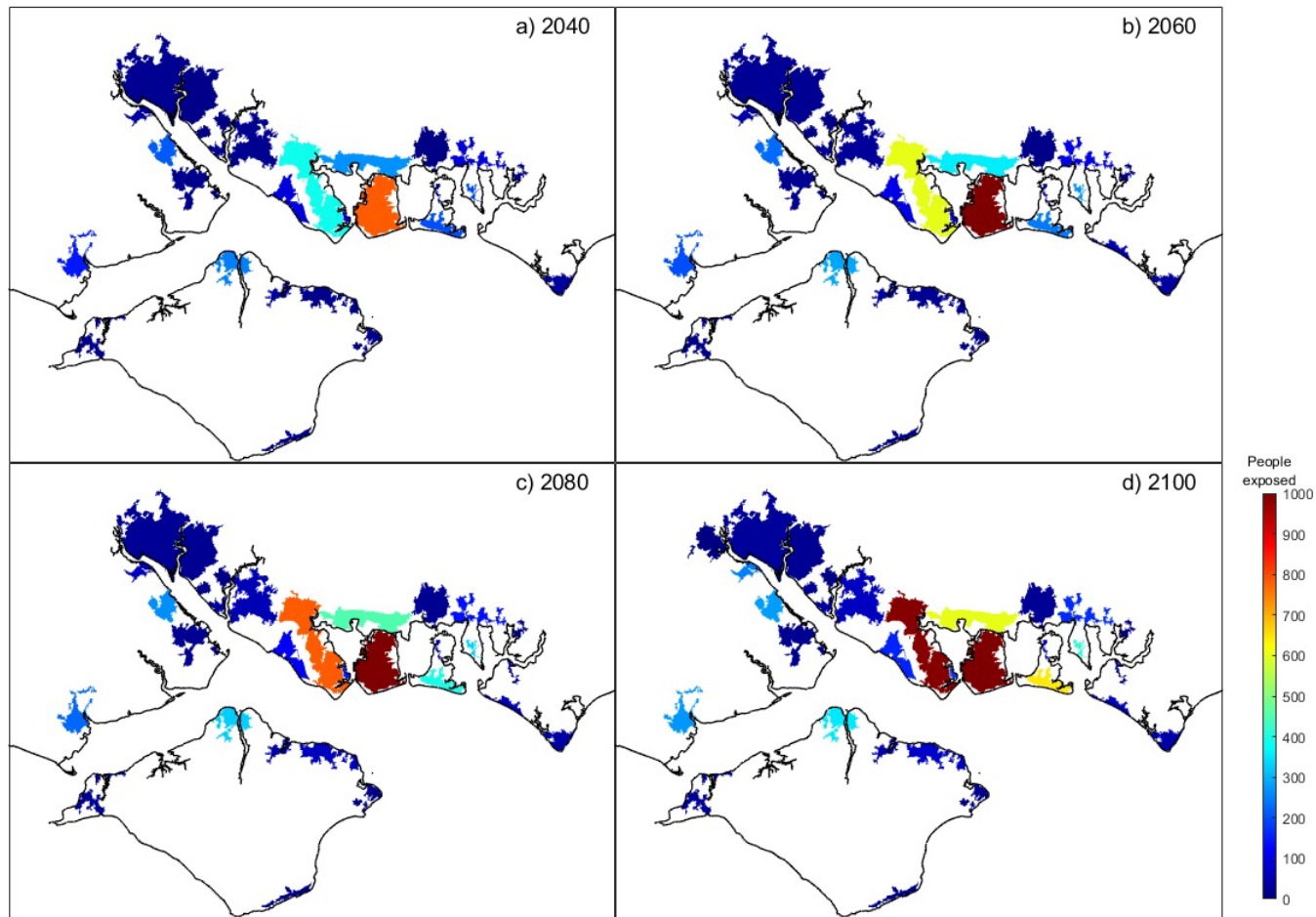
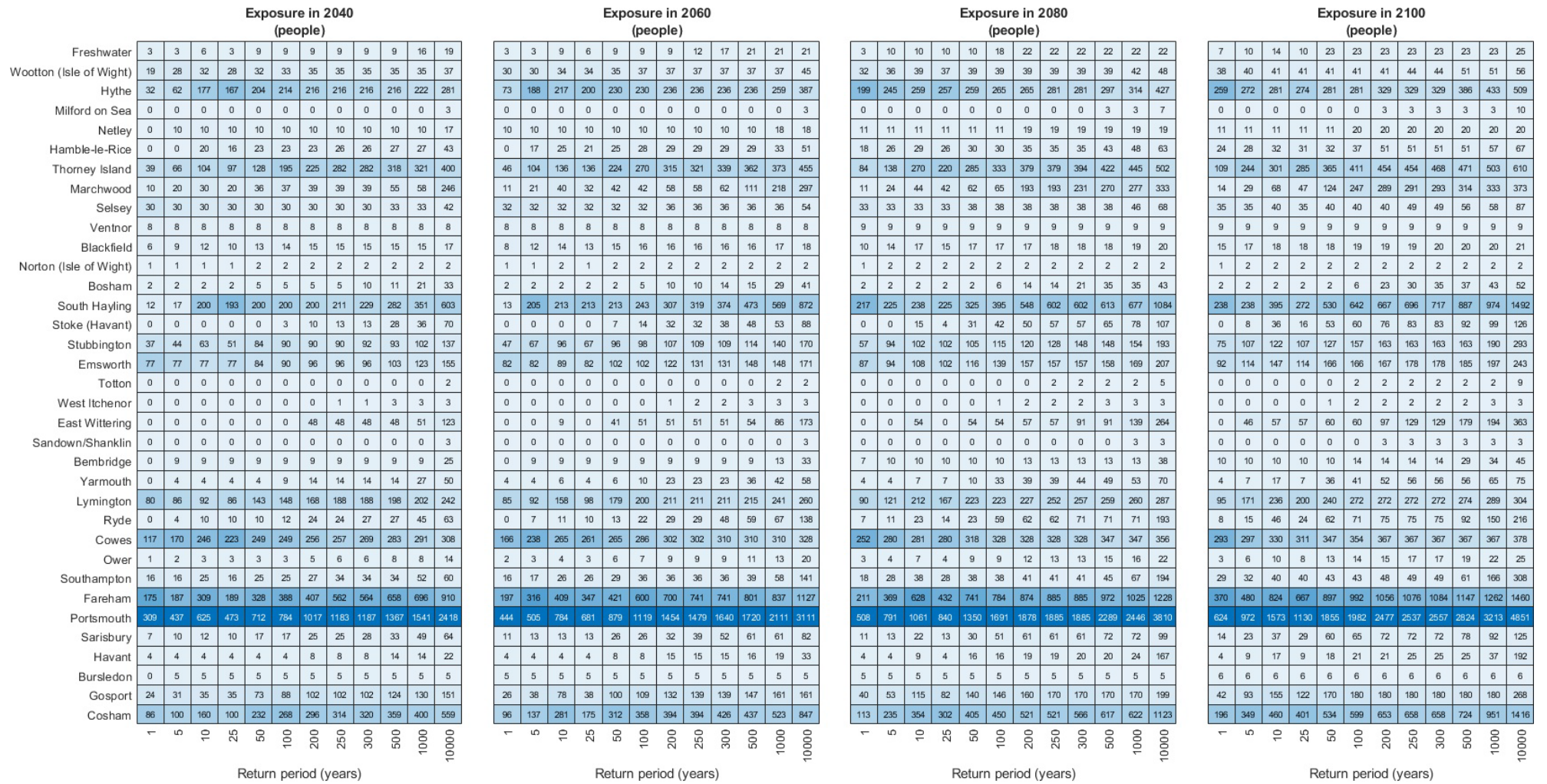


Figure 7.8 Map of future exposure to a 1 in 100-year event for the main built-up areas of the Solent under a "business as usual" scenario, considering a minimum flood depth of 0.3m



## Chapter 7



### 7.3.2 Future risk of coastal flooding

The second sub-objective is to estimate the number of people at risk of coastal flooding for the remainder of the 21<sup>st</sup> century. For this purpose, the exposure to individual extreme water levels is integrated across their probabilities to obtain the expected annual damage (Figure 7.10). This results in 1,520 people/year EAD for the year 2020. EAD increases by a third (376 people/year) from 2020 to 2040, and it increases at a similar rate after 2040. There is a growth of 33.28% from 2040 (1869 people/year) to 2060 (2,527 people/year). The same augmentation rate is seen from 2060 to 2080, going from 2,527 to 3,369 people/year. For the last timestep between 2080 and 2100, the rate of growth is moderately increased to 35.98%, reaching a maximum of 4,581 people/year by 2100.

Considering the 2020 average household income for England of £35,900, the EAD estimates of people are equivalent to £148 million/year in 2020, £184 million/year in 2040, £245 million/year in 2060, £327 million/year in 2080, and £445 million/year by the end of the century.

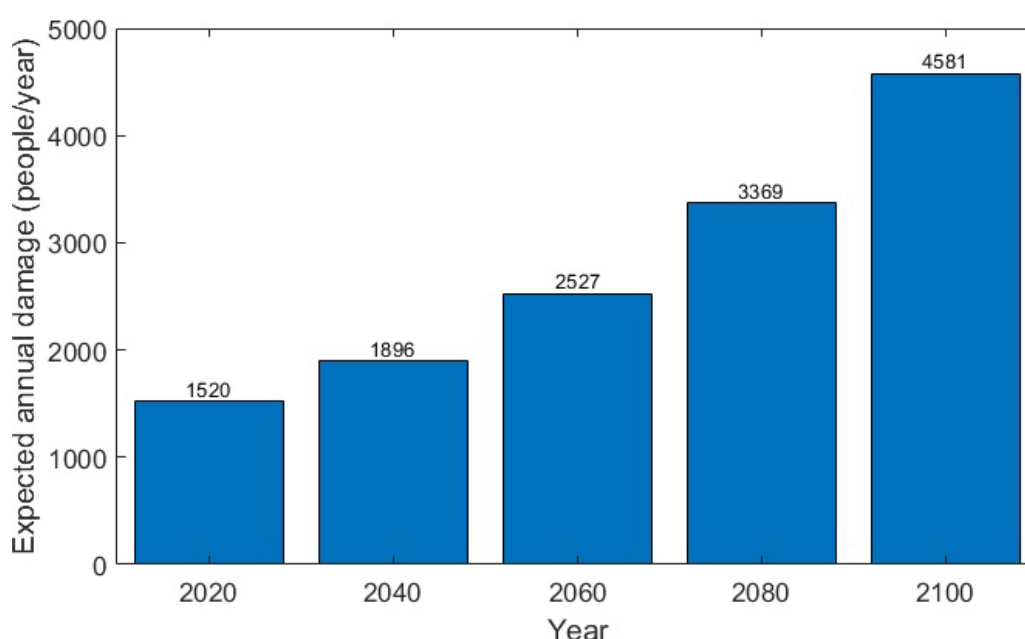


Figure 7.10 Expected annual damage projections for the Solent, considering a minimum depth of flood of 0.3m

EAD is estimated for the first four main storylines presented in Table 7.3. The results presented in Figure 7.11 show that for a best-case scenario, risk steadily increases up to the year 2060.

However, these increments appear to slow down after this year producing 1,127 people/year at risk, which is 650 people/year less at risk of flooding than a business as usual scenario by 2100. An almost constant increment in risk is seen for a business as usual scenario, reaching a maximum of 1,770 by the year 2100. Comparing the best case (1,127 people/year by 2100) and the worst case

(3,060 people/year by 2100) scenarios under present management for the year 2100 results in a difference of over 1,930 people/year. For both worst-case scenarios, these increments are exponential and particularly heightened after 2080. Following the present management strategies results in a decrement of 375 people/year than those projected with no active intervention.

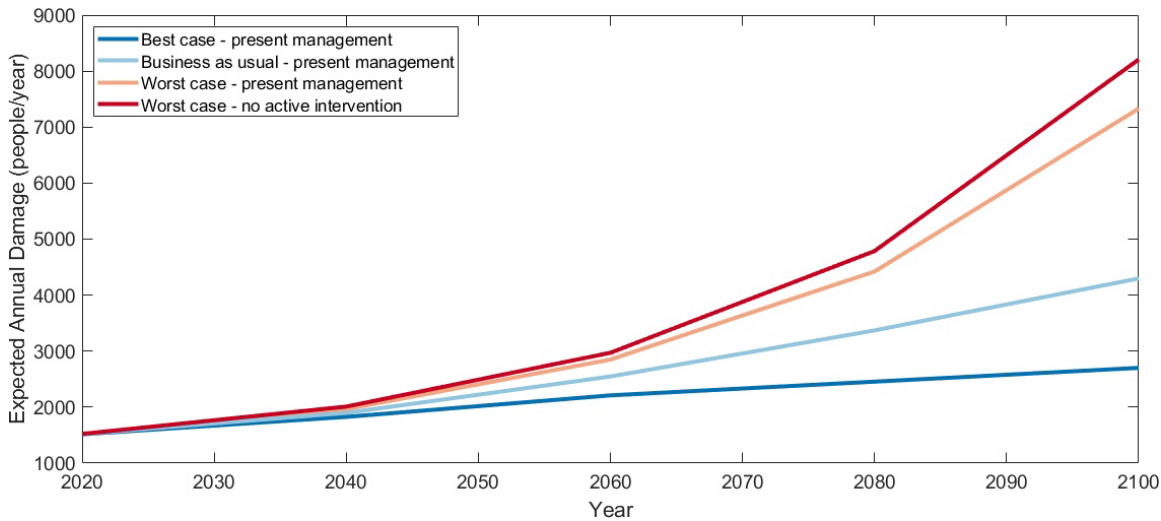


Figure 7.11 Future expected annual damage for four main storylines of SPRC factor configuration

In addition to the scenarios above, the EAD is presented for three scenarios that assume a link between population growth and climate change (Figure 7.12). In all of these, the increment in defence standard of protection is set equal to RCP 8.5. SCEN 1 overlaps with the result of a best-case scenario as both assume the lowest population growth and sea-level rise, combined with a high increment in the standard of protection. Similarly, SCEN 2 and a BAU scenario are closely tied. However, the former considers a higher standard of protection for future defences. This leads to a decrement of 250 people at risk by the year 2100. This difference increases to 750 people/year when SCEN 3 and worst-case–present management are compared for the same year.

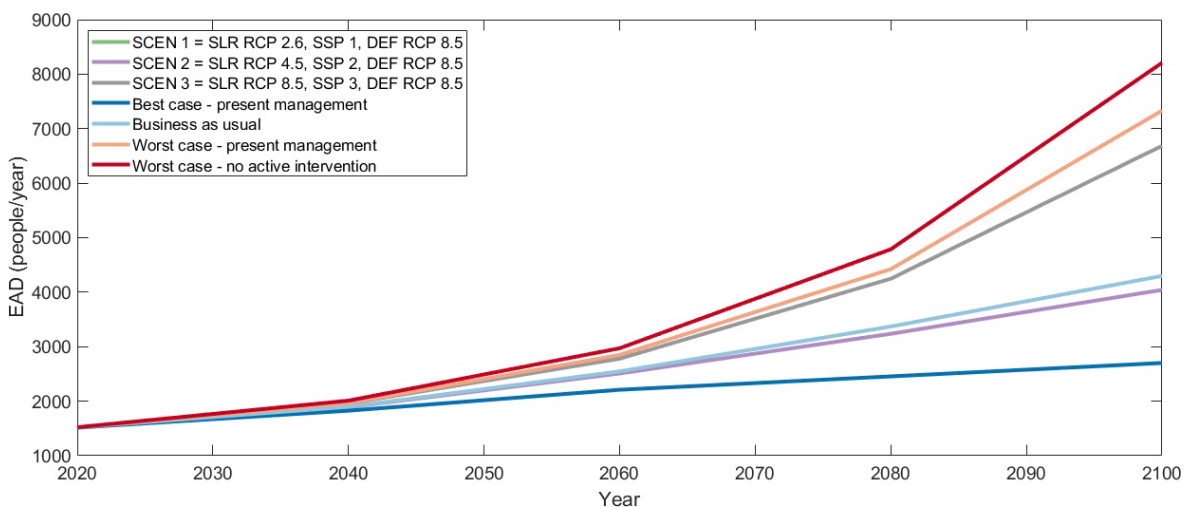


Figure 7.12 Future expected annual damage for the four main storylines and three additional scenarios relating sea level rise to population growth.



Expected annual damage in terms of people is estimated for the main built-up areas presented in Figure 3.3. This is done for the first four storylines presented in Table 7.3. In all cases, the city of Portsmouth presents the largest EAD (Figure 7.13). Focus is given to Portsmouth as it holds a similar share of the Solent's EAD as the combined total of all the rural areas within the region. Under the present coastal management approaches, its risk increases from 339 to 554 people/year between 2020 and 2100 for a best-case scenario. Assuming the worst-case scenario under present management (i.e. high sea-level rise, high population growth and low increments of defence height), the EAD more than triples for the city by the year 2100, reaching a maximum of 1,828 people/year. Under the storylines built around the present coastal management, the city of Portsmouth shares an average of 20% of the Solent's EAD. Assuming no active intervention, its share increases to 25.3%.

Other cities located in the vicinity of Portsmouth also show substantial levels of risk (Figure 7.14). Cosham, located north of Portsmouth, is projected to follow a similar trend to Portsmouth but on a smaller magnitude. It is only in the best-case scenario that EAD increases by less than 100% from the year 2020 to 2100 (Figure 7.13). For the rest of the storylines, the increments range between three and five times their 2020 EAD by the year 2100. At the west of Portsmouth, Fareham reaches a maximum EAD of 482 people/year by 2100 with BAU (Figure 7.14). This number decreases to 292 people/year under a best-case scenario and almost doubles, reaching 909 people/year for a worst-case—present management scenario. Interestingly, Fareham only shows a slight difference when the worst-case scenarios for present management and no active intervention are compared. At the opposite end of the Solent, Lymington experiences a decrement in the EAD for a best-case scenario, where EAD is reduced to less than half of its 2020 value by 2100. However, this trend is not sustained for the worst-case scenarios, where EAD increases by almost fourfold between 2020 and 2100.

For the rest of the urban areas, not shown in Figure 7.13, EAD increases by a factor of two for a best-case scenario and a factor of 4 under business as usual for the period between 2020 and 2100. However, these numbers are severely increased with a worst-case scenario. Even following the present management could result in 1,229 people/year EAD, which is more than ten times the EAD of these areas for 2020 (129 people/year) (Figure 7.13). Without any active intervention, the rate of increase is similar, reaching a maximum of 1,280 people/year by the end of the century. For the rural areas in the region, the greatest enlargements come for the worst-case scenarios, and EAD is increased by 327% to 370% for present management and no active intervention, respectively.

EAD people/year Best case scenario Present management						EAD people/year Business as usual					EAD people/year Worst case scenario Present management					EAD people Worst case scenario No active intervention							
	2020	2040	2060	2080	2100		2020	2040	2060	2080	2100		2020	2040	2060	2080	2100		2020	2040	2060	2080	2100
Cosham	85	101	119	152	188		85	105	139	204	306		85	105	158	299	510		85	105	165	298	513
Cowes	124	152	188	210	227		124	157	212	270	299		124	161	230	292	360		124	161	230	297	364
Emsworth	64	74	76	76	79		64	77	83	93	109		64	76	84	106	154		64	76	84	106	154
Fareham	170	192	208	275	292		170	198	283	342	482		171	198	300	474	909		171	199	301	481	911
Hythe	51	69	131	155	197		51	64	145	227	267		51	75	153	254	314		51	74	143	230	305
Lymington	78	84	84	60	33		78	87	97	119	148		78	88	105	161	250		78	90	117	175	273
Portsmouth	339	403	472	518	554		340	416	526	732	924		340	419	644	976	1828		340	423	669	1102	2255
Selsey	29	28	28	28	27		29	29	31	33	35		29	28	31	34	42		29	35	48	102	214
Stubbington	36	43	51	57	70		36	44	62	80	96		36	47	62	94	132		36	47	62	94	132
Thorney Island	38	60	78	93	113		38	62	90	133	201		38	66	110	206	369		38	66	116	235	410
Other main urban areas	129	158	276	306	396		129	171	309	481	626		129	179	348	649	1229		129	182	362	686	1280
Rural areas	377	462	499	525	525		376	487	570	656	805		375	524	624	877	1233		375	552	674	981	1397
Solent	1520	1826	2210	2455	2701		1520	1897	2547	3370	4298		1520	1966	2849	4422	7330		1520	2010	2971	4787	8208

Figure 7.13 Future expected annual damage (EAD – people/year) for main built-up areas at risk at the Solent under four main storylines.

EAD (people/year) distribution for the main built up areas of the Solent under a business as usual scenario - present manage

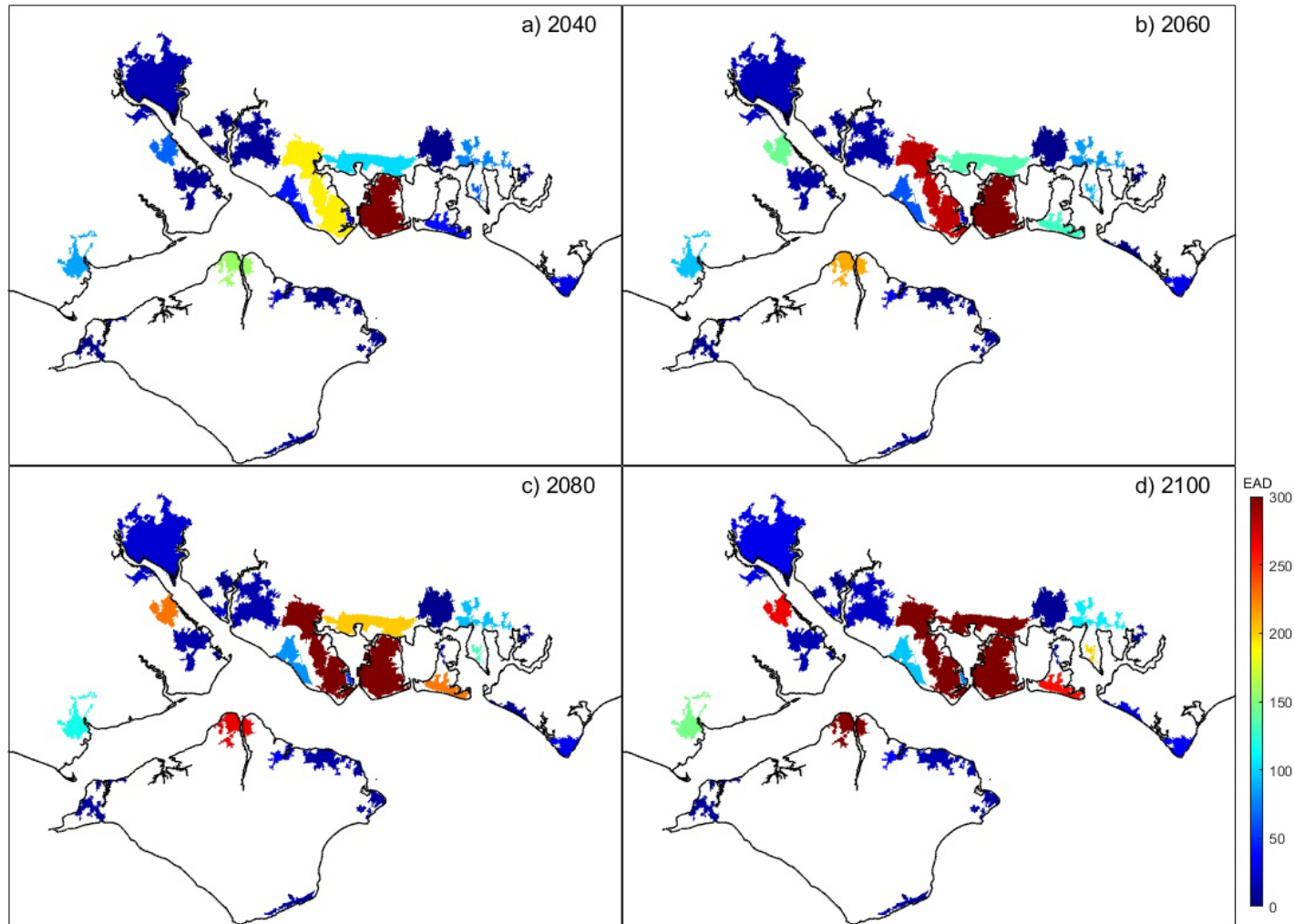


Figure 7.14 Map of future expected annual damage (people/year) at the main built-up areas of the Solent under a business as usual storyline

### 7.3.3 Uncertainty in future exposure and risk of coastal flooding

The third sub-objective of this chapter is to quantify the uncertainty in coastal flood exposure and risk caused by climatic, socio-economic, and coastal management scenarios. Figure 7.15 presents the range of uncertainty in the level of exposure caused by each return period at the Solent from the year 2020 as a baseline up until the year 2100. The spread of results increases as a function of the return period and the year under scrutiny. The variance is such for some return periods that the lowest exposure they cause is equivalent to a smaller magnitude event. For instance, a 1 in 1,000-year event can generate exposure of over 12,00 people by the year 2100. This is equivalent to almost the highest exposure produced by a 1 in 5-year event for the same year.

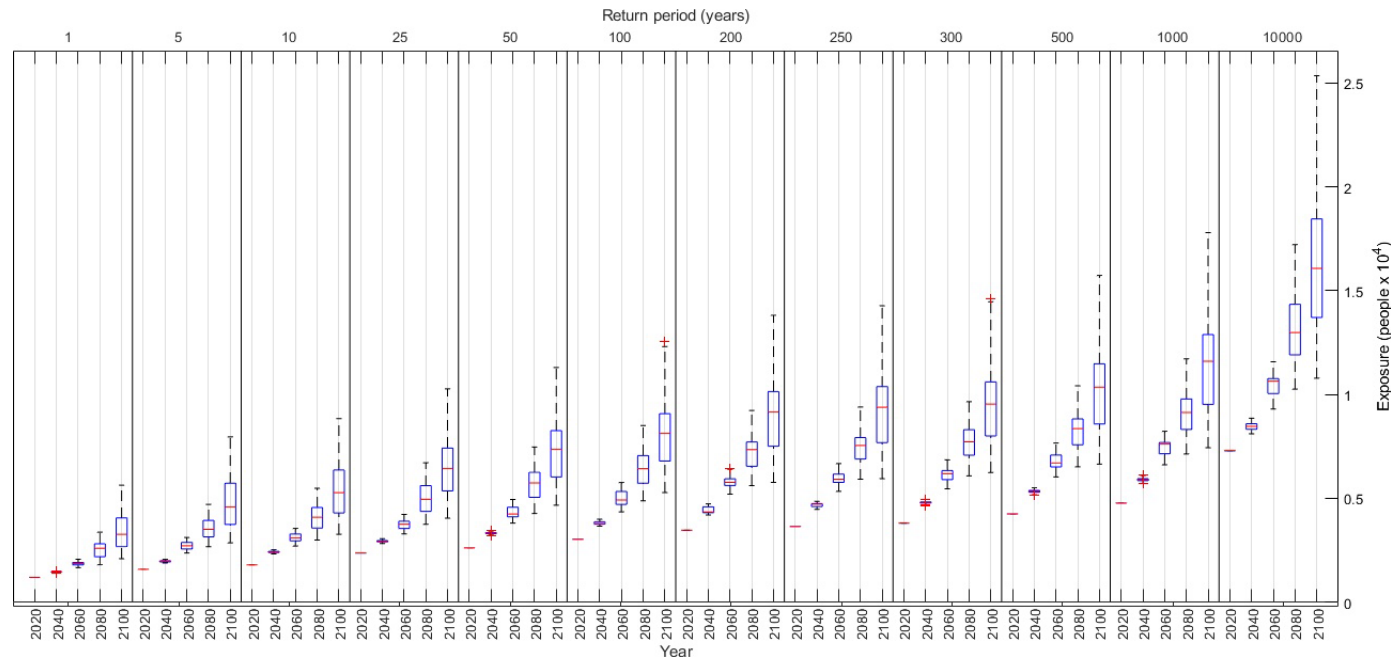


Figure 7.15 Future uncertainty in the level of exposure of the Solent to different return periods.

One of the critical elements of the present assessment is understanding the factors that will drive exposure in the future and those that generate the highest uncertainty. The results of Figure 7.16 can be decomposed based on the input factors of each simulation. Following a business as usual scenario, it is clear that the increment in sea level from 2020 up until 2100 is the primary driver of increased exposure (Figure 7.16.a). The variability in exposure generated from the uncertainty in each component is analysed by performing simulations where all but one component are kept to their BAU value. The component in which variability is being analysed is tested for each of its three settings in every timestep. For instance, the variance produced by sea-level rise is studied by running the inundation model with flood defences kept at a BAU height, whilst the extreme water levels are increased by the rates of RCP2.6, RCP4.5 and RCP8.5 (Figure 7.16.b).

On its own, sea-level rise creates the largest variability. For instance, the exposure to a 1 in 100-year event ranges by up to 5,000 people for the year 2100. The results of this event for the end of the century range from 7,200 people under an RCP2.6 to more than 11,200 with RCP8.5 (Figure 7.16.b). Population growth comes second, causing uncertainty of 2,500 people (Figure 7.16.d). SSP1 leads to 6,400 people being threatened in 2100, whilst SSP3 results in 8,900 people being exposed for the same year. Lastly, the variability in defence height produces the least uncertainty for exposure to a 1 in 100-year event, with a variance of just over 800 people between RCP 8.5 (7,450 people) and RCP 2.6 (8,270) by 2100 (Figure 7.16.c).

The same remains true for the rest of the return periods analysed (Figure 7.17). In all cases, it is the sea-level rise (variance in the sources) that generate the largest standard deviations. This is followed by the uncertainty in population growth (receptors) and, lastly, by the uncertainty in defence height (pathways). It can be appreciated that for all the estimates, the standard deviation increases as a function of the return period. In the same way, uncertainty is increased as the study moves from 2040 to 2100.

Interestingly, for almost all the return periods and timesteps, the standard deviation obtained by only including the variability in the sources is higher than the standard deviation estimates when all the components are variable (Figure 7.17). For the year 2040, the uncertainty when either sources or pathways are analysed sees a decrement when the return period goes above 1 in 200-years. The same is true for the overall variance. However, this does not occur when the receptors are the only variable factor. The results of Figure 7.16 and Figure 7.17 are obtained by incorporating the variability of one component whilst the rest are kept to their “business as usual” value. In reality, there are interactions between components that can lead to more stable and less variable results.

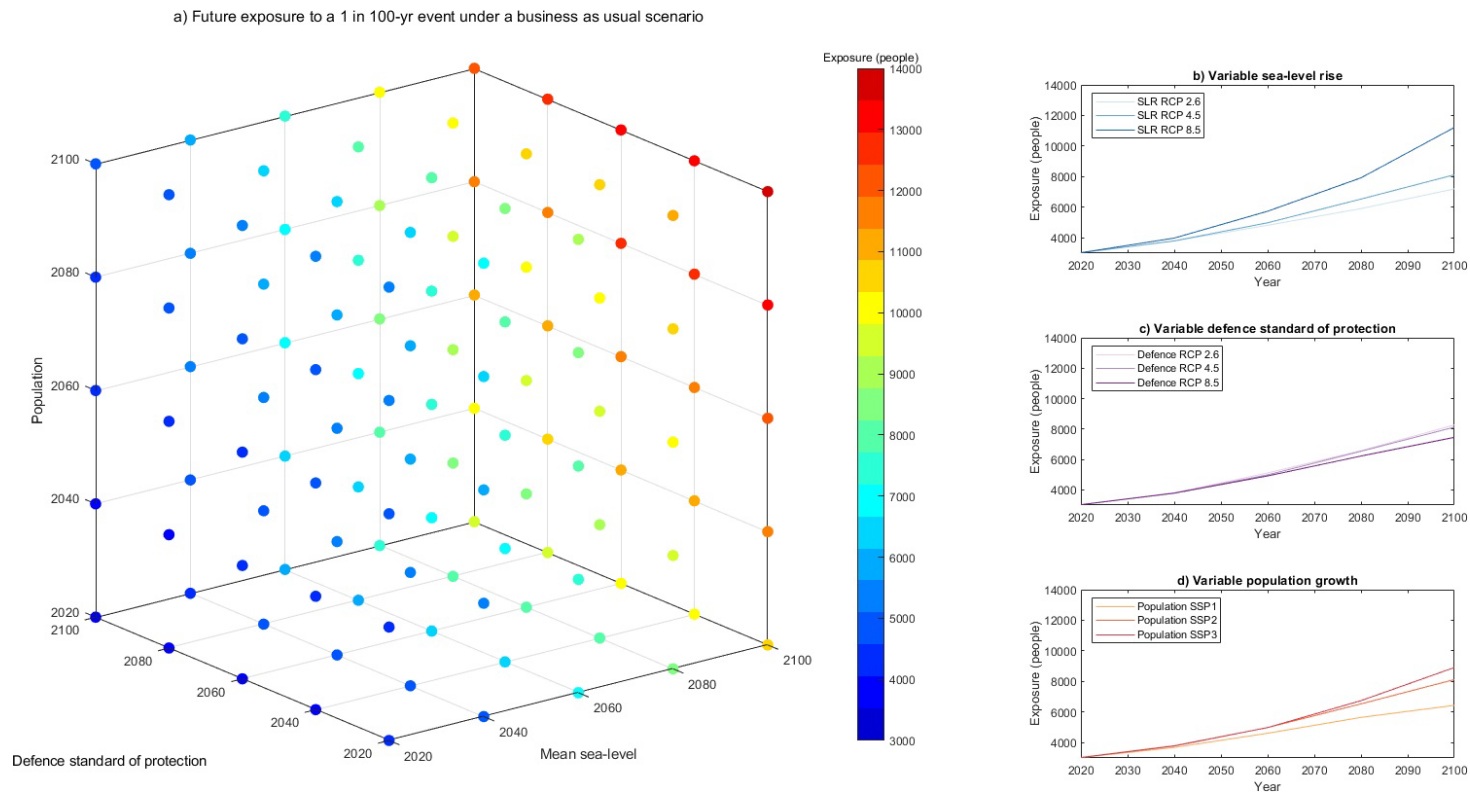


Figure 7.16 Uncertainty in future exposure to a 1 in 100-year event based on the evolution of the SPRC input factors. Subplot a) shows the estimates when all components vary. For subplots b to d, the components which are not analysed are kept to their business as usual value.

Standard deviation (people) year 2040					Standard deviation (people) year 2060				Standard deviation (people) year 2080				Standard deviation (people) year 2100				
Return period (years)	1	33	5	24	33	125	16	82	124	512	44	231	470	1195	119	508	1063
	5	55	11	32	54	268	30	119	230	709	132	319	628	1749	208	713	1525
	10	60	11	39	57	265	61	138	253	755	93	365	724	1823	195	819	1624
	25	79	5	47	76	298	24	163	287	1039	83	440	901	1996	302	1001	1805
	50	66	12	54	70	423	44	184	364	1104	204	514	979	2045	389	1145	1931
	100	110	12	61	106	490	100	215	446	1030	194	581	1016	2104	436	1263	2103
	200	222	7	70	180	397	21	250	387	1065	100	653	1051	2351	505	1422	2308
	250	69	1	77	100	455	34	257	431	1037	134	671	1028	2429	451	1458	2387
	300	82	9	78	95	454	39	269	436	1043	279	687	1043	2506	432	1482	2436
	500	90	13	87	106	592	48	290	507	1164	268	757	1139	2568	282	1609	2585
1000	123	16	96	131	397	26	331	451	1354	112	812	1335	2861	322	1802	2875	
10000	238	53	137	220	607	57	461	646	2243	272	1154	2021	4487	847	2497	4195	
	Sources	Pathways	Receptors	All	Sources	Pathways	Receptors	All	Sources	Pathways	Receptors	All	Sources	Pathways	Receptors	All	

Figure 7.17 Standard deviation caused by the individual SPRC components on the exposure to different future extreme water levels. Each column presents the uncertainty generated by one component while the remainder are kept to their business as usual value.

The effect of the interactions between components on the overall uncertainty in future coastal flood exposure is explored. Two components are varied whilst the remainder is kept at its BAU value (Figure 7.18). In this case, the largest standard deviations are caused by the joint effect of uncertainties in sea-level rise (sources - S) and population growth (receptors – R). However, the standard deviation caused by S&R is lower than that caused solely by the sources. The uncertainty generated by the sources (S) and defence height (pathways – P) comes second. However, it is close to that of the S&R. Lastly, combining the uncertainties of pathways and receptors creates the lowest exposure variabilities. These trends are kept throughout the 21<sup>st</sup> century. In almost all cases, the variance produced by S&P is 18% lower than that of S&R for 2040. However, there is a small decrement in this difference with time (Figure 7.18). The variance of S&P is 14% lower than the one produced by S&R in 2060 and 13% lower in 2080 and 2100.



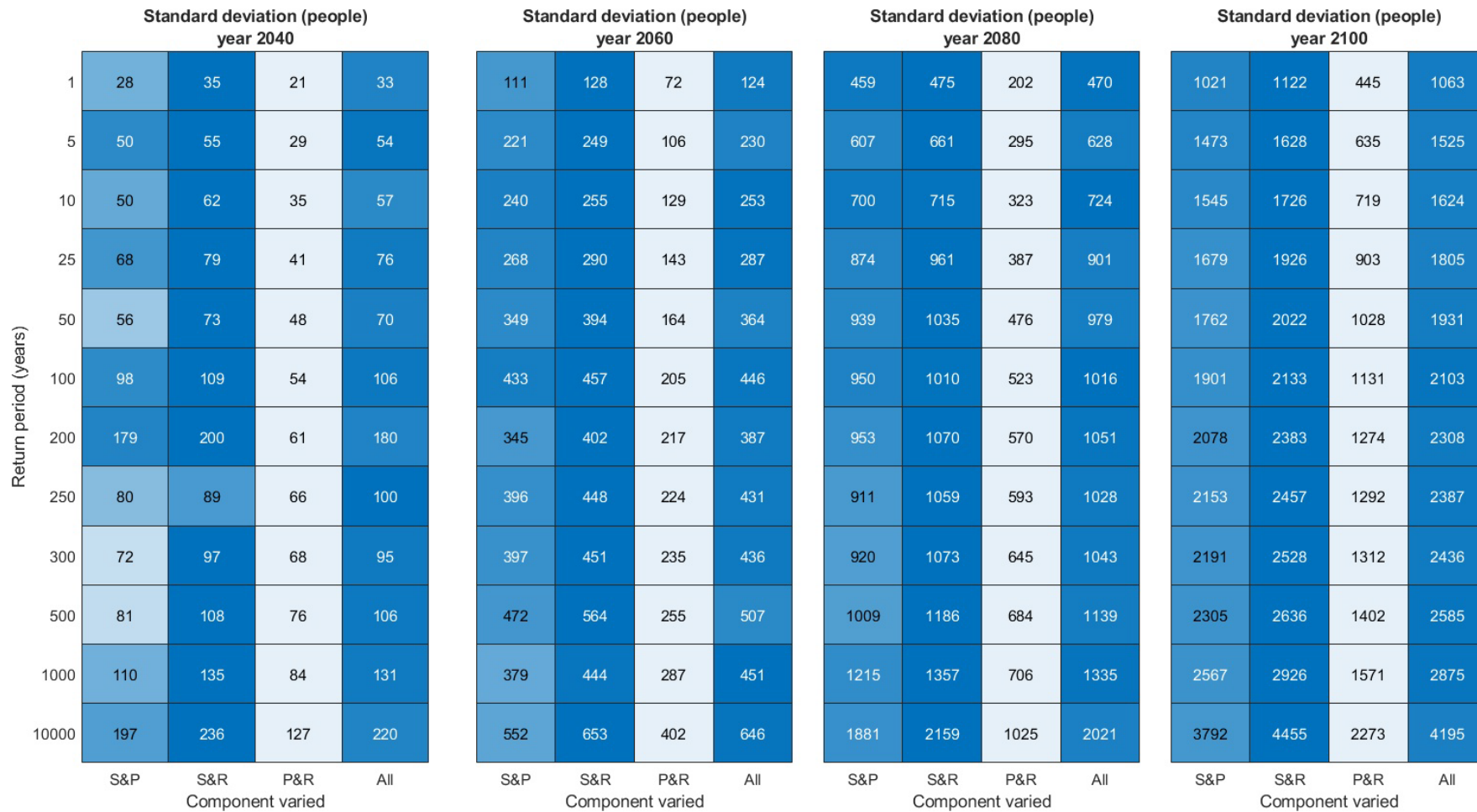


Figure 7.18 Standard deviation on exposure to future extreme water levels caused by the variance of two SPRC components. The remainder variable is kept to its business as usual value

It is then necessary to analyse the variance in the EAD caused by the SPRC components. This is assessed by estimating the results considering all the possible combinations of states of each variable. The results of Figure 7.19 show that uncertainty increases with the length of time of the estimates. For the year 2040, the uncertainty between the minimum EAD (1,826 people/year) and maximum (1,976 people/year) values is 150 people/year, which equals 7.91% of the mean EAD for the same year (1,896 people/year). The uncertainty for 2060 is equivalent to 25% (639 people/year) of the mean EAD of 2,526 people, ranging from a minimum EAD of 2,210 people/year and a maximum estimated EAD of 2,849 people/year. By 2080, the uncertainty is more than 58% of the mean EAD of 3,368 people/year. Finally, for the year 2100, the uncertainty exceeds 104% of the mean value (4,422 people/year). These figures show the uncertainty in EAD when all components are variable (Figure 7.19). However, it is necessary to identify the components which a) drive future coastal flood risk and b) generate the largest uncertainties.

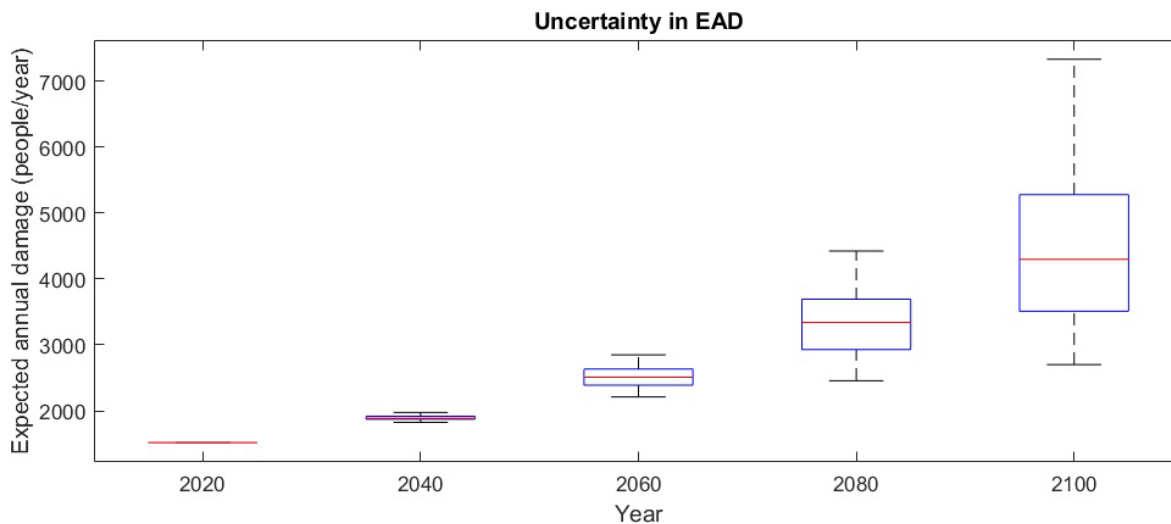


Figure 7.19 Uncertainty in future projections of expected annual damage caused by variations on the SPRC components

First, the influence of each component on the future EAD is analysed. This is done by estimating the EAD when one variable changes and comparing it to the previous timestep value. For the period between 2020 and 2040, the three sea-level rise scenarios increase the EAD by a similar magnitude. SLR RCP 2.6 causes an increment of 276 people/year, RCP 4.5 of 283 people/year and RCP 8.5 of 355 people/year. Defence improvement does not appear to produce substantial changes, with an average reduction of 37 people/year. Population growth increases EAD on a smaller magnitude than that caused by SLR. Interestingly, SSP2, the middle range scenario, appears to cause the largest increments in this period with 117 people/year (72 for SSP1 and 108 for SSP3). Overall, the effect of individual variations on the SPRC component on EAD from 2020 to 2040 is relatively uniform.

Looking at the period between 2040 and 2060, sea-level rise starts to dominate the changes in EAD. The variation between the increments caused by each RCP SLR scenario is visibly larger, ranging from 445 to 737 people/year for RCP2.6 and RCP8.5, respectively. Similar to this, the effect of increasing the height of flood defences starts to be appreciated. However, increasing the height of these structures only reduced EAD by only 25, 37 and 65 people/year for defence improvement RCP2.6, RCP4.5 and RCP 8.5, respectively. The changes produced by population growth are similar to those seen for the 2020-2040 period, with increments of 29, 122 and 132 people/year under SSP1, SSP2 and SSP3, respectively.

Sea level rise between the years 2060 and 2080 produces increments of over 400 and 1200 people/year for the lowest and highest SLR scenarios. Defence improvement continues to decrease EAD at a lower rate with a maximum decrement of 100 people/year. For the first time, population growth causes a decrease in EAD. Under SSP1, EAD decreases by 28 people/year. However, EAD increases by 147 and 233 people/year for the rest of the population growth scenarios.

Lastly, for the period between 2080 and 2100, the lowest SLR adds an extra 587 people/year to the 2080 EAD. This increment is fivefold under RCP 8.5, resulting in an additional 2,110 people/year expected to experience coastal flooding every year. Increasing the height of coastal flood defences continues to mitigate EAD. However, even the highest effect of defence improvement (decreasing EAD by 147 people/year) accounts for a quarter of the increments produced by the lowest rate of SLR. For this period, population growth under scenario SSP1 decreases EAD by 85 people/year. This is similar to the decrement in EAD produced by the lowest increment in defence height (84 people/year). Similarly, EAD increases by 435 people/year from 2080 to 2100 under SSP3, an increment that is similar to that produced by RCP2.6 (587 people/year).

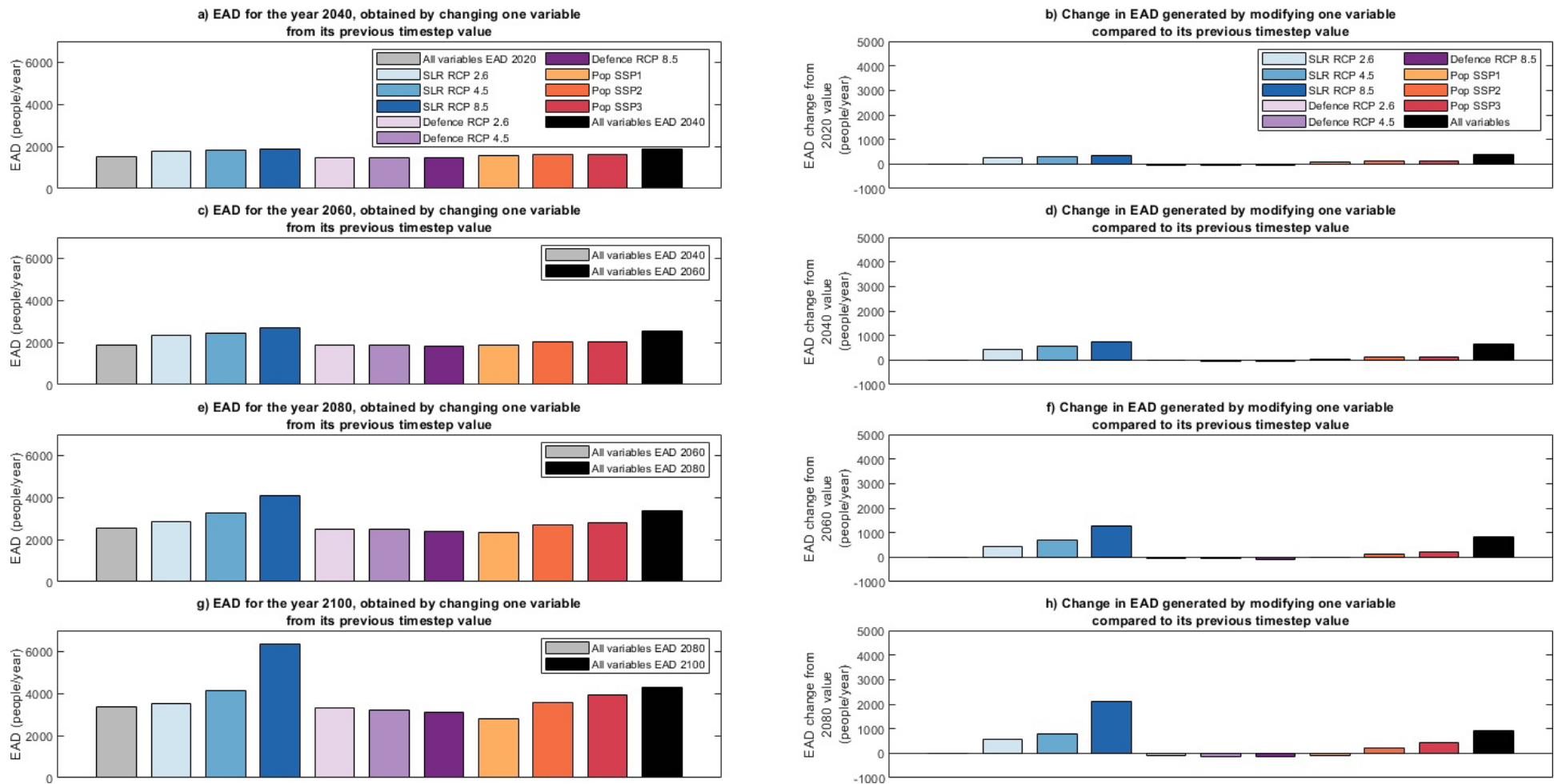


Figure 7.20 Evolution of expected annual damage based on changes in the SPRC components. The potential individual and combined effect of component evolution on EAD is projected using the different SPRC scenarios at each timestep.

Following the identification of the main drivers of EAD, it is necessary to assess the uncertainty generated by each input. For this, the model is tested for the variations of the SPRC components. By doing so, the increments generated by, for instance, each of the three sea-level rise scenarios can be assessed. As done in the exposure assessment, the analysis initiates by varying one component while the remaining variables are set to their BAU value (Figure 7.21). In this case, the uncertainty in the sources (i.e. in sea-level rise) cause the largest standard deviation. In second place comes the uncertainty generated by the receptors (i.e. population growth). The difference between the standard deviation created by sea-level rise and that generated by population growth is of only 18 people/year (36.74%) for the year 2040 (Figure 7.21). However, this increases to a difference of almost 43% by the year 2100, as the sources generate an STD of 1,556 people/year, whilst the receptors only yield an STD of 668 people/year.

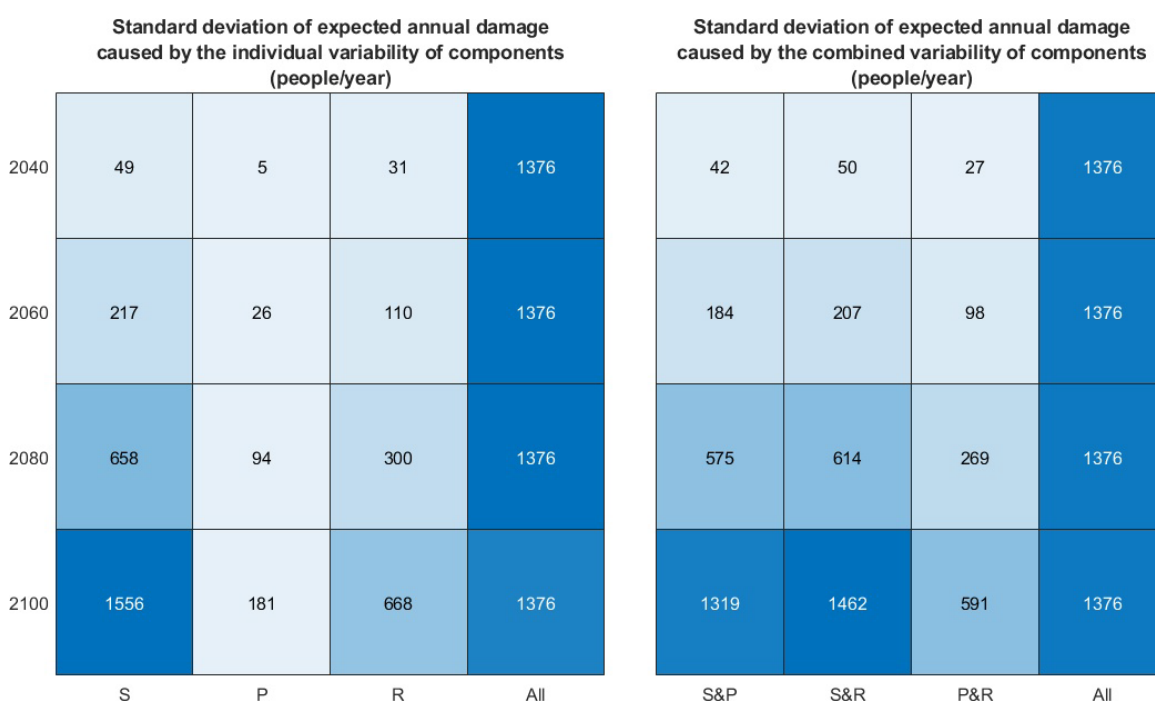


Figure 7.21 Standard deviation of EAD results obtained by maintaining one component constant at its business as usual value (RCP 4.5 for sea-level rise and defence height increments, SSP2 for population growth) while the rest are varied.

## 7.4 Discussion

The present chapter analyses objective three, which is to determine how flood risk may evolve over the remainder of the 21<sup>st</sup> century with future sea-level rise and population growth, considering future coastal management strategies. Three sub-objectives are defined to aid in the development of this objective. The findings of each sub-objective are discussed in sections 7.4.1 to 0.

### 7.4.1 Future exposure to coastal flooding

The first sub-objective of this chapter is to analyse the future exposure to coastal flooding at the Solent. The analysis first started by showing the influence of a minimum depth threshold to determine the number of people exposed to coastal flooding. The data indicate that with introducing a minimum depth of 0.1m, the estimates of risk are decreased by almost fifty per cent. Although such a depth could be considered as nuisance flooding, it highlights the effect this has on flood risk estimates.

For the present study, a minimum depth of 0.3m is selected as the threshold to cause damage to people and assets, which results in a decrement of over 57% from the results obtained without a minimum depth. Interestingly, the effect of this threshold decreases with time. One of the reasons for this is that, even though higher sea levels are likely to increase the overall floodplain, their effect is more likely to first impact areas with low elevation. This, in turn, would increase the extent of the area flooded to higher depths, decreasing the gap between their added area and the total area of the floodplain. When a higher depth is required to produce damage, the estimates are decreased by up to two thirds.

As mentioned in previous chapters, a minimum flood depth of 0.3m is selected as it would cause damage to buildings even under low water velocities. However, this threshold should be dynamic within the study area as it is highly dependent on the characteristics of each property. Unfortunately, there is not enough publicly available information on this matter. Furthermore, the use of an elevation model where all the human-made structures are removed results in inaccurate overestimation of the velocity of the floods.

Considering the flood threshold of 0.3m and a business as usual scenario, the assessment finds that exposure to a 1 in 100-year event almost triples from 2040 to 2100, although the increments are smaller for events with a lower probability. As seen on the historical assessment, it is the areas in the vicinity of Portsmouth that see the highest levels of exposure throughout the 21<sup>st</sup> century. Interestingly, the rate of increments in the number of people exposed is not equal for the

whole area. It has been shown that for areas such as Fareham, the increments are relatively low compared to those seen at Portsmouth. This can be tied to the assumption of each section of the Solent maintaining their present-day share of the population throughout the 21<sup>st</sup> century,

#### **7.4.2 Future risk of coastal flooding**

The second sub-objective is to estimate the future levels of coastal flood risk at the Solent. These are given for seven main scenarios. Expected annual damage is projected to steadily increase from 1,520 people/year in 2020 to more than 4,580 people/year by 2100 under a business as usual scenario. For a best-case scenario, CFR can be expected to tend to a plateau by the end of the century. There is high uncertainty on the path that coastal flood risk will follow in the area, causing the large spread of results seen when BAU and a worst-case scenario are compared. However, there are combinations of factors that are more feasible than others. For instance, it is rather unlikely that “no active intervention” occurs for the whole region. As presented at the NSSMP (NFDC, 2010), an average of 30% of coastal flood defences will follow such a scenario (Figure 7.4), and it is likely that these will be non-critical defences. Furthermore, additional assumptions can be made to decrease the uncertainty in CFR estimates. It is possible that, if coastal defence height is to be raised under HTL, this will be done assuming the highest future rate of SLR, as done in Portsmouth by the Coastal Partners. Assuming that this will be the case, the spread of results is reduced. Furthermore, the population growth SSP scenarios developed by IIASA can be linked to the RCP scenarios by the IPCC, as shown by van Vuuren and Carter (2013). This has been presented for scenarios SCEN 1, SCEN 2 and SCEN 3, which closely follow the best case, business as usual and worst-case scenarios, respectively, under present management. There are few assessments available looking at the uncertainty in EAD on a regional level. However, the magnitude of the variance seen in the EAD by the end of the century is in line with the trends found by Rohmer et al. (2021) on a global scale.

#### **7.4.3 Uncertainty in future exposure and risk of coastal flooding**

The third and last sub-objective is to quantify the uncertainty in exposure and risk estimates produced by climate change, socio-economic drivers and coastal management strategies. For the present assessment, the evolution climatic stressors are introduced with the variation of the sources of flood risk, mainly through sea-level rise. SLR is extremely likely to increase the frequency and severity of extreme weather events (Church et al., 2013, Taherkhani et al., 2020). However, its effect is simplified for the present assessment and only considered to increase the height of the extreme water levels. The rates of SLR used in the analysis and obtained from the UKCP18 report, which estimate them using probabilistic projections. However, there is high

uncertainty in these rates as there are still knowledge gaps on the physical processes of climate change and the resulting changes in sea level (Le Bars, 2018). These uncertainties are passed on to the risk estimates, resulting in the sources being identified as primarily responsible for increasing future risk and creating the largest variabilities. Identifying sea-level rise as the main source of uncertainty agrees with previous uncertainty assessments in coastal flood risk estimates (e.g. Vousdoukas et al., 2018a). Furthermore, the findings agree with what has been presented in global and regional assessments in terms of the importance of sea-level rise as the primary driver of future flood risk (Le Cozannet et al., 2015, Dayan et al., 2021, Rohmer et al., 2021). It is interesting to see that, without the influence of the rest of the components, the sources would cause uncertainties of a larger magnitude than those expected when all the components are varied. This could indicate a dampening effect on the uncertainty caused by the interactions between components.

In terms of the local importance of the sources, the areas at the east of the Solent are the most impacted by variations in the EWL height. It should be reminded that the present assessment does not consider the effect of waves. This is an important limitation to the analysis as these could increase the volume of water entering the area, particularly for the eastern region of the Solent. Furthermore, the frequency and magnitude of waves can be expected to be enhanced by climate change. Deepening the foreshore by increasing the sea level could lead to waves travelling further inland. Even though it is controlled by sediment processes, deeper seas could shift the breaking zone closer to the existing line of defences, ultimately resulting in higher loads applied to the coastal structures.

The second factor affecting the uncertainty in coastal flood risk estimates is the evolution of the receptors, i.e. population change. There is high uncertainty on the evolution of coastal populations, not only for the Solent but for England and the world as a whole (Neumann et al., 2015). To overcome this, three population growth scenarios are used to represent the range of plausible futures. The likelihood of occurrence of each population growth scenario, as developed by IIASA, is highly linked through feedback mechanisms to the climatic factors of the RCPs. However, the combination of all SSPs and RCPs is explored to understand the influence of this factor on coastal flood risk uncertainty.

The baseline assumption for the present assessment is that increments in population and future development will occur within the existing urban areas and that there will be no migration from the area. These assumptions have profound implications for coastal flood risk. Even if no changes in the sources or the pathways occur, the increasing numbers of people and equivalent assets are expected to be located within the existing and future coastal floodplain. Although changes in sea



level are presented as the largest driver of risk and uncertainty, the presence of people or assets determines the consequences of water entering an area.

The distributions presented in Figure 7.6 depict the number of people present in different sections of the Solent. Although the rate of increase is maintained equal throughout the Solent, this is unlikely to occur. Large urban areas have historically attracted development due to the presence of services, employment opportunities and additional socio-economic factors. However, Neumann et al. (2015) find that this trend is becoming less dominant for prosperous economies such as that of the UK. Unfortunately, there is high uncertainty in how this would apply at a regional scale, leading to the simplification above. This results in areas already densely populated and with a high level of risk for the year 2020, seeing these increase throughout the 21<sup>st</sup> century for almost all population growth scenarios. Most notable are the built-up areas within the vicinity of Portsmouth.

The assumptions made on the evolution of the receptors in the area are unlikely to occur in reality. Population growth will lead to a need for new housing development. This is likely to enlarge the urban area and possibly extend it onto the floodplain, even though this is discouraged by the government (Environment Agency, 2020b). However, there are landlocked areas where urban expansion is not entirely possible, such as Portsea Island, where Portsmouth is located. Here, the population could reach constant numbers and possibly decrease in the future. Hauer (2017) explored the effect of sea-level rise on coastal population, finding an unforeseen projected migration from landlocked areas, a trend that is yet to be widely seen in England. Migration from the area and development outside of the existing urban footprint and the existing floodplain could result in considerable reductions in the levels of threat (Merkens et al., 2018)

Additionally, future developments are likely to have a vertical nature, with the capacity to host more than one household. This means that the direct consequences could only be experienced by those living in lower levels, while the rest will only suffer from indirect impacts. Furthermore, the present assessment does not consider the possibility of migration from the area, as it is still not well understood the dynamics between coastal flood risk and migration as the latter is also affected by other socio-economic factors (McMichael et al., 2020, Neumann et al., 2015).

Lastly, the pathways generate the least uncertainties in the flood risk estimates. For this component, two main coastal management strategies are analysed. Firstly, one that assumes no active intervention, meaning that present defences are no longer maintained and left to deteriorate with time. In reality, this is very unlikely to occur as the presence of assets and infrastructure near the coast will require constant protection. The findings of this scenario can be used as a baseline to determine the benefits of maintaining or upgrading coastal defences.

However, it would be necessary to conduct a more in-depth assessment that identifies the protection given by individual and groups of coastal structures.

In the second pathway scenario, where present management is considered, the information on the management strategies for each section of the coast is obtained from the Nort Solent Shoreline Management Plan and the Isle of Wight Shoreline Management Plan. It can be seen that, for most coastal flood defences, the management strategy is to hold the existing line of defences. The Environment Agency defines this as maintaining or upgrading the level of protection given by the coastal assets. Neither the NSSMP nor the IOWSMP clearly indicate whether HTL will be reached by maintaining or upgrading the SoP. For this assessment, HTL is assumed to be equivalent to maintaining the standard of protection through time. Unfortunately, there is no clear guidance on what this implies in practical terms, as the SMPs do not indicate how often the standard of protection is to be matched to the level of threat.

For the present study, the assumption is that the defence upgrades will follow the rate of sea-level rise. Given this, the findings indicate that holding the existing line of defences is not an appropriate approach for maintaining or decreasing the level of future threat. A plausible option is to follow a more proactive approach such as that seen for Portsea Island by the Coastal Partners. Although the underlying principle is to hold the existing line of defences, the SoP is being increased to a higher level, including allowance for sea-level rise. This approach is projected to have a long-lasting effect on coastal flood risk. Interestingly, the city of Portsmouth has already benefitted from an equivalent approach. It has been shown in Chapter 5 that the substantial increment in defence height seen between 1940 and 1960 had a long-running effect on risk management for the 20<sup>th</sup> century.

Increasing the standard of protection on its own makes up for over 63% and 30% of the low end of the projected SLR under RCP2.6 and RCP8.5, respectively, by 2100. By further increasing the total height of defences to account for SLR, their standard of protection would be above the 1 in 10,000-yr extreme water level of 2020. Including these safety margins could delay the need for further upgrades.

## 7.5 Conclusions

Objective three is set to determine the future evolution of coastal flood risk for the Solent, given the variability on the SPRC components. To achieve this aim, three sub-objectives are defined.

The first sub-objective is to estimate the future exposure to coastal flooding at the Solent. This reveals that the areas identified with the highest risk of coastal flooding at present will continue

to maintain the level of risk throughout the century. In particular, the areas in the vicinity of Portsmouth harbour will experience the largest risk of coastal flooding. However, the results indicate significant uncertainties for exposure to individual extreme water levels, with variabilities of more than 100% for the most extreme water levels by the year 2100.

The second sub-objective is to estimate the number of people at risk of coastal flooding for the remainder of the 21<sup>st</sup> century. The present assessment calculates mean expected annual damages of 1,900 people/year by 2040, 2,520 people/year by 2060, 3,370 people/year by 2080 and 4,580 people/year by 2100. These are equivalent to £184 million/year in 2040, £245 million/year by 2060, £327 million/year in 2080, and £445 million/year by the end of the century considering the 2020 average annual household income. The range of uncertainty in EAD is similar to that of the exposure to individual extreme water levels, with a clear increment in the variability as the estimates extend in time. It is interesting to see that, unlike for the historical assessment, the risk estimates follow a more steady rate of increment as there are no sudden changes projected for the SPRC components.

The third and last sub-objective is to quantify the uncertainty in coastal flood exposure and risk caused by climatic, socio-economic, and coastal management scenarios. The baseline assumptions are that climate change would create the largest uncertainties while population growth would be the main driver of future risk. Contradictory to the baseline assumption, population growth is not the main driver of future risk in the area. Instead, sea-level rise and its subsequent effect on the extent of the floodplain reigns as the driver of increased future risk. The analysis confirms that uncertainties in future sea-level rise cause the highest variability in coastal flood risk estimates for the Solent. Interestingly, when only the effect of sea-level rise was included in the assessment, the uncertainty in the risk estimates was larger than when all components varied. However, this is unlikely to occur and, although still dominant, the effect of sea-level rise is lessened by its interactions with population growth and defence improvement.

In this sense, population growth becomes the second driver of uncertainty in the estimates. However, the underlying assumptions are no migration from the area and that population growth occurring within the present urban extent are unlikely to occur, particularly in densely populated areas with a high level of threat, such as Portsmouth. In reality, both of these conditions are ruled by socio-economic and environmental factors, increasing their complexity and the underlying epistemic uncertainty in the assessment.

Lastly, the effectiveness of the present coastal management strategies on reducing and maintaining the levels of risk throughout the 21<sup>st</sup> century is assessed. The findings indicate that increasing the height of defences at a rate equivalent to that of sea-level rise will not be sufficient

to mitigate the effect of climate change and population growth. Instead, it is suggested that proactive management strategies could have a long-lasting effect on coastal flood risk. A clear example of this is that seen in Portsea Island by the Coastal Partners, where the standard of protection is not only improved, but the project considers a safety margin for future sea-level rise. Such an approach has proved beneficial in the Netherlands and even at the Solent, where an equivalent technique was seen between 1940 and 1960, with a positive, long-lasting effect. This could be implemented for critical areas of the Solent. However, the Solent would benefit from the adoption of an adaptive approach to coastal flood risk management. Following such a strategy would require constant monitoring of the evolution of the SPRC components (Nicholls, 2018). This would provide coastal managers with the information necessary to plan the actions necessary to maintain or decrease the future levels of coastal flood risk. This flood risk management strategy has already been adopted in the Thames Estuary, where some key indicators of risk are monitored every five years, and a full review of the protection plans is conducted every ten years (Environment Agency, 2012).

## **Chapter 8    Synthesis of the past, present and future evolution of coastal flooding at the Solent, England**

### **8.1    Introduction**

This chapter presents a synthesis of the work conducted throughout this thesis and the three objectives specifically. A synthesis of the thesis is given in section 8.2. It starts by reminding the reader of the overarching aim of this work. This is followed by explaining the selection of the Solent as a case study and the basics of the analysis. Next, the three objectives set to complete the overall aim are presented, as well as their baseline assumptions, the methodology to complete them, and their main findings. Lastly, the evolution of coastal flood risk at the Solent from the beginning of the 20<sup>th</sup> century up to the end of the 21<sup>st</sup> century is discussed. Next, a discussion of the main findings of each of the thesis objectives is given in section 8.3. The implications are discussed in section 8.4, and the limitations of the assessment are given in section 8.5. Lastly, the recommendations for future work are presented in section 8.6.

### **8.2    Synthesis**

The overall aim of this PhD thesis has been to analyse the evolution of coastal flooding in the Solent, UK, and quantify the influence each component of the SPRC conceptual framework has on past, present and future coastal flood risk levels. The south of England, and particularly the Solent, is selected as a case study region as it has a broad history of coastal flooding that has shaped the urban evolution of the area. The Solent has experienced numerous coastal flood events (Ruocco et al., 2011). Some of the most severe include the events of December 1989 (Davison et al., 1993, Stripling et al., 2008, Ruocco et al., 2011), March 2008 (Wadey et al., 2013) and the winter storms of 2013/2014 (Wadey et al., 2015b), causing widespread flooding in the region. Furthermore, the Solent is home to a variety of coastal environments, including densely populated cities, rural areas and protected sections of the coast. These factors create the opportunity to transfer the knowledge acquired to other areas of the UK and more widely worldwide. In addition to this, there is richness in data available for this region that allows for a better understanding of the coastal processes, ultimately leading to more accurate assessments of coastal flood risk. Furthermore, a number of recent studies have analysed some aspects of coastal flooding in the region (e.g. Ruocco et al., 2011, Quinn et al., 2012, Wadey et al., 2012,

Stevens et al., 2015, Ozsoy et al., 2016). The work of the present thesis is conducted using a rapid 2D inundation model of the region. The baseline characteristics of the area, such as the terrain elevation, the friction given by the types of land use, are set, and only particular characteristics of the extreme water levels and coastal structures are modified depending on the objective analysed. The results of the inundation model are coupled with different population distribution models to determine the number of people and assets exposed to extreme coastal water events.

Three main objectives were defined to achieve the aim. The first objective is to assess how coastal flood risk has evolved at the Solent over the 20<sup>th</sup> century. The baseline assumption for this objective is that population growth was the main driver of risk for this period, whilst improvement of the coastal defences regulated the level of threat. The study initiates by digitizing historical maps to determine the extent of the urban area. These are coupled with census data to determine the number and distribution of people across the Solent. Having determined the population distribution for each of the 20-year timesteps analysed, it is necessary to determine the extent of the floodplain for different extreme water levels. The input factors of the inundation model are modified to represent the increments in mean sea-level seen over the 20<sup>th</sup> century. Additionally, the presence of defences was to be modified to represent the improvements in coastal protection. Unfortunately, there is little to no information on when coastal defences were placed in the area. The study attempts to overcome this by identifying them on the historical maps. Unfortunately, the level of detail of these documents prevented it. Therefore, the study assumes that the coastal defences found in present-day datasets have been present throughout the 20<sup>th</sup> century. The only information available in this regard is the rate by which defence height was improved for the city of Portsmouth. Given the limitations above, it is assumed that all defences in the area followed the trend of improvement of Portsmouth's structures. The analysis is then conducted varying the conditions of population growth, defence improvement and historical sea-level rise.

The historical assessment confirms the baseline assumption of objective one that population growth is the leading cause of increased coastal flood risk during the 20<sup>th</sup> century. Although migration occurred from critical areas such as Portsmouth for a few decades, the overall increment in the extent of the urban area led to more people and assets under threat. The analysis also finds that the defence improvements seen prior to 1960, likely caused by the implementation of the first coastal protection act of 1949, and the learnings from the 1953 north sea flood, led to attenuating the increased flood risk rate. Even though sea-level rise contributed to enlarging the floodplain, its influence over the 20<sup>th</sup> century is minor compared to population growth. Moreover, SLR only overtakes the influence of defence improvement after 1980.

The second objective of this thesis was to determine the present level of coastal flood risk for the Solent and identifying the sources of uncertainty in these estimates. The baseline hypothesis for objective two is that uncertainties in extreme water levels are the largest sources of uncertainty in coastal flood risk estimates. In addition, it was expected to find that variabilities in the height of coastal defences control the level of threat. The analysis was conducted by incorporating the mean values and variability of each of the input factors on both the inundation and population distribution models. In the case of the inundation model, data on the height of extreme water levels and the presence of flood defences were obtained from the EA and CCO. In the case of population distribution, a high-resolution model was developed with the latest information from the 2011 England census and data on urban development by the Ordnance Survey.

The uncertainties explored as part of objective two include the selection of the length of the synthetic storm surge curve used for the analysis. The information used to assess this component was obtained from analysing the tide gauge records of the region and identifying the characteristics of the 100 largest surge events. Secondly, the analysis incorporates the uncertainties in the probabilistic estimates of extreme water levels provided by the Environment Agency. As mentioned, uncertainties in the height of defences are expected to dictate the level of threat in the area. Unfortunately, there is no data available to determine the accuracy of the information reported in national datasets. Instead, a new modelled defence height dataset was created with information derived from high-resolution DTM and DSM models. The differences between the EA data and that derived from elevation models are used to portray inaccuracies in the reported standard of protection of coastal structures. Regarding uncertainty in population distribution, there is no available data to determine the accuracy of the model developed in the present study. Instead, the study explores the differences in the risk estimates obtained with the high-resolution population model against those obtained when data from the global population model WorldPop is used. In general, two approaches are followed to assess the uncertainty in the risk estimates. The first one involves scenarios that dictate the behaviour of the input components. The second one makes use of a variance-based approach to determine the sensitivity of the results to the input parameters.

The results of objective two reveal that for the year 2020, an average of 1,488 people/year are expected to be affected by coastal flooding in the Solent region, with a variance of  $\pm 460$  people/year (5% and 95% confidence). These numbers indicate a decrease in the level of risk from the year 2000 to 2020, likely caused by the improvement of defences in Portsea Island. Analysing the uncertainty in the estimates reveals that the uncertainties in extreme water level height create the most significant variance on the risk estimates, confirming the initial hypothesis. This is confirmed with the variance-based approach. Lastly, comparing the results obtained with the

high-resolution population model to those estimates with WorldPop data show considerable differences for small floodplains (i.e. those obtained with low return periods). However, these differences decrease as the magnitude of the extreme water levels increases. For some of the largest return periods, the results obtained with WorldPop doubled the values found with the high-resolution model.

The third and last objective was to determine how coastal flood risk might evolve over the remainder of the 21<sup>st</sup> century considering climatic and socio-economic stressors. The initial hypothesis for objective three was that population growth would be the primary driver of coastal flood risk. At the same time, uncertainties in future sea-level rise will create the largest uncertainties for the risk estimates. The inputs for the inundation model are modified to represent the plausible futures. First, the height of the extreme water levels is modified based on three sea-level rise scenarios. Two baseline scenarios explore the future of coastal defences. The first one where no active intervention occurs representing a do-nothing scenario. The second one accounts for the current coastal management strategies. For the latter, the rates of SLR are used to increase the height of coastal defences. In the case of population, three population growth scenarios were used. These cover low, medium and high population growth projections. The assessment assumes that development will occur within the existing urban footprint, and no migration from the area will occur. This means that every area of the Solent will maintain its present share of the country's population throughout the 21<sup>st</sup> century.

The assessment found an average of 1,900 people/year at risk of coastal flooding in 2040, 2,530 people/year by 2060, 3,370 people/year by 2080 and 4,580 people/year by 2100. The uncertainties that accompany these estimates are seen to increase the further in time the projections are made. For the year 2040, there is a 7.91% uncertainty on the estimates. This increases to 25% by 2060, 58% by 2080, and reaches a maximum of 104% by 2100. Analysing the influence of the inputs, it is found that uncertainties in sea-level rise create the largest uncertainties for the risk estimates. Furthermore, sea-level rise is identified as the primary driver of increments in risk for the 21<sup>st</sup> century. Although the analysis does not identify population growth as the main cause for increments in exposure, it is highlighted that changes in the population do play a significant role in the future levels of threat. Based on the assumptions made from the present coastal management strategies, it is found that these are not effective to control or reduce the level of threat posed by climate change and population growth. Finally, as seen in the historical assessment of objective one, the city of Portsmouth, along with urban areas in its vicinity, are the main contributors to the Solent's EAD. Portsmouth is found to contribute almost 20% of the total EAD.



Altogether, it can be seen that the Solent has experienced a relatively constant increment in the level of coastal flood risk. Its past growth can be attributed to socio-economic factors, particularly population growth and development at the floodplain. Looking at the future and given the assumptions made in the assessment, it is expected that the level of threat will rapidly increase (Figure 8.1). The current coastal management strategies are found to be insufficient to overcome the effect of climate and population change, with the former projected to be the main driver of coastal flood risk at the Solent.

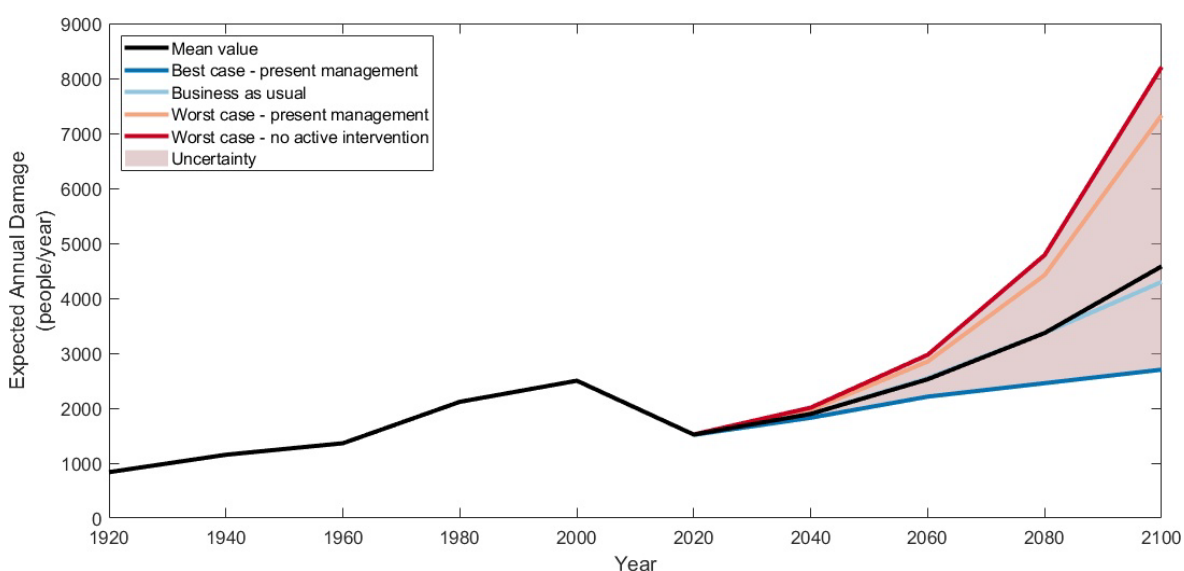


Figure 8.1 Evolution of coastal flood risk at the Solent, UK, over the 20<sup>th</sup> and 21<sup>st</sup> century as estimated in the present study.

### 8.3 Discussion

This thesis has analysed the evolution of coastal flood risk across the Solent, UK. Firstly, a historical assessment was conducted to determine the factors that drove risk in the 20<sup>th</sup> century. This was to identify key relationships or patterns that can be used in other areas with similarities to Solent. In general, it is found that population growth was the main driver of coastal flood risk for the area in the 20<sup>th</sup> century. Before now, there has been little to no research conducted analysing the past evolution of coastal flooding. The few research available also find population growth, or socio-economic factors, to be the drivers of risk during the 20<sup>th</sup> century for the Netherlands (VanKoningsveld et al., 2008) and a smaller region of the Solent previously assessed (Stevens et al., 2015)

Even though population growth increased the consequences of flooding, this was not always the case for every area within the region. The data suggest that migration from Portsmouth after 1930 led to a decrease in the level of risk. Further to this, it is found that after the first half of the

century, defence improvement had a long-lasting effect on risk. It is not clear why such improvement occurred, but it can be attributed to three main factors. The first one is that the increments in population led to a demand for protection from coastal threats, although this seems unlikely. Secondly, it is possible that some of the structures that act now as flood protection were built for other purposes during the second world war. Thirdly and as mentioned in Chapter 4, the introduction of the first coastal protection act in 1949 and the lessons learned from the 1953 North Sea flood could have led to an increased awareness of the threat posed by coastal flooding. It can be seen that, although it increases the height of the extreme water levels, the rate of sea-level rise for the 20<sup>th</sup> century was not a triggering factor for coastal flood risk.

It is interesting to analyse the interaction between the aforementioned factors. It can be assumed that the government and general population were aware of the threat posed by extreme coastal water levels. Unfortunately, it appears that up until recent years, there were no regulations or spatial planning that limited development at the floodplain, which led to the present urban footprint. Instead, it could be suggested that the flood risk management strategies were based on the implementation of defences. These findings can serve as guidance for areas that are yet to experience the level of urbanisation seen at the Solent. Instead of permitting indiscriminate development at the coastal zone, governments and ruling bodies should establish the areas prone to flooding and discourage or prevent urban development.

Secondly, a present-day assessment of risk was conducted to determine the level of threat, the uncertainty in coastal flood risk estimates and the largest sources of uncertainty. This aims to shed light on the drivers of uncertainty so that assets can be focused and efforts can be made to narrow any knowledge gaps. The results indicate an average of 8,300 people exposed to a 1 in 200-year event (with a zero-depth threshold). This number is 25% smaller than the estimates by Wadey et al. (2012) for the same conditions. Interestingly, this difference is incremented when a flood depth threshold of 1m is introduced. Wadey et al. (2012) find the equivalent of 504 people exposed to a 1 in 200-year extreme sea level, whilst the present thesis obtains 2,621 people under threat for the same condition. These differences can be attributed to the baseline assumptions and data used for the assessment. Firstly, Wadey et al. (2012) estimate the volume of water that would enter the floodplain through overflow, overtopping and breaching, and inputs this as a constant volume flowing inside the floodplain. As explained in section 3.4, this is likely to result in more extensive floodplains as there is no consideration of the effect that the water level on the landwards face of the defences will have on the discharge above the structure (drowned weir effect). This explains why Wadey et al. (2012) results for a no depth threshold are larger than the estimates of this thesis.

Secondly, Wadey et al. (2012) does not consider the presence of inland flood defences offering protection from rivers. Even though these structures do not prevent water from entering the floodplain, they can affect and limit the spread of water within the floodplain by creating basins. Incorporating such defences can lead to a smaller and deeper floodplain, leading to the larger estimate of exposure found in the present assessment when a minimum depth of 1m is selected.

The analysis suggests that uncertainties in extreme water level height generate the largest variabilities in present-day risk estimates. As mentioned in the literature review, extensive research is being conducted analysing this component. These range from studies doing data archaeology to extend tide gauge records to those looking at more advanced methods to calculate the EWL heights (e.g. Muis et al., 2016, Muis et al., 2017, Wahl et al., 2017, MacPherson et al., 2019). Both groups of assessments should ultimately lead to more accurate estimates. However, the preliminary assessment for objective two revealed substantial gaps in the EA coastal defence dataset. This highlights that, at present, incomplete information on coastal defence presence can lead to inaccurate risk estimates. Unfortunately, these gaps could have easily been overlooked as the EA dataset is meant to be a complete source of information. As mentioned, one of the benefits of using the Solent as a case study is the richness of data for this region, which allowed to complement the EA data with information from additional sources. Wing et al. (2019) developed a model to identify the presence and height of defences from elevation data which could be used for such purpose. Government and coastal management bodies must conduct reviews and systematically update the information on the presence, condition and standard of protection of these structures. This would lead to better asset management and more accurate assessments of the level of threat.

In terms of population distribution, the results obtained with the low-resolution model are seen to overestimate the number of people exposed to coastal flooding. This is expected as these population distributions are built using indirect information, such as land cover and cell phone data (Tatem, 2017). The comparison with the high-resolution dataset indicated that these differences are particularly relevant for high probability extreme water levels and decrease as the return period increases. Smith et al. (2019) produced a similar assessment for developing regions, finding the results obtained using WorldPop and the LandScan dataset to be up to 64% larger than those estimates with a high-resolution model.

Lastly, the future level of coastal flood risk for the Solent was projected. This aimed to understand the plausible range of futures and identify the decisions that could shape the evolution of risk for the area. Given the assumptions made, the results suggest that climate change will be the main driver of increased coastal flood risk throughout the 21<sup>st</sup> century. Global and regional assessments

concur with this finding (e.g. Muis et al., 2015, Muis et al., 2017, Rohmer et al., 2021, Taherkhani et al., 2020, Lincke et al., In preparation, 2021). This is a worrying warning for the future, as even under the most conservative climate change scenarios, global mean sea level is expected to increase. Accepting the reality of this can help to focus on the remaining drivers of risk. It is found that population growth is the second most crucial trigger for increased risk. Two main assumptions are made in terms of population growth at the Solent. Firstly, that migration from the area will not occur. There are various climatic and socio-economic factors that will determine the veracity of this assumption, which fall beyond the scope of the present work. Furthermore, it is not well understood how the population will react to increasing coastal threats, and any assumptions are almost as valid as the no migration scenario. Secondly, the analysis considers that the present-day urban extent will be maintained in the future. This is also unlikely as growing populations demand new housing, amenities and workplaces, which could lead to new development occurring both outside and within the floodplain. As mentioned, development at the floodplain is discouraged but not forbidden by the government, providing protection measures are placed. If development occurs within the floodplain, it would be necessary to determine the minimum standard of protection required for individual properties. Including such information in risk assessments would require splitting the consequences into direct and indirect, as the protected properties would only experience the latter for extreme sea levels below their standard of protection.

Further to the above, one of the assessment's key findings is that the current management strategies are unlikely to be sufficient in maintaining or decreasing the threat level for the future. This, based on the assumption that the standard of protection is to be increased following the rate of sea-level rise. It is suggested that following a more proactive approach where the current standard of protection is increased, including an allowance for the highest future sea-level rise, could be an appropriate measure to mitigate the effect of climate and socio-economic stressors. Such an approach has been suggested by previous authors as suitable for England (e.g. de la Vega-Leinert and Nicholls, 2008). The benefits of such flood risk management strategies are particularly visible in the Netherlands, where most flood defences have a standard of protection at or above the 1 in 1,000-year event extreme water level (Kabat et al., 2009, Jonkman et al., 2018).

The framework developed has been applied to the Solent. However, the approach was designed to be applied on a similar or larger scale anywhere. All the data and information used in this thesis are publicly available. Even if some of the data is not available on a local scale or high-resolution, the effect of using a modelled information and global datasets has been presented in Chapter 6.

It is suggested that the methods described in this thesis should be first used in other areas of the UK. Particular attention should be given to guaranteeing that the presence of coastal defences is well documented and incorporated into the assessment. This could help highlight and quantify the epistemic uncertainties in the EA flood dataset. By applying the approach presented in this thesis, future assessments could look at the influence of each input factor on the evolution of coastal flood risk in the UK. If this method is applied to other areas, and considering the findings and implications of this thesis, it is expected to find population growth to be the initial driver of CFR. However, once there is an established presence of people and assets, it will be the combination of natural stressors and flood management strategies dictating the level of risk. Conducting a similar assessment in other regions could indicate if the findings of the present study and assumptions drawn from their analysis are unique to the study site or show spatial and temporal patterns. Furthermore, coastal managers could look at the findings of objective one and apply the learnings to areas where the evolution of the SPRC components might follow a similar pattern to those seen at the Solent.

## 8.4 Implications

Based on the findings of this thesis, the following five recommendations are made for the Solent:

1. **Development of spatial planning aimed at steering development away from the floodplain.** Unfortunately, the present-day directives highly discourage development in these areas but do not forbid it. The presence of assets will set the foundations for future risk in these areas, even if this is not evident at present, as it happened during the 20<sup>th</sup> century at the Solent.
2. **The Solent should move towards a proactive approach for coastal flood risk management.** A feasible strategy could identify the areas with the highest level of threat, providing them with enhanced protection that includes an allowance for climate change.
3. **If protecting the areas at risk is not a feasible option, the government could promote migration from areas with high levels of risk.** Abandonment of areas continuously subject to flooding could be a suitable solution to flood risk management. However, the population is unlikely to accept these changes, even when the risk is evident.
4. **In some cases where increasing populations are met with a scarcity of land area, an “attack” management approach could be implemented.** This method consists of claiming land by advancing it seawards and building upwards to accommodate for future sea-level rise (Nicholls, 2018). This has been proposed as a suitable solution for Portsmouth (ICE, 2010). However, it would be necessary to consider such strategies' implications on the SAC's and SPA's surrounding Portsea Island.

5. **The local population could become part of the risk management solutions.** This could be done through partnership funding, where the principle is to share the costs of protection measures between government and local authorities/residents. Furthermore, local populations should be encouraged to insure their property and assets to spread the potential financial costs of flooding with the government (van der Plank et al., 2021).
6. **Adopt an adaptive approach to coastal flood risk management.** Such a framework is an effective tool to deal with the uncertainty in the future evolution of the SPRC components (Nicholls, 2018). The adaptive approach is based on monitoring the behaviour of the drivers of risk to identify the measures necessary to maintain or reduce the level of risk. A good example of this management strategy is the Thames Estuary plan, where monitoring of its key risk indicators is conducted every five years, and a full review of the protection plans is done every ten years (Environment Agency, 2012).

These suggestions are kept broad and straightforward to cover the main focus points of coastal flood risk management for the Solent. A more in-depth assessment at a city level could help determine which of the strategies above is the most appropriate approach for each area.

## 8.5 Limitations

The present assessment has benefitted from the use of the most up to date information and methods. However, modelling and representing the interactions between nature and people require generalizations and simplifications that limit the accuracy of the analysis. Below, key limitations are briefly discussed.

Firstly, conducting a coastal flood risk assessment required simplifications, such as the selection of a 50m resolution. This resolution is selected as it provides a middle ground between accuracy and the computational expense of processing the inundation model. However, this could cause problems, particularly in densely populated areas where slight variations in the extent of the floodplain could lead to under/overestimates of risk. In the same sense, using a digital terrain model where all artificial structures are removed is likely to create more extensive flood plains. The use of an inundation model that allows for an adaptive mesh would be a valuable tool for the Solent, as areas such as Portsmouth could be modelled in more detail. In contrast, less exposed and less populated areas could maintain a coarse resolution.

Secondly, there is a lack of uniformity and availability of information. For instance, the historical analysis highlighted the changes in the census resolution. This is noticeable looking at the change in risk from 1980 to 2000. During this period, the population of the Solent increased, and no substantial defence improvement nor changes in the extent of the urban footprint occurred.

However, decrements in the level of risk can be seen for some areas, which can only be attributed to changes in the resolution of population data. This is a good example of the influence of population distribution in coastal flood risk, particularly for low-elevation-densely populated areas. Although high-resolution population distribution and its implications on privacy is a sensitive topic in the UK, the data on a postcode level could be made available for research purposes, which would lead to more accurate estimates of risk.

One of the benefits of selecting the Solent as a case study is the richness in the information available for the area, which proved crucial for coastal defences. As mentioned, the Environment Agency provides information on the characteristics of the defences in the area. Critical gaps were identified and filled with information from other sources. However, it might not be possible to identify and fill these gaps for other areas. In addition to this, there is uncertainty on the accuracy of the information of the defences included in the dataset. Most of the time, the EA staff visually assess the condition and standard of protection of these structures. Even though guidance on assessing the defences is available, the outcome is up to the judgement of the person conducting the inspection. Both of these limitations could be overcome with site visits and technical assessments of the coastal structure.

One of the strengths of the present assessment is that coastal, river and pluvial flood defences are included in a coastal flood risk assessment at the Solent for the first time. However, the latter are assumed to remain unmodified for the remainder of the 21<sup>st</sup> century. In reality, climate change has the potential to modify environmental conditions, and these structures will likely require modifications and improvements.

## 8.6 Recommendations for future research

Strengths and limitations have been found during the development of this thesis. The following paragraphs give suggestions for future research based on the findings of each objective.

### Based on objective one, the historical assessment of risk

As mentioned, one of the central constrictions for the historical assessment is the lack of information on coastal defences and when these were built. Further research should be conducted aimed at identifying when these were placed. In addition, data archaeology could give a better perspective of if and when these have been upgraded. This knowledge would be crucial for a more thorough evaluation and could help understand the interaction between urban development and coastal protection.

### Based on objective two, the assessment of present-day risk

One of the critical limitations of the analysis is the exclusion of wave action. Future research should consider this component, which is likely to increase the estimates of risk. However, it would be necessary to couple the inundation model with a morphodynamic assessment of the foreshore. By doing so, it would be possible to determine the conditions faced by waves and how these might vary depending on the magnitude of the storms.

The sensitivity assessment finds that risk estimates are highly sensitive to information on coastal defences. Further to this, the preliminary assessment finds the primary source of uncertainty is the lack of information on coastal defences. The same is found to be applicable in almost all published work on coastal flooding (Lincke et al., In preparation, 2021). Further research aimed at developing tools for automated detection of flood defences, such as Wing et al. (2019), could benefit future assessments. As mentioned, it is difficult to perform detailed assessments of coastal defences on large scale projects such as that of this thesis. In general, key attributes such as the location and height of the defences are the minimum required to consider the presence of defences in the study site. Ideally, this would be accompanied by information on the type of defence (e.g. sea-wall), standard of protection and residual life.

In addition to this, further research on coastal flooding on a regional scale could benefit from using an adaptive mesh for increased accuracy in areas identified with high risk. The results obtained from this exercise can be compared to those used with a square grid model to understand the bias caused by low/high-resolution analysis.

### *Based on objective three, the analysis of future coastal flood risk*

Research on the feedback mechanisms between climatic stressors and migration is required. Most of the research available bases their analysis on the assumption that no migration from exposed areas will occur. Unfortunately, the effect of climate change on coastal populations has only started to be seen in recent decades, leading to a lack of subjects for analysis. It is imperative to generate a more in-depth understanding of the effect of climate change on coastal communities.

Dealing with the uncertainty in each SPRC component will require adaptive approaches to coastal flood risk management. Future research should be conducted to determine the feasibility of such an approach at the Solent and the requirements for its application in the area. Furthermore, research should look at the feasibility and effectiveness of implementing natural or “soft” engineering approaches to managing flood risk. These have gained popularity in recent years due to their ability to adapt to evolving coastal threats.

The methodology presented in this thesis is applicable to wider areas and different timescales. In general, there are three minimum datasets required to apply this method. The resolution and



additional data needs depend on the characteristics of the assessment. The three basic datasets required are, in order of importance:

1. A digital elevation model. Depending on data availability, this could be a simple elevation model derived from satellite data such as SRTM, or high-resolution models obtained with LIDAR. It is important to consider that although higher resolution models have the potential of providing more accurate results, their use can be computationally expensive. Furthermore, FRA are subject to the quality and accuracy of the rest of the input parameters. For instance, there is no use for a high-resolution model when there is limited data on defence presence or accurate estimates of EWL.
2. Extreme water level data. These could be as simple as an arbitrary water level or derived from tide gauge analysis as done by the EA. More refined assessments would usually require a water curve that presents the variance of EWL with time.
3. Information on the receptors of risk. The term receptors, as explained in section 2.3.3, can range from the area of land subject to flooding to the number of people and assets at risk. The need for this component lies in the metric used for the assessment.



## Chapter 9 Conclusions

The overall aim of this thesis has been to determine the past, present-day and future evolution of coastal flooding at the Solent, UK, as well as to understand the drivers of coastal flood risk. This region has a long history of flood events, and coastal flooding continues to pose a significant threat for the area. The work centred on three research objectives. A synthesis of the work conducted for each objective, their main findings and the implications are presented in Chapter 8. The following paragraphs present the key conclusions drawn from their analysis.

Objective 1 was to assess how coastal flood risk evolved at the Solent, UK, over the period of 1920 to 2000. This objective sought to answer the question: *What were the main driving factors of coastal flood risk at the Solent from 1920 to 2000?*. This is the first publicly available assessment of the regional evolution of coastal flood risk from 1920 to 2000, analysing human and nature interactions and their role in the level of threat. The analysis finds that population growth was the dominant driver of risk for this period. The presence of people and assets in areas under threat set the basis for the present-day and future risk as almost no abandonment of areas prone to flooding has occurred. As research tends to focus on climatic stressors, the learnings of this objective show that it should be a priority to establish exclusion zones for development in areas that might follow a similar trend of urbanisation as the Solent.

Objective 2 was to quantify the largest sources of uncertainty in coastal flood risk at present. This aimed to answer the research question: *Which SPRC components generate the largest variability and uncertainty for present flood risk analysis?*. The study highlights the variability in extreme water level height as the largest source of uncertainty. However, the underlying lack of data on defence presence is critical for coastal flood risk assessments. Even though research to improve the accuracy of the probabilistic extreme water levels is encouraged, the focus should be given to improving the quantity and quality of data available on coastal flood defences. Promising works are being conducted to collect information on global defence presence and on identifying the presence of these structures with elevation data. It would be beneficial for the community of coastal managers to contribute information to produce more accurate regional, national and global assessments.

Objective 3 was to determine how flood risk may evolve over the remainder of the 21<sup>st</sup> century with future sea-level rise and population growth, considering future coastal management strategies. This objective sought to answer the research question: *What will be the primary driver of coastal flood risk, and what generates the most significant uncertainties in the next 80 years for the Solent?*. The analysis indicates that the present-day level of risk is very likely to increase

throughout the 21<sup>st</sup> century. Given the input parameters, it is found that mean sea-level rise will be the primary driver of this risk. Furthermore, the results indicate that the current coastal management strategies will not be sufficient to mitigate the effect of climate change and socio-economic factors on the level of threat. Some critical areas could benefit from a more proactive approach where critical flood defences are identified and their standard of protection heightened, including an allowance for the highest projected sea-level rise. This technique has proved beneficial in the Netherlands and even at the Solent, where an equivalent technique was seen between 1940 and 1960, with a positive, long-lasting effect. However, the Solent would benefit from the adoption of an adaptive approach to coastal flood risk management, where the evolution of the SPRC components is constantly monitored to determine the actions necessary to maintain or reduce the level of risk.

Altogether, for the first time, this single study has explored the past, present and future interactions between the components of coastal flood risk and their influence on the level of threat posed for the Solent. This research provides a look at the interaction between natural and human stressors and their role in the level of threat. The work has been conducted with the development of a novel approach to analyse the evolution of coastal flood risk at a regional level. A combination of probabilistic and non-probabilistic approaches have been employed to quantify the uncertainty in the present-day and future estimates of coastal flood risk caused by epistemic and aleatory uncertainties. The insights found with these assessments have helped to understand the factors and decisions that led to the present levels of risk. Furthermore, it has given an indication of what the future might hold for other areas of the UK and the world that might follow a similar track of development as that seen for the Solent. Overall, the findings of this thesis can inform today's coastal management strategies in the UK and more widely.

## Appendix A Accuracy of the hydrodynamic model

This appendix assesses the accuracy of the hydrodynamic model used in this thesis. This is done by examining the model's ability to replicate the flood event of March 10, 2008. This event is selected as there is a richness of data on the locations impacted by flooding.

### A.1 Coastal flood event March 10, 2008

On March 9, 2008, a low depression travelling across the north Atlantic from southeast Greenland travelled over Ireland and across the Midlands into the North Sea (Wadey et al., 2013). On the following day, the storm's passage and subsequent surge coincided with a high tide, causing a maximum still water level of 2.77m in Portsmouth (Wadey et al., 2013), equivalent to a 1 in 7.5-year EWL (Table 6.2). The maximum EWL occurred around midday March 10, 2008, with flood warnings allowing local residents to abandon the threatened areas. Wadey (2013) provides a synthesis of the locations at the Solent where flooding occurred on March 10, 2008. The data was gathered from reports by the EA and local news outlets. Table 9.1 shows the roads and areas flooded during this event. It can be seen that widespread flooding occurred, although it has been highlighted that most of the affected areas experience nuisance flooding, except for the caravan park at Selsey, where severe flooding occurred with thirty people needing rescuing (BBC, 2008).

Table 9.1 Summary of flood locations and failure mechanisms on 10 March 2008. Data from Wadey (2013)

Number	Area	Sites recorded as flooded	Defence failure mechanism
1	Lymington	Quay street	Overflow
2	Beaulieu	Palace Lane	
3	Lepe	Lepe Road	Overtopping
4	Calshot	Clashot Road	Overflow
5	Hythe	Shore Road & Sailing club	
6		The Promenade and Prospect Place	
7		Cracknore Hard	
8		Magazine Lane	

Number	Area	Sites recorded as flooded	Defence failure mechanism
9	Totton	Downs Park Crescent and Downs Park Road	Overflow and non-coastal flooding
10		Commercial Road	
11		Itchen: Saltmead	
12	Southampton East	St Denys: Priory Road	
13		Woodmill Lane and Oliver Road	
14	Weston	Weston Parade	Overtopping
15	Warsha and Hamble	Passage Lande and Shore Road	Overflow
16	Wallington	Wallington Shore Road and Delme Drive	Overflow and non-coastal flooding
17	Hamble	Rope Walk, Well Lane and Green Lane	
18		Blundell Lane	
19	Old Portsmouth	East Street & Broad Street, Ferry terminal and Camber Quay	Overflow/Overtopping
20	West Portsea	The Hard	
21	Southsea	Clarance Esplanade and "rock gardens"	Overtopping
22	Hayling Island	Southwood Road, Creek Road, Nutbourne Road and Bosmere Road	
23	Havant	High Street	
24	Emsworth	Bridge Road, Bath Road and Mill Pond	Overflow
25		A256, Queen Street and Lumley Road	

<b>Number</b>	<b>Area</b>	<b>Sites recorded as flooded</b>	<b>Defence failure mechanism</b>
26	Bosham	Shore Road, Bosham Lane, Stumps Lane, The Drive, High street and Harbour Road	
27	Selsey	West Sands Caravan Park	Overtopping/Breaching
28	Newport	Medina Way, Sea Street and the Quay	Overflow/non-coastal flooding
29	East Cowes	Esplanade	
30	West Cowes	Brunswick Street, Medina Road, Bridge Road, Fountain & Town Quays, High Street, Red Funnel Ferry terminal	Overflow/Overtopping
31		Egypt and Prince's Esplanade	
32		Marine Parade	
33		Marsh Road and Rew street	
34	Yarmouth	Bridge Road, Quay street, The quat and River Road	Overflow
35	Eastern Yar	Yaverland Road	Overtopping
36		Freshwater Bay	

## A.2 Hydrodynamic simulation setup

The hydrodynamic model presented in Chapter 4 is used to model a flood with the characteristics of that of March 10, 2008. The input parameters such as the location of the boundary conditions and hydraulic roughness map presented in sections 4.2.1 and 4.2.2, respectively, are used for this simulation. The only aspect modified is the height of the extreme water level, which is set to 2.77m at Portsmouth. As mentioned in section 4.2.1, the mean surge curve obtained with the analysis of tide gauge data is added to the MHWS curve. The surge curve is adjusted so that the added height matches the height of the EWL (Figure 9.1). It should be noticed that the EWL distribution shown in Figure 6.2 is maintained for this simulation. The present-day flood defences are used for the simulation. However, the height of the defences in Portsmouth is modified as the works to improve their standard of protection started in 2015 (Coastal Partners, n.d.).

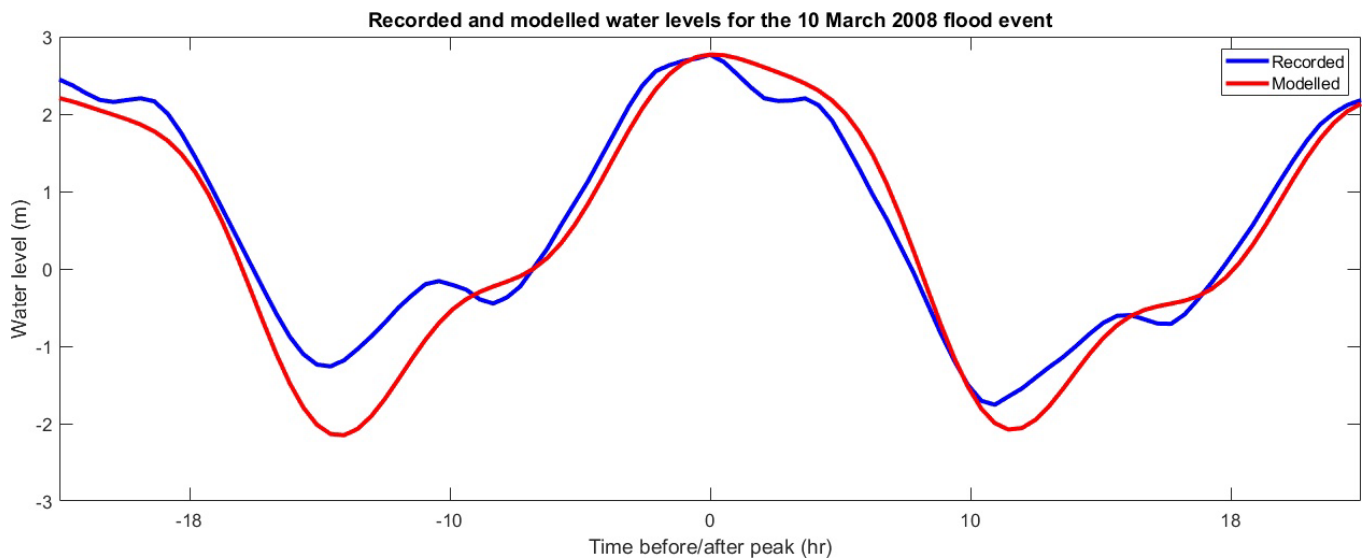


Figure 9.1 Recorded and modelled water curve for the 10 March 2008 flood event



### **A.3 Results of the hydrodynamic simulation of the 10 March 2008 flood event**

Figure 9.2 shows the outline obtained when modelling the March 10, 2008 flood event. It is not possible to gauge the accuracy of the model to replicate the extent of the flood as there is not enough accurate information on all the locations where flooding occurred, nor the depth and extent of areas affected. Instead, the locations presented in Table 9.1 are used to assess the accuracy of the modelled flood outline. In total, 74% of the locations where flooding was registered were identified as flooded using the model output. Furthermore, 85% of the locations where the reported defence failure mechanisms included overflow are located within the modelled flood extent. This is relevant as this thesis only considers overflow for the assessment.

Furthermore, the water curve resulting from adding the mean storm surge curve obtained to the MHWS curve appears to capture the behaviour of the water curve registered on 10 March 2008. Overall, the model appears to yield sensible flood outlines, where only the areas with a low elevation and those with a history of coastal flooding are within the modelled flood extent. As mentioned, some of the locations in Table 9.1 are not within the modelled floodplain. This is likely caused by not including waves in the assessment. Furthermore, the event of March 10, 2008, was accompanied by “gales and blustery showers” (BBC, 2008), which likely enhanced the magnitude of the flood. A similar validation of a hydrodynamic model for the Solent was conducted by Wadey (2013), who mentions that the effect of rainfall was incorporated by adding 0.1m to the boundary water levels. This 0.1m was determined by Wadey (2013) through “trial and error”.

Considering the above, the hydrodynamic model presented in Chapter 4 and used throughout this thesis is regarded as accurate in the representation of plausible coastal flood extents.

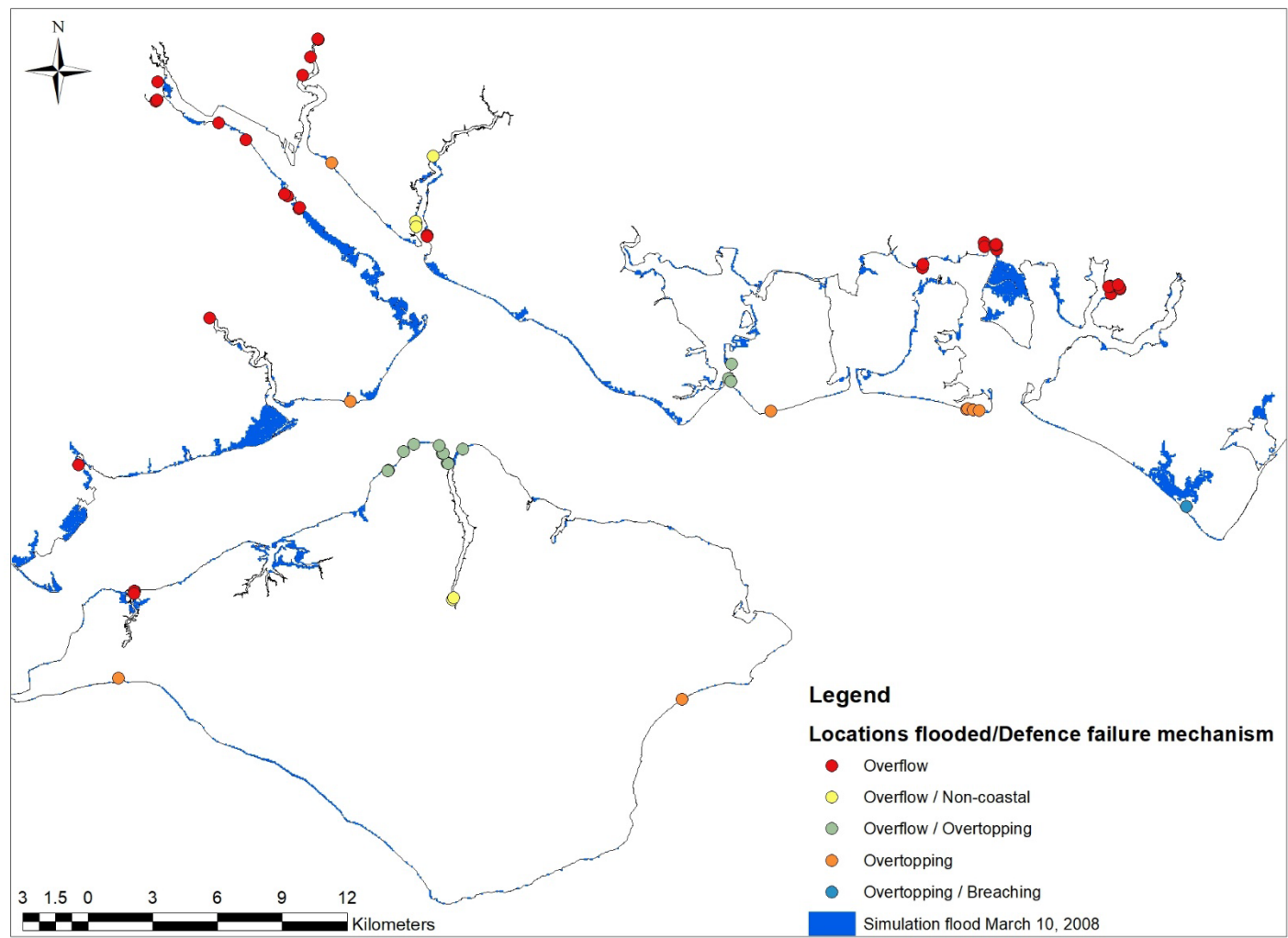


Figure 9.2 Modelled flood outline of the March 10, 2008 event, and the locations reported as flooded by Wadey (2013).

## List of References

- ABPMER. n.d. *OMREG - Medmerry* [Online]. Available: <https://www.omreg.net/query-database/103-medmerry/> [Accessed].
- ABRAMSON, D. M. & REDLENER, I. 2012. Hurricane sandy: lessons learned, again. *Disaster Med Public Health Prep*, 6, 328-9.
- ANDERSEN, T. L. & BURCHARTH, H. F. 2004. Crest Level Assessment of Coastal Structures by Full-Scale Monitoring, Neural Network Prediction and Hazard Analysis On Permissible Wave Overtopping - CLASH.
- ANDERSON, J. R. 1976. *A land use and land cover classification system for use with remote sensor data*, US Government Printing Office.
- APEL, H., THIEKEN, A. H., MERZ, B. & BLOSCHL, G. 2004. Flood risk assessment and associated uncertainty. *Natural Hazards and Earth System Sciences*, 295-308.
- ARMSTRONG, S. B., LAZARUS, E. D., LIMBER, P. W., GOLDSTEIN, E. B., THORPE, C. & BALLINGER, R. C. 2016. Indications of a positive feedback between coastal development and beach nourishment. *Earth's Future*, 4, 626-635.
- ARNS, A., WAHL, T., HAIGH, I. D., JENSEN, J. & PATTIARATCHI, C. 2013. Estimating extreme water level probabilities: A comparison of the direct methods and recommendations for best practise. *Coastal Engineering*, 81, 51-66.
- ASSOCIATED BRITISH PORTS. 2021. *Port information* [Online]. Available: [https://www.southamptonvts.co.uk/Port\\_Information/](https://www.southamptonvts.co.uk/Port_Information/) [Accessed].
- AVEN, T., BARALDI, P., FLAGE, R. & ZIO, E. 2013. *Uncertainty in risk assessment: the representation and treatment of uncertainties by probabilistic and non-probabilistic methods*, John Wiley & Sons.
- BATES, P. D., DAWSON, R. J., HALL, J. W., HORRITT, M. S., NICHOLLS, R. J., WICKS, J. & MOHAMED AHMED ALI MOHAMED, H. 2005. Simplified two-dimensional numerical modelling of coastal flooding and example applications. *Coastal Engineering*, 52, 793-810.
- BATES, P. D., HORRITT, M. S. & FEWTRELL, T. J. 2010. A simple inertial formulation of the shallow water equations for efficient two-dimensional flood inundation modelling. *Journal of Hydrology*, 387, 33-45.
- BATSTONE, C., LAWLESS, M., TAWN, J., HORSBURGH, K., BLACKMAN, D., MCMILLAN, A., WORTH, D., LAEGER, S. & HUNT, T. 2013. A UK best-practice approach for extreme sea-level analysis along complex topographic coastlines. *Ocean Engineering*, 71, 28-39.
- BATTJES, J. 1988. Surf-zone dynamics. *Annual Review of Fluid Mechanics*, 20, 257-291.
- BAXTER, P. J. 2005. The east coast Big Flood, 31 January-1 February 1953: a summary of the human disaster. *Philos Trans A Math Phys Eng Sci*, 363, 1293-312.
- BBC. 2008. Evacuations as waves flood park. *BBC NEWS*, 10 March 2008.
- BENN, J., KITCHEN, A., KIRBY, A., FOSBEARY, C., FAULKNER, D., LATHAM, D. & HEMSWORTH, M. 2019. *Culvert, screen and outfall manual*, CIRICA.

## List of References

- BESLEY, P. 1998. Wave overtopping of seawalls, design and assessment manual. *R&D technical report W178*.
- BOZA, X. 2018. *The Reconstruction and Analysis of Historical Coastal Flood Events from 1800's in the Solent, UK*. Masters MSc Dissertation, University of Southampton.
- BRANDER, L. M., FLORAX, R. J. G. M. & VERMAAT, J. E. 2006. The Empirics of Wetland Valuation: A Comprehensive Summary and a Meta-Analysis of the Literature. *Environmental & Resource Economics*, 33, 223-250.
- BROWN, C., CHATTERTON, J. & PURCELL, A. 2014. Asset performance tools - asset inspection guidance.pdf>. In: AGENCY, E. (ed.).
- BRUNNER, G. W. 2010. HEC-RAS river analysis system user's manual version 4.1. Davis CA.
- BUIJS, F., SIMM, J., WALLIS, M. & SAYERS, P. 2007. Performance and reliability of flood and coastal defences. *Environment Agency, London*.
- BUIJS, F. A., HALL, J. W., SAYERS, P. B. & VAN GELDER, P. H. A. J. M. 2009. Time-dependent reliability analysis of flood defences. *Reliability Engineering & System Safety*, 94, 1942-1953.
- BUREAU, R. 1971. Convention on Wetlands of International Importance. Gland, Switzerland.
- BURGESS, K., JAY, H. & NICHOLLS, R. J. 2007. 16 Drivers of coastal erosion. *Future Flooding and Coastal Erosion Risks*, 267.
- BURHENNE, S., JACOB, D. & HENZE, G. P. Sampling based on Sobol' sequences for Monte Carlo techniques applied to building simulations. *Proc. Int. Conf. Build. Simulat*, 2011. 1816-1823.
- CABINET OFFICE 2015. National Risk Register of Civil Emergencies.
- CABINET OFFICE 2020. National Risk Register 2020 edition.
- CAFLISCH, R. E. 2008. Monte Carlo and quasi-Monte Carlo methods. *Acta Numerica*, 7, 1-49.
- CASCIATI, F. & FARAVELLI, L. 1991. *Fragility analysis of complex structural systems*, Research Studies Press.
- CCO. 2014. *Regional Coastal Monitoring Programmes: Cell 5 Defences 2014* [Online]. Channel Coastal Observatory. Available: <https://www.coastalmonitoring.org/ccoresources/shapefiles/> [Accessed].
- CHARLIER, R. H., CHAINEUX, M. C. P. & MORCOS, S. 2005. Panorama of the history of coastal protection. *Journal of Coastal Research*, 21, 79-111.
- CHRISTIE, E. K., SPENCER, T., OWEN, D., MCIVOR, A. L., MÖLLER, I. & VIAVATTENE, C. 2018. Regional coastal flood risk assessment for a tidally dominant, natural coastal setting: North Norfolk, southern North Sea. *Coastal Engineering*, 134, 177-190.
- CHURCH, J. A., CLARK, P. U., CAZENAVE, A., GREGORY, J. M., JEVREJEVA, S., LEVERMANN, A., MERRIFIELD, M. A., MILNE, G. A., NEREM, R. S., NUNN, P. D., PAYNE, A. J., PFEFFER, W. T., STAMMER, D. & UNNIKRISHNAN, A. S. 2013. Sea Level Change. In: STOCKER, T. F., QIN, D., PLATTNER, G.-K., TIGNOR, M., ALLEN, S. K., BOSCHUNG, J., NAUELS, A., XIA, Y., BEX, V. & MIDGLEY, P. M. (eds.) *Climate Change 2013: The Physical Science Basis. Contribution of Working Group I to the Fifth Assessment Report of the Intergovernmental Panel on*

- Climate Change*. Cambridge, United Kingdom and New York, NY, USA.: Cambridge University Press.
- COASTAL PARTNERS. n.d. *Local Authority for Portsmouth: Projects, maintenance and repairs for Portsmouth coastline* [Online]. Available: <https://coastalpartners.org.uk/authority/portsmouth/> [Accessed].
- COLLINS, M. B. & ANSELL, K. 2000. *Solent science: a review*, Elsevier.
- COULTHARD, T. J., NEAL, J. C., BATES, P. D., RAMIREZ, J., DE ALMEIDA, G. A. M. & HANCOCK, G. R. 2013. Integrating the LISFLOOD-FP 2D hydrodynamic model with the CAESAR model: implications for modelling landscape evolution. *Earth Surface Processes and Landforms*, 38, 1897-1906.
- COWELL, P. J. & THOM, B. G. 1994. Morphodynamics of coastal evolution. *Coastal evolution: Late Quaternary shoreline morphodynamics*, 33-86.
- CUI, L., GE, Z., YUAN, L. & ZHANG, L. 2015. Vulnerability assessment of the coastal wetlands in the Yangtze Estuary, China to sea-level rise. *Estuarine, Coastal and Shelf Science*, 156, 42-51.
- CURTIS, K. J. & SCHNEIDER, A. 2011. Understanding the demographic implications of climate change: estimates of localized population predictions under future scenarios of sea-level rise. *Population and Environment*, 33, 28-54.
- DALAL, I. L., STEFAN, D. & HARWAYNE-GIDANSKY, J. Low discrepancy sequences for Monte Carlo simulations on reconfigurable platforms. 2008 International Conference on Application-Specific Systems, Architectures and Processors, 2008. IEEE, 108-113.
- DAVISON, M., CURRIE, I. & OGLEY, B. 1993. *The Hampshire and Isle of Wight Weather Book*, Westerham, Froglets Publications Ltd.
- DAWSON, R., HALL, J. & DAVIS, J. 2004. Performance-based management of flood defence systems. *Proceedings of the Institution of Civil Engineers - Water Management*, 157, 35-44.
- DAWSON, R. J., DICKSON, M. E., NICHOLLS, R. J., HALL, J. W., WALKDEN, M. J. A., STANSBY, P. K., MOKRECH, M., RICHARDS, J., ZHOU, J., MILLIGAN, J., JORDAN, A., PEARSON, S., REES, J., BATES, P. D., KOUKOULAS, S. & WATKINSON, A. R. 2009. Integrated analysis of risks of coastal flooding and cliff erosion under scenarios of long term change. *Climatic Change*, 95, 249-288.
- DAWSON, R. J., PEPPE, R. & WANG, M. 2011. An agent-based model for risk-based flood incident management. *Natural Hazards*, 59, 167-189.
- DAYAN, H., LE COZANNET, G., SPEICH, S. & THIÉBLEMONT, R. 2021. High-End Scenarios of Sea-Level Rise for Coastal Risk-Averse Stakeholders. *Frontiers in Marine Science*, 8.
- DE ALMEIDA, G. A. M., BATES, P., FREER, J. E. & SOUVIGNET, M. 2012. Improving the stability of a simple formulation of the shallow water equations for 2-D flood modeling. *Water Resources Research*, 48.
- DE LA VEGA-LEINERT, A. C. & NICHOLLS, R. J. 2008. Potential Implications of Sea-Level Rise for Great Britain. *Journal of Coastal Research*, 2008.
- DE MOEL, H., ASSELMAN, N. E. M. & AERTS, J. C. J. H. 2012. Uncertainty and sensitivity analysis of coastal flood damage estimates in the west of the Netherlands. *Natural Hazards and Earth System Sciences*, 12, 1045-1058.

## List of References

- DEFRA 2003. Flood and Coastal Defence R&D Programme: Flood risk to people Phase 1 R&D Technical Report FD2317/TR. *In*: AGENCY, D. E. (ed.). London SW1P 3JR.
- DEFRA 2006. Shoreline management plan guidance - volume 2 - Procedures. *In*: DEPARTMENT FOR ENVIRONMENT, F. R. A. (ed.). London: Department for Environment, Food and Rural Affairs.
- DI BALDASSARRE, G. 2012. *Floods in a changing climate: inundation modelling*, Cambridge University Press.
- DI LEVA, C. & TYMOWSKI, W. 2000. The Ramsar Convention on Wetlands: the Role of 'Urgent National Interests' and 'Compensation' in Wetland Protection. *Bonn: IUCN Environmental Law Centre*.
- DIGIMAP. 2021. *Summary of Maps, Scales and Dates* [Online]. Available: [https://digimap.edina.ac.uk/webhelp/historic/historicdigimaphelp.htm#about\\_historic\\_maps/map\\_summary.htm](https://digimap.edina.ac.uk/webhelp/historic/historicdigimaphelp.htm#about_historic_maps/map_summary.htm) [Accessed].
- DUARTE, C. M., MIDDELBURG, J. J. & CARACO, N. 2005. Major role of marine vegetation on the oceanic carbon cycle. *Biogeosciences*, 2, 7.
- EASTERLING, J. C. 1991. *Portsmouth Sea Defences: Towards 2050*.
- EMERY, K. & AUBREY, D. G. 1991. Impact of sea-level/land-level change on society. *Sea Levels, Land Levels, and Tide Gauges*. Springer.
- ENGLISH HERITAGE 2015. Roman and Medieval Sea and River Flood Defences.
- ENGMAN, E. T. 1986. Roughness coefficients for routing surface runoff. *Journal of Irrigation and Drainage Engineering*, 112.
- ENVIRONMENT AGENCY 2001. *Lessons learned: Autumn 2000 Floods.*, Bristol, Environment Agency.
- ENVIRONMENT AGENCY 2012. Thames Estuary 2100: TE2100 Plan. *In*: AGENCY, E. (ed.). Charlton, London SE7 8LX.
- ENVIRONMENT AGENCY 2016. The costs and impacts of the winter 2013 to 2014 floods.
- ENVIRONMENT AGENCY 2017. Spatial Flood Defences (including standardised attributes): Product Description.
- ENVIRONMENT AGENCY 2018. Coastal flood boundary conditions for the UK: 2018 update; Technical summary report. Environment Agency.
- ENVIRONMENT AGENCY 2020a. AIMS Spatial Flood Defences (inc. standardised attributes). *In*: ENVIRONMENT AGENCY (ed.).
- ENVIRONMENT AGENCY 2020b. National Flood and Coastal Erosion Risk Management Strategy for England.
- ENVIRONMENT AGENCY. n.d.-a. *Environment Agency Geomatics: Accuracy & Resolution* [Online]. Available: [https://experience.arcgis.com/experience/753ad2ebd3554fa696885b8c366c3049/page/page\\_16/?views=view\\_19](https://experience.arcgis.com/experience/753ad2ebd3554fa696885b8c366c3049/page/page_16/?views=view_19) [Accessed].

- ENVIRONMENT AGENCY. n.d.-b. *Environment Agency Geomatics: DSM & DTMs* [Online]. Available: [https://experience.arcgis.com/experience/753ad2ebd3554fa696885b8c366c3049/page/page\\_16/?views=view\\_19](https://experience.arcgis.com/experience/753ad2ebd3554fa696885b8c366c3049/page/page_16/?views=view_19) [Accessed].
- EVANS, E. 2004. *Foresight: Future Flooding. Scientific Summary*, Department of Trade and Industry.
- FINKL, C. W. 2004. Coastal classification: systematic approaches to consider in the development of a comprehensive scheme. *Journal of Coastal research*, 20, 166-213.
- FLIKWEERT, J. & SIMM, J. 2008. Improving performance targets for flood defence assets. *Journal of Flood Risk Management*, 1, 201-212.
- FORESIGHT 2011. Migration and Global Environmental Change - Final Project Report: Executive summary. In: SCIENCE, T. G. O. F. (ed.). London.
- FOX-KEMPER, B., HEWITT, H. T., XIAO, C., AÐALGEIRSDÓTTIR, G., DRIJFHOUT, S. S., EDWARDS, T. L., GOLLEDGE, N. R., HEMER, M., KOPP, R. E., KRINNER, G., MIX, A., NOTZ, D., NOWICKI, S., NURHATI, I. S., RUIZ, L., SALLÉE, J.-B., SLANGEN, A. B. A. & YU, Y. 2021. Ocean, Cryosphere and Sea Level Change. In: MASSON-DEMLOTTE, V., ZHAI, P., PIRANI, A., CONNORS, S. L., PEAN, C., BERGER, S., CAUD, N., CHEN, Y., GOLDFARB, L., GOMIS, M. I., HUANG, M., LEITZELL, K., LONNOY, E., MATTHEWS, J. B. R., MAYCOCK, T. K., WATERFIELD, T., YELEKCI, O., YU, R. & ZHOU, B. (eds.) *Climate Change 2021: The Physical Science Basis. Contribution of Working Group I to the Sixth Assessment Report of the Intergovernmental Panel on Climate Change*. Cambridge University Press.
- FRENCH, J., BURNINGHAM, H., THORNHILL, G., WHITEHOUSE, R. & NICHOLLS, R. J. 2016. Conceptualising and mapping coupled estuary, coast and inner shelf sediment systems. *Geomorphology*, 256, 17-35.
- FRITZ, H. M., BLOUNT, C. D., THWIN, S., THU, M. K. & CHAN, N. 2009. Cyclone Nargis storm surge in Myanmar. *Nature Geoscience*, 2, 448-449.
- FÜHRBÖTER, A., DETTE, H. H. & GRÜNE, J. 1977. Response of Sea Dykes Due to Wave Impacts. *Coastal Engineering* 1976.
- GOULDBY, B., SAMUELS, P., KLIJN, F. & MESSNER, F. 2005. Language of risk-project definitions. *Floodsite project report T32-04-01*.
- GOULDBY, B., SAYERS, P., MULET-MARTI, J., HASSAN, M. A. A. M. & BENWELL, D. 2008. A methodology for regional-scale flood risk assessment. *Proceedings of the Institution of Civil Engineers - Water Management*, 161, 169-182.
- HABITATS DIRECTIVE 1992. Council Directive 92/43/EEC of 21 May 1992 on the conservation of natural habitats and of wild fauna and flora. *Official Journal of the European Union*, 206, 7-50.
- HAIGH, I., NICHOLLS, R. & WELLS, N. 2010. Assessing changes in extreme sea levels: Application to the English Channel, 1900–2006. *Continental Shelf Research*, 30, 1042-1055.
- HAIGH, I., NICHOLLS, R. & WELLS, N. 2011. Rising sea levels in the English Channel 1900 to 2100. *Proceedings of the Institution of Civil Engineers - Maritime Engineering*, 164, 81-92.
- HAIGH, I. D., COOPER, N., HARRIS, J., SWIFT, R., BUTCHER, P., TRIPP, I. & KERMODE, T. 2004a. Developing an improved understanding of storm surge propagation in the Solent.

## List of References

- HAIGH, I. D., COOPER, N., HARRIS, J., SWIFT, R., BUTCHER, P., TRIPP, I. & KERMODE, T. Developing an Improved Understanding of Storm Surge Propagation in the Solent. 39th DEFRA flood and coastal management conference, June 29–July 1 2004 2004b. York, UK.
- HAIGH, I. D. & NICHOLLS, R. J. 2017. Coastal Flooding. *MCCIP Science Review*, 108-114.
- HAIGH, I. D., NICHOLLS, R. J., PENNING-ROWSELL, E. & SAYERS, P. 2020. Impacts of climate change on coastal flooding, relevant to the coastal and marine environment around the UK. *Marine Climate Change Impact Partnership Science Review 2020*, 546-565.
- HAIGH, I. D., OZSOY, O., WADEY, M. P., NICHOLLS, R. J., GALLOP, S. L., WAHL, T. & BROWN, J. M. 2017. An improved database of coastal flooding in the United Kingdom from 1915 to 2016. *Sci Data*, 4, 170100.
- HAIGH, I. D., WADEY, M. P., GALLOP, S. L., LOEHR, H., NICHOLLS, R. J., HORSBURGH, K., BROWN, J. M. & BRADSHAW, E. 2015. A user-friendly database of coastal flooding in the United Kingdom from 1915-2014. *Sci Data*, 2, 150021.
- HAIGH, I. D., WADEY, M. P., WAHL, T., OZSOY, O., NICHOLLS, R. J., BROWN, J. M., HORSBURGH, K. & GOULDBY, B. 2016. Spatial and temporal analysis of extreme sea level and storm surge events around the coastline of the UK. *Sci Data*, 3, 160107.
- HALL, J., SAYERS, P. & DAWSON, R. 2005. National-scale Assessment of Current and Future Flood Risk in England and Wales. *Natural Hazards*, 36, 147-164.
- HALL, J. W., DAWSON, R. J., SAYERS, P. B., ROSU, C., CHATTERTON, J. B. & DEAKIN, R. 2003. A methodology for national-scale flood risk assessment. *Proceedings of the Institution of Civil Engineers - Water and Maritime Engineering*, 156, 235-247.
- HALL, J. W., SAYERS, P. B., WALKDEN, M. J. & PANZERI, M. 2006. Impacts of climate change on coastal flood risk in England and Wales: 2030-2100. *Philos Trans A Math Phys Eng Sci*, 364, 1027-49.
- HALLEGATTE, S. 2008. An adaptive regional input-output model and its application to the assessment of the economic cost of Katrina. *Risk Anal*, 28, 779-99.
- HALLEGATTE, S., GREEN, C., NICHOLLS, R. J. & CORFEE-MORLOT, J. 2013. Future flood losses in major coastal cities. *Nature Climate Change*, 3, 802-806.
- HALLEGATTE, S. & PRZYLUSKI, V. 2010. The Economics of Natural Disasters: Concepts and Methods. *Policy Research Working Paper*, 5507.
- HALLEGATTE, S., RANGER, N., MESTRE, O., DUMAS, P., CORFEE-MORLOT, J., HERWEIJER, C. & WOOD, R. M. 2011. Assessing climate change impacts, sea level rise and storm surge risk in port cities: a case study on Copenhagen. *Climatic change*, 104, 113-137.
- HANSON, S., NICHOLLS, R., RANGER, N., HALLEGATTE, S., CORFEE-MORLOT, J., HERWEIJER, C. & CHATEAU, J. 2010. A global ranking of port cities with high exposure to climate extremes. *Climatic Change*, 104, 89-111.
- HAUER, M. E. 2017. Migration induced by sea-level rise could reshape the US population landscape. *Nature Climate Change*, 7, 321-325.
- HAUER, M. E., EVANS, J. M. & MISHRA, D. R. 2016. Millions projected to be at risk from sea-level rise in the continental United States. *Nature Climate Change*, 6, 691-695.
- HAY, C. C., MORROW, E., KOPP, R. E. & MITROVICA, J. X. 2015. Probabilistic reanalysis of twentieth-century sea-level rise. *Nature*, 517, 481-484.



- HELTON, J. C., JOHNSON, J. D., SALLABERRY, C. J. & STORLIE, C. B. 2006. Survey of sampling-based methods for uncertainty and sensitivity analysis. *Reliability Engineering & System Safety*, 91, 1175-1209.
- HENDRY, A., HAIGH, I. D., NICHOLLS, R. J., WINTER, H., NEAL, R., WAHL, T., JOLY-LAUGEL, A. & DARBY, S. E. 2019. Assessing the characteristics and drivers of compound flooding events around the UK coast. *Hydrology and Earth System Sciences*, 23, 3117-3139.
- HINKEL, J., FEYEN, L., HEMER, M., COZANNET, G., LINCKE, D., MARCOS, M., MENTASCHI, L., MERKENS, J. L., MOEL, H., MUIS, S., NICHOLLS, R. J., VAFEIDIS, A. T., WAL, R. S. W., VOUSDOKAS, M. I., WAHL, T., WARD, P. J. & WOLFF, C. 2021. Uncertainty and bias in global to regional scale assessments of current and future coastal flood risk. *Earth's Future*.
- HINKEL, J., LINCKE, D., VAFEIDIS, A. T., PERRETTE, M., NICHOLLS, R. J., TOL, R. S., MARZEION, B., FETTWEIS, X., IONESCU, C. & LEVERMANN, A. 2014. Coastal flood damage and adaptation costs under 21st century sea-level rise. *Proc Natl Acad Sci U S A*, 111, 3292-7.
- HINKEL, J., NICHOLLS, R. J., VAFEIDIS, A. T., TOL, R. S. J. & AVAGIANOU, T. 2010. Assessing risk of and adaptation to sea-level rise in the European Union: an application of DIVA. *Mitigation and Adaptation Strategies for Global Change*, 15, 703-719.
- HOGARTH, P., HUGHES, C. W., WILLIAMS, S. D. P. & WILSON, C. 2020. Improved and extended tide gauge records for the British Isles leading to more consistent estimates of sea level rise and acceleration since 1958. *Progress in Oceanography*, 184.
- HOLDGATE, M. W. 1979. *A perspective of environmental pollution*, Cambridge University Press.
- HOLTHUIJSEN, L. H. 2010. *Waves in oceanic and coastal waters*, Cambridge university press.
- HOOZEMANS, F. M., STIVE, M. J. & BIJLSMA, L. A global vulnerability assessment: vulnerability of coastal areas to sea-level rise. Coastal Zone'93, 1993. ASCE, 390-404.
- HORSBURGH, K. & HORRITT, M. 2006. The Bristol Channel floods of 1607 - reconstruction and analysis. *Weather*, 61, 272-277.
- HUGO, G. 2011. Future demographic change and its interactions with migration and climate change. *Global Environmental Change*, 21, S21-S33.
- ICE 2010. FACING UP TO RISING SEA-LEVELS: RETREAT? DEFEND? ATTACK?
- IIASA 2018. SSP Database (Shared Socioeconomic Pathways) - Version 2.0. In: ANALYSIS, T. I. I. F. A. S. (ed.) V 2.0 ed.
- IPCC 2014. Climate Change 2014: Synthesis Report. Contribution of Working Groups I, II and III to the Fifth Assessment Report of the Intergovernmental Panel on Climate Change. In: PACHAURI, R. K. & MEYER, L. A. (eds.). Geneva, Switzerland.
- IPCC 2019. Summary for Policymakers. In: PÖRTNER, H.-O., ROBERTS, D. C., MASSON-DELMOTTE, V., ZHAI, P., TIGNOR, M., POLOCZANSKA, E., MINTENBECK, K., ALEGRÍA, A., NICOLAI, M., OKEM, A., PETZOLD, J., RAMA, B. & WEYE, N. M. (eds.) *IPCC Special Report on the Ocean and Cryosphere in a Changing Climate*.
- IPCC 2021. Summary for Policymakers. In: MASSON-DEMLLOTTE, V., ZHAI, P., PIRANI, A., CONNORS, S. L., PEAN, C., BERGER, S., CAUD, N., CHEN, Y., GOLDFARB, L., GOMIS, M. I., HUANG, M., LEITZELL, K., LONNOY, E., MATTHEWS, J. B. R., MAYCOCK, T. K., WATERFIELD, T., YELEKCI, O., YU, R. & ZHOU, B. (eds.) *Climate Change 2021: The Physical Science Basis*.

## List of References

- Contribution of Working Group I to the Sixth Assessment Report of the Intergovernmental Panel on Climate Change*. Cambridge University Press.
- JONKMAN, S. N., VOORTMAN, H. G., KLERK, W. J. & VAN VUREN, S. 2018. Developments in the management of flood defences and hydraulic infrastructure in the Netherlands. *Structure and Infrastructure Engineering*, 14, 895-910.
- KABAT, P., FRESCO, L. O., STIVE, M. J. F., VEERMAN, C. P., VAN ALPHEN, J. S. L. J., PARMET, B. W. A. H., HAZELEGER, W. & KATSMAN, C. A. 2009. Dutch coasts in transition. *Nature Geoscience*, 2, 450-452.
- KEBEDE, A. S. & NICHOLLS, R. J. 2011. Exposure and vulnerability to climate extremes: population and asset exposure to coastal flooding in Dar es Salaam, Tanzania. *Regional Environmental Change*, 12, 81-94.
- KEBEDE, A. S., NICHOLLS, R. J., HANSON, S. & MOKRECH, M. 2012. Impacts of climate change and sea-level rise: a preliminary case study of Mombasa, Kenya. *Journal of Coastal Research*, 28, 8-19.
- KELMAN, I. 2002. *Physical flood vulnerability of residential properties in coastal, eastern England*. Citeseer.
- KERINS, D. 2014. Hampshire flood chaos 'becomes a risk to life'. *Southern Daily Echo*.
- KIUREGHIAN, A. D. & DITLEVSEN, O. 2009. Aleatory or epistemic? Does it matter? *Structural Safety*, 31, 105-112.
- KRON, W. 2013. Coasts: the high-risk areas of the world. *Natural hazards*, 66, 1363-1382.
- LAGMAY, A. M. F., AGATON, R. P., BAHALA, M. A. C., BRIONES, J. B. L. T., CABACABA, K. M. C., CARO, C. V. C., DASALLAS, L. L., GONZALO, L. A. L., LADIERO, C. N., LAPIDEZ, J. P., MUNGICAL, M. T. F., PUNO, J. V. R., RAMOS, M. M. A. C., SANTIAGO, J., SUAREZ, J. K. & TABLAZON, J. P. 2015. Devastating storm surges of Typhoon Haiyan. *International Journal of Disaster Risk Reduction*, 11, 1-12.
- LARSON, M., ERIKSON, L. & HANSON, H. 2004. An analytical model to predict dune erosion due to wave impact. *Coastal Engineering*, 51, 675-696.
- LAUSTRUP, C., MADSEN, H. T., JENSEN, J. & POULSEN, L. 1991. Dike failure calculation model based on in situ tests. *Coastal Engineering 1990*.
- LE BARS, D. 2018. Uncertainty in Sea Level Rise Projections Due to the Dependence Between Contributors. *Earth's Future*, 6, 1275-1291.
- LE COZANNET, G., ROHMER, J., CAZENAVE, A., IDIER, D., VAN DE WAL, R., DE WINTER, R., PEDREROS, R., BALOUIN, Y., VINCHON, C. & OLIVEROS, C. 2015. Evaluating uncertainties of future marine flooding occurrence as sea-level rises. *Environmental Modelling & Software*, 73, 44-56.
- LEFEBVRE, A., THOMPSON, C. E. L. & AMOS, C. L. 2010. Influence of *Zostera marina* canopies on unidirectional flow, hydraulic roughness and sediment movement. *Continental Shelf Research*, 30, 1783-1794.
- LEWIS, M., HORSBURGH, K., BATES, P. & SMITH, R. 2011. Quantifying the Uncertainty in Future Coastal Flood Risk Estimates for the U.K. *Journal of Coastal Research*, 276, 870-881.
- LHOMME, J., SAYERS, P., GOULDBY, B., SAMUELS, P., WILLS, M. & MULET-MARTI, J. 2008. Recent development and application of a rapid flood spreading method.

- LICHTER, M., VAFEIDIS, A. T. & NICHOLLS, R. J. 2010. Exploring Data-Related Uncertainties in Analyses of Land Area and Population in the “Low-Elevation Coastal Zone” (LECZ). *Journal of Coastal Research*, 27.
- LINCKE, D., HINKEL, J., MENGEL, M. & NICHOLLS, R. J. In preparation, 2021. Attributing the drivers of industrial age and 21st century coastal flood exposure and risk.
- LOWE, J. A., HOWARD, T. P., PARDAENS, A., TINKER, J., HOLT, J., WAKELIN, S., MILNE, G., LEAKE, J., WOLF, J. & HORSBURGH, K. 2009. UK Climate Projections science report: Marine and coastal projections.
- LUTZ, W., BUTZ, W. P. & SAMIR, K. E. 2014. *World population and human capital in the twenty-first century*, OUP Oxford.
- MACPHERSON, L. R., ARNS, A., DANGENDORF, S., VAFEIDIS, A. T. & JENSEN, J. 2019. A Stochastic Extreme Sea Level Model for the German Baltic Sea Coast. *Journal of Geophysical Research: Oceans*, 124, 2054-2071.
- MATTHIES, H. G. QUANTIFYING UNCERTAINTY: MODERN COMPUTATIONAL REPRESENTATION OF PROBABILITY AND APPLICATIONS. 2007 Dordrecht. Springer Netherlands, 105-135.
- MCALINDEN, B. 2015. *Managed realignment at Medmerry, Sussex* [Online]. Institution of Civil Engineers. Available: <https://www.ice.org.uk/knowledge-and-resources/case-studies/managed-realignment-at-medmerry-sussex> [Accessed].
- MCGRANAHAN, G., BALK, D. & ANDERSON, B. 2007. The rising tide: assessing the risks of climate change and human settlements in low elevation coastal zones. *Environment and Urbanization*, 19, 17-37.
- MCMICHAEL, C., DASGUPTA, S., AYEB-KARLSSON, S. & KELMAN, I. 2020. A review of estimating population exposure to sea-level rise and the relevance for migration. *Environ Res Lett*, 15, 123005.
- MCMILLAN, A., BATSTONE, C., WORTH, D., TAWN, J., HORSBURGH, K. & LAWLESS, M. 2011. Coastal flood boundary conditions for UK mainland and islands. Project SC060064/TR2: Design sea levels.
- MERKENS, J.-L., LINCKE, D., HINKEL, J., BROWN, S. & VAFEIDIS, A. T. 2018. Regionalisation of population growth projections in coastal exposure analysis. *Climatic Change*, 151, 413-426.
- MERKENS, J.-L., REIMANN, L., HINKEL, J. & VAFEIDIS, A. T. 2016. Gridded population projections for the coastal zone under the Shared Socioeconomic Pathways. *Global and Planetary Change*, 145, 57-66.
- MEYER, V., BECKER, N., MARKANTONIS, V., SCHWARZE, R., VAN DEN BERGH, J. C. J. M., BOUWER, L. M., BUBECK, P., CIAVOLA, P., GENOVESE, E., GREEN, C., HALLEGATTE, S., KREIBICH, H., LEQUEUX, Q., LOGAR, I., PAPYRAKIS, E., PFURTSCHALLER, C., POUSSIN, J., PRZYLUSKI, V., THIEKEN, A. H. & VIAVATTENE, C. 2013. Review article: Assessing the costs of natural hazards – state of the art and knowledge gaps. *Natural Hazards and Earth System Sciences*, 13, 1351-1373.
- MINIKIN, R. 1963. Winds, Waves and Maritime Structures: Studies in Harbour Making and in the Protection of Coasts, 2nd Rev. Ed., *Griffin, London*, 294.
- MONDAL, P. & TATEM, A. J. 2012. Uncertainties in measuring populations potentially impacted by sea level rise and coastal flooding. *PLoS One*, 7, e48191.

## List of References

- MUIS, S., GUNERALP, B., JONGMAN, B., AERTS, J. C. & WARD, P. J. 2015. Flood risk and adaptation strategies under climate change and urban expansion: A probabilistic analysis using global data. *Sci Total Environ*, 538, 445-57.
- MUIS, S., VERLAAN, M., NICHOLLS, R. J., BROWN, S., HINKEL, J., LINCKE, D., VAFEIDIS, A. T., SCUSSOLINI, P., WINSEMIUS, H. C. & WARD, P. J. 2017. A comparison of two global datasets of extreme sea levels and resulting flood exposure. *Earth's Future*, 5, 379-392.
- MUIS, S., VERLAAN, M., WINSEMIUS, H. C., AERTS, J. C. & WARD, P. J. 2016. A global reanalysis of storm surges and extreme sea levels. *Nat Commun*, 7, 11969.
- NARAYAN, S., HANSON, S., NICHOLLS, R. J., CLARKE, D., WILLEMS, P., NTEGEKA, V. & MONBALIU, J. 2012. A holistic model for coastal flooding using system diagrams and the Source-Pathway-Receptor (SPR) concept. *Natural Hazards and Earth System Sciences*, 12, 1431-1439.
- NARAYAN, S., NICHOLLS, R. J., CLARKE, D., HANSON, S., REEVE, D., HORRILLO-CARABALLO, J., LE COZANNET, G., HISSEL, F., KOWALSKA, B., PARDA, R., WILLEMS, P., OHLE, N., ZANUTTIGH, B., LOSADA, I., GE, J., TRIFONOVA, E., PENNING-ROWSELL, E. & VANDERLINDEN, J. P. 2014. The SPR systems model as a conceptual foundation for rapid integrated risk appraisals: Lessons from Europe. *Coastal Engineering*, 87, 15-31.
- NASA. n.d. *Global Rural-Urban Mapping Project (GRUMP)*, v1 [Online]. Available: <https://sedac.ciesin.columbia.edu/data/collection/grump-v1> [Accessed].
- NÉELZ, S. & PENDER, G. 2008. Desktop review of 2d hydraulic modelling packages.
- NÉELZ, S. & PENDER, G. 2009. Desktop review of 2D hydraulic modelling packages. Environment Agency.
- NÉELZ, S. & PENDER, G. 2010. *Benchmarking of 2D Hydraulic Modelling Packages*, Bristol, Environment Agency.
- NÉELZ, S. & PENDER, G. 2013. *Benchmarking the latest generation of 2D hydraulic modelling packages*, Bristol, Environment Agency.
- NEUMANN, B., VAFEIDIS, A. T., ZIMMERMANN, J. & NICHOLLS, R. J. 2015. Future coastal population growth and exposure to sea-level rise and coastal flooding--a global assessment. *PLoS One*, 10, e0118571.
- NFDC 2010. North Solent Shoreline Management Plan.
- NICHOLLS, R., ZANUTTIGH, B., VANDERLINDEN, J. P., WEISSE, R., SILVA, R., HANSON, S., NARAYAN, S., HOGGART, S., THOMPSON, R. C., VRIES, W. D. & KOUNDOURI, P. 2015. Developing a Holistic Approach to Assessing and Managing Coastal Flood Risk. *Coastal Risk Management in a Changing Climate*.
- NICHOLLS, R. J. 2004. Coastal flooding and wetland loss in the 21st century: changes under the SRES climate and socio-economic scenarios. *Global Environmental Change*, 14, 69-86.
- NICHOLLS, R. J. 2018. Adapting to Sea-Level Rise. *Resilience*.
- NICHOLLS, R. J., HANSON, S., HERWEIJER, C., PATMORE, N., HALLEGATTE, S., CORFEE-MORLOT, J., CHÂTEAU, J. & MUIR-WOOD, R. 2008. Ranking Port Cities with High Exposure and Vulnerability to Climate Extremes.

- NICHOLLS, R. J., HOOZEMANS, F. M. & MARCHAND, M. 1999. Increasing flood risk and wetland losses due to global sea-level rise: regional and global analyses. *Global Environmental Change*, 9, S69-S87.
- NOAA 2018. Costliest U.S. tropical cyclones tables updated.
- O'CONNOR, J. E. & COSTA, J. E. 2004. The World's Largest Floods, Past and Present - Their Causes and Magnitudes. *U.S. Geological Survey Circular*, 1254, 13.
- ONS. 2013. *2011 Census: Population and household estimates for the United Kingdom, March 2011* [Online]. Available: <https://www.ons.gov.uk/peoplepopulationandcommunity/populationandmigration/populationestimates/bulletins/populationandhouseholdestimatesfortheunitedkingdom/2011-03-21> [Accessed].
- ONS. 2016. *The modern census* [Online]. Available: <https://www.ons.gov.uk/census/2011census/howourcensusworks/aboutcensuses/censushistory/themoderncensus> [Accessed].
- ONS. 2020. *Average household income, UK: financial year ending 2019* [Online]. Available: <https://www.ons.gov.uk/peoplepopulationandcommunity/personalandhouseholdfinances/incomeandwealth/bulletins/householddisposableincomeandinequality/financialyearending2019> [Accessed].
- ONS. n.d.-a. *A quick guide to 1991 and earlier Censuses* [Online]. Available: <https://www.ons.gov.uk/census/2001censusandearlier/aquickguideto1991andearliercensuses# census-geography-1801-2001> [Accessed 2021].
- ONS, O. F. N. S. 2011. *2011 Census: Characteristics of Built-Up Areas* [Online]. Available: <https://www.ons.gov.uk/peoplepopulationandcommunity/housing/articles/characteristics of built up areas/2013-06-28> [Accessed].
- ONS, O. F. N. S. n.d.-b. *2001 Census and earlier* [Online]. Available: <https://www.ons.gov.uk/census/2001censusandearlier> [Accessed].
- ORDNANCE SURVEY 2016. MasterMap Topography Layer: User guide and Technical specification.
- ORDNANCE SURVEY 2017. OS TERRAIN 5: User guide and technical specification.
- OWEN, M. 1980. Design of seawalls allowing for wave overtopping. *Report Ex*, 924, 39.
- OZSOY, O., HAIGH, I. D., WADEY, M. P., NICHOLLS, R. J. & WELLS, N. C. 2016. High-frequency sea level variations and implications for coastal flooding: A case study of the Solent, UK. *Continental Shelf Research*, 122, 1-13.
- PAIK, J. K. 2018. *Ultimate Limit State Analysis and Design of Plated Structures*,.
- PALMER, M., HOWARD, T., TINKER, J., LOWE, J., BRICHENO, L., CALVERT, D., EDWARDS, T., GREGORY, J., HARRIS, G., KRIJNEN, J., PICKERING, M., ROBERTS, C. & WOLF, J. 2018. UKCP18 Marine report. In: ENVIRONMENT AGENCY, M. O. (ed.).
- PAWLOWICZ, R., BEARDSLEY, B. & LENTZ, S. 2002. Classical tidal harmonic analysis including error estimates in MATLAB using T\_TIDE. *Computers & Geosciences*, 28, 8.
- PEDROZO-ACUÑA, A., DAMANIA, R., LAVERDE-BARAJAS, M. A. & MIRA-SALAMA, D. 2015. Assessing the consequences of sea-level rise in the coastal zone of Quintana Roo, México: the costs of inaction. *Journal of Coastal Conservation*, 19, 227-240.

## List of References

- PENNING-ROWSELL, E. C. 2015. A realistic assessment of fluvial and coastal flood risk in England and Wales. *Transactions of the Institute of British Geographers*, 40, 44-61.
- PENNING-ROWSELL, E. C., SULTANA, P. & THOMPSON, P. M. 2013. The 'last resort'? Population movement in response to climate-related hazards in Bangladesh. *Environmental Science & Policy*, 27, S44-S59.
- PERCIVAL, S., GATERELL, M. & TEEUW, R. 2019. Urban neighbourhood flood vulnerability and risk assessments at different diurnal levels. *Journal of Flood Risk Management*, 12.
- PITT, M. 2008. *Learning lessons from the 2007 floods*, Pitt Review.
- PRELL, C., HUBACEK, K. & REED, M. 2009. Stakeholder Analysis and Social Network Analysis in Natural Resource Management. *Society & Natural Resources*, 22, 501-518.
- PUGH, D. T. 1987. *Tides, surges and mean sea-level*, John Willey and Sons.
- QUINN, A. D. F. 1972. Design and construction of ports and marine structures.
- QUINN, N., ATKINSON, P. M. & WELLS, N. C. 2012. Modelling of tide and surge elevations in the Solent and surrounding waters: The importance of tide–surge interactions. *Estuarine, Coastal and Shelf Science*, 112, 162-172.
- QUINN, N., LEWIS, M., WADEY, M. P. & HAIGH, I. D. 2014. Assessing the temporal variability in extreme storm-tide time series for coastal flood risk assessment. *Journal of Geophysical Research: Oceans*, 119, 4983-4998.
- RAGAS, A. M., HUIJBREGTS, M. A., HENNING-DE JONG, I. & LEUVEN, R. S. 2008. Uncertainty in Environmental Risk Assessment: Implications for Risk-Based Management of River Basins. *Integrated Environmental Assessment and Management*, 5, 10.
- RENARDY, M., JOSLYN, L. R., MILLAR, J. A. & KIRSCHNER, D. E. 2021. To Sobol or not to Sobol? The effects of sampling schemes in systems biology applications. *Math Biosci*, 337, 108593.
- RIAH, K., VAN VUUREN, D. P., KRIEGLER, E., EDMONDS, J., O'NEILL, B. C., FUJIMORI, S., BAUER, N., CALVIN, K., DELLINK, R., FRICKO, O., LUTZ, W., POPP, A., CUARESMA, J. C., KC, S., LEIMBACH, M., JIANG, L., KRAM, T., RAO, S., EMMERLING, J., EBI, K., HASEGAWA, T., HAVLIK, P., HUMPENÖDER, F., DA SILVA, L. A., SMITH, S., STEHFEST, E., BOSETTI, V., EOM, J., GERNAAT, D., MASUI, T., ROGELJ, J., STREFLER, J., DROUET, L., KREY, V., LUDERER, G., HARMSSEN, M., TAKAHASHI, K., BAUMSTARK, L., DOELMAN, J. C., KAINUMA, M., KLIMONT, Z., MARANGONI, G., LOTZE-CAMPEN, H., OBERSTEINER, M., TABEAU, A. & TAVONI, M. 2017. The Shared Socioeconomic Pathways and their energy, land use, and greenhouse gas emissions implications: An overview. *Global Environmental Change*, 42, 153-168.
- ROHMER, J., LINCKE, D., HINKEL, J., LE COZANNET, G., LAMBERT, E. & VAFEIDIS, A. T. 2021. Unravelling the Importance of Uncertainties in Global-Scale Coastal Flood Risk Assessments under Sea Level Rise. *Water*, 13.
- ROYAL HASKONING 2008. Technical analysis of defence failures—Summer floods 2007. 9T0505.
- RUOCCO, A. C., NICHOLLS, R. J., HAIGH, I. D. & WADEY, M. P. 2011. Reconstructing coastal flood occurrence combining sea level and media sources: a case study of the Solent, UK since 1935. *Natural Hazards*, 59, 1773-1796.
- SALTELLI, A., ANNONI, P., AZZINI, I., CAMPOLONGO, F., RATTO, M. & TARANTOLA, S. 2010. Variance based sensitivity analysis of model output. Design and estimator for the total sensitivity index. *Computer Physics Communications*, 181, 259-270.

- SANTAMARÍA-GÓMEZ, A., GRAVELLE, M., DANGENDORF, S., MARCOS, M., SPADA, G. & WÖPPELMANN, G. 2017. Uncertainty of the 20th century sea-level rise due to vertical land motion errors. *Earth and Planetary Science Letters*, 473, 24-32.
- SAVAGE, J. T. S., PIANOSI, F., BATES, P., FREER, J. & WAGENER, T. 2016. Quantifying the importance of spatial resolution and other factors through global sensitivity analysis of a flood inundation model. *Water Resources Research*, 52, 9146-9163.
- SAYERS, P., HALL, J., DAWSON, R., ROSU, C. & BSC, R. D. 2002. Risk assessment of flood and coastal defences for strategic planning (RASP)—a High Level Methodology.
- SAYERS, P., HORRITT, M., CARR, S., KAY, A., MAUZ, J., LAMB, R. & PENNING-ROWSELL, E. 2020. Third UK Climate Change Risk Assessment (CCRA3): Future flood risk. *Research undertaken by Sayers and Partners for the Committee on Climate Change. Published by Committee on Climate Change, London.*
- SEENATH, A. 2015. Modelling coastal flood vulnerability: Does spatially-distributed friction improve the prediction of flood extent? *Applied Geography*, 64, 97-107.
- SHARMA, G. 2017. Pros and cons of different sampling techniques. *International journal of applied research*, 3, 749-752.
- SIMM, J., GOULDBY, B., SAYERS, P., FLIKWEERT, J., WERSCHING, S. & BRAMLEY, M. 2008. Representing fragility of flood and coastal defences: Getting into the detail. *Flood Risk Management: Research and Practice*
- SKINNER, C. J., COULTHARD, T. J., PARSONS, D. R., RAMIREZ, J. A., MULLEN, L. & MANSON, S. 2015. Simulating tidal and storm surge hydraulics with a simple 2D inertia based model, in the Humber Estuary, U.K. *Estuarine, Coastal and Shelf Science*, 155, 126-136.
- SLATER, J. 2009. Conservation area 27 - Hilsea Lines (scheduled Ancient Monument). In: COUNCIL, P. C. (ed.).
- SMALLS, C. & NICHOLLS, R. J. 2003. A global analysis of human settlement in coastal zones. *Journal of Coastal Research*, 19, 15.
- SMITH, A., BATES, P. D., WING, O., SAMPSON, C., QUINN, N. & NEAL, J. 2019. New estimates of flood exposure in developing countries using high-resolution population data. *Nat Commun*, 10, 1814.
- SOBOL, I. M. 1998. On quasi-monte carlo integrations. *Mathematics and computers in simulation*, 47, 103-112.
- SPENCER, T., SCHUERCH, M., NICHOLLS, R. J., HINKEL, J., LINCKE, D., VAFEIDIS, A. T., REEF, R., MCFADDEN, L. & BROWN, S. 2016. Global coastal wetland change under sea-level rise and related stresses: The DIVA Wetland Change Model. *Global and Planetary Change*, 139, 15-30.
- STANCZAK, G. & OUMERACI, H. 2012. Modeling sea dike breaching induced by breaking wave impact-laboratory experiments and computational model. *Coastal Engineering*, 59, 28-37.
- STEVENS, A. J. 2017. *The historic evolution of coastal flood exposure in the UK*. Doctoral Thesis, University of Southampton.
- STEVENS, A. J., CLARKE, D., NICHOLLS, R. J. & WADEY, M. P. 2015. Estimating the long-term historic evolution of exposure to flooding of coastal populations. *Natural Hazards and Earth System Sciences*, 15, 1215-1229.

## List of References

- STIVE, M. J. F., COWELL, P. J. & NICHOLLS, R. J. 2008. Impacts of Global Environmental Change on Beaches, Cliffs and Deltas. *In: SLAYMAKER, O., SPENCER, T. & EMBLETON-HAMANN, C. (eds.) Geomorphology and Global Environmental Change* International Association of Geomorphologists.
- STRIPLING, S., BRADBURY, A. P., COPE, S. N. & BRAMPTON, A. H. 2008. Understanding Barrier Beaches.
- TAHERKHANI, M., VITOUSEK, S., BARNARD, P. L., FRAZER, N., ANDERSON, T. R. & FLETCHER, C. H. 2020. Sea-level rise exponentially increases coastal flood frequency. *Sci Rep*, 10, 6466.
- TATEM, A. J. 2017. WorldPop, open data for spatial demography. *Sci Data*, 4, 170004.
- TENG, J., JAKEMAN, A. J., VAZE, J., CROKE, B. F. W., DUTTA, D. & KIM, S. 2017. Flood inundation modelling: A review of methods, recent advances and uncertainty analysis. *Environmental Modelling & Software*, 90, 201-216.
- THORNE, C. 2014. Geographies of UK flooding in 2013/4. *The Geographical Journal*, 180, 297-309.
- TOWNEND, I. 2007. A conceptual Model of Southampton Water. *In: AGENCY, E. (ed.)*.
- TURNER, R. K., SUBAK, S. & ADGER, W. N. 1996. Pressures, trends, and impacts in coastal zones: interactions between socioeconomic and natural systems. *Environmental management*, 20, 159-173.
- UNITED NATIONS, D. O. E. A. S. A., POPULATION DIVISION 2015. World Population Prospects: The 2015 Revision, Key Findings and Advance Tables.
- USGS. n.d. *USGS EROS Archive - Digital Elevation - Shuttle Radar Topography Mission (SRTM) Non-Void Filled* [Online]. Available: [https://www.usgs.gov/centers/eros/science/usgs-eros-archive-digital-elevation-shuttle-radar-topography-mission-srtm-non?qt-science\\_center\\_objects=0#qt-science\\_center\\_objects](https://www.usgs.gov/centers/eros/science/usgs-eros-archive-digital-elevation-shuttle-radar-topography-mission-srtm-non?qt-science_center_objects=0#qt-science_center_objects) [Accessed].
- VAN DER MEER, J. W. 2017. Wave run-up and overtopping. *Dikes Aimd Revetments*. Routledge.
- VAN DER PLANK, S., BROWN, S. & NICHOLLS, R. J. 2021. Managing coastal flood risk to residential properties in England: integrating spatial planning, engineering and insurance. *International Journal of Disaster Risk Reduction*, 52.
- VAN VUUREN, D. P. & CARTER, T. R. 2013. Climate and socio-economic scenarios for climate change research and assessment: reconciling the new with the old. *Climatic Change*, 122, 415-429.
- VAN VUUREN, D. P., EDMONDS, J., KAINUMA, M., RIAHI, K., THOMSON, A., HIBBARD, K., HURTT, G. C., KRAM, T., KREY, V., LAMARQUE, J.-F., MASUI, T., MEINSHAUSEN, M., NAKICENOVIC, N., SMITH, S. J. & ROSE, S. K. 2011. The representative concentration pathways: an overview. *Climatic Change*, 109, 5-31.
- VANKONINGSVELD, M., MULDER, J. P. M., STIVE, M. J. F., VANDERVALK, L. & VANDERWECK, A. W. 2008. Living with Sea-Level Rise and Climate Change: A Case Study of the Netherlands. *Journal of Coastal Research*, 242, 367-379.
- VELEGRAKIS, A. 2000. Geology, geomorphology and sediments of the Solent System. *In: COLLINS, M. & ANSELL, K. (eds.) Solent Science - A Review*. Elsevier Science.
- VINET, F., LUMBROSO, D., DEFOSSEZ, S. & BOISSIER, L. 2011. A comparative analysis of the loss of life during two recent floods in France: the sea surge caused by the storm Xynthia and the flash flood in Var. *Natural Hazards*, 61, 1179-1201.



- VOUSDOKAS, M. I., BOUZOTAS, D., GIARDINO, A., BOUWER, L. M., MENTASCHI, L., VOUKOUVALAS, E. & FEYEN, L. 2018a. Understanding epistemic uncertainty in large-scale coastal flood risk assessment for present and future climates. *Natural Hazards and Earth System Sciences*, 18, 2127-2142.
- VOUSDOKAS, M. I., MENTASCHI, L., VOUKOUVALAS, E., VERLAAN, M., JEVREJEVA, S., JACKSON, L. P. & FEYEN, L. 2018b. Global probabilistic projections of extreme sea levels show intensification of coastal flood hazard. *Nat Commun*, 9, 2360.
- WADEY, M. P. 2013. *Understanding Defence Failures and Coastal Flood Events: a Case Study Approach*. Doctor of Philosophy, University of Southampton.
- WADEY, M. P., COPE, S. N., NICHOLLS, R. J., MCHUGH, K., GREWCOCK, G. & MASON, T. 2015a. Coastal flood analysis and visualisation for a small town. *Ocean & Coastal Management*, 116, 237-247.
- WADEY, M. P., HAIGH, I. D., NICHOLLS, R. J., BROWN, J. M., HORSBURGH, K., CARROLL, B., GALLOP, S. L., MASON, T. & BRADSHAW, E. 2015b. A comparison of the 31 January–1 February 1953 and 5–6 December 2013 coastal flood events around the UK. *Frontiers in Marine Science*, 2.
- WADEY, M. P., NICHOLLS, R. J. & HAIGH, I. 2013. Understanding a coastal flood event: the 10th March 2008 storm surge event in the Solent, UK. *Natural Hazards*, 67, 829-854.
- WADEY, M. P., NICHOLLS, R. J. & HUTTON, C. 2012. Coastal Flooding in the Solent: An Integrated Analysis of Defences and Inundation. *Water*, 4, 430-459.
- WAHL, T., HAIGH, I. D., NICHOLLS, R. J., ARNS, A., DANGENDORF, S., HINKEL, J. & SLANGEN, A. B. A. 2017. Understanding extreme sea levels for broad-scale coastal impact and adaptation analysis. *Nat Commun*, 8, 16075.
- WAHL, T., MUDERSBACH, C. & JENSEN, J. 2011. Assessing the hydrodynamic boundary conditions for risk analyses in coastal areas: a stochastic storm surge model. *Natural Hazards and Earth System Sciences*, 11, 2925-2939.
- WAVERLEY 1954. Report of the Departmental Committee on Coastal Flooding. In: HOME OFFICE, SCOTTISH OFFICE, MINISTRY OF HOUSING AND LOCAL GOVERNMENT & MINISTRY OF AGRICULTURE AND FISHERIES (eds.). London.
- WELCH, A. C., NICHOLLS, R. J. & LÁZÁR, A. N. 2017. Evolving deltas: Coevolution with engineered interventions. *Elem Sci Anth*, 5.
- WEMELSFELDER, P. J. 1939. Wetmatigheden in het optreden van stormvloed. *De Ingenieur*, 54 jg., nr. 9 (8/3/'39), blz B31-35.
- WHITE, G. F. 1942. *Human adjustment to floods: a geographical approach to the flood problem in the United States*. The University of Chicago.
- WILLIAMS, J., HORSBURGH, K. J., WILLIAMS, J. A. & PROCTOR, R. N. F. 2016. Tide and skew surge independence: New insights for flood risk. *Geophysical Research Letters*, 43, 6410-6417.
- WILLOUGHBY, N., GRIMBLE, R., ELLENBROEK, W., DANSO, E. & AMATEKPOR, J. 2001. The wise use of wetlands: identifying development options for Ghana's coastal Ramsar sites. *Hydrobiologia*, 458, 221-234.
- WING, O. E. J., BATES, P. D., NEAL, J. C., SAMPSON, C. C., SMITH, A. M., QUINN, N., SHUSTIKOVA, I., DOMENEGHETTI, A., GILLES, D. W., GOSKA, R. & KRAJEWSKI, W. F. 2019. A New

## List of References

- Automated Method for Improved Flood Defense Representation in Large-Scale Hydraulic Models. *Water Resources Research*, 55, 11007-11034.
- WINKLER, R. L. 1996. Uncertainty in probabilistic risk assessment. *Reliability Engineering & System Safety*, 54, 127-132.
- WONG, P. P., LOSADA, I. J., GATTUSO, J.-P., HINKEL, J., KHATTABI, A., MCINNES, K. L., SAITO, Y. & SALLENGER, A. 2014. Coastal systems and low-lying areas. *Climate change*, 2104, 361-409.
- WONG, T. E. & KELLER, K. 2017. Deep Uncertainty Surrounding Coastal Flood Risk Projections: A Case Study for New Orleans. *Earth's Future*, 5, 1015-1026.
- WOODWORTH, P. L., BLACKMAN, D. L., PUGH, D. T. & VASSIE, J. M. 2005. On the role of diurnal tides in contributing to asymmetries in tidal probability distribution functions in areas of predominantly semi-diurnal tide. *Estuarine, Coastal and Shelf Science*, 64, 235-240.
- WORLDPOP. 2021. *WorldPop methods* [Online]. Available: <https://www.worldpop.org/methods> [Accessed].
- ZHANG, J. 2020. Modern Monte Carlo methods for efficient uncertainty quantification and propagation: A survey. *WIREs Computational Statistics*, 13.

